Mutational analysis and protein interactions of Epstein-Barr virus protein Zta, with reference to ZtaRh, a homologue from Cercopithecine herpesvirus-15

by

Questa Hope Karlsson

PhD Biochemistry

University of Sussex

Submitted December 2011

I hereby declare that this thesis has not been and will not be, submitted in whole or in part to another University for the award of any other degree.

Signature: .....

Acknowledgments

I would like to take this opportunity to thank the many people who have helped me during my PhD studies.

The members of the lab have always been fantastic in helping me, both through their friendship and technical expertise. Thank you to Michelle, Helen, Andrea and Sandra, from the West lab and to Sharada, Kay, Winston and Bryony from the Sinclair lab. In particular, the other PhD students, Celine, Sarah and Kirsty, have been wonderful in their help and support.

My supervisor, Alison, has probably never expected me to still be her student after so long but she has always been so supportive and positive, especially when I have faced increasing demands in my life.

I would like to thank my two wonderful sons and daughter, Oliver, Noah and Phoebe, who all made an appearance during my studies, for keeping me smiling and providing an inspiration for finishing. My husband and inspiration, Sam, has been instrumental in motivating me and helping at home and with our children. Without my wonderful mother coming from New Zealand to stay with us to look after the children, this journey would have been so much more difficult, if not impossible. Also: thank you to my friends, in particular, Dawn and Ellie, for helping with childcare and always being available when I needed a break. And thank you to both my sisters; to Melda for making me feel closer to home; and to Finda for her proof-reading help.

I would like to remember two very special people who passed away during my PhD: Lizzie was a wonderful, enthusiastic friend and colleague and is still greatly missed. My father, David, was probably one of the few retired people without a scientific background who enjoyed reading books on genetics and biology and I cherish the support and encouragement he gave me.

Table of Contents

Figures and Tables

Abbreviations

amino acids	aa
Acquired Immunodeficiency Syndrome	AIDS
Bam HI-A rightward transcript	BART
B-cell receptor	BCR
Burkitts lymphoma	BL
basepairs	bp
Zta basic region domain mutant	BZta
CCAAT/enhancer binding protein α	C/EBPα
chloramphenicol acetyltransferase	CAT
cyclin dependent kinase	cdk
Cyclin Dependent Kinase	CDK
Cercopithecine herpes virus 15	Ce-HV15
Cytomegalovirus	CMV
methylated cytosine	Cp
carboxyl-terminus	CT
Zta CT domain mutant	CTZta
EBV Encoded RNA	EBER
Epstein-Barr Nuclear Antigen	EBNA
Epstein Barr Virus	EBV
enzymatic chemiluminescence	ECL
Electrophoretic Mobility Shift Assay	EMSA
Fluorescence Activated Cell Sorting	FACS
Fold Difference	FD
glycoprotein	gp
histone acyl transferases	HAT
Hodgkin's Disease	HD
Histone deacetylase 1	HDAC1
Human epithelial kidney	HEK
Human Herpes Virus	HHV
6x-histidine	his
Human immunodeficiency virus	HIV
Hodgkin's Lymphoma	HL
Hodgkin and Reed-Sternberg cells	HRS
Herpes simplex virus	HSV
immediate early	IE
immunoglobulin	Ig
Infectious mononucleosis	IM
interferon	INF
in vitro translation	IVT
Kilodalton	kDa
Kaposi's sarcoma-associated herpesvirus	KSHV
Lymphocryptovirus	LCV
Latent Membrane Protein	LMP
micro-RNAs	miRNAs
Nasopharyngeal Carcinoma	NPC
Origin of lytic replication	oriLyt

origin of plasmid replication	oriP
Phosphate-Buffered Saline	PBS
Proliferating Cell Nuclear Antigen	PCNA
Polymerase Chain Reaction	PCR
propidium iodide	PI
Post-transplant lymphoproliferative disease	PTLD
Quantitative Polymerase Chain Reaction	QPCR
retinoic acid receptor	RAR
Rhesus Macaque LCV	RhLCV
RhLCV BRLF1	RhRp
BRLF1 promoter	Rp
R transactivator	Rta
S-adenosyl homocysteine	SAH
S-adenosyl methionine	SAM
sodium dodecyl sulphate	SDS
SDS-Polyacrylamide Gel Electrophoresis	SDS-PAGE
Simian-human chimeric immunodeficiency virus	SHIV
ski protein	SKIP
transforming growth factor β1	TGFβ1
the tumour necrosis factor	TNF
terminal repeat regions	TR
TNF receptor activated death domain protein	TRADD
TNF receptor activated family	TRAF
Varicella Zoster virus	VSV
X-linked lymphoproliferative disease	XLP
Zta coiled coil domain mutant	ZipZta
BZLF1 promoter	Zp
Zta Response Element	ZRE

Abstract

Epstein Barr Virus (EBV) is a γ-herpesvirus infecting around 95% of the human population. EBV infection is life-long and asymptomatic in the majority of individuals, however EBV is associated with Nasopharyngeal Carcinoma, Burkitt's lymphoma and Hodgkin's lymphoma. The transcription factor Zta is an immediate early gene of EBV able to reactivate the virus from latency, cause cell cycle arrest and bind to sequence specific DNA elements. Cercopithecine herpesvirus-15 is a closely related virus, infecting rhesus monkeys, with a homologue to Zta; ZtaRh. A comparison of features of these proteins may be informative about critical residues in each protein. Binding to almost all response elements is conserved between the two proteins. A Zta response element (ZRE3Rh) in the CeHV-15 Rta gene promoter that is not functional for either protein was identified. ZRE3 from EBV is methylation dependent for Zta binding. Analysis of ZRE3 using competition EMSA assays has shown the importance of methylation of individual CpG motifs. ZtaRh is compromised in reactivating EBV from latency and this appears to be mediated by changes at the extreme C-terminus. ZtaRh is unable to cause G1 cell cycle arrest, however this function maps to the transactivation domain. Known binding partners of Zta were cloned to enable investigation of binding by ZtaRh or other mutants. Co-transfection of p53 and Zta resulted in rapid degradation of both proteins. Co-transfection of C/EBPα and Zta produced a larger additional Zta species. Neither effect was seen with a Zta CT mutant. RNA from HEK293-ZKO cells transfected with Zta or a C-terminal Zta mutant was analysed using a QPCR array probing 595 human genes associated with cancer, revealing possible host cell proteins influenced by Zta. Further information on the precise mechanisms of Zta could contribute to the development of future therapies for the prevention or treatment of EBV related diseases.

Chapter 1 Introduction

1.1 Introduction to Herpes viruses

Herpesviridae are a family of enveloped, doubled stranded DNA viruses. This type of virus can cause both latent and lytic infection, enabling a life-long infection of the host (Roizman and Baines, 1991). There are around 90 species of herpesviridae that infect many types of animals. There are 8 herpes viruses that infect humans including herpes simplex I and II, cytomegalovirus and Epstein Barr Virus (Table 1.1). All these viruses are capable of causing disease in humans including chicken pox (Varicella zoster virus), oral and genital herpes (herpes simplex virus 1 and 2) and Kaposi's sarcoma (Kaposi's sarcoma-associated herpesvirus). Herpes viruses are classified into 3 sub-families generally according to the location during latency. Alpha herpes viruses are situated in neurons during latency, beta herpes viruses in T lymphocytes and other cells and gamma herpes viruses reside in lymphocytes. Although this criteria is not strictly accurate, for example Roseolovirus is a beta herpes virus but can latently infect lymphocytes, this classification is supported by nucleotide and protein homology (Davison, 2002).

HHV	Name	Sub Family	Target cell type	Main Disease Associations
1	Herpes simplex-1 (HSV-1)	Alpha	Mucoepithelia	Oral and genital herpes, Herpes keratitis
2	Herpes simplex-2 (HSV-2)	Alpha	Mucoepithelia	Genital and oral herpes
3	Varicella Zoster virus (VZV)	Alpha	Mucoepithelia	Chickenpox, shingles
4	Epstein-Barr Virus (EBV)	Gamma	B lymphocyte, epithelia	Infectious mononucleosis, Nasopharyngeal carcinoma, Burkitts's lymphoma
5	Cytomegalovirus (CMV)	Beta	Epithelia, monocytes, lymphocytes	Cytomegalovirus-retinitis
6	Herpes lymphotropic virus	Beta	Lymphocytes	Roseola infantum
7	Human herpes virus-7 (HHV-7)	Beta	T lymphocytes	Roseola infantum
8	Kaposi's sarcoma- associated herpes virus (KSHV)	Gamma	Endothelial cells	Kaposi's sarcoma

Table 1.1: Human herpes viruses (HHV)

1.1.1 Gamma herpes virus

The gamma herpesviridae contains two genera; the Lymphocryptoviruses, including Epstein Barr Virus (EBV), and the Rhadinoviruses, including Kaposi's sarcoma associated herpesvirus (KSHV). EBV and KSHV are the two gammaherpes viruses that infect humans. KSHV is a causative agent for Kaposi's sarcoma which generally occurs in immunocompromised patients (Moore and Chang, 1995). Gammaherpes viruses infecting other species are also associated with cancer including porcine gammaherpesvirus infecting pigs (Ehlers *et al.*, 1999). The Rhadinovirus Herpesvirus saimiri causes T cell lymphomas in several monkey species except the natural spider monkey host (Fickenscher and Fleckenstein, 2001).

1.2 Epstein Barr Virus

1.2.1 Identification of EBV

In Uganda in 1958 Denis Burkitt identified a type of lymphoma that caused jaw tumours in children (Burkitt, 1958), and reviewed in (Thompson and Kurzrock, 2004). The distribution of Burkitt's lymphoma was distinctive climatically and geographically. Subsequent work by Anthony Epstein, Yvonne Barr and Bert Achong identified virus particles in tumour samples using electron microscopy (Epstein *et al.*, 1965). This virus was called Epstein Barr Virus. Detection of the virus in DNA in the lymphomas and experimental induction of tumours in monkeys established EBV as the first virus identified as causing human tumours (Epstein *et al.*, 1965).

1.2.2 EBV Background

EBV (human herpes virus 4) belongs to the genus lymphocryptovirus (LCV). EBV infection is usually transmitted through salvia contact. Infection of young children is generally asymptomatic, however primary infection in young adults can cause infectious mononucleosis. This delayed infection and resultant infectious mononucleosis is more prevalent in developed countries. In both cases a lifelong latent infection of B cells is established, which is present in about 95% of adults (Thompson and Kurzrock, 2004). In healthy carriers the pathological effects of the virus are controlled by the immune system so infection is asymptomatic and the virus persists. Other diseases, including nasopharyngeal carcinoma and Hodgkin's and non-Hodgkin's

lymphomas, are associated with EBV in patients with compromised immune systems. This is covered in more detail in section 1.3. There are 2 sub-types of EBV; EBV-1 and EBV-2. The major differences between the sub-types are in the nuclear protein genes EBNA2, EBNA3A, EBNA3B and EBNA3C which vary between the strains by 16% - 47% in protein sequence (Sample *et al.*, 1990). EBV-1 is more efficient at transforming B-cells *in vitro* and is the more prevalent sub-type in most populations. However the incidence of EBV-2 is increased in populations with endemic Burkitt's lymphoma including equatorial Africa and New Guinea (Young *et al.*, 1987).

1.2.3 EBV Structure

EBV has a double-stranded DNA core within an icosahedral nucleocapsid, surrounded by a protein tegument and encased in an outer envelope covered in glycoprotein spikes (Figure 1.2). The glycoprotein spikes include gp350/220, which is required for virus entry into B cells. Gp350/220 binds with high affinity to the complement receptor type 2 (CD21, CR2) on B cells (Nemerow *et al.*, 1987).

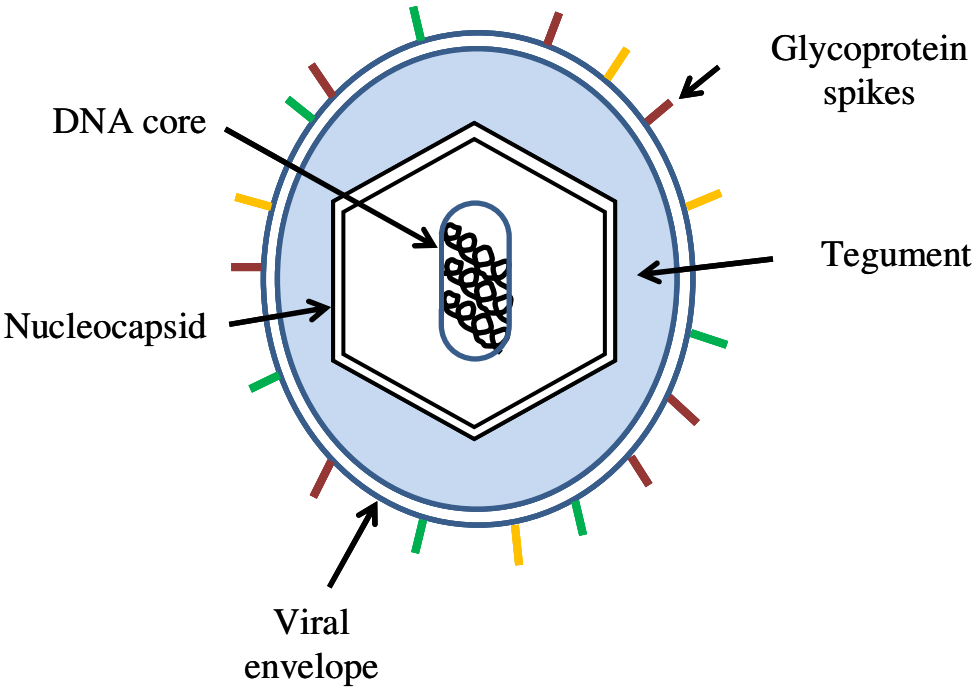

Figure 1.2: Basic structure of Epstein Barr virus and other herpes viruses

The EBV genome is approximately 172 kbp long and contains over 85 protein encoding genes (Thompson and Kurzrock, 2004), NCBI). The genome contains terminal repeat regions (TR) at both ends as well as tandem internal repeat sequences (Kieff and Rickinson, 2007). Upon infection the terminal repeats anneal together in the nucleus of the infected cell to form a viral episome. The genome is maintained as an episome during the latent cycle, replicating once during each cell division. The EBV genome contains 3 distinct origins of replication; the origin of plasmid replication, OriP, is utilised during episome replication. During the replicative lytic cycle, the origin of lytic replication, oriLyt, is used for rolling circle replication. There are 2 copies of oriLyt in most strains of EBV. The multiple genome DNA molecules are cut into genome lengths at the TR and then packaged and released from the cell (Kieff and Rickinson, 2007).

1.2.4 EBV Infection

Primary infection of EBV commonly occurs through salivary contact (Niederman *et al.*, 1976) and occurs in the tonsillar area known as the oropharynx. In the course of infection, both lymphocytes and epithelial cells are infected. However in the process of this infection it is unclear whether the initial infection occurs in circulating B-lymphocytes in the lymphoepithelium of Waldeyers ring or in tonsillar epithelial cells. If the virus does not initially infect epithelial cells then the host epithelial membrane must be crossed to access B cells, either through physical wounds or leakiness from inflammation (Shannon-Lowe and Rowe, 2011).

Lytic replication in oral epithelial cells has been observed in both oral hairy leukoplakia lesions from AIDS patients (Greenspan *et al.*, 1985) and more recently in epithelial tongue cells in viral carriers (Herrmann *et al.*, 2002). However patients with B-Cell deficient X-linked agammaglobulinemia, who lack mature B-cells, appear to be resistant to EBV infection, which implies that the oral epithelial infection requires B-cell involvement (Faulkner *et al.*, 1999). *In vitro* experiments have shown that infection of epithelial cells is 1000 times more efficient when the virus is associated via gp350 to CD21 of a B-cell (Shannon-Lowe *et al.*, 2006). This demonstrates that association of EBV with B-cells may be important for both B-cell and epithelial infection (Shannon-Lowe and Rowe, 2011).

Attachment of the virus to both B-cells and epithelial cells occurs through interactions between different viral glycoproteins and human cell surface proteins.

The EBV gp350/220 membrane glycoprotein attaches to the CD21 receptor on the B lymphocyte surface (Nemerow *et al.*, 1985). This interaction causes cross-linking of CD21 and a series of events including tyrosine kinase activation, increased mRNA synthesis and expression of IL-6 and surface CD23 (reviewed in (Thompson and Kurzrock, 2004). This results in delivery of the now uncoated viral genome to the nucleus. Here the linear DNA circularises into an episome and the latent cycle commences (Figure 1.3).

The EBV proteins gH and gL associate and may operate as a ligand to epithelial cells (Molesworth *et al.*, 2000), although the receptor has not been identified. In addition the EBV protein BMRF2 is a ligand to several integrins and appears to be important for infection in polarized epithelial cells (Tugizov *et al.*, 2003). Fusion of the viral envelope to both cell types requires the core fusion machinery which is composed of three viral proteins gH, gL and gB (Spear and Longnecker, 2003).

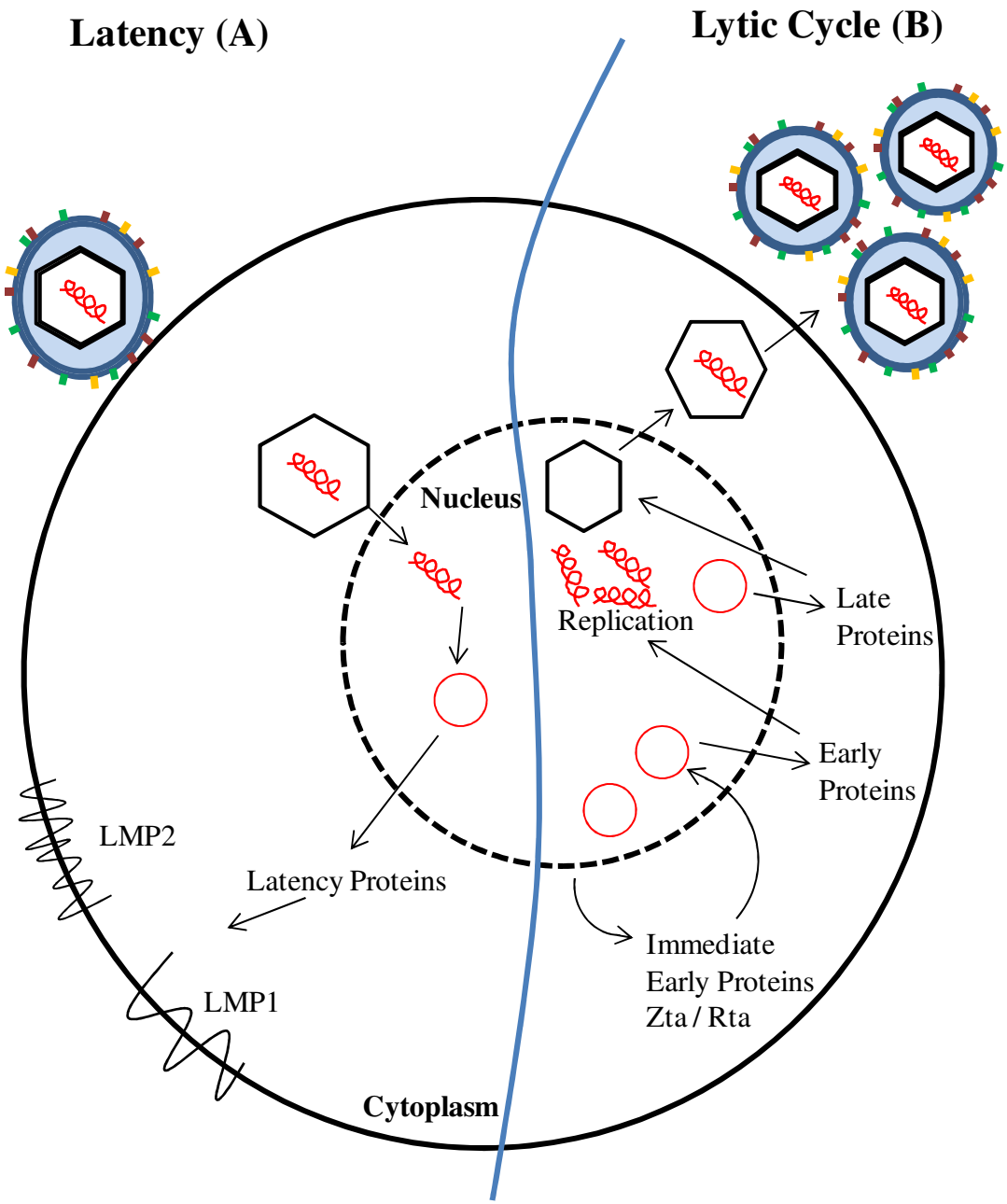

Figure 1.3: Infection of a B lymphocyte by EBV
The glycoprotein gp350/220 binds to the cell surface receptor CD21 on the B lymphocyte surface. EBV can then penetrate the cell via endocytosis and the viral genome circularises in the nucleus. EBV can then establish a latent infection (A), expressing only a few genes including Latent Membrane Proteins (LMPs). Alternatively the lytic cycle program (B) leads to the production of new virions. This diagram was adapted from http://www2.ujf-grenoble.fr/pharmacie/laboratoires /gdrviro/groupedrouet/archive/2003/recherche.html

1.2.5 Latency

1.2.6 Establishment of Latency in B cells

For viral persistence in the host, the viral genome must be maintained in host cells that avoid death and evade immune responses while activating cellular proliferation pathways (Thompson and Kurzrock, 2004). The actions of the genes expressed after infection increase host cell survival and proliferation. These circumstances could contribute to the association of EBV and cancer. Infected B-lymphocytes are triggered to proliferate, entering S-phase 24 - 48 hours post infection (Rowe, 1999).

In a similar manner to other herpesviruses, EBV maintains a lifelong infection in the host cell. One or more episomal copies of the viral genome are maintained in the nucleus. As the host cell replicates, the episomes also replicate once each cell division, using the host cell machinery. This period of the viral lifecycle is called latency. At this stage there is a much restricted pattern of viral gene expression. The genes involved are listed below:

6 EBV Nuclear Antigens (EBNA 1, 2, 3A 3B, 3C and LP)
3 Latent Membrane Proteins (LMP 1, 2A, 2B)
2 small non-coding EBV RNAs – (EBER 1 and 2)
Bam HI-A rightward transcripts - (BARTs)
27 micro-RNAs (miRNAs)
(Swaminathan, 2008)

There are 4 distinct patterns of EBV latent gene expression observed in infected lymphocytes, with a subset of the genes expressed in different cells and malignancies. Quiescent memory B-cells express a latency 0 profile. The non-protein-coding genes are expressed in latency 0 but the 9 protein-coding latent genes are not (Table 1.4). The other 3 expression profiles, latency I, II and III, are identified in cells during different disease states as detailed in Table 1.4.

	0	I	II	III
Cell Type	Quiescent B-cell	BL	HD NPC	IM PTLD
Promoter		Qp	Qp	Wp/Cp
EBNA-1	-	+	+	+
EBNA-2	-	-	-	+
EBNA-3A, 3B, 3C	-	-	-	+
EBNA-LP	-	-	-	+
LMPs	(LMP2A) +	(LMP2A) +	+	+
EBERs	+	+	+	+
BARTs	?	+	+	+
miRNAs	?	+	+	+

Table 1.4: Expression profiles of Latency 0, I, II and III
Expression profiles are shown for Latency 0 (Quiescent memory B-cells), I (Burkitt's Lymphoma (BL) cells), II (Hodgkin's Disease (HD) and Nasopharyngeal Carcinoma (NPC) cells) and III (Infectious mononucleosis (IM) and post-transplantation lymphoproliferative disease (PTLD). Expression (+) of the protein / RNA or not (-) is shown. Expression of BARTs and miRNAs in latency 0 is unknown.

1.2.7 EBNAs

EBNA1 is a phosphoprotein that binds to DNA in a sequence specific way. It is required for replication and maintenance of the viral genome so is key to maintaining the latent infection of EBV (Middleton and Sugden, 1994). Viruses lacking a functional EBNA1 are unable to establish a latent infection in B-cells (Lee *et al.*, 1999).
EBNA1 is expressed in all three disease associated latent states, being transcribed by the Qp promoter in latency I and II and by the Wp and Cp promoters in latency III (Figure 1.5). At the origin of plasmid replication (OriP) there are 2 EBNA1 binding elements, both composed of multiple 18bp EBNA1 binding sites. The Family of Repeats site contains 20 EBNA1 binding sites and the dyad symmetry site contains 4 (Wysokenski and Yates, 1989). Binding to these sites initiates plasmid replication. The promoter Qp is key to maintaining levels of EBNA1 in the cell and is subject to a negative auto-regulation feedback system by EBNA1 binding to 2 downstream binding sites (Sample *et al.*, 1992).

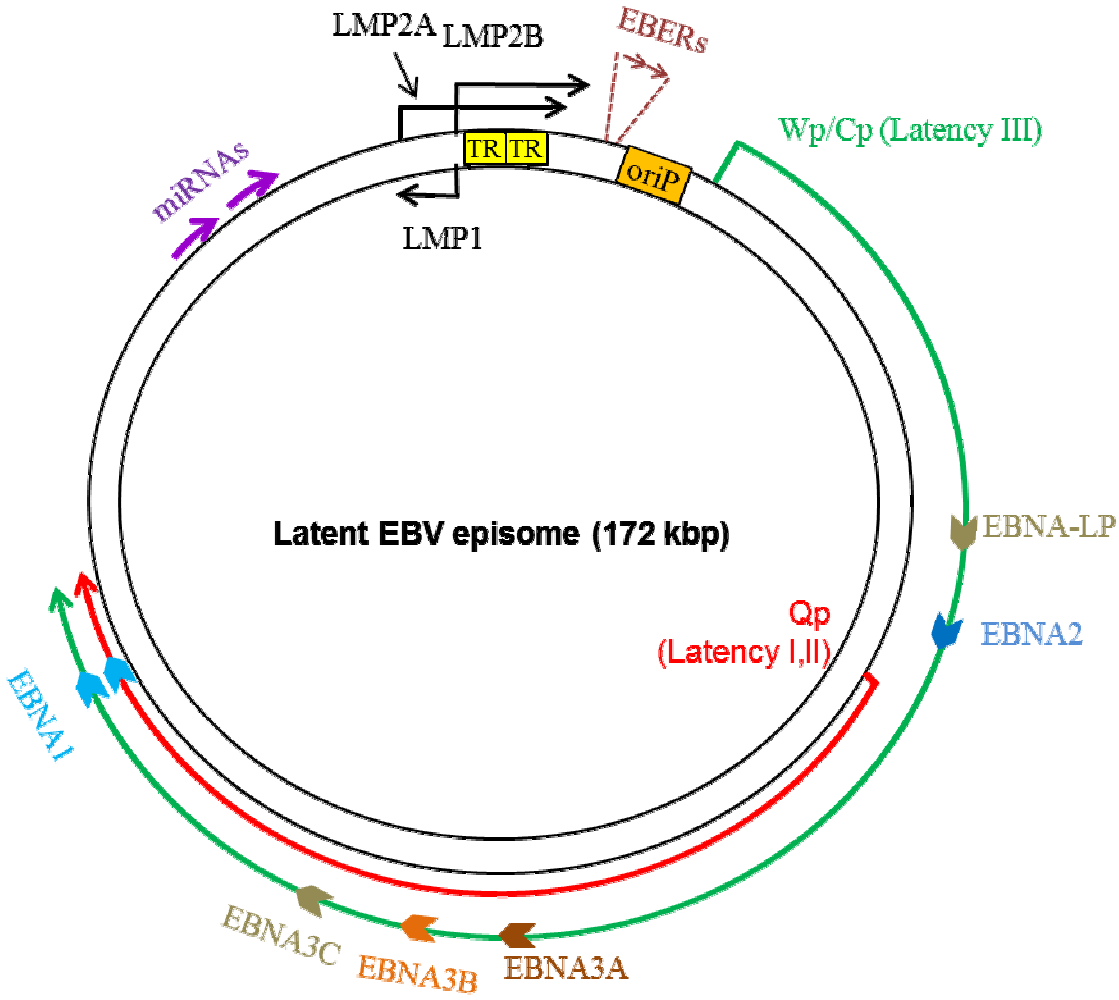

Figure 1.5: Schematic Diagram of the Latent EBV genome
Following entry into the nucleus, the linear EBV genome forms an episome through the ligation of the terminal repeats (TR). Transcription of the latent membrane proteins LMP1, LMP2A and LMP2B are shown as black arrows. LMP2A and LMP2B are composed of multiple exons located either side of the TR region. The green arrowed line represents transcription during latency III, when all the EBNAs are transcribed from either the Cp or Wp promoter. The red arrowed line represents transcription from Qp during latency I and II encoding EBNA1 only. Purple arrows indicate the two clusters of BART miRNAs. (Diagram adapted from (Murray and Young, 2001))

EBNA1 also assists EBV in immune system evasion. A series of glycine-glycine-alanine repeat sequences within the protein disrupt ubiquination and proteosomal degradation of EBNA1. This prevents MHC class I antigen presentation of fragments of EBNA1 at the cell surface to the immune system. (Levitskaya *et al.*, 1997).

EBNA2, along with EBNA-LP, is one of the first genes detected upon infection of a primary B-cell, being detected within 12 to 16 hours of EBV infection (Alfieri *et al.*, 1991). It has a key role in B-cell transformation as demonstrated by Cohen and colleagues with an EBV strain lacking EBNA2 that was unable to transform B-cells (Spear and Longnecker, 2003).

EBNA2 is an indirect transcriptional activator of both cellular and viral genes. Initiated by the promoter Wp, EBNA2 is a transcriptional activator of the Cp promoter. The Cp promoter is in turn responsible for the expression of most latent EBV proteins (Young and Rickinson, 2004). EBNA2 operates through interaction with transcription factors such as the cellular RBP-Jκ (Recombining Binding Protein suppressor of hairless) (Waltzer *et al.*, 1994). In the absence of EBNA2 , Cp activation is repressed through RBP-Jκ binding with a co-repressor complex, also including Histone deacetylase 1 (HDAC1) and the ski-interacting protein (SNW1, SKIP) (Waltzer *et al.*, 1995; Zhou *et al.*, 2000). EBNA2 interacts with the chromatin remodelling protein hSNF5/Ini1, disrupting the nucleosome and allowing transcriptional machinery access to the Cp promoter. Cellular genes upregulated by EBNA2 include CD23, a cell surface marker of activated B-cells, the proto-oncogene c-myc and the EBV receptor, CD21 (reviewed in (Young and Rickinson, 2004)).

The other gene expressed early in EBV infection is EBNA-LP (leader protein or EBNA5). Together EBNA2 and EBNA-LP can push quiescent B-cells from G0 to G1 of the cell cycle. This is achieved by inducing cyclin-D2 (Sinclair *et al.*, 1994) and possibly through interaction with p53 and Rb (Szekely *et al.*, 1993). EBNA-LP varies in size due to exon skipping, resulting in a variable number of W repeats (reviewed in (Rowe, 1999)).

The EBNA3 family is comprised of 3 proteins; EBNA3A, EBNA3B and EBNA3C. They are encoded by three adjacent genes in the viral genome. All three are transcriptional regulators with EBNA3A and EBNA3C being critical for B-cell transformation (Tomkinson *et al.*, 1993). All three EBNA3 proteins interact with RBP-Jκ, inhibiting binding to transcriptional targets, including inhibition of the EBV Cp promoter (Waltzer *et al.*, 1996). This has the effect of repressing EBNA2 activity. In addition EBNAC3 interacts with histone deacetylase 1 (HDAC1) along with RBP-Jκ which results in chromatin remodelling at Cp (Radkov *et al.*, 1999).

1.2.8 LMPs

The three latent membrane proteins, LMP1, LMP2A and LMP2B are transmembrane proteins.

LMP1 contains 6 transmembrane domains and a cytoplasmic tail. It is essential for the proliferation of EBV infected B-cells (Kilger *et al.*, 1998). LMP1 is a constitutively active receptor that mimics CD40 in a ligand-independent manner (Gires *et al.*, 1997). CD40 is an important cell surface marker for B-cells that have been activated by antigen, with roles in proliferation and differentiation. Two regions in the cytoplasmic tail of LMP1 bind to members of the tumour necrosis factor (TNF) receptor activated family (TRAFs) and to TNF receptor activated death domain protein (TRADDs). As LMP1 lacks kinase activity these proteins act as adaptor proteins to activate the NFκB signalling pathway (Huen *et al.*, 1995). The transcription factor NFκB has a key cellular role in the regulation of cell growth and apoptosis. It can induce expression of cytokines including lymphotoxin, an autocrine growth factor for transformed B-cells by binding to the respective promoter (Thompson *et al.*, 2003). In addition LMP1 influences other signalling pathways, including the JAK/STAT pathway which can be activated by LMP1 interacting with JAK3 (Gires *et al.*, 1999). LMP1 also exhibits the ability to inhibit apoptosis through elevation of Bcl-2 levels (Rowe *et al.*, 1994). Through a combination of these actions LMP1 is closely implicated in oncogenesis with EBV in latency II and III such as Hodgkin's Disease and Nasopharyngeal carcinoma.

The gene LMP-2 encodes the two proteins, LMP-2A and LMP-2B, which are not essential for B-cell immortalisation (Rochford *et al.*, 1997). The 2 proteins differ in the NH_2-terminal domain. Exon 1 LMP-2A contains a 118 amino acid cytoplasmic

domain, containing an immunoreceptor tyrosine-based activation motif. This domain is missing from LMP-2B. This domain of LMP-2A is functional in the prevention of activation of the lytic cycle by inhibiting the signal transduction from immunoglobulin cross-linking of the B-cell receptor (Fruehling and Longnecker, 1997). This effect may be modulated by LMP-2B, although the exact role of LMP-2B is unclear.

1.2.9 EBERs

EBER1 and EBER2 are non-polyadenylated, non-coding RNAs of 167 and 172 nucleotides and are found in all stages of latency (reviewed in (Thompson and Kurzrock, 2004). They are the most abundant RNAs in most EBV cells, often with more than $5x10^6$ copies per cell (Lerner *et al.*, 1981). The EBERs have been shown *in vitro* to bind to the cellular Protein kinase R (PKR) and inhibit its activity in translational inhibition and apoptosis (Clarke *et al.*, 1990). However it is unclear if this effect is replicated *in vivo*, mainly as EBERs are localised to the nucleus and PKR is cytoplasmic. EBERs interact with the autoantigen La and ribosomal protein L22. La enhances the stability or translation of mRNAs and L22 forms part of the large ribosomal subunit which binds RNA. EBER binding to these proteins causes nuclear sequestering, however there is not significant depletion of L22 from the ribosomes and La levels also remain high (Swaminathan, 2008). Komano and colleagues have shown that both EBERs can confer apoptotic resistance via bcl-2 induction in Burkitt's lymphoma cells, promoting their survival (Komano *et al.*, 1999). It is possible that EBERs act as a transcriptional regulator to protect EBV under *in vivo* stress conditions (Swaminathan, 2008). The precise role of these RNAs in EBV latency is not yet clear but the ubiquitous expression and evolutionary conservation suggest an important function.

1.2.10 BARTs

BamHI-A rightward transcripts (or complementary strand transcripts) are spliced RNAs with a common 3' open reading frame and a poly-adenylation site. They are present in many EBV infections and especially prevalent in NPC cells. It is unclear if protein products of these transcripts exist. Predicted products can modulate both RBP-Jκ and its interaction with EBNA-2 and the Notch pathway through RAK (Smith *et al.*, 2000; Zhang *et al.*, 2001).

1.2.11 miRNAs

Micro RNAs (miRNAs) are small non-coding RNAs approximately 22 nucleotides long. MiRNAs modulate translation by inhibiting translation or promoting degradation of mRNAs through incorporation into a RNA-inducing silencing complex (RISC) as well as binding directly to complementary sequences in the genome (reviewed in (Bartel, 2004)).

In EBV, miRNAs are encoded in the *Bam*HI A region of the genome (BART miRNAs) and from the *Bam*HI H region (BHRF1 miRNAs). Expression or miRNAs varies markedly between cell types. In NPC cells BART miRNAs are strongly expressed, while BHRF1 miRNAs are not detected. Transformed B cells preferentially express BHRF1 miRNAs. In latency III under Cp or Wp promoter activity BHRF miRNAs are thought to originate from splicing of the EBNA transcripts (Swaminathan, 2008). Possible targets of the EBV miRNAs include IFN-inducible T-cell attracting chemokine CXCL-11 which may result in host inhibition of the interferon response (Xia *et al.*, 2008). In addition the miRNAs may target at least 2 EBV genes, BALF5 and LMP1 (Swaminathan, 2008).

1.2.12 Latency Types

In a healthy EBV carrier there is a low stable proportion of infected B-lymphocytes of about 1-50 in 10^6 cells (Wagner *et al.*, 1992). These cells are in latency 0 and express a highly restricted range of latent viral genes. In order to achieve this state, a newly infected B-lymphocyte must progress through different stages of latent gene expression as shown in Figure 1.6. This mimics the activation of B-cells by antigen, also resulting in production of memory B-cells (reviewed in (Thorley-Lawson and Gross, 2004).

After EBV infection or antigen activation, B-cells cluster at the germinal centre of the lymph nodes where proliferation and differentiation occur (Macsween and Crawford, 2003). Upon initial infection, EBV initiates a latency III or growth pattern of gene expression, during which all the latent genes are expressed (Table 1.4). This induces cell proliferation and induction of the B-cell activation markers including CD23. EBV has the ability to transform or immortalise B-lymphocytes so that they continue to proliferate, expanding the pool of circulating EBV positive memory B-cells. EBNA-2, EBNA-3A, EBNA-3C and LMP1 are essential for transformation.

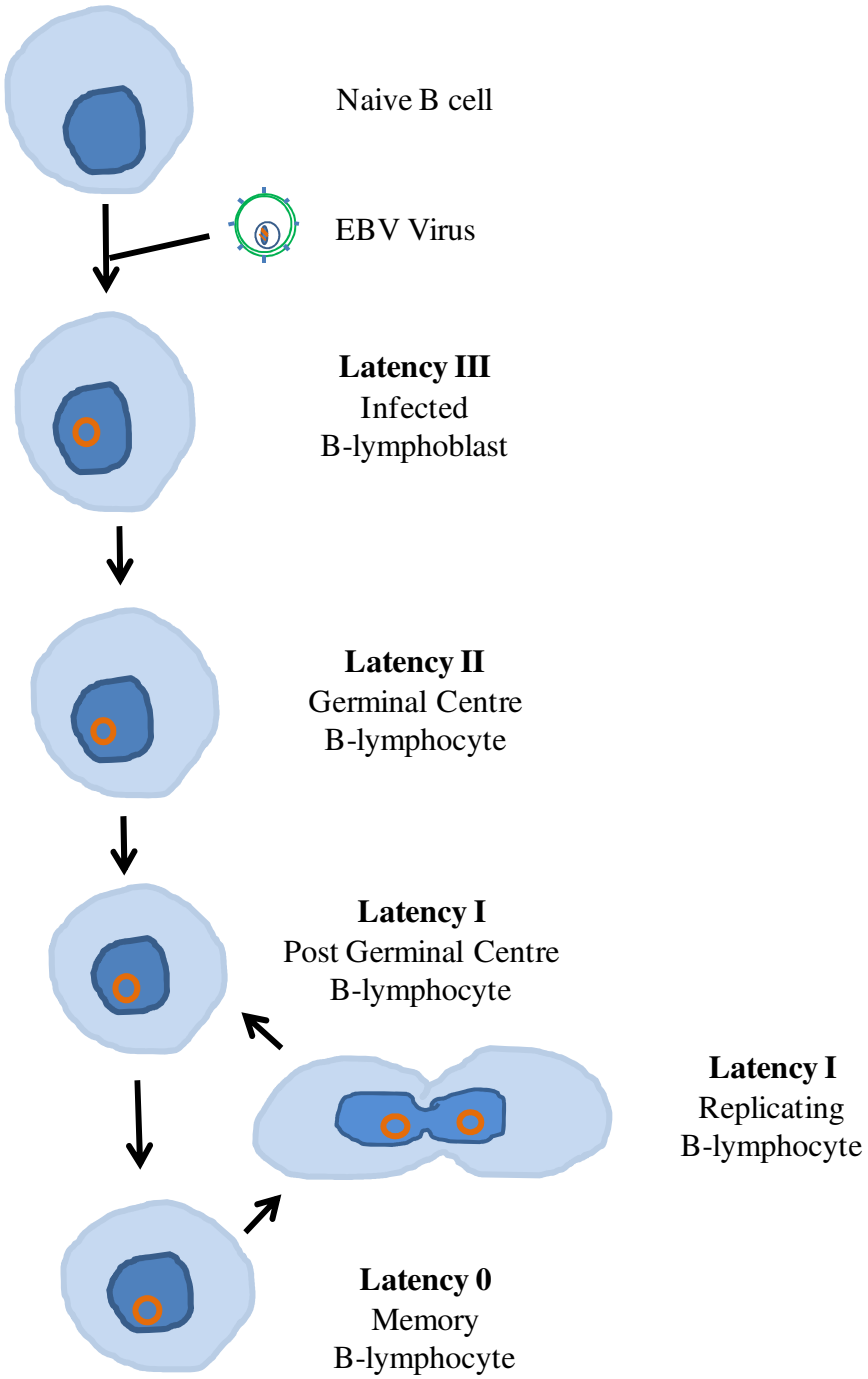

Figure 1.6: Steps in establishment and maintenance of EBV infection in B-cells
Naive B-cells are infected by EBV and activation of the latency III program activates cells to become proliferating lymphoblasts. In the germinal centre differentiation under latency II occurs to produce a memory B-cell. During replication of the memory B-cell a switch to latency I occurs, expressing EBNA1 to enable replication of the viral episome. (adapted from (Thorley-Lawson and Gross, 2004))

An antigen activated B-cell in the germinal centre is protected from apoptosis by the action of antigen-specific helper T-cells. To avoid apoptosis, an EBV infected cell must substitute these rescue signals by the action of genes expressed during latency II. This pattern of expression of EBNA1 and the LMPs is also seen in Hodgkin's disease and nasopharyngeal carcinoma.

On exit from the germinal centre and entry into the peripheral circulation, expression of all protein coding genes is shut down. During the occasional division of an EBV positive memory B-cell, a latency I pattern of expression is enacted to express EBNA1 and allow concerted replication of the episome. Latency I is also observed in Burkitt's lymphoma cells (Niedobitek *et al.*, 1995).

1.3 EBV Associated diseases

EBV was first discovered through association with Burkitt's lymphoma and has since been linked with several other diseases and cancers (Figure 1.7). In order for EBV to be oncogenic it must fulfil four criteria;

i. Maintain viral genome in host cell
ii. Not destroy the cell
iii. Prevent cell from becoming a target of the immune system
iv. Activate cellular growth pathways

A person is vulnerable to EBV associated malignancies when the host immune system is suppressed such as in patients with AIDS or immunosuppression following organ transplantation.

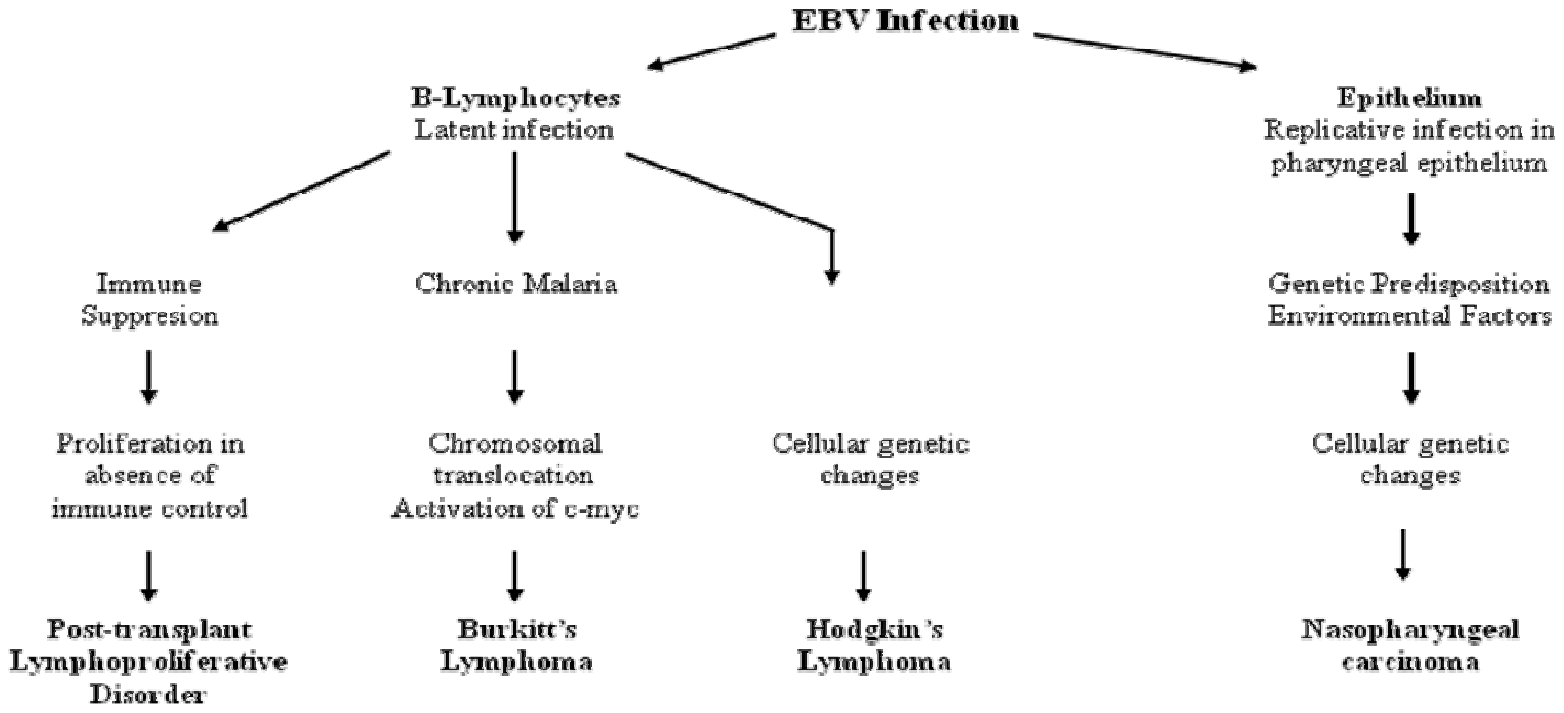

Figure 1.7: Diagram of Cancer development and EBV
Modified from (http://info.cancerresearchuk.org/cancerstats/causes/infectiousagents/epsteinbarrvirus/)

1.3.1 Infectious Mononucleosis

Infectious mononucleosis (IM) or glandular fever is normally caused by delayed primary EBV infection of adolescents and young adults. It is characterised by fever, pharyngeal inflammation and enlarged lymph nodes and spleen. IM is rare in the developing countries as primary infection in these areas occurs almost universally in early childhood. A causative link to EBV was established in 1968 (Henle *et al.*, 1968). In IM, as in normal primary infection, EBV infected cells proliferate, progress through the germinal centre and mature into memory B-cells. During IM up to 50% of the memory B-cells may be infected with EBV (Hochberg *et al.*, 2004).
The immune response in IM is characterised by an increased proportion of lymphocytes (lymphocytosis), in particular CD8+ cytotoxic T cells. This enables lysis of infected B-cells but is also responsible for IM symptoms due to the release of high levels of cytokines including IL2 and INFγ (Foss *et al.*, 1994). There is a correlation between the level of T cell activation and clinical severity of IM (Williams *et al.*, 2004). During this initial phase of infection B-cells display a latency III gene expression profile. This is followed by latency II expression, which produces a much lower immune response in the patient (Williams and Crawford, 2006).

In most cases symptoms diminish after 4-6 weeks but relapses can occur for up to 12 months. During this period the level of EBV+ memory B cells may remain higher than in a normal carrier (Vetsika and Callan, 2004).

1.3.2 X-linked lymphoproliferative disease

X-linked lymphoproliferative disease (XLP) is a rare X-linked genetic condition with a mutation in the gene Signalling Lymphocytic Activation Molecule (SLAM) - Associated Protein (SAP) (Sayos *et al.*, 1998). SAP is a cytoplasmic signal transduction molecule that is expressed in activated T cells and NK cells. The transmembrane glycoprotein SLAM, which is member of the Ig superfamily, is expressed on T, B and dendritic cells. Levels are upregulated on activated CD4+ and CD8+ T cells and binding by specific antibody leads to proliferation of T cells and production of cytokines including INFγ (Garcia *et al.*, 2001). Binding of SAP to SLAM inhibits production of INFγ. An absence of functional SAP results in deregulation of the host immune response to viral infection. XLP patients develop severe and often

fatal IM-like responses to EBV infection with an uncontrolled proliferation of cytotoxic T cells, resulting in hepatic necrosis and bone marrow failure (reviewed in (Williams and Crawford, 2006)).

1.3.3 Post Transplant Lymphoproliferative disease

Post Transplant Lymphoproliferative disease (PTLD) is a proliferation of B-lymphocytes which may occur following organ transplantation. To ensure immune acceptance of the transplanted organ the cytotoxic T cell response of host immune system is suppressed by drugs. The lack of a complete T cell response to EBV infection allows abnormal proliferation of EBV+ B lymphocytes, normally expressing a latency III type infection (reviewed in (Williams and Crawford, 2006)). This often presents as a single clonal lesion. The level of immunosuppression the patient receives is a major risk factor for PTLD. As this varies with the type of organ transplanted, the incidence of PTLD varies widely (Williams and Crawford, 2006). PTLD can occur in up to 33% of patients who have received a multi-organ transplant but less than 1% of stem cell transplant recipients. 50% of PTLD occurs as a result of primary EBV infection and this is more common in children as they are more likely to be EBV naive at transplantation (Ho *et al.*, 1985). A similar tumour is seen in late-stage AIDS patients who have lost T cell control due to HIV infection.

1.3.4 Nasopharyngeal carcinoma

Nasopharyngeal carcinoma (NPC) is a tumour arising from squamous epithelial cells in the post-nasal space. It has a high incidence in South East Asia and a moderate incidence in Southern and Northern Africa and Polynesia but is rare elsewhere in the world. There is also an increased prevalence in some populations including the Inuit population of North America and Greenland (Jemal *et al.*, 2011). 70% of NPC tumours are composed of undifferentiated cells and all these carcinomas are associated with EBV, demonstrating a type II latency pattern. LMP1 is potentially important in NPC development as it is expressed in most NPC cells, can inhibit differentiation of squamous epithelium and can induce tumours in animal models (reviewed in (Crawford, 2001)). Genetic and environmental factors are also considered to be important in NPC development (Chang and Adami, 2006).

1.3.5 Hodgkin's Lymphoma

Hodgkin's Lymphoma (HL) is characterised by the presence of large multinucleate Hodgkin and Reed-Sternberg (HRS) cells. It is the most common lymphoma in young people and there is a 3 fold increased risk of HL with a history of IM (Gutensohn and Cole, 1980). EBV is found in about 50% of HL cases in Western countries with a higher association in some developing countries (reviewed in (Crawford, 2001). The EBV genome is found in a subset of HRS cells, which express high levels of LMP1 in a latency II pattern. HRS cells originate from germinal centre B cells with Ig gene rearrangements and defective Ig transcription (Marafioti *et al.*, 2000). The presence of high levels of LMP1 may provide additional cellular proliferation and apoptosis resistance signals. The EBV genomes in HRS cells are monoclonal which suggests that EBV infection is an early event in development of the tumour (Anagnostopoulos *et al.*, 1989). Although there is evidence for an oncogenic role for EBV in HL the details are still unclear.

1.3.6 Burkitt's Lymphoma

Burkitt's lymphoma is an aggressive lymphoma with two types; endemic with EBV present and sporadic with an inconsistent association with EBV. Almost all BL tumours arising in Africa are endemic BL containing EBV but only approximately 20% of tumours in North America and Europe contain EBV (Crawford, 2001). Generally the EBV genome is found in the form of multiple nuclear episomes and in some instances with chromosomal integration. The genomes are clonal suggesting EBV infection occurs early in carcinogenesis. The only EBV gene expressed is EBNA1, along with EBERs, suggesting a latency I profile. Although the carcinogenic potential of this expression is questionable, lymphoid tumours have developed in EBNA1 transgenic mice (Wilson *et al.*, 1996) and bcl-2 induction by EBERs may provide an anti-apoptotic advantage (Komano *et al.*, 1999).

BL tumours all demonstrate one of three chromosomal translocations which brings the oncogene c-myc under the control of an Ig gene, resulting in constitutive expression. BL incidence is geographically associated with malarial regions. This may be due to continuous B-cell activation by chronic malaria infection which leads to a large number of EBV+, proliferating B-cells. This provides greater opportunity for a critical oncogenic translocation to occur. The translocations are different in endemic and non-endemic BL but it is not known if EBV has any causative effect on endemic

translocation (reviewed in (Thompson and Kurzrock, 2004)). The Akata Burkitt's lymphoma cell line is able to induce tumours in mice. However if EBV is lost from the Akata cell line it is not able to induce these tumours and decreased growth is observed. If Akata cells are re-infected with EBV, induction is re-established (Shimizu *et al.*, 1994).

1.4 Lytic Cycle

In common with other herpesviruses, the infection strategy of EBV consists of life-long latency in the host, punctuated at intervals by reactivation of the lytic cycle in a small proportion of the latently infected cellular population. This type of replication is needed for infection and propagation of the virus. Lytic reactivation probably occurs in latently infected memory B-cells that differentiate further as a response to antigen stimulation via binding to B-cell receptor (BCR) or as a result of stress (Amon and Farrell, 2005). The lytic cycle proceeds via staged expression of viral proteins, resulting in the production of infectious virions that enable the EBV genome to be transmitted to new hosts. The highly regulated reactivation process is initiated by the immediate early (IE) gene BZLF1 (Rooney *et al.*, 1989), which expresses Zta (Z, Zebra, EB1). Zta is essential for the reactivation of EBV from latency as cells with a BZLF1 knockout virus are unable to reactivate the lytic cycle (Feederle *et al.*, 2000). In addition transfection with short interfering RNA (siRNA) directed against BZLF1 renders cells defective in reactivation (Chang *et al.*, 2004). Zta auto-activates the Zta promoter (Zp) as well as the Rta promoter (Rp) of the BRLF1 gene (Feederle *et al.*, 2000). These two IE transcriptional transactivators co-operate to push the transition from latency to lytic cycle, triggering a gene expression cascade of over 80 EBV genes (Kenney *et al.*, 1989; Takada and Ono, 1989). The early genes encode proteins responsible for initiating viral DNA replication and include the viral DNA polymerase. This is followed by the expression of late genes which encode nucleocapsid and virion structural proteins. As EBV virions are shed from the host cell by budding, the lytic cycle does not necessarily lead to lysis of the host cell. Serological evidence has suggested that prior to the onset of NPC, Burkitt's lymphoma and Hodgkin's disease, there is reactivation of EBV lytic replication (Mueller *et al.*, 1989; Chan *et al.*, 1991) which suggests that the lytic cycle may contribute to the development of some EBV-associated diseases (Israel and Kenney, 2005).

The following section focuses on the structure and function of Zta, the product of the immediate early gene BZLF1.

1.4.1 Zta Structure

Zta is a member of the leucine zipper family of transcription factors (reviewed in (Sinclair, 2003).

Zta is a 245 amino acid protein, comprised of four distinct functional domains; an N-terminal transactivation domain, a basic DNA contact domain, a coiled-coil (zipper) dimerisation domain and a unique C-terminal domain (Figure 1.8A). The central basic and zipper domains form a long α-helix. This 35kDa protein operates as a homodimer *in vivo*.

The crystal structure of Zta bound to DNA has been determined (Petosa *et al.*, 2006) (Figure 1.8B). This reveals that unlike other bZip proteins, the C terminal domain folds back in an anti-parallel direction to the α-helix and interacts with the zipper domain. It is probable that this interaction has a stabilising effect on dimerisation and so is important for the function of Zta (Petosa *et al.*, 2006; Sinclair, 2006). The nine extreme C terminal amino acids are missing from the crystal structure so the full extent of the interaction is yet to be determined.

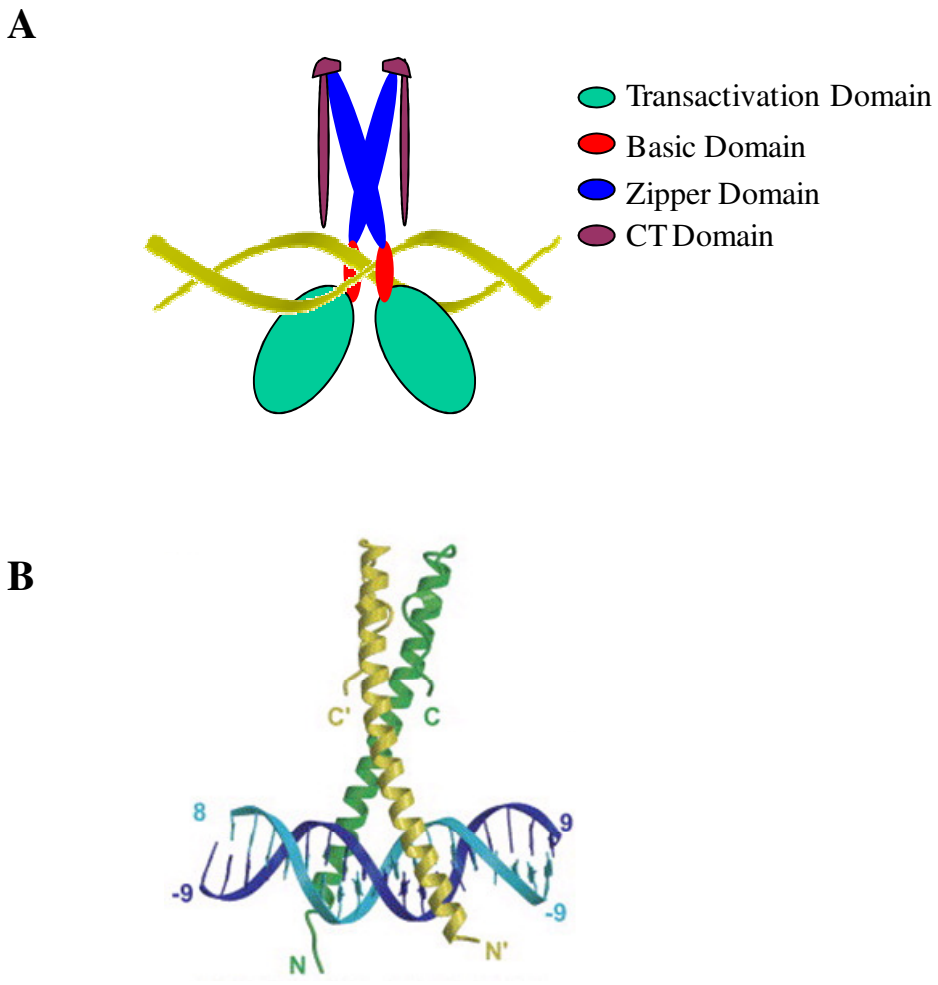

Figure 1.8: The structure of Zta
A shows a cartoon with the four domains of Zta, operating as a homodimer and in association with DNA (yellow). B shows the crystal structure of Zta, bound to a ZRE (Petosa *et al.*, 2006) This model does not include the N-terminal transactivation domain or the 9 extreme C-terminal residues.

Leucine zipper family members include C/EBPα, GCN4 and the transforming proteins c-fos, c-jun and c-myc. Alignment of these proteins shows a shared region of structural homology, composed of a leucine residue every seven amino acids (Landschulz *et al.*, 1988). The leucine zipper motif is a super-secondary structure that forms the basis of the dimerisation domain for these proteins, which all interact with DNA as homo or heterodimers. The heptad repeat of leucine residues forms a hydrophobic core for a coiled-coil structure (O'Shea *et al.*, 1989). All these transcription factors also contain a

basic DNA contact domain adjacent to the coiled-coil zipper and so are termed bZIP proteins. A third common domain is the transactivation domain.

Although Zta contains coiled-coil zipper, basic DNA binding and transactivation domains, it differs from canonical bZIP proteins due to a lack of the heptad repeat of leucine residues. These positions are substituted by other hydrophobic amino acids. The resulting strength of the coiled-coil is weaker than in other bZIP proteins (Hicks *et al.*, 2001).

1.4.2 Regulation of the BZLF1 promoter (Zp)

Zta is produced from either a monocistronic 0.8 kb mRNA transcript controlled by the BZLF1 promoter or a 2.9 kb transcript controlled by the BRLF1 promoter (Figure 1.9). The larger bicistronic transcript contains 2 open reading frames and encodes both Zta and Rta proteins (Manet *et al.*, 1989; Sinclair *et al.*, 1991). BRRF1, an early gene, is also located in this region and is transcribed in the opposite direction from a separate promoter (Figure 1.9).

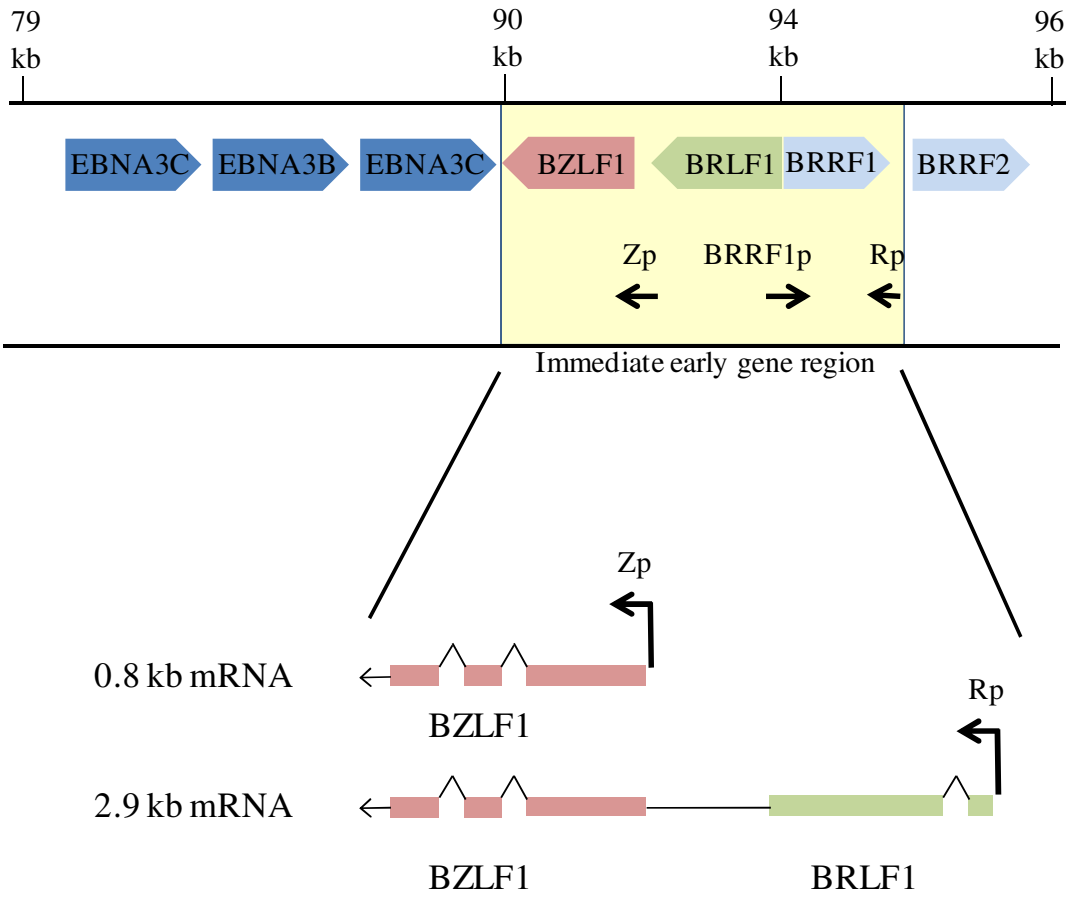

Figure 1.9: Diagram of the two BZLF1 mRNA transcripts in the EBV genome
BZLF1 is transcribed from either Zp as a 0.8kb monocistronic mRNA or from Rp as a 2.9kb bicistronic mRNA, that also encodes BRLF1. The 3 promoters, Zp, Rp and BRRF1p within the immediate early gene region are shown. (not drawn to scale) Adapted from (Rooney *et al.*, 1989) and www.ncbi.nlm.nih.gov

Initial activation of the lytic cycle occurs through expression of Zta through the BZLF1 promoter Zp. The EBV lytic cycle can be chemically induced by several methods in EBV positive cell lines, including phorbol esters, (e.g. TPA), IgG, transforming growth factor β1 (TGFβ1) and HDAC inhibitors.

The B-cell receptor (BCR) is activated via cross-linking of surface IgG which leads to an increase in cytosolic calcium concentration, following a release of calcium from the endoplasmic reticulum (reviewed in (Scharenberg *et al.*, 2007). This results in the activation and nuclear localisation of cellular transcription factors, inducing Zp to express Zta (Daibata *et al.*, 1990; Speck *et al.*, 1997).

Several host cell factors regulate Zp, acting through multiple cis-acting elements (Figure 1.10A). There are 4 types of binding elements, ZI, ZII, ZIII and ZV. ZI sites A-D are negative regulatory elements in the absence of a lytic cycle signal (Flemington and Speck, 1990c). MEF2D, SP1 and Sp3 bind to the ZI binding sites (Liu *et al.*, 1997a; Liu *et al.*, 1997b). Histone deacetylase complexes are recruited to MEF2D in latently infected B-cells, resulting in transcriptional repression (Gruffat *et al.*, 2002). Under some conditions, e.g. TPA addition, the ZI sites can act as positive regulators (Flemington and Speck, 1990c).

The ZII site in Zp binds multiple factors including CREB, c-jun, ATF1/2 and C/EBPα (Flemington and Speck, 1990c; Wang *et al.*, 1997; Adamson *et al.*, 2000; Wu *et al.*, 2004). In contrast to the ZI sites, the ZII site is essential for Zp activation (Flemington and Speck, 1990c; Daibata *et al.*, 1994). However in the presence of Zta, ZII is dispensable and Zp is auto-regulated through the Zta binding sites, ZIIIA and ZIIIB (Flemington and Speck, 1990a). This suggests that activation of Zp occurs in two stages; firstly transactivation by cellular transcription factors at ZI and ZII results in a low level of Zta expression and secondly newly expressed Zta binds to ZIII sites. This results in a higher level of Zta expression and activation of the lytic cycle (Flemington and Speck, 1990a).

The ZV motif, which is located close to the transcription start site, binds the zinc finger protein ZEB and is a strong negative regulator of Zp activation. Binne et al showed that deletion of ZV greatly increased the promoter activation following IgG cross-linking (Binne *et al.*, 2002).

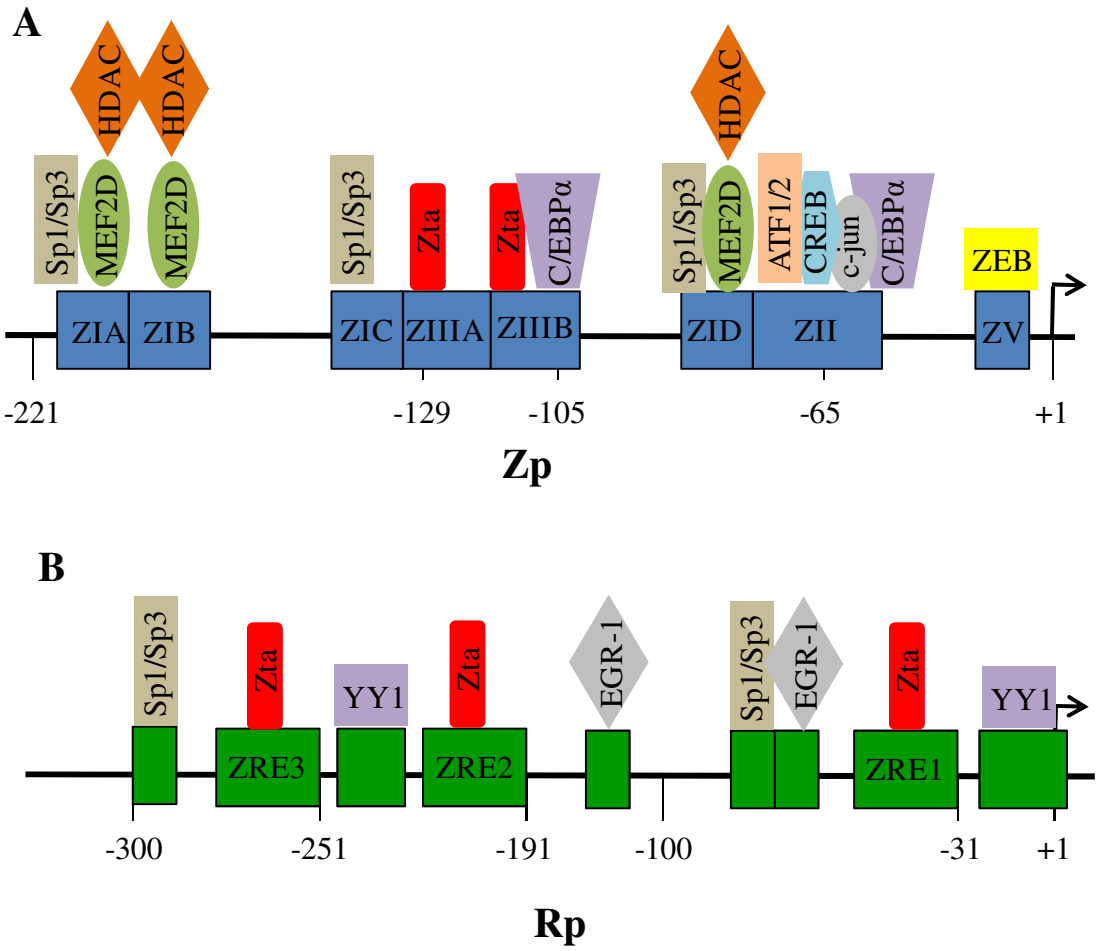

Figure 1.10: cis-acting elements and transcription factors of IE promoters Zp and Rp
A. The BZLF1 promoter, Zp, contains ZI, ZII and ZIII cis-acting elements. An additional element, ZV, inhibits transcription from the promoter in uninduced cells. MEF2D-HDAC, SP1 and Sp3 bind to the ZI binding sites. The ZII element binds multiple factors and is essential for promoter activation in the absence of Zta. Zp is auto-regulated through the 2 ZIII Zta binding sites. B. The BRLF1 promoter, Rp, contains 3 Zta Response Elements (ZREs) as well as Sp1/Sp3 and EGR-1 binding sites. Negative regulation can occur through 2 YY1 sites.

1.4.3 Regulation of the BRLF1 promoter (Rp)

The essential second step in reactivation of EBV from latency by Zta is activation of another immediate early transcription factor, Rta (Figure 1.10B). This occurs through Zta interaction with three Zta Response Elements (ZREs) in the Rp promoter; ZRE1, ZRE2 and ZRE3. Both ZRE2 and ZRE3 contain CpG motifs, which are very likely to be methylated during the latent phase *in vivo* (Robertson and Ambinder, 1997; Tao and Robertson, 2003). Zta has demonstrated the novel ability to selectively bind methylated response elements (Bhende *et al.*, 2004). CpG containing ZREs may only be recognised when methylated or binding is enhanced, while binding to non CpG ZREs is not influenced by methylation status. In addition Rp contains several important Sp1/Sp3 binding sites which are required for constitutive activity (Zalani *et al.*, 1992; Ragoczy and Miller, 2001). BCR cross-linking and TPA induction both result in increased levels of EGR-1 (Krappmann *et al.*, 2001) and Rp contains two EGR-1 binding sites (Zalani *et al.*, 1995). This suggests that EGR-1 may regulate expression of Rp. Negative regulation of Rp occurs through two YY1 binding sites (Zalani *et al.*, 1997).

1.4.4 Zta as a transcription factor (viral and cellular)

The α-helical DNA binding domain of Zta comprises the mostly basic amino acids 172 to 198 (Packham *et al.*, 1990; Petosa *et al.*, 2006). As Zta is required to form a homodimer to bind DNA, the adjacent dimerisation domain is also important for binding function (Hicks *et al.*, 2003). As described in section 1.4.1, Zta differs from other bZip proteins due to a lack of leucine residues in the coiled-coil (Kouzarides *et al.*, 1991) and it possesses a unique CT domain that folds back and stabilises the dimerisation domain (Petosa *et al.*, 2006). This unusual structure of Zta may permit it to recognise a wider range of DNA binding sites than other bZIP proteins (Farrell *et al.*, 1989; Lieberman *et al.*, 1990; Sinclair, 2006). The shorter dimerisation domain present in Zta may allow greater flexibility in the homodimer (Petosa *et al.*, 2006; Schelcher *et al.*, 2007). The residues that directly contact DNA during binding are almost identical in c-Fos, c-Jun and Zta and are analogous to the Zta amino acids 182, 185, 186, 189 and 190 (Glover and Harrison, 1995). The exception is amino acid 186 which is a serine in Zta and an alanine in c-Fos and c-Jun. Mutation S186A in Zta results in a mutant that

cannot bind selected ZRE sites, for example in Rp, but retains binding ability to Ap1 sites and other ZREs (Francis *et al.*, 1997; Adamson and Kenney, 1998). This residue is important for Zta recognition of a broad range of binding sites.

ZRE motifs are found in the promoters of many early EBV genes (Urier *et al.*, 1989; Flemington and Speck, 1990a). When two or more ZREs are located in a promoter, the effect on transactivation is synergistic (Carey *et al.*, 1992). Zta is also able to facilitate a transcription favouring DNA conformation by interacting directly with histone acetylating complexes such as CBP and p300 to acetylate chromatin (Adamson and Kenney, 1999; Zerby *et al.*, 1999). Zta interacts with the transcription factor C/EBPα to form a stable complex that is capable of activating promoters, including Zp, through binding to C/EBPα binding sites (Wu *et al.*, 2004).

ZREs within the human genome are common and Zta can exert a transcriptional effect on host cell genes. Affected genes include c-fos (Flemington and Speck, 1990b), IL-10 (Mahot *et al.*, 2003), TGF-β (Cayrol and Flemington, 1995), tyrosine kinase TKT (Lu *et al.*, 2000) and matrix metalloproteinases 1 and 9 (Yoshizaki *et al.*, 1999; Lu *et al.*, 2003). The immunosuppressive cytokines IL-10 and TGFβ may be induced by Zta to suppress host cell immune response (Israel and Kenney, 2005). The function in EBV persistence or transmission for other host genes activated by Zta is unclear, but potentially could contribute to oncogenesis (Israel and Kenney, 2005). Matrix metalloproteinases have been shown to play a role in metastatic spread and IL-10 is a growth factor for B cell tumours.

1.4.5 Interaction with Cellular proteins

Zta interacts directly with a number of cellular proteins, providing another mechanism for Zta to modify the cellular environment. Like many other viruses, EBV influences the tumour suppressor protein p53 and this is mediated by Zta. There have been conflicting reports of both activating and inhibitory effects on p53 by Zta (Mauser *et al.*, 2002b, Dreyfus *et al.*, 2000). These two distinctive, opposing methods of p53 regulation appear to be dependent on p53 phosphorylation state, cell type and stage of lytic replication (Sato *et al.*, 2010.) p53 is transiently induced by Zta during the early stages of lytic replication resulting in cell cycle arrest (Cayrol and Flemington, 1996b).

In the later stages of lytic replication Zta is a component in an ubiquitin ligase complex, targeting p53 for degradation and resulting in S-phase conditions (Sato *et al.*, 2009). Zta and p53 also interact directly and over-expression of either protein inhibits the transactivation ability of the other (Tarakanova et al., 2007). In a similar way, direct interaction between Zta and NFκB p65 results in negative regulation of Zta transactivation function (Gutsch *et al.*, 1994). Other Zta-interacting negative regulators include the retinoic acid receptors RXRα and RARα (Pfitzner *et al.*, 1995; Sista *et al.*, 1995).

Positive regulation of Zta function occurs through an interaction with the histone acetylase and transcriptional co-activator CBP (Adamson and Kenney, 1999). Zta interaction with the N-terminus of CBP occurs through both the transactivation and zipper domains of Zta. The interaction results in the recruitment of histone acyl transferases (HAT), destabilising the nucleosome structure and forming a more open chromatin structure for the basal transcription machinery, thus allowing transactivation of genes (Adamson and Kenney, 1999). Interaction between Zta and C/EBPα leads to stabilisation and increased levels of C/EBPα. In turn C/EBPα transactivates the cycle dependent kinase inhibitor p21, contributing to G1 cell cycle arrest (Wu *et al.*, 2003; Wu *et al.*, 2004).

1.4.6 Zta and EBV replication

In addition to functioning as a transcription factor, Zta plays a direct role as a replication factor, binding directly to the origin of lytic replication (oriLyt) (Schepers *et al.*, 1996).

Expression of Zta and six early genes including the EBV DNA polymerase catalytic subunit (BALF5) and polymerase processivity factor (BMRF1) are essential for viral genome replication (Fixman *et al.*, 1992). The other genes encode a helicase/primase complex (BBLF2/3, BBLF4, and BSLF1) and a DNA binding protein (BALF2).

The EBV genome contains two highly related oriLyts; Left and Right, located approximately opposite each other on a circularised genome, within a duplicated segment (DS) of the genome. A separate third replication origin, oriP, is utilised for EBV plasmid replication during latent infection (Yates *et al.*, 1984). Each oriLyt spans

approximately 1000bp and they are essentially identical. oriLyt is comprised of an upstream and a downstream component separated by approximately 400bp (Hammerschmidt and Sugden, 1988). The upstream component contains four ZRE motifs and binding by Zta to these sites is required for replication from oriLyt (Fixman *et al.*, 1992; Schepers *et al.*, 1996). Both the DNA binding and transactivation domains of Zta are required for oriLyt binding (Schepers *et al.*, 1996). In addition there are three ZREs located downstream of the downstream component but these are not essential for replication (Schepers *et al.*, 1996).

The formation of an initiation complex at oriLyt is the first step in lytic replication, requiring Zta binding at the upstream ZREs and binding of transcription factors ZBP-89 and SP1 to the downstream component (Baumann *et al.*, 1999). Binding of Zta is thought to recruit other essential viral components to this complex (Gao *et al.*, 1998), (reviewed in (Tsurumi *et al.*, 2005)). The six essential EBV replication proteins work together as the replication machinery at the replication fork. Replication then proceeds in a two stage process, with initial replication generating two copies of the genome with fewer supercoils and nucleosomes (Pfuller and Hammerschmidt, 1996). These genomes then provide the template for rolling circle replication, generating large head-to-tail DNA concatamers, which are then cleaved into genome length units for virion packaging (Cho and Tran, 1993). The EBV genome is replicated 100-1000 fold during this process (Tsurumi *et al.*, 2005).

Zta functions in multiple ways to allow lytic replication of the EBV genome. As a transcription factor, Zta induces the expression of essential EBV replicative enzymes, recruits these enzymes to oriLyt and provides the platform for formation of the initiation complex.

1.4.7 The Cell Cycle

During the course of the cell cycle DNA is replicated and division of the parent cell into two daughter cells occurs. This process consists of four main phases: G1, S, G2 and M phases (Figure 1.11). Non-proliferative cells are maintained in a state of quiescence termed G0 phase. G1 phase is characterised by cell growth and preparation for DNA replication including the synthesis of required enzymes. During S phase replication of DNA occurs, resulting in a doubling of cellular DNA content. Following S phase,

preparation for cell division occurs during G2. During M phase or mitosis the DNA and cellular components are divided into two daughter cells. The cell cycle is regulated by checkpoints to ensure required conditions and components are available for continuation of the next phase and integrity of replicated DNA is maintained (reviewed in (Vermeulen *et al.*, 2003)). The two main checkpoints are G1/S and G2/M. Progression through these checkpoints is regulated by protein phosphorylation by specific protein kinases. These heterodimeric kinases are comprised of a regulatory subunit, called a cyclin and a catalytic subunit, called a cyclin dependent kinase (cdk).

Progression of the cell through the G1/S checkpoint is mainly controlled by the protein kinases cdk 4, 6/cyclin D and cdk2/cyclin E. Together cdk4,6/cyclin D and cdk2/cyclinE cause hyper-phosphorylation of Rb, resulting in dissociation from E2F. This frees the transcription factor E2F to initiate transcription of key S-phase-promoting genes required for DNA replication.

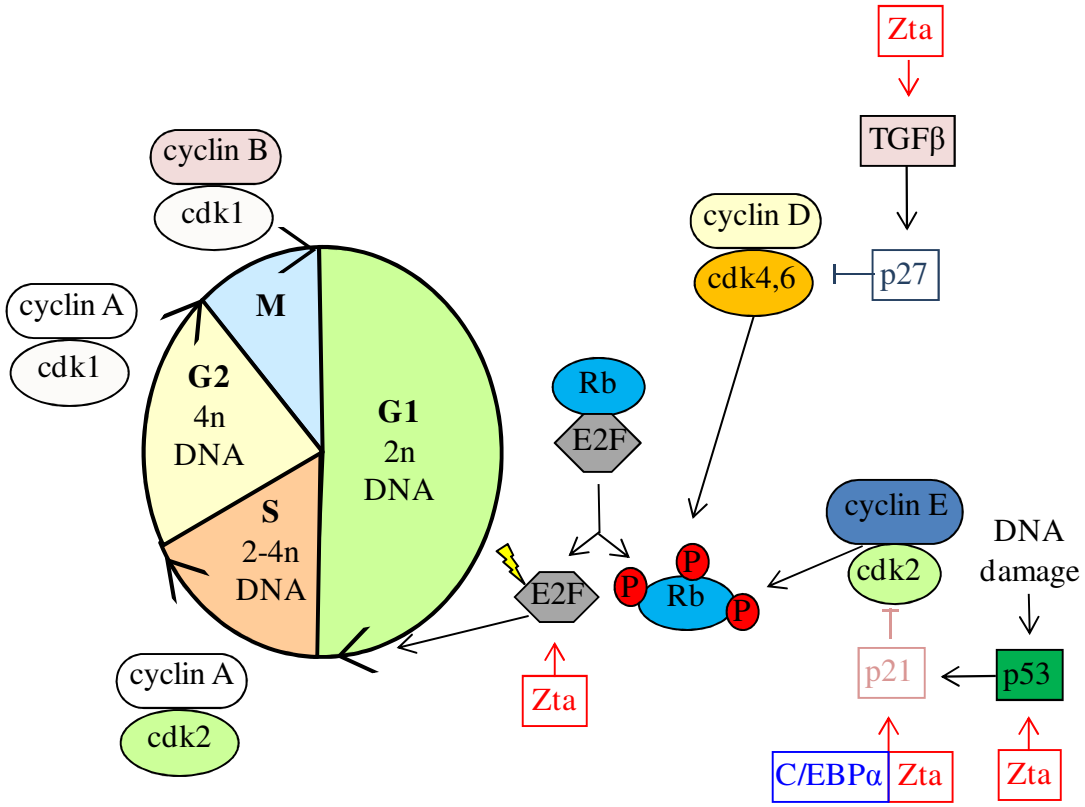

Figure 1.11: Cell cycle progression and Zta
Diagram of the cell cycle and control points of the G1/S checkpoint that are influenced by the expression of Zta. Critical cyclin/cdk complexes for progression and DNA content is shown for each phase of the cell cycle.

1.4.8 EBV, Zta and the Cell Cycle

EBV lytic replication is inhibited when the host cell enters S-phase so manipulation of the cell cycle is important to allow replication of the virus (Takase *et al.*, 1996). Zta has been shown to inhibit progression through the cell cycle via several different mechanisms (Figure 1.11). Zta is able to signal via the cyclin dependent kinase inhibitor p21 through either a p53-dependent or independent mechanism. Zta can cause cell cycle arrest at G1 via upregulation of p53. The increased level of p53 in turn activates expression of p21, leading to inhibition of cdk2/cyclin E (Cayrol and Flemington, 1996a; Cayrol and Flemington, 1996b). This results in a reduction of Rb phosphorylation and halts cell cycle progression. In addition Zta is able to upregulate p21 and thus promote G1 cell cycle arrest via a p53-independent mechanism (Rodriguez et al., 1999). This requires a stabilising interaction between Zta and C/EBPα and results in transcriptional activation of p21 (Wu et al., 2003; Wu et al., 2004).

Zta-mediated inhibition of cdk4,6/cyclin D occurs when Zta interacts with TGFβ, resulting in activation of the cdk inhibitor p27 (Cayrol and Flemington, 1996b; Rodriguez *et al.*, 1999). p27 inhibits formation of cdk4,6/cyclin D, resulting in a reduction of Rb phosphorylation. Zta has also been shown to directly induce expression of E2F and cyclin E (Mauser *et al.*, 2002a). The interaction of Zta with several different control points in the G1/S checkpoint is likely to contribute to the cell growth arrest function of Zta.

Kudoh and colleagues have shown that S-phase cdks are required for viral replication (Kudoh *et al.*, 2004). They proposed that the elevation of cyclins E/A and accumulation of hyper-phosphorylated Rb is characteristic of post-G1/S cells and that these S-phase-like conditions are required for EBV DNA replication (Kudoh *et al.*, 2003; Kudoh *et al.*, 2004).

The ability of Zta to cause cell cycle arrest is dependent on the cell type (Cayrol and Flemington, 1996a; Cayrol and Flemington, 1996b; Flemington, 2001; Mauser *et al.*, 2002a). Zta demonstrates the ability to mediate cell cycle arrest at G1/S in HeLa and LCL cell lines and in human fibroblasts cells. However in human keratinocytes and

EBV-infected gastric carcinoma cells Zta appears to instead promote cell cycle progression (Mauser *et al.*, 2002a).

In contrast to the lytic cycle, EBV encoded genes in latency have cell cycle promoting activity, allowing EBV to cause growth transformation upon infection of naive B lymphocytes (reviewed in (Flemington, 2001)).

Residues within the basic region of Zta have been shown to be important for Zta to mediate cell cycle arrest and to reactivate EBV from latency (Kolman *et al.*, 1996). This connection raises the possibility that the cell cycle arrest function of Zta is a requirement for EBV lytic cycle activation.

Rta, which is induced by Zta, may also have an effect on the cell cycle through interactions with E2F and pRb (Swenson *et al.*, 1999).

1.4.9 Zta and immune response

Zta has a key role in reducing the host cell immune response to lytic infection by EBV. This is exerted through several different mechanisms as detailed below.

Zta is able to inhibit the expression of MHC class I on the cell surface, thus limiting the immune presentation of viral antigens (Keating *et al.*, 2002). IFN-γ is an important component in the host response to viral infection, inducing cellular protein with direct anti-viral effects (Morrison *et al.*, 2001). Zta can inhibit the signalling pathway of the cytokine IFN-γ, decreasing activation of a number of important downstream IFN-γ targets including CIITA, p48 and class II MHC surface expression (Morrison *et al.*, 2001). This is achieved by Zta via inhibition of STAT1 tyrosine phosphorylation and nuclear localisation. In addition Zta causes down-regulation of the IFN-γ receptor (Morrison *et al.*, 2001). This may also be key for promoting B cell infection as EBV virus produced in cells expressing MHC class II preferentially infect epithelial cells and virus produced in MHC class II negative cells preferentially infect B cells (Borza and Hutt-Fletcher, 2002).

Promyelocytic leukaemia (PML) bodies are structures in the nucleus that are induced by expression of type I and II interferons and are thought to have an antiviral, apoptotic function (Bernardi and Pandolfi, 2003). Several viruses encode proteins that disperse PML bodies (Chee *et al.*, 2003) and Zta expression has also been shown to disperse

these structures (Adamson and Kenney, 2001). As sumo-I modification is essential for the formation of PML bodies, this may in part be due to competition for sumo-I as Zta is sumo-modified at lysine 12 (Adamson and Kenney, 2001).

Zta also inhibits expression of the receptor for tumour necrosis factor (TNF), thus repressing TNF cytokine signalling (Bristol *et al.*, 2010). As part of an immune response TNFα induces key inflammatory genes as well as cellular apoptosis. However both these functions are abrogated in the presence of Zta (Morrison and Kenney, 2004).

1.4.10 Lytic cycle Therapies

The cause of most EBV-associated diseases is the ability of EBV to transform and immortalise cells promoting tumour formation, not as a result of lytic reactivation. However a novel approach to treat EBV malignancies is therapeutic induction of the lytic cycle in tumour cells (Westphal *et al.*, 1999). This could be achieved by introduction of the IE genes. Delivery of BZLF1 and BRLF1 using adenoviruses in nude mice resulted in the inhibition of EBV+ tumour cells (Feng *et al.*, 2002). Lytically infected cells express viral protein kinases that are capable of converting a nucleoside analogue to the active form (Moore *et al.*, 2001). This is cytotoxic as the host DNA polymerase is inhibited and this effect is transferred to neighbouring cells. Induction of the lytic cycle in tumour cells, in conjunction with administration of the nucleoside analogue gancyclovir is a possible treatment for EBV positive tumours (Faller *et al.*, 2001; Mentzer *et al.*, 2001).

1.5 Lymphocryptoviruses

EBV is a member of the lymphocryptovirus (LCV) genus, along with about 50 different LCVs that have been identified in both New and Old World primates (Ehlers *et al.*, 2010). Many of the LCVs that have been identified in primates are closely related to EBV. The *in vivo* infection of the related LCVs also closely resembles the natural history of EBV infection (Wang *et al.*, 2001). Asymptomatic, lifelong infection of most occurs in infancy and LCV-induced tumours arise in immune-suppressed primates (reviewed in (Wang *et al.*, 2001)). This identifies simian LCVs as a valuable model system to provide a better understanding about EBV.

1.6 Aims

Aim 1: To investigate the effect of methylated ZREs on Zta binding and function including the methylation sensitive Zta mutant C189S

As methylation of some Zta Response Elements is critical for Zta binding and appears to play an important role in viral lytic activation, I hypothesize that conformational differences between Zta and the methylation sensitive Zta mutant C189S are permissive for enhanced binding to ZREs containing a methylated CpG motif.

Aim 2: To compare DNA binding specificity, lytic reactivation and the promotion of cell cycle arrest function of RhZta and Zta.

The two related lymphocryptoviruses, EBV and Rhesus Macaque LCV, share a similar pathogenesis and repertoire of genes. I hypothesize that the RhLCV protein ZtaRh is functionally equivalent to the EBV protein Zta, in terms of DNA binding specificity, lytic reactivation and the promotion of cell cycle arrest.

Aim 3: To investigate how Zta and mutants of Zta interact with various host cell proteins. This includes known interacting partners as well as investigating potentially novel Zta interactions.

Interactions with a variety of viral and cellular host proteins are critical for the functions of Zta. Several of these interactions occur through the zipper dimerization domain, which is contacted by the CT domain. I hypothesize that alterations to the extreme CT of Zta reduce the ability of Zta to contact some interacting partner proteins.

Chapter 2 Materials and Methods

2.1 Materials

2.1.1 Plasmids

Plasmid name	Method	Source
pSP64-Z(L243A-F245A)	Cloning	Generated by Celine Schelcher
pSP64-Zta F245A	Cloning	Generated by Celine Schelcher
pSP64-Zta L243A	Cloning	Generated by Celine Schelcher
pSP64-Zta N244A	Cloning	Generated by Celine Schelcher
pBabe -Z(L243A-F245A)	*In vitro* transcription	Generated by Questa Karlsson
pBabe -Zta F245A	*In vitro* transcription	Generated by Questa Karlsson
pBabe -Zta N244A	*In vitro* transcription	Generated by Questa Karlsson
pBabe-his-ZtaRh	*In vitro* transcription	Generated by Questa Karlsson
pBabe-his-Zta	*In vitro* transcription	Generated by Questa Karlsson
pBabe-Zta L243A	*In vitro* transcription	Generated by Questa Karlsson
pcDNA3-Flag-C/EBPα	*In vitro* transcription	(Schelcher *et al.*, 2005)
pSP64- Zta C189S	*In vitro* transcription	(Schelcher *et al.*, 2005)
pSP64-Zta	*In vitro* transcription	(Hicks *et al.*, 2003)
pBluescript-ZtaRh	*In vitro* transcription cloning	Generated by Mirjam Meyer
pGL2- EBVΔZRE3	Luciferase assay	Generated by Questa Karlsson
pGL2- RhLCV RhRp	Luciferase assay	Generated by Questa Karlsson
pGL2-EBV Rp	Luciferase assay	Generated by Questa Karlsson
pGL2-Rh+ZRE3	Luciferase assay	Generated by Questa Karlsson
pBABE Puro	Transfection of cells	(Morgenstern and Land, 1990)
pBabe-Rh_LNF	Transfection of cells	Generated by Questa Karlsson
pBABE-Zta	Transfection of cells	(Hicks *et al.*, 2001)

Plasmid name	Method	Source
pBABE-Zta C189S	Transfection of cells	(Schelcher *et al.*, 2005)
pBabe-Zta_IΔΔ	Transfection of cells	Generated by Questa Karlsson
pcDNA3	Transfection of cells	Invitrogen
pcDNA3-flag-BGLF4	Transfection of cells	(Tarakanova *et al.*, 2007)
pcDNA3-flag-BMRF1	Transfection of cells	Generated by Questa Karlsson
pcDNA3-flag-NFκB p65	Transfection of cells	Generated by Questa Karlsson
pcDNA3-flag-p53	Transfection of cells	Addgene
pcDNA3-flag-RARα	Transfection of cells	Generated by Questa Karlsson
pcDNA3-flag-RXRα	Transfection of cells	Generated by Questa Karlsson
pmaxGFP	Transfection of cells FACS	Amaxa

Table 2.1: Plasmids

2.1.2 Oligonucleotides

N.B. Primer pairs used in site directed mutagenesis (sdm) are reverse complements of each other so only one primer sequence is shown. For EMSA probes the ZRE is shown in blue and methylated residues in red.

Name	Sequence (5'→3')	Method
To create EBV Rp	(a)ctgcacaccggacgcgttgtcgtcgggagataaaagt (b)ctgcacaccggctcgagctttaaaaaggccggctgac	Cloning
To create his-ZtaRh	(a)caccggggatccatgcatcatcatcatcatcatatggaccccagcttgcctcctg (b)caccgggaattcttatataagatcttcatggataatgtctgg	Cloning
To create pcDNA3-flag-BMRF1	(a)ctgcacaccggggatccatggattataaagatgatgatgataaaatggaaaccactcagactctccg (b)ctgcacaccgggaattcttaaatgaggggttaaaggcctg	Cloning
To create pcDNA3-flag-NFκB p65	(a)ctgcacaccggggatccatggattataaagatgatgatgataaaatggacgaactgttcccccct (b)ctgcacaccggaagctttaggagctgatctgactcagc	Cloning

Name	Sequence (5'→3')	Method
To create EBV Rp	(a)ctgcacaccggacgcgttgtcgtcgggagataaaagt (b)ctgcacaccggctcgagctttaaaaaggccggctgac	Cloning
To create his-ZtaRh	(a)caccggggatccatgcatcatcatcatcatcatatggaccccagcttgcctcctg (b)caccgggaattcttatataagatcttcatggataatgtctgg	Cloning
To create pcDNA3-flag-BMRF1	(a)ctgcacaccggggatccatggattataaagatgatgatgataaaatggaaaccactcagactctccg (b)ctgcacaccgggaattcttaaatgaggggttaaaggcctg	Cloning
To create pcDNA3-flag-RARα	(a)ctgcacaccggggatccatggattataaagatgatgatgataaaatggccagcaacagcagctcctgc (b)ctgcacaccgggaattctcacggggagtgggtggc	Cloning
To create pcDNA3-flag-RXRα	(a)ctgcacaccggctcgagatggattataaagatgatgatgataaaatggacaccaaacatttcctgccg (b)ctgcacaccgggaattcctaagtcatttggtgcggcg	Cloning
To create RhLCV RhRp	(a)ctgcacaccggacgcgtcggcgtggggaaataaaagt (b)ctgcacaccggctcgaggacaaaataggctggctgaca	Cloning
AP-1	(a) gatccatgactcagaggaaaacatacg (b) cgtatgttttcctctgagtcatggatc	EMSA
oriLyt (ZRE1)	(a) ccttaaagtattacacagag (b) ctctgtgtaatactttaagg	EMSA
oriLyt 1	(a)gatctaaggtattgcacagcgccc (b)gatcgggcgctgtgcaatacctta	EMSA
oriLyt 6	(a)gatcggattagtgtgccacggtga (b)gatctcaccgtggcacactaatcc	EMSA
oriLyt 7	(a)gatccgtgctctgactcatatttc (b)gatcgaaatatgagtcagagcacg	EMSA
RhLCV ZRE3 methylated	(a)gatccagcacacpgccpggattttgc (b)gatcgcaaaatccpggcpgtgtgctg	EMSA
RhLCV ZRE3 unmethylated	(a)gatccagcacacgccggattttgc (b)gatcgcaaaatccggcgtgtgctg	EMSA
ZRE1 (Rp)	(a) gatctcttttatgagccattggca (b) tgccaatggctcataaaagagatc	EMSA
ZRE2 (Rp)	(a) gatcaagcttatgagcgattttat (b) gatcataaaatcgctcataagctt	EMSA
ZRE2 methylated	(a) gatcaagcttatgagcpgattttat (b) gatcataaaatcpgctcataagctt	EMSA

Name	Sequence (5'→3')	Method
To create EBV Rp	(a) ctgcacaccggacgcgttgtcgtcgggagataaaagt (b) ctgcacaccggctcgagctttaaaaaggccggctgac	Cloning
To create his-ZtaRh	(a) caccggggatccatgcatcatcatcatcatcatatggaccccagcttgcctcctg (b) caccgggaattcttatataagatcttcatggataatgtctgg	Cloning
To create pcDNA3-flag-BMRF1	(a) ctgcacaccggggatccatggattataaagatgatgatgataaaatggaaaccactcagactctccg (b) ctgcacaccgggaattcttaaatgaggggttaaaggcctg	Cloning
ZRE3 (Rp)	(a) gatctcaaaattcgcgatgctata (b) gatctatagcatcgcgaattttga	EMSA
ZRE3 me(0)	(a) gatctcaaaattcgcgatgctata (b) gatctatagcatcgcpgaattttga	EMSA
ZRE3 me(1')	(a) gatctcaaaattcgcpgatgctata (b) gatctatagcatcgcgaattttga	EMSA
ZRE3 me(-1')	(a) gatctcaaaattcpgcgatgctata (b) gatctatagcatcgcgaattttga	EMSA
ZRE3 me(1', 0)	(a) gatctcaaaattcgcpgatgctata (b) gatctatagcatcgcpgaattttga	EMSA
ZRE3 me(-1', -2)	(a) gatctcaaaattcpgcgatgctata (b) gatctatagcatcpgcgaattttga	EMSA
ZRE3 me(-1', -2, 1', 0)	(a) gatctcaaaattcpgcpgatgctata (b) gatctatagcatcpgcpgaattttga	EMSA
ZRE3 me(-2)	(a) gatctcaaaattcgcgatgctata (b) gatctatagcatcpgcgaattttga	EMSA
ZREIIIB	(a) gtacattagcaatgcctg (b) caggcattgctaatgtac	EMSA
BBLF2/3	(a) ctggcatcctccgagtctt (b) cgagttcatcctgggctt	QPCR
BHLF1	(a) gggacactgcactaccgcca (b) cgccaggaaccccggctg	QPCR
BLLF1	(a) agaatctgggctgggacgtt (b) cgagatacaatgcgacca	QPCR
BRLF1	(a) cagaaagtcttccaagccatcc (b) caaacagacgcagccatgag	QPCR
BZLF1	(a) ctatcaggacctgggagggc (b) cacagcacacaaggcaaagg	QPCR
L32	(a) caacattggttatgcaagcaaca (b) tgacgttgtggaccaggaact	QPCR
LMP1	(a) aagaaggccaaaagctgc (b) ctgttcatcttcgggtgc	QPCR
B-globin Forward	(a) ggcaaccctaaggtgaaggc (b) ggtgagccaggccatcacta	QPCR

Name	Sequence (5'→3')	Method
To create EBV Rp	(a)ctgcacaccggacgcgttgtcgtcgggagataaaagt (b)ctgcacaccggctcgagctttaaaaaggccggctgac	Cloning
To create his-ZtaRh	(a)caccggggatccatgcatcatcatcatcatcatatggaccccagcttgcctcctg (b)caccgggaattcttatataagatcttcatggataatgtctgg	Cloning
To create pcDNA3-flag-BMRF1	(a)ctgcacaccggggatccatggattataaagatgatgatgataaaatggaaaccactcagactctccg (b)ctgcacaccgggaattcttaaatgaggggttaaaggcctg	Cloning
EBV polymerase (BALF5)	(a)agtccttcttggctagtctgttga (b)ctttggcgcggatcctc	QPCR (Gallagher *et al.*, 1999)
To create BZta	(a)cgggtggcttccagaaaatgccgggccaggttaagaatctgctgcagcactaccgtgaggtggctgc	sdm
To create CTZta	(a1)gttgactccattatcccccggacaccagatattatccacgaggatctcttaaatttctaactcccg (a2)ccggacaccagatattatccacgaggatctcatataactcccgttattgaaaccacgcctgcttc	sdm
To create pBabe-Rh_LNF	(a)ccggacaccagacattatccatgaagatctttaaatttctaagaattcgccagcacagtggtcgacctg	sdm
To create pBabe-Zta_IΔΔ	(a)cacgaggatctcatataattctaactcccg	sdm
To create pGL2-EBVΔZRE3	(a)ctggtttatagcaccgtcaattttgactgca	sdm
To create pGL2 -Rh+ZRE3	(a)cgacccagcacatcgcaattttgcctgcaat	sdm
To create ZipZta	(a1)gccgggccaggtttaagaatctgctgcagcactaccgtg (a2)gccaaatcatctgaaaatgacaggctgcgcatcctgatgaagcagatgtgcccaagcctggatgttgac (a3)ccaaatcatctgaaaatgaaaggctgcgcatcctgatgaagc	sdm

Table 2.2: Oligonucleotides

2.1.3 Buffers

Buffer	Composition	Method
Sample loading buffer (6X)	0.25% (w/v) Bromphenol blue, 0.25% (w/v) xylene cyanole FF, 40% (w/v) sucrose (Sigma)	Agarose gel
TBE	0.89M Tris-Borate, 20mM Na_2EDTA, pH 8.3 (Fisher)	Agarose gel EMSA
Calcium Chloride	3M $CaCl_2$ (Promega)	Calcium phosphate Transfection
HBS (2x)	50 mM HEPES, 280 mM NaCl, 1.5 mM Na_2HPO_4, pH 7.1 (Promega)	Calcium phosphate Transfection
PBS	10mM Tris-Base, 150mM NaCl, 1mM EDTA, pH 7.4 (Sigma)	Cell culture
Freezing solution	85% (v/v) FBS, 15% (v/v) DMSO	Cell line storage
Alkaline phosphatise buffer (10x)	25 mM Tris-HCl, 1 mM $MgCL_2$, 0.1 mM $ZnC1_2$, 50% (v/v) glycerol, pH 7.6 (Roche)	Cloning
Ligation buffer (10x)	660 mM Tris-HCl, 50 mM $MgCl_2$, 50 mM DTT, 10 mM ATP, pH 7.5. (Roche)	Cloning
Restriction Enzyme buffer A (10x)	330 mM Tris acetate, 100 mM Mg-acetate, 660 mM K-acetate, 5mM Dithiothreitol (DTT) (Roche)	Cloning
Restriction Enzyme buffer B (10X)	100 mM Tris-HCl, 1 M NaCl, 50 mM $MgCl_2$, 10 mM 2-mercaptoethanol pH 8 (Roche)	Cloning
Restriction Enzyme buffer H (10X)	0.5 M Tris-HCl, 1 M NaCl, 100 mM $MgCl_2$, 10 mM Dithioerythritol, pH 7.5 (Roche)	Cloning
EMSA binding buffer (5x)	50mM Tris-HCl (pH 7.5), 5mM $MgCl_2$, 2.5mM EDTA, 2.5mM DTT, 250mM NaCl, 20% glycerol, 0.25 mg/ml poly (dI-dC).poly(dI-dC) (Promega)	EMSA
Fixing solution	10% (v/v) acetic acid, 20% (v/v) ethanol	EMSA
SP6 transcription buffer (5x)	400mM HEPES-KOH, 160mM $MgCl_2$, 10mM spermidine, 200mM DTT, pH 7.5 (Promega)	*In vitro* transcription
TFBI	30mM KAc, 50mM $MnCl_2$, 100mM KCl, 10mM $CaCl_2.2H_20$, 15% glycerol (v/v)	Competent bacteria
TFBII	10mM NaMOPs, 75mM $CaCl_2$, 10mM KCl 15% glycerol	Competent bacteria
Elution buffer (EB)	10mM Tris-Cl, pH 8.5	Mini-Prep Maxi-Prep
Pfx buffer	50mM Tris-HCl, 50mM KCl, 1mM DTT, 0.1 mM EDTA, 50% glycerol (v/v), pH 8 (Invitrogen)	PCR
TE buffer	10 mM Tris, 1 mM EDTA, pH 8.0	Probe labelling

Buffer	Composition	Method
Lysis buffer	10% glycerol, 2mM EDTA, 0.1% NP40, 2mM DTT, 150mM NaCl, 10mM NaF in PBS	Pulldowns
Lysis buffer (Qiagen)	50 mM NaH_2PO_4, 10 mM imidizole, 0.05% Tween 20, pH to 8.0 with NaOH	Pulldowns
Lysis buffer (Zou et al, 2007)	1% NP-40, 10mM imidizole in PBS	Pulldowns
Wash /Nickel binding buffer	20mM imidizole, 0.5% NP-40 in PBS	Pulldowns
Wash buffer (Qiagen)	50 mM NaH_2PO_4, 300 mM NaCl, 20 mM imidizole, 0.05% Tween 20, pH to 8.0 with NaOH	Pulldowns
Wash buffer (Zou et al, 2007)	1% NP-40, 20mM imidizole in PBS	Pulldowns
SYBR Green Master Mix	HotStarTaqTM DNA Polymerase, QuantiTect SYBR Green PCR Buffer, dNTPs mix including dUTP, SYBR Green I, ROX and 5mM $MgCl_2$	Quantitative real time PCR
Laemmli Protein Sample buffer	2% SDS, 10% glycerol, 5% 2-mercaptoethanol, 0.002% bromphenol blue, 0.0625 Tris HCl (Sigma)	SDS-PAGE
MOPS SDS running buffer (20x)	1M MOPS (2-(N-morpholino) propane sulfonic acid), 1M Tris-Base, 69.3mM SDS, 20.5mM EDTA (Invitrogen)	SDS-PAGE
Protogel resolving buffer	0.375 M Tris-HCl and 0.1% SDS, pH 8.8 (National Diagnostics)	SDS-PAGE
Protogel stacking buffer	0.125 M Tris-HCl and 0.1% SDS, pH 6.8 (National Diagnostics)	SDS-PAGE
Tris-Glycine SDS buffer (10x)	0.25M Tris base, 1.92M glylcine, and 1% (w/v) SDS	SDS-PAGE
Ponceau-S concentrate (10X)	2% (w/v) Ponceau-S, 30% (v/v) Trichloroacetic acid, 30% (v/v) Sulphosaliylic acid (Sigma)	Western blotting
Blocking solution	5% dried milk (w/v), 10mM Tri-Base pH 7.4, 150mM NaCl, 1mM EDTA, 0.1% Tween 20 (v/v).	Western blotting
ECL buffer A	250mM luminol, 90mM P-Coumaric acid, 100mM Tris, pH 8.5	Western blotting
ECL buffer B	1.92% H_2O_2 (v/v), 100mM Tris, pH 8.5	Western blotting
PBS-Tween	10mM Tris-Base, 150mM NaCl, 1mM EDTA, 0.1% Tween 20 (v/v), pH 7.4	Western blotting
Transfer buffer	0.025M Tris, 0.192M Glycine, 15% methanol (v/v)	Western blotting

Table 2.3: Buffers

2.1.4 Antibodies

Type	Name	Source
Primary	BZ1 mouse monoclonal	Gift from Professor Martin Rowe
Primary	Cdk2 mouse monoclonal	Santa Cruz Biotechnology
Primary	Monoclonal α-Flag M2 mouse	Sigma
Primary	α-penta-his	Qiagen
Primary	Bcl2 mouse	Santa Cruz Biotechnology
Secondary	ECL α-mouse HRP-linked	GE Healthcare
Secondary	Polyclonal rabbit-α-mouse Ig	Dako
Tertiary	Protein A, peroxidase-linked	Amersham

Table 2.4: Antibodies

2.1.5 Enzymes

Name	Manufacturer	Method
Alkaline phosphatase	Roche	Cloning
BamHI restriction enzyme	Roche	Cloning
Dpn1 restriction enzyme	Roche	Site directed mutagenesis
EcoRI restriction enzyme	Roche	Cloning, linearisation of plasmid DNA
HindIII restriction enzyme	Roche	Cloning
ImProm-II™ Reverse Transcriptase	Promega	cDNA Synthesis
Polynucleotide kinase (PNK)	Roche	DNA labelling
P*fx* DNA polymerase	Invitrogen	PCR reaction
RQ1 RNAse-free DNAse	Promega	*In vitro* transcription
RNasin® Ribonuclease Inhibitor	Promega	*In vitro* translation
SP64 RNA polymerase	Promega	*In vitro* transcription
SYBR Green	Qiagen	Quantitative Real Time PCR
T4 DNA ligase	Roche	Ligation
T7 RNA polymerase	Promega	*In vitro* transcription

Name	Manufacturer	Method
XhoI restriction enzyme	Roche	Cloning, linearisation of plasmid DNA

Table 2.5: Enzymes

2.1.6 Kits

Name	Manufacturer	Method
QIAquick PCR purification kit	Qiagen	PCR purification
QIAprep Maxi-Prep	Qiagen	Maxi-prep
QIAprep Mini-Prep	Qiagen	Mini-prep
RNeasy	Qiagen	Total RNA extraction
ImProm-II™ Reverse Transcription System	Promega	Reverse Transcription
RiboMax Large Scale RNA production systems: SP6 and T7	Promega	*in vitro* transcription
Rabbit Reticulocyte Lysate System	Promega	*in vitro* translation
Profection Mammalian Transfection Systems	Promega	Transfection
Effectene Transfection Kit	Qiagen	Transfection
Luciferase Assay System	Promega	Luciferase Assay

Table 2.6: Kits

2.1.7 Radioactivity

The radioisotopes [^{35}S] Methionine (*in vitro* translated protein labelling for EMSA) and [γ^{33}P] ATP (EMSA probe labelling) were purchased from Amersham Biosciences.

2.2 Methods

2.2.1 Cell Culture

2.2.1.1 Cell Lines

Human epithelial HeLa cells (Jones *et al.*, 1971; Verma and Hansch, 2006) were grown in Dulbecco's modified Eagle's medium (Invitrogen) containing 10% (v/v) Fetal Bovine Serum, 100U/ml penicillin, 100 µg/ml streptomycin and 2mM L-glutamine. These cells were utilised to investigate cell arrest as demonstrated by Cayrol and Flemington (Cayrol and Flemington, 1996a). Human embryonic kidney (HEK) 293 cells were grown in RPMI medium (Invitrogen) containing 10% (v/v) Fetal Bovine Serum, 100U/ml penicillin, 100 µg/ml streptomycin and 2mM L-glutamine. These cells were selected as they are easily grown and transfected so are good for protein expression experiments. HEK 293 cells containing the B95-8 EBV strain lacking the BZLF1 gene (HEK293-ZKO cells) (Feederle *et al.*, 2000) were grown in RPMI medium (Invitrogen) containing 10% (v/v) Fetal Bovine Serum, 100U/ml penicillin, 100 µg/ml streptomycin, 2mM L-glutamine and 100 µg/ml hygromycin. The hygromycin maintains selection for the recombinant virus in HEK293-ZKO cells. Cells were grown at 37°C in a humidified 5% CO_2 incubator. These cells provide a system for reactivating the EBV lytic cycle via the transfection of a functional Zta or Zta mutant.

2.2.1.2 Storage and recovery of cell lines

80% confluent cells were washed in PBS then spun at 283 xg for 5 minutes. The pellet was resuspended in 1/6 original volume freezing solution and 2ml aliquoted to each sterile cryogenic tube. Tubes were frozen in isopropanol cryogenic boxes overnight at -80°C, before being transferred to liquid nitrogen storage.

To recover cell lines, tubes were removed from liquid nitrogen and thawed at 37°C. Thawed cells were added to 10mls of media, spun at 145 xg for 10mins to remove freezing solution, and the pellet was then resuspended in 10 ml media. Cells were then plated in a small flask and placed in incubator at 37°C.

2.2.1.3 Determination of cell count

A small aliquot of cells were removed from the media and placed in a Neubauer Hematocytometer. Using a light microscope the total number of cells in the four

squares was counted. To determine the number of cells/ml, the following equation was used:

Number of cells/ml = (total cells counted/4) x 10,000

2.2.1.4 Calcium Phosphate Transfection (HeLa cells)

Calcium phosphate transfection was performed using the Promega Calcium Phosphate ProFection Mammalian Transfection System. $3x10^5$ HeLa cells were plated in a 10cm plate. The following day 30µg of plasmid DNA was mixed with 250µl HEPES 2x Buffered Saline (HBS) and 250µl H_2O. 30µl of 2.5M $CaCl_2$ was added to each tube, mixed and incubated at room temperature for 20 minutes. This was added drop by drop to the cells. Media was changed the next day and cells were harvested after 48 hours and washed twice in PBS.

2.2.1.5 Effectene Transfection (HEK293-ZKO and HEK cells)

Cells were plated in 6-well plates at $4x10^5$ cells per well in 2mls of media. Transfection was done using the Qiagen Effectene Transfection Kit. 0.8µg plasmid DNA was combined with 100µl EC buffer and 3.2µl enhancer. This was vortexed and incubated for 5 minutes at room temperature. 4µl of effectene was added, then vortexed and incubated for 10 minutes at room temperature. 1ml of RPMI medium was added and the mixture was added directly to the well. Cells were incubated for 48-96 hours before harvesting. Cells were washed twice in PBS and harvested.

2.2.1.6 FACS

Cells were transfected with a GFP vector along with the experimental expression vector. A fraction of cells were analysed by flow cytometry to determine the transfection efficiency as shown by the proportion of cells expressing GFP.

A second fraction of cells were resuspended in 500µl 80% ethanol and incubated at 4°C for one hour. Cells were centrifuged at 145 xg for 5 minutes and the cell pellet was resuspended in 200µl propidium iodide (PI) stain. 5µl of RNAseA was added to each sample and samples were incubated at room temperature in the dark for 20 minutes. The distribution of cells in the cell cycle was determined by flow cytometry to detect the amount of fluorescent PI bound to DNA in each cell.

2.2.2 Protein Gels

2.2.2.1 SDS-PAGE

Cells were washed in PBS and lysed in an equal volume of Laemmli Protein Sample buffer (Sigma). Samples were vortexed for 30 seconds, heated for 10 minutes at 95°C and spun at >10,000xg for 10 minutes. Samples were loaded into a pre-cast 12% Bis-Tris NuPAGE gel (Invitrogen) or a 12% homemade gel (see below). Seeblue marker (Invitrogen) was loaded into one lane for size determination. NuPAGE gels were run for 50 minutes at 200 volts in MOPS SDS running buffer (Invitrogen).

2.2.2.2 Acrylamide gels

Gels were made using a BioRad Mini-PROTEAN 3 gel casting system.

Resolving gel mix for 12% gel

40ml 30% Protogel (37.5:1 Acrylamide to Bisacrylamide) (National Diagnostics)
26ml Protogel resolving buffer
34ml H_20

Stacking gel mix

22ml 30% Protogel (37.5:1 Acrylamide to Bisacrylamide) (National Diagnostics)
25ml Protogel stacking buffer
53ml H_2O

To initiate polymerisation of 10ml of resolving gel mix, 40µl of ammonium persulfate and 5µl of TEMED were added. This was poured into the mould to 1cm below the bottom of the wells, layered with butan-1-ol and allowed to polymerise. 20µl of ammonium persulfate and 4µl of TEMED to was added to 5ml of stacking gel mix. Butan-1-ol was removed from the mould and polymerising stacking gel mix was poured in. The well comb was put in and the gel left to polymerise. Samples were loaded and run for 50 minutes at 200 volts in 1x Tris-Glycine SDS buffer.

2.2.2.3 Western Blotting

Following electrophoresis, proteins were transferred onto a nitrocellulose membrane in a Bio-Rad Transblot tank for 90 minutes at 75V in transfer buffer. To check proteins

had transferred to the membrane, it was incubated with PonceauS red stain (Sigma) for one minute with agitation and then rinsed with deionised water to remove background staining and reveal protein bands. The membrane was then blocked for 1 hour in blocking solution. The blots were incubated overnight with agitation at 4°C with the primary antibody. The following day membranes were washed three times in PBS-Tween for 10 minutes. A secondary horseradish peroxidase linked antibody was selected against the animal in which the primary antibody was generated. Detection was performed by incubating the membrane with the secondary antibody for one hour. For some blots a three layer western blot was carried out, with rabbit-α-mouse immunoglobulins as the secondary antibody and protein A-HRP as the tertiary antibody. Membranes were again washed three times for 10 minutes with PBS-Tween after antibody incubation. The immune complexes were observed using enzymatic chemiluminescence (ECL).

To detect proteins the membrane was incubated with equal amounts of ECL buffer A and buffer B for one minute. Buffer was removed and the membrane was covered with saran wrap. A piece of film was exposed to the ECL treated membrane in a cassette and developed to reveal antibody specific bands.

2.2.3 *In vitro* transcription and translation

2.2.3.1 *In vitro* transcription

In vitro transcription was performed using Promega RiboMAX Large Scale RNA Production Systems. Plasmid DNA was linearised using an appropriate restriction enzyme prior to the transcription reaction.

Reactions from the SP6 promoter were assembled as follows:

Component	**Volume**
SP6 5x Transcription Buffer	20µl
rNTPs (100mM)	20µl
linear plasmid DNA (1µg/µl)	10µl
Nuclease free H_2O	40µl
SP6 Enzyme mix	10µl
Total	**100µl**

Reactions were incubated at 37°C for 4 hours.

For genes under control of the T7 promoter, reactions were assembled as follows:

Component	**Volume**
RiboMAX Express T7 2x Buffer	10µl
linear plasmid DNA (1µg/µl)	1µl
Nuclease free H_2O	7µl
T7 Express Enzyme mix	2µl
Total	**20µl**

Reactions were incubated at 37°C for 30 minutes.

In order to remove template DNA RQ1 RNase-free DNAse was added to both reaction types at a concentration of 1U/1µg template DNA and incubated at 37°C for 15 minutes.

2.2.3.2 Phenol-chloroform extraction and ethanol precipitation

RNA was extracted using phenol-chloroform extraction and ethanol precipitation. One volume of phenol:chloroform:isoamyl alcohol (25:24:1) was added to the sample and mixed by vortexing for one minute. Samples were centrifuged at 4°C for two minutes at >10,000xg, forming distinct separation between the upper aqueous and lower organic phases. The aqueous phase was transferred to a new tube and one volume of chloroform:isoamyl alcohol (24:1) was added. The components were mixed and spun as previously. The aqueous phase was transferred to a fresh tube and spun for ten seconds at >10,000xg to sediment any residual chloroform which was removed from the bottom of the tube. 0.1 volumes of 3M sodium acetate and 2.5 volumes of ethanol were added to the sample. Samples were incubated on ice for five minutes then spun at >10,000xg for ten minutes at 4°C. The liquid layer was removed leaving the white RNA pellet at the bottom of the tube. The pellet was washed with 70% ethanol then spun as previously for 3 minutes. Any remaining liquid layer was removed and the tubes were air dried for five minutes. RNA was resuspended in H_2O to the starting volume and quantified using an eppendorf BioPhotometer.

2.2.3.3 *In vitro* translation

In vitro translation was performed as below using the Promega Rabbit Reticulocyte Lysate Translation System (Nuclease-Treated).

Component	**Volume**
Rabbit Reticulocyte Lysate	35 µl
Amino acid -minus methionine (1mM)	1 µl
RNasin Ribonuclease inhibitor (40U/µl)	1 µl
RNA (1µg/µl)	2 µl
[^{35}S] methionine	2 µl
Nuclease free H_2O	9 µl
Total	**50 µl**

Reactions were incubated at 30°C for 90 minutes.

Negative control reactions containing all components except RNA were also performed.

2µl of each reaction was run with Laemmli sample buffer on a NuPAGE Novex 12% Bis-Tris gel (Invitrogen) in MOPS buffer at 200V for 50 minutes. The gel was fixed in fixing solution and dried under vacuum. Gels were exposed overnight to an Amersham Phosphor Storage screen and detected by phosphorimaging using a Molecular Dynamics STORM 860 phosphorimager. Relative signal strength was determined using ImageQuant software version 5.1 (Molecular Dynamics). Proteins were diluted with negative control reaction to ensure equivalent concentration for subsequent EMSA experiments.

2.2.4 Molecular Biology

2.2.4.1 Polymerase Chain Reaction (PCR)

Primers were prepared to a 100 µM stock concentration and then to a working concentration of 10 µM in nuclease free water.

Each PCR reaction was prepared as below:

10X Pfx Buffer	5.0 µl
10 mM dNTPs	1.5 µl
50 mM $MgSO_4$	1.0 µl
Forward primer (10 µM)	1.5 µl
Reverse primer (10 µM)	1.5 µl
Platinum Pfx DNA polymerase	0.5 µl
Template DNA (1-200ng)	0.5 - 1.5 µl
dH_20	to 50 µl

Reactions were amplified on a Techne TC-512 PCR machine using the cycling conditions below:

94°C	2 minutes	
94°C	15 seconds	30 - 35 cycles
50-65°C	30 seconds	
68°C	60 seconds	
4°C	hold	

The annealing temperature used varied between 50°C and 65°C, dependent on the melting temperature of the primers used, according to the following formula:

Primer melting temperature = 4(G + C) + 2(A + T)°C

Following a PCR reaction, samples were purified using QIAquick columns (Qiagen), following the protocol of the QIAquick PCR Purification Kit (Qiagen). DNA was stored at -20°C.

2.2.4.2 Determination of nucleic acid concentration

The concentration of DNA and RNA was determined using an Eppendorf BioPhotometer by measuring the absorbance of a sample at two wavelengths; 260 and 280 nm. Distilled water was used as a blank reading and 1 µl sample was added to 49 µl distilled water and the absorbance was read at both wavelengths.

The ratio of 260/280 determines the purity of the sample; a ratio of approximately 2.0 is expected for pure RNA and a ratio of approximately 1.8 is expected for pure DNA.

2.2.4.3 Agarose Gel Electrophoresis

1-2% agarose gels were used to analyse DNA. The percentage agarose (w/v) was resuspended in 1X Tris-Borate EDTA (TBE) and heated until the agarose was completely dissolved. When partially cool, 1 µl of 1000 X Ethidium bromide per ml of solution was added. The gel was poured into a mould and a comb added to create the wells. 1 X loading buffer was added to samples. A molecular weight marker of either PstI or HindIII λ DNA (Sigma) was run alongside samples. Gels were run in 1 X TBE buffer for up to sixty minutes at 100 volts and was visualised under UV light using a Uvitech BTS-2.M.

PCR products and digested vectors were extracted from agarose gels using a QIAquick Gel Extraction Kit (Qiagen) following the standard protocol.

2.2.4.4 Genomic DNA Extraction

DNA was extracted from cells using Promega Wizard Genomic DNA extraction kit. 600µl of Nuclei Lysis solution was added to each cell pellet and pipetted to lyse cells. 3µl RNaseA (4mg/ml) was added and incubated at 37°C for 30 minutes then cooled to room temperature. 200µl Protein Precipitation solution was added, vortexed and chilled on ice for 5 minutes. Samples were centrifuged for 4 minutes at >10,000xg. DNA was precipitated from the supernatant using ethanol precipitation. DNA was rehydrated in 100µl H_2O.

2.2.4.5 Isolation of total RNA

RNA extraction was performed using Qiagen RNeasy kit. Cells were harvested and centrifuged at 167xg for 10 minutes. Pellets were resuspended in 350µl lysis buffer and 350µl of 70% ethanol was added. Samples were loaded into a RNeasy column, centrifuged at >10,000xg for 15 seconds and flow-through was discarded. 700µl of washing buffer was loaded into column, centrifuged at >10,000xg for 15 seconds and flow-through was discarded. A second 500 µl wash using a washing buffer containing

ethanol was performed using same centrifugation steps. This was repeated twice. RNA was eluted into a clean tube using 40µl of RNAse-free water and RNA was stored at -20°C.

2.2.4.6 cDNA synthesis

cDNA was synthesised from total RNA extracted from cells using the ImPromII Reverse Transcription System (Promega). 1µg of RNA was mixed with 0.5µg of Random Primer in 5µl. This was incubated at 70°C for 5 minutes and placed on ice for 5 minutes. The following reverse transcription mixture was assembled:

Component	**Volume**
RNA + random primers	5.0 µl
ImPromII 5x reaction buffer	4.0 µl
$MgCl_2$ (25mM)	3.2 µl
dNTPs mix (10mM)	1.0 µl
RNasin RNAse inhibitor (20U)	0.5 µl
ImPromII Reverse transcriptase	1.0 µl
RNase free H_2O	To a final volume of 15µl

This was incubated at 25°C for 5 minutes to anneal random primers to RNA. Extension was performed at 42°C for 1 hour. The enzyme deactivated at 70°C for 15 minutes. cDNA samples were stored at -20°C.

2.2.4.7 Quantitative Real-Time PCR (QPCR)

A standard curve of each primer set was created from an undiluted sample using a dilution series of the DNA for each primer set individually.
Samples were diluted 1/10. A master-mix with the following components was made and dispensed into wells of a 96-well plate:

Component	**Volume**
SYBR Green (Qiagen)	12.5 µl
Forward primer	1.0 µl (10µM)
Reverse primer	1.0 µl (10µM)
H_2O	9.5 µl

1µl of each sample (in duplicate) was added to the master-mix.

The QPCR reaction conditions using an Applied Biosystems 7500 Realtime PCR system were:

50°C	2 minutes		
95°C	10 minutes		
95°C	15 seconds	}	40 cycles
60°C	1 minute	}	
95°C	15 seconds		
60°C	1 minute		
95°C	15 seconds		

The QPCR results were analysed using ABI 7500 system SDS software, ensuring sample values fell within the standard curves obtained.
Melting curve analysis was performed for each reaction to ensure contamination, mispriming or primer-dimer artefact was not affecting results.

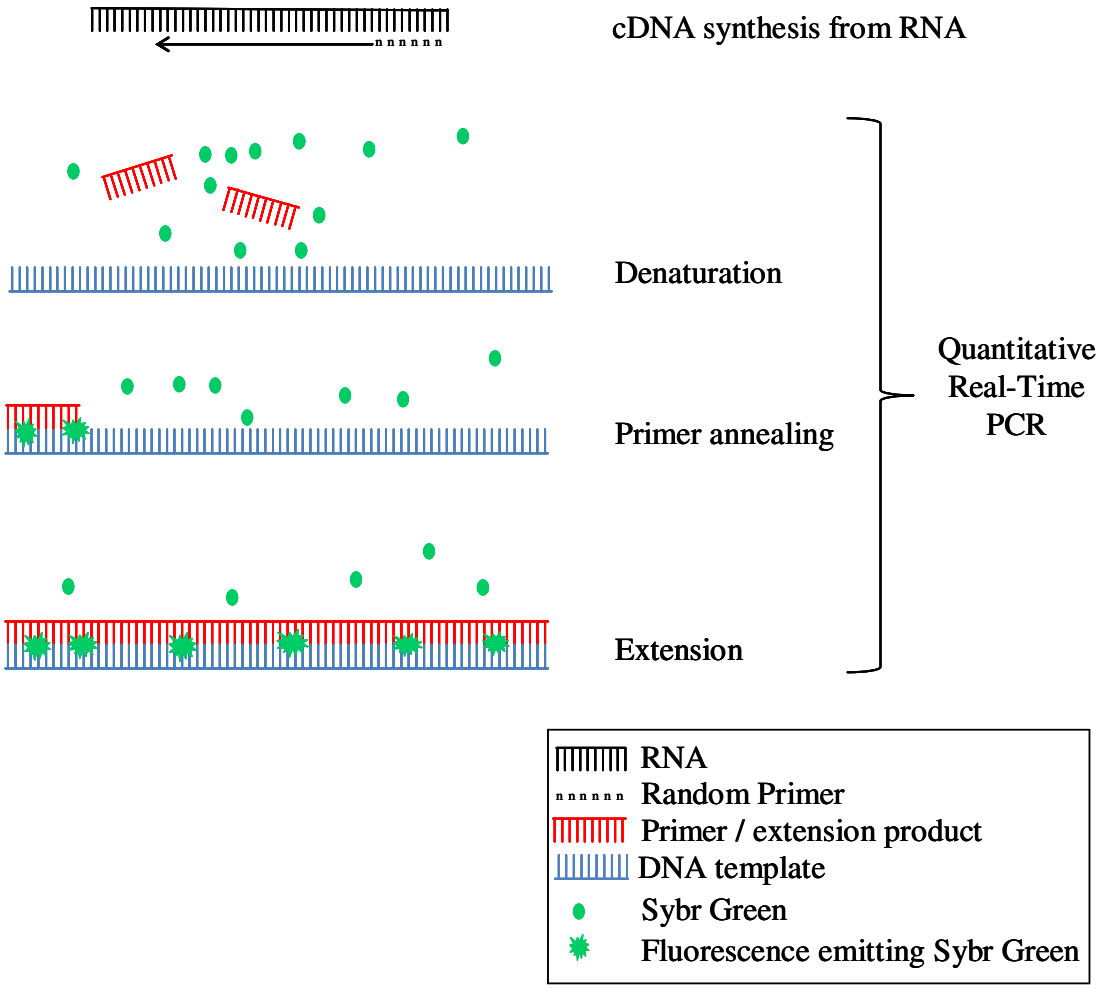

Figure 2.7: Diagram of SYBR Green Quantitative Real-time PCR
cDNA is synthesized from RNA via reverse transcription. cDNA is denatured and specific primers anneal in the prescence of Sybr Green dye. Sybr Green binds to double stranded DNA causing fluorescence. The level of fluorescence is measured during each cycle of amplification, allowing quantification of the DNA product.

2.2.4.8 Site directed mutagenesis

Site directed mutagenesis was performed using mismatched primers to introduce the desired sequence change. Primers were designed with the desired mutation in the middle of the primer with 10-15 matching bases either side.

Component	**Volume**
10x pfx buffer	5.0 µl
$MgSO_4$ (50mM)	1.0 µl
dNTPs (10mM)	1.5 µl
Forward primer	1.5 µl
Reverse primer	1.5 µl
Template DNA (50µg/µl)	1.0 µl
pfx enzyme	1.0 µl
H_2O	37.5 µl
Total	**50.0 µl**

PCR conditions:

Temperature	Time	
95°C	5 minutes	
95°C	30 seconds	} 18 cycles
55°C	1 minute	
65°C	4 minutes	
68°C	7 minutes	

PCR products were incubated with 1µl Dpn1 enzyme for 1 hour at 37°C to specifically digest the methylated template DNA.

2.2.4.9 Subcloning

The vector and DNA insert were digested using the same restriction enzymes for one hour at 37°C. The vector reaction was treated with alkaline phosphatase for 1 hour at 37°C to remove the 5'phosphate group and stop re-ligation of the plasmid DNA. DNA insert and vector were run on a 1% agarose gel and purified using the Qiagen gel extraction kit. The vector and insert were ligated at a 1:3 ratio, with 1 unit of T4 DNA

ligase and 1µl of ligase buffer (10X) to a final volume of 10µl. The reaction was placed at 4°C overnight. Modifications to ligation ratio, enzyme concentration and temperature were used when the initial ligation was unsuccessful. Colonies were picked and amplified, and plasmids extracted using Qiagen mini prep kit. To ensure the presence of the insert, the plasmid was digested with the same restriction enzymes and analysed by agarose gel electrophoresis. Samples were sent for sequencing (MWG Biotechnology) for confirmation.

2.2.5 Microbiology

2.2.5.1 Creating Competent Bacteria

Under aseptic conditions Top 10 bacteria (Invitrogen) were streaked on to an LB agar plate and incubated overnight at 37°C. A single colony was picked from the plate and grown overnight in 20 ml LB broth without antibiotic at 37°C, shaking at 220 rpm. The overnight culture was diluted in 100 ml LB broth and transferred to a 2 L flask, then returned to the heated shaker until the optical density at 600 nm wavelength (OD600) was in the range of 0.5-0.9. A further 400 ml LB broth was added to the culture and grown until the OD600 was 0.6. Cultures were swirled in a water ice bath to cool, and then centrifuged at 2683xg for fifteen minutes. Cells were resuspended in 100 ml TFBI buffer then centrifuged at 2683xg for eight minutes. Pellets were resuspended in 20 ml ice cold TFBII buffer. 100 µl aliquots of bacterial cells were frozen at -80°C.

2.2.5.2 Transformation

1µl of plasmid DNA was added to chemically competent cells (E. coli equivalent to Top10), and incubated on ice for 30 minutes. Samples were heat shocked at 42°C for 30 seconds following by the addition of 250µl of S.O.C. medium (Invitrogen) and incubated in a shaker at 220 rpm for 1 hour at 37°C. Bacteria were streaked onto a LB agar plate containing 100µg/ml of ampicillin.

Qiagen mini and maxi preps were performed as recommended in the kit.

2.2.6 Electrophoretic Mobility Shift Assay (EMSA)

2.2.6.1 Probe labelling

For EMSA reactions oligos approximately 25 bp long with the 7 bp binding site in the centre were utilised.
The following reaction was performed to generate an end- labelled oligionucleotide:

Component	**Volume**
10µM oligionucleotide a	1.0 µl
^{33}P γATP (25 µCi)	5.0 µl
PNK enzyme	0.5 µl
10x PNK buffer	1.0 µl
Ultrapure H_2O	2.5 µl

The reaction was incubated at 37°C for 30 minutes, then heated at 65°C for 10 minutes to inactivate the kinase enzyme.

2µl of 10µM unlabelled complementary reverse probe was added. This was then denatured at 95°C for 2 minutes and annealed at 65°C for 10 minutes and 37°C for 30 minutes. 90µl of TE buffer was added to each reaction and purified using G25 spin columns to remove unlabelled nucleotides. 200µl of TE buffer was added to the purified probe. This double stranded, radiolabelled DNA probe was now ready for use in EMSA reactions.

2.2.6.2 Electrophoretic Mobility Shift Assay (EMSA)

The following components were assembled for EMSA reactions:

Component	**Volume**
in vitro translated protein	0.5 - 2.0 µl
5x binding buffer	2.0 µl
0.1M DTT	0.4 µl
labelled probe	1.0 µl
H_2O	To final volume of 10µl

Reactions were incubated at room temperature for 20 minutes.
1µl or 0.5µl of protein was respectively used for ½ and ¼ size reactions. A control containing all reaction components, except RNA in the *in vitro* translation (IVT), controls for binding by proteins contained in the Rabbit reticulocyte lysate. A reaction containing no protein was also included.

2µl of 5x Novex TBE Hi-Density Sample Buffer (Invitrogen) was added to each sample then run on a Novex 6% DNA retardation gel (Invitrogen) with 0.5x TBE buffer at 100V for 45 minutes. Gels were fixed in fixing buffer for 1 hour then dried under vacuum and exposed to a phosphor storage screen. Results were visualised using a phosphor imager (Molecular Dynamics Storm 860). Quantitation of band size was used to determine the relative binding efficiencies. It was important to determine that there was excess probe in each reaction, seen as bands at the bottom of the gel. This determines that the binding reaction is not limited due to lack of probe.

2.2.6.3 Competition EMSA

In addition to the components for an EMSA reaction, unlabelled double-stranded test competitor probe was created for each probe to be assessed. 50µl of each 10µM probe were mixed then denatured at 95°C for 2 minutes and annealed at 65°C for 10 minutes and 37°C for 30 minutes. This unlabelled test competitor probe was diluted to 6x, 10x, 20x, 50x, 75x and 100x strength of the probes.

A labelled standard probe that was known to produce strong EMSA reactions was selected and the following reactions were assembled:

Component	**Volume**
5x binding buffer	2.0 µl
0.1M DTT	0.4 µl
labelled standard probe	1.0 µl
unlabelled test competitor probe (6x-100x)	1.0 µl
in vitro translated protein	0.5 - 2 µl
H_2O	To final volume of 10µl

Proteins were added after probes to reactions to ensure equal binding time for each probe.
Reactions were incubated for 20 minutes, then analysed on a single gel as for EMSA reactions.

2.2.7 Luciferase Assay

2.2.7.1 SssI methylation

10µg of vector was incubated with 50U SssI enzyme, NEB Buffer 2 (to 1x), 1 µl of 32mM S-adenosylmethionine (SAM) and H_20 for 1 hour at 37°C. The reaction was stopped by incubating at 65°C for 20 minutes. Mock-methylation reactions excluding enzyme were also performed for each vector as a control. Reactions were digested with the methylation-dependent restriction enzyme BstUI, which is unable to digest CpG methylated DNA. Protection from digestion in this reaction confirmed methylation.

2.2.7.2 Luciferase Assay

Transfected cells were harvested after 24 hours, washed in PBS and lysed with 900µl of 1x Luciferase Cell Lysis Reagent (Promega). Cell lysates were collected by centrifugation. 20µl of each sample was added in duplicate to a 96 well plate. 50µl of Luciferase Assay Reagent was added to each well. Bioluminescence was measured for a 10 second read on a luminometer using Stingray software (Dazdaq).

2.2.8 Pulldowns

HEK293 cells were co-transfected with vectors containing pBabe his-Zta and flag-pcDNA3 experimental vector, as well as controls comprised of his-Zta or experimental vector with the complementary empty vector (pBabe or flag-pcDNA3). Cells were harvested and lysed with lysis buffer after 48 hours. Samples were placed on ice for 30 minutes then underwent three freeze/thaw cycles (freezing with liquid nitrogen and thawing at 37°C). Samples were spun at 380xg for 10 minutes. HIS-Select Nickel Affinity Gel was washed 3 times in wash/Nickel binding (binding) buffer then resuspended in binding buffer. Sample supernatant was incubated with the gel overnight rotating at 4°C. Samples were spun at 380xg, 4°C for 2 minutes. The supernatant was removed and kept for analysis. The gel was washed three times as previously then the starting volume of binding buffer was added. 1 volume of sample

buffer was added before denaturing at 95°C for 10 minutes and running on a protein gel. Gels were then western blotted with BZ1 and flag antibodies.

Chapter 3 Methylation of Zta Response Elements

3.1 Introduction

3.1.1 DNA Methylation

Methylation of DNA is an epigenetic mechanism typically associated with negative regulation of gene expression. It plays a crucial role in modulating expression of both cellular and viral genes. DNA methylation typically occurs at CpG motifs. DNA methyltransferase enzymes convert the cytosine residue on both strands to 5-methylcytosine (Figure 3.1A). The cytosine methyl donor is S-adenosyl methionine (SAM), yielding S-adenosyl homocysteine (SAH) and 5-methylcytosine (Klose and Bird, 2006). As CpG motifs are palindromes, full methylation consists of two methylated cytosine residues positioned diagonally on complementary DNA strands (Figure 3.1B). The DNA methyltransferase enzyme DNMT1 acts on hemi-methylated DNA to methylate the complementary cytosine, for example during DNA replication, thus maintaining full methylation of the CpG site.

CpG motifs are often arranged in clusters called CpG islands, which are present in the 5' regulatory regions of many genes. These regions are predominantly unmethylated and are often sites of transcription initiation (Deaton and Bird, 2011). Control of gene expression via DNA methylation occurs via two mechanisms; inhibition of transcription factor binding to DNA recognition sequences that are methylated and methyl-CpG-binding proteins and associated co-repressors leading to transcriptional silencing and chromatin remodelling in areas of DNA methylation (Klose and Bird, 2006).

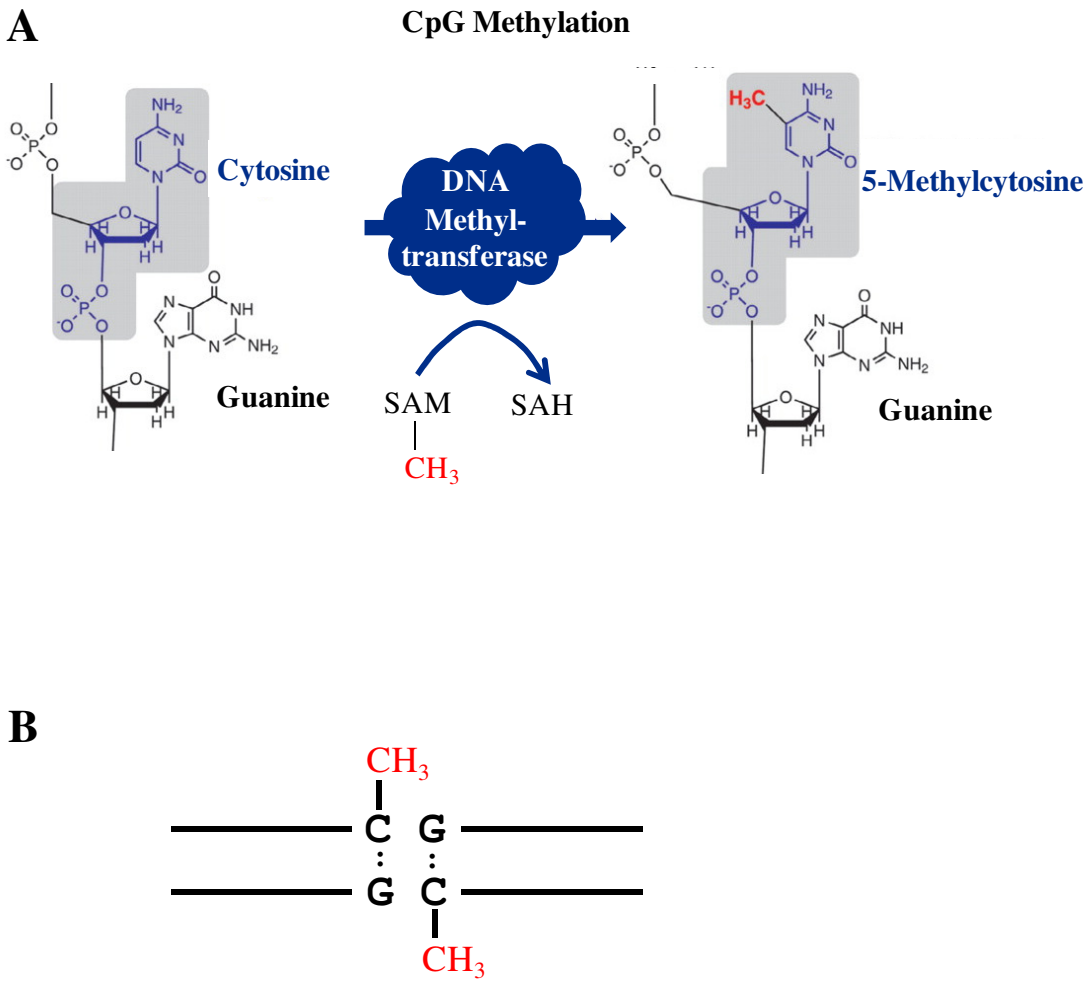

Figure 3.1: CpG methylation
A. Mechanism of CpG methylation. CpG motifs consist of a cytosine residue followed by a guanine residue. Methylation of the cytosine within a CpG motif is catalyzed by DNA methyltransferases which transfer the methyl group from S-adenosyl methionine (SAM-CH3) to cytosine. The methylation reaction yields S-adenosyl homocysteine (SAH) and 5-methylcytosine.
B. As a CpG motif is palindromic, a second cytosine is located on the complementary DNA strand.
A is adapted from (Maxwell *et al.*, 2009)

3.1.2 Methylation in EBV

EBV DNA is unmethylated when infecting cells but becomes progressively methylated by host cell processes (Kalla *et al.*, 2010), resulting in extensive methylation in latent infection (Robertson and Ambinder, 1997). Methylation of the viral DNA is an essential requirement for lytic cycle activation (Kalla *et al.*, 2010). The EBV genome is extensively methylated in both Burkitt's lymphoma and nasopharyngeal carcinoma (Lo and Huang, 2002; Li *et al.*, 2005). DNA methylation is the main control mechanism for regulating the promoter switch from Wp to Cp after primary B cell infection as well as being critical to regulation of the latency promoter Cp (Tierney *et al.*, 2000). This occurs via both direct inhibtion of transcription factor binding and recruitment of repressor proteins to methylated DNA (reviewed in (Tao and Robertson, 2003)).

The use of DNA methylation inhibitors such as 5-azacytidine in EBV related tumours may permit re-expression of viral genes, allowing recognition and specific killing by the immune system or anti-viral drugs ((Tao and Robertson, 2003).

3.1.3 Zta and Methylation

A key study by Bhende et al (Bhende *et al.*, 2004) established that methylation of ZRE2 and ZRE3 in the BRLF1 promoter enhanced the interaction with Zta. This interaction is considered crucial for lytic cycle activation.

The ability of Zta to demonstrate enhanced binding to CpG methylated, sequence specific binding sites is highly unusual for a transcription factor (Bhende *et al.*, 2004). Recently the transcription factor C/EBPα has been discovered to have enhanced binding to a methylated CRE binding site, while the same unmethylated site is preferentially bound by CREB (Rishi *et al.*, 2010). Other examples of proteins with the ability to distinguish between methylated and unmethylated DNA are proteins without specific DNA-binding ability, for example the methyl bindings MeCP2, MDB1, MDB2, MDB4 and Kaiso (Prokhortchouk *et al.*, 2001; Klose and Bird, 2006)

In the experiments conducted by Bhende et al (Bhende *et al.*, 2004) only two of the four possible CpG sites in Rp ZRE3 were methylated (ZRE3 me(-1', -2)) (Figure 3.2A). This paper did not explain why the probe was not fully methylated as is the condition *in vivo*.

As methylation of ZRE3 increases the ability of Zta to bind, I wanted to further investigate if binding was affected by using a fully methylated ZRE3 probe (ZRE3 me(-1', -2, 1', 0)), in place of the probe with two methylated sites (Figure 3.2B).

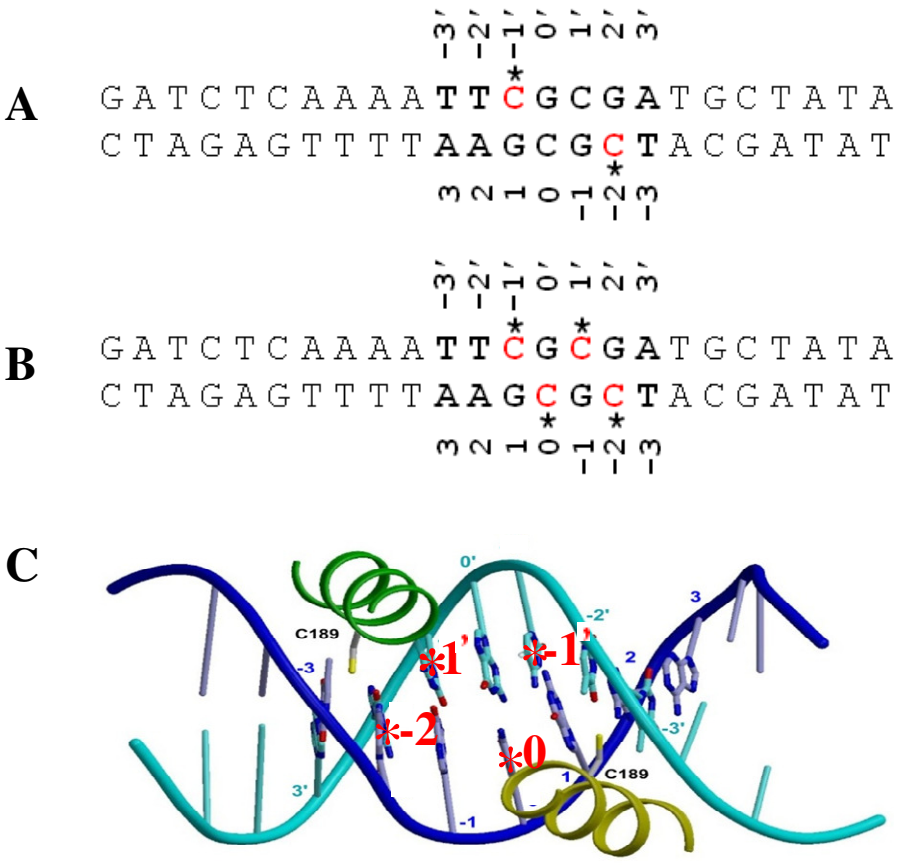

Figure 3.2: Methylation of ZRE3 EMSA probes
A. The methylation state used by Bhende et al (Bhende *et al.*, 2004) is shown. The binding site is in bold and methylated CpG motifs are marked in red with an asterisk. The latent EBV genome is likely to be fully methylated so we investigated the fully methylated probe shown in **B**. **C.** The structure of the DNA binding site of Zta from Petosa et al (Petosa *et al.*, 2006) in association with Zta, shown in green and yellow. The red asterixes show the position of the four potential methylation sites as labelled.

ZREs can be classified into three classes (Karlsson *et al.*, 2008b). Class I ZREs contains no CpG methylation sites so binding by Zta is not affected by methylation status. Class II ZREs contain a CpG site and Zta can bind to the non-methylated motif, however binding is enhanced by methylation. Class III ZRE motifs contain one or two CpG motifs. Zta is only able to bind to the methylated site and there is no or very poor binding in the unmethylated state. The gene Rta contains three ZREs in the promoter, one of each class. Rp ZRE1 is an example of a class I ZRE, Rp ZRE2 is class II and Rp ZRE3 is class III.

The DNA binding redox-sensitivity of Zta is regulated by Cys-189, a cysteine residue, located in the basic region (Wang *et al.*, 2005). A Zta mutant, ZtaC189S, containing a serine residue at this key position is unable to activate the lytic cycle (Schelcher *et al.*, 2005; Wang *et al.*, 2005) (Figure 3.3).

Competition EMSAs can be used to examine the impact of methylation on binding and to establish if ZRE3 with no methylation was compromised or completely defective in binding. This method would also examine the individual contribution of each methyl-cytosine. This could aid modelling of the interaction between Zta and the methylated ZRE3 DNA binding site (Figure 3.2C).

My initial aim in this chapter is to establish if binding to Zta is increased with a fully methylated, rather than half-methylated probe. I will also examine the individual contribution of each methyl-cytosine in the ZRE3 binding site and investigate the effect of different methylation patterns on the methylation sensitive Zta mutant C189S.

A

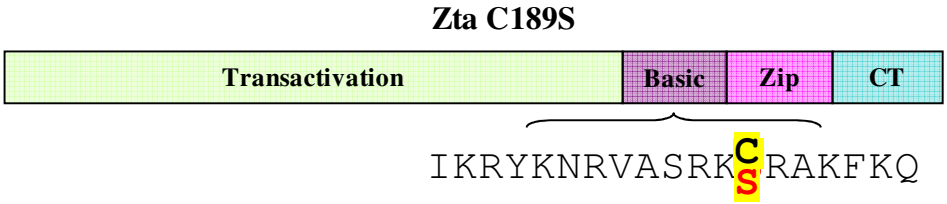

B

Function	Zta	C189S
Reactivate lytic cycle	+	-
Viral gene transactivation	+	-
Binding to ZREs	+	+/-
Dimer formation	+	+
Mediate cell cycle arrest	+	-

Figure 3.3: Summary of Zta C189S functions
A. The mutant ZtaC189S has a single cysteine residue in the basic region of Zta converted to a serine. This residue potentially has a role in redox sensitivity and is highly conserved in BZip proteins. C189S has been shown by Dr Celine Schelcher to be deficient in several key functions of Zta (Schelcher *et al.*, 2005) as summarised in **B**. C189S is unable to reactivate the lytic cycle or transactivate the viral genes *BRLF1*, *BMLF1* and *BMRF1*. Binding to ZRE ZIIIB and methylated ZRE3 was compromised while binding to ZRE2 was unaffected. C189S is able to form dimers as wild type Zta but is unable to mediate cell cycle arrest in HeLa cells.

3.2 Results

3.2.1 Competition EMSA

Electrophoretic Mobility Shift Assay (EMSA) reactions are an *in vitro* method to assess protein-DNA interactions. The protein and double-stranded DNA probe are combined to allow binding, before submitting for gel electrophoresis. If binding has occurred between the protein and DNA probe, the resulting protein-DNA complex will travel more slowly during electrophoresis. This causes a visible band shift, when compared to unbound protein and probe, confirming that binding occurred.

Competition EMSA experiments utilise the EMSA method to ascertain relative binding affinity of a protein for different binding sites (Figure 3.4). A non-labelled test competitor probe and a labelled standard probe compete for binding to the protein. A standard DNA oligo, known to bind efficiently to the protein, is radio-labelled then annealed to an unlabelled complementary oligo. This created a double-stranded, labelled EMSA probe which is used in a binding reaction with non-labelled, double-stranded test competitor probe and *in vitro* translated Zta protein. If the test competitor probe binds efficiently to the protein, less of the labelled standard will be able to bind, resulting in weaker EMSA bands. EMSA reactions are run on a non-denaturing gel, fixed, dried and quantitated using a phosphorimager.

For the following experiments the standard probe used was methylated ZRE2. This was chosen as it is has a high affinity for Zta binding. The sequence of the ZRE2 oligo is GATCATAAAATC*GCTCATAAGCTT, containing the underlined ZRE2 binding site and methylated during oligo synthesis as indicated with an asterix. This approximate length of oligo is used to provide surrounding sequence to facilitate binding to the specific site in the centre of the probe but is short enough to limit the possibility of other potential binding sites. This was radio-labelled with ^{33}P γATP before annealing to create a labelled, double-stranded probe.

A constant amount of labelled standard probe was used in each reaction with an increasing amount of unlabelled ZRE3 test competitor probe (6x, 10x, 20x, 50x, 75x and 100x excess).

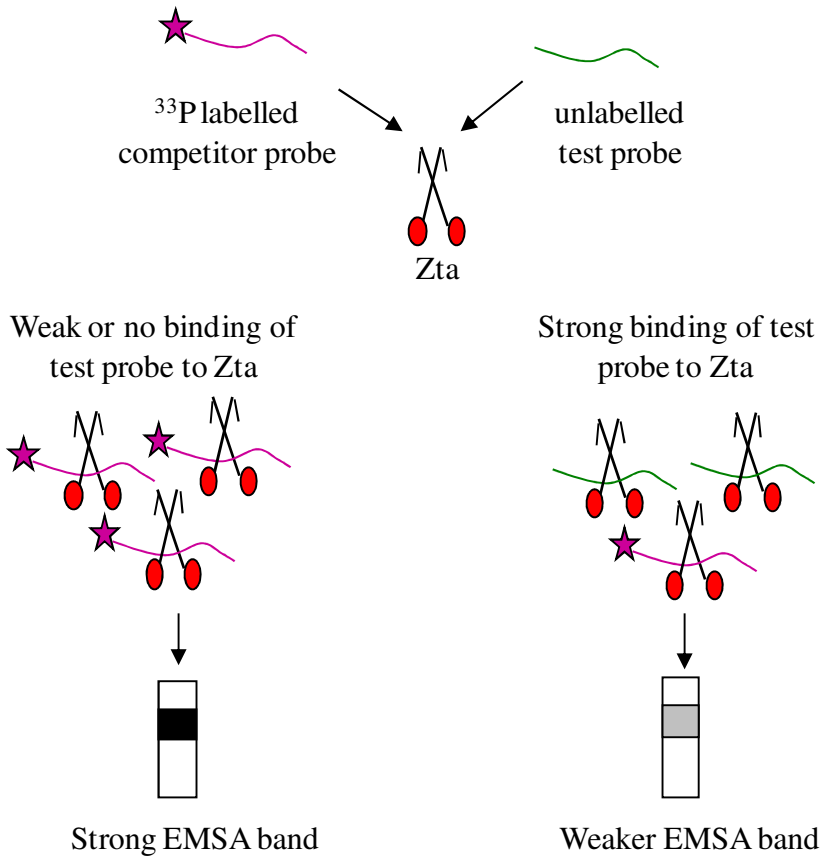

Figure 3.4: Schematic of Competition EMSA method

A probe that is known to bind well to Zta was radiolabelled with [^{33}P]. In the following experiments ZRE2 (GATCATAAAATCGCTCATAAGCTT) was used. A constant amount of this competitor probe was added with unlabelled test probe (ZRE3) to unlabelled *in vitro* translated Zta protein in an EMSA binding reaction. If the test probe is unable to bind efficiently to Zta there is no competition to the labelled probe, resulting in a strong EMSA band, as seen in the left panel. However if the test probe is a strong binding partner for Zta, less binding to the competitor probe will occur, giving a weak EMSA band as seen on the right.

In the initial experiment I compared binding efficiency of a ZRE3 probe methylated at two positions (ZRE3 me(-1', -2)), as used by Bhende et al (Bhende *et al.*, 2004), to unmethylated ZRE3 probe (Figure 3.5A) or fully methylated ZRE3 probe (ZRE3 me(-1', -2, 1', 0)) (Figure 3.5B). All experiments were duplicated.

The graphs in Figure 3.5C show the percentage of labelled standard probe that is competed from binding to Zta at increasing excesses of unlabelled test competitor probe. As little as 20x excess of ZRE3 me(-1', -2) was able to compete with the labelled probe for Zta binding. In contrast even 100x excess unmethylated ZRE3 probe was unable to compete. This demonstrates that methylation is absolutely required for Zta to bind to ZRE3.

Fully methylated ZRE3 me(-1', -2, 1', 0) was slightly better at competing for Zta binding than ZRE3 me(-1', -2). At 20x excess ZRE3 me(-1', -2, 1', 0) competed 16% better. This data suggests that full methylation of ZRE3 generates a stronger binding site for Zta than the version previously tested, however this would need to be repeated. As the fully methylated site is most likely to represent the situation *in vivo*, it reinforces the relevance of methylation-dependent binding to this site.

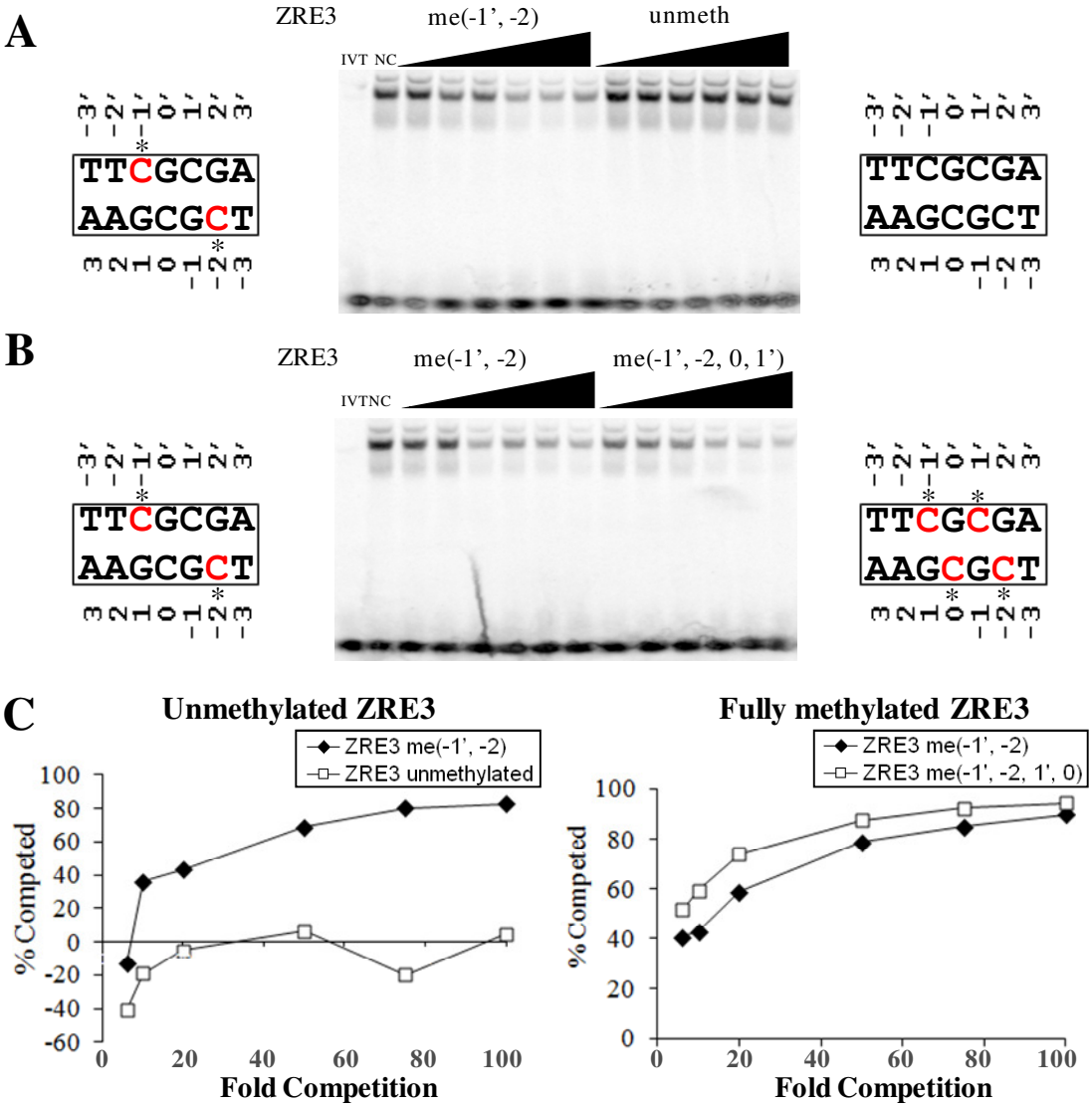

Figure 3.5: Competition EMSA of Rp ZRE3 methylation
Competition EMSAs were performed using increasing amounts of unlabelled ZRE3 competitor probe (6, 10, 20, 50, 75 and 100x excess). A constant amount of labelled probe ([^{33}P] labelled ZRE2 - GATCATAAAATCGCTCATAAGCTT) was included in each EMSA reaction. Unlabelled *in vitro* translated Zta was generated in Promega Rabbit Reticulocyte Lysate. EMSA reactions were separated on SDS-PAGE gels which were then fixed, dried and quantitated using a phosphoimager. The left hand side of each gel uses the unlabelled ZRE3 methylated probe (me –1', -2) as shown on the far left. The right hand side of each gel uses an unlabelled ZRE3 probe with the methylation status shown to the right of the gel. Panel **A** shows competition with ZRE3 unmethylated. Panel **B** tests ZRE3 with all 4 possible sites methylated (ZRE3 me(-1', -2, 0, 1')). Translation reaction omitting RNA (IVT) is a control in lane 1 and reaction with no competitor probe (NC) is lane 2. Both experiments were duplicated and quantitated in the graphs in **C**. The graphs show the average percentage of the labelled probe that is competed from binding at varying excesses of unlabelled probe.

3.2.2 Contribution of Individual Methylation Sites

I used the same technique to investigate the individual contribution of each of the four methylation sites within ZRE3. Oligos with a single methylation of each of the four possible CpG cysteines were ordered (Sigma). Each singly methylated ZRE3 oligo was used to create a double-stranded unlabelled EMSA probe. The four probes, ZRE3 me(-2), ZRE3 me(-1'), ZRE3 me(0) and ZRE3 me(1'), were used for competition EMSA using the labelled ZRE2 probe as a standard competitor. All four test probes were individually able to compete for binding (Figure 3.6). The strongest binding was demonstrated by the probe ZRE3 me(1') (Figure 3.6D). At 75x excess to the standard probe, the detected binding of the standard probe was reduced by 82%. This probe was not appreciably different at binding Zta from the half-methylated probe, ZRE3((-1', -2), used in the Bhende at al experiments (Bhende *et al.*, 2004). The other three methylation sites showed considerably lower levels of binding than ZRE3((-1', -2). However all three single sites were able to reduce standard binding at 75x excess. ZRE3 me(-2) was able to reduce standard binding by 32% (Figure 3.6A), ZRE3 me(0) produced a 15% reduction in binding (Figure 3.6C) and ZRE3 me(-1') reduced binding by 5% at 75x excess (Figure 3.6B). All experiments were duplicated.

3.2.3 ZtaC189S

The methylation sensitive mutant, ZtaC189S, may be important as a selective tool in understanding the importance of methylation dependent binding by Zta. I decided to quantify the reduced binding demonstrated by ZtaC189S using competition EMSA.

As shown in Figure 3.7A, ZtaC189S and Zta bind equally to the unmethylated version of ZRE2. However binding of ZtaC189S to methylated ZRE2 is reduced by 50% (Figure 3.7B), compared with Zta. This result was significantly different using a Mann-Whitney U test (U=16, n1 = n2 = 4, P=0.02857). Neither protein showed detectable binding to unmethylated ZRE3 in these assays. Binding to methylated ZRE3 was greatly compromised for ZtaC189S with both ZRE3 me(-1', -2) (25%) and me(-1', -2, 0, 1') (21%) (Figure 3.7 C,D). Both results were significant using a a Mann-Whitney U test (U=16, n1 = n2 = 4, p=0.02857). Experiments were repeated four times.

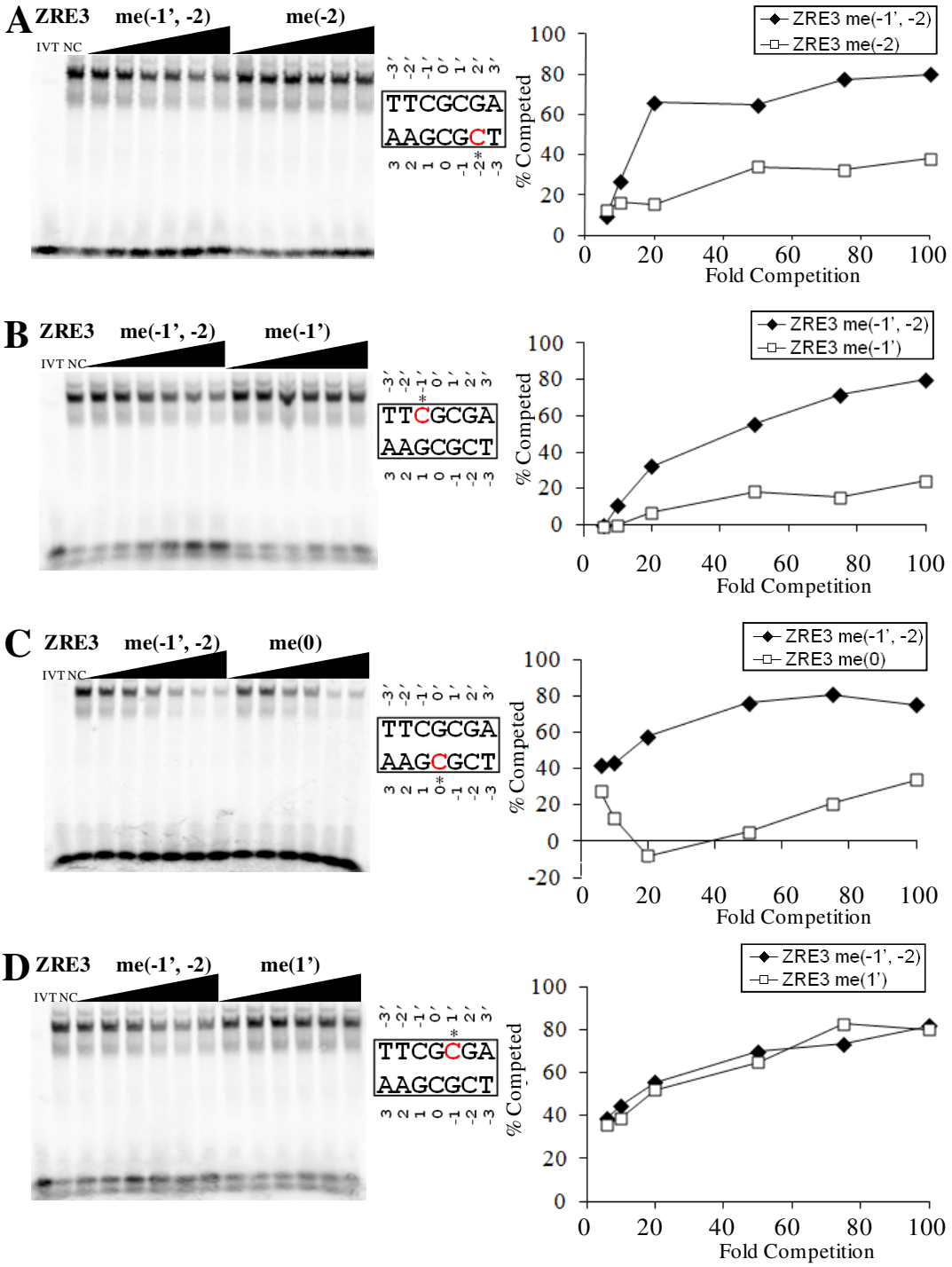

Figure 3.6: Individual contribution of ZRE3 methylation sites
Competition EMSAs were performed and analysed as in Figure 3.5. Each of the four individual potential methylation sites in Rp ZRE3 were methylated in turn as shown to the right of each gel; (**A**) ZRE3 me(-2), (**B**) ZRE3 me(-1'), (**C**) ZRE3 me(0), and (**D**) ZRE3 me(1'). Competition was compared to ZRE3 me(-1', -2).

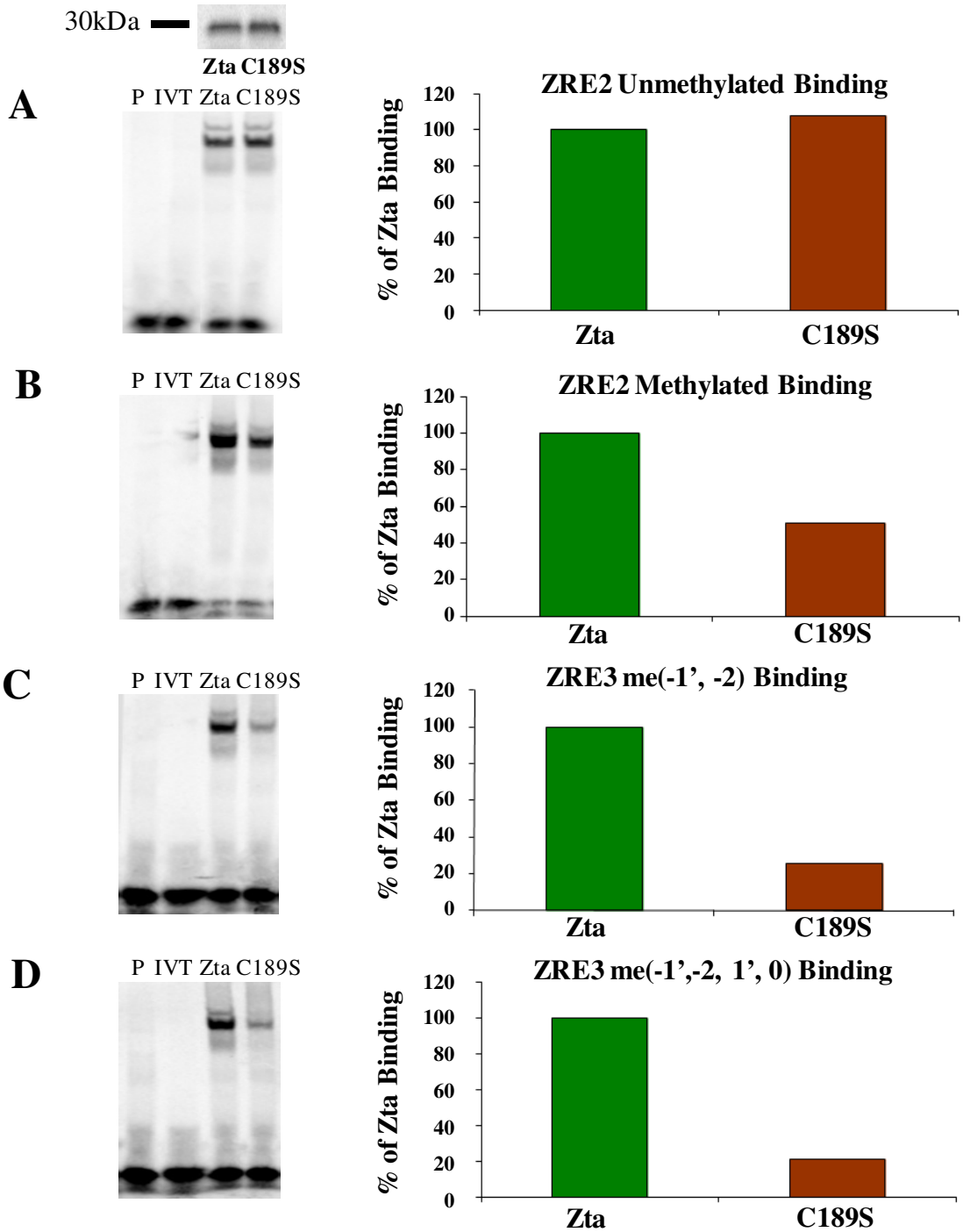

Figure 3.7: Comparison of Zta and ZtaC189S binding to Rp ZRE2 and ZRE3
EMSAs were performed on *in vitro* translated proteins Zta and ZtaC189S for unmethylated (**A**) and methylated (**B**) Rp ZRE2 and half (**C**) and fully (**D**) methylated Rp ZRE3. Input protein is shown at the top. Probe alone is in lane 1 and translation reaction omitting RNA (IVT) as a control is in lane 2. Experiments were repeated 4 times and the average percentage of Zta binding is shown.

3.2.4 Modelling

The crystal structure of Zta bound to an AP1 site (Petosa *et al.*, 2006) was the basis of structural modelling of Zta bound to methylated ZRE2 and ZRE3 performed by Carlos Petosa and colleagues at EMBL, Grenoble. Figure 3.8A describes the nomenclature used in these models, the two DNA half sites are designated left and right and the CpG motifs are 1 and 2. The difference in the modelling of ZRE2 and ZRE3 is in right DNA half-site as the 2 base-pair difference (+1 and +2) occurs at this position. The models provide an explanation for three key experimental observations; the lack of affinity for unmethylated ZRE3, enhanced binding to methylated ZRE2 and ZRE3 and loss of affinity for methylated ZRE3 by mutant C189S.

Firstly the binding affinity of Zta for unmethylated ZRE3 is greatly diminished in comparison to ZRE2 or AP1. In the crystal structure Zta makes base-specific interactions with Asn-182 and Arg-190 (Petosa *et al.*, 2006). Arg-190 interacts in an asymmetrical manner that is conserved for the ZRE sites. Asn-182 contacts via basepairs ±2 in AP1. ZRE2 is divergent at -2 and ZRE3 at +2 and -2 (Figure 3.8A). This means that the Asn-182 contact is disrupted in the left DNA half-site for ZRE2 and is completely disrupted for ZRE3. It is probable that the additional disruption of this interaction with ZRE3 accounts for the loss of affinity Zta has for this site.

The modelling can also explain the enhanced binding to ZRE2 and ZRE3 in the methylated state. Methylation of motif 1 introduces a direct contact between Cytosine$^{1'}$ methyl group and Ser-186^{Left} (Petosa *et al.*, 2006) and is further enhanced by a hydrophobic contact between Cys-189^{Left} and the cytosine^{-2} methyl group (Karlsson *et al.*, 2008a) (Figure 3.8D). Ser-186^{Left} and Cys-189^{Left} simultaneously interact with the two methyl groups that comprise motif 1. These are the 2 methyl groups (1' and -2) that I demonstrated to be able to compete most effectively for Zta binding. The position of the DNA and protein helices are not equivalent for both motifs. CpG motif 2 is offset by 1 bp relative to the bZIP helix and in contrast to motif 1, interacts with both left and right bZIP helices. The aromatic ring of cytosine$^{-1'}$ has a π-cation interaction with the guanidino group of Arg-190^{Left} (Figure 3.8B).

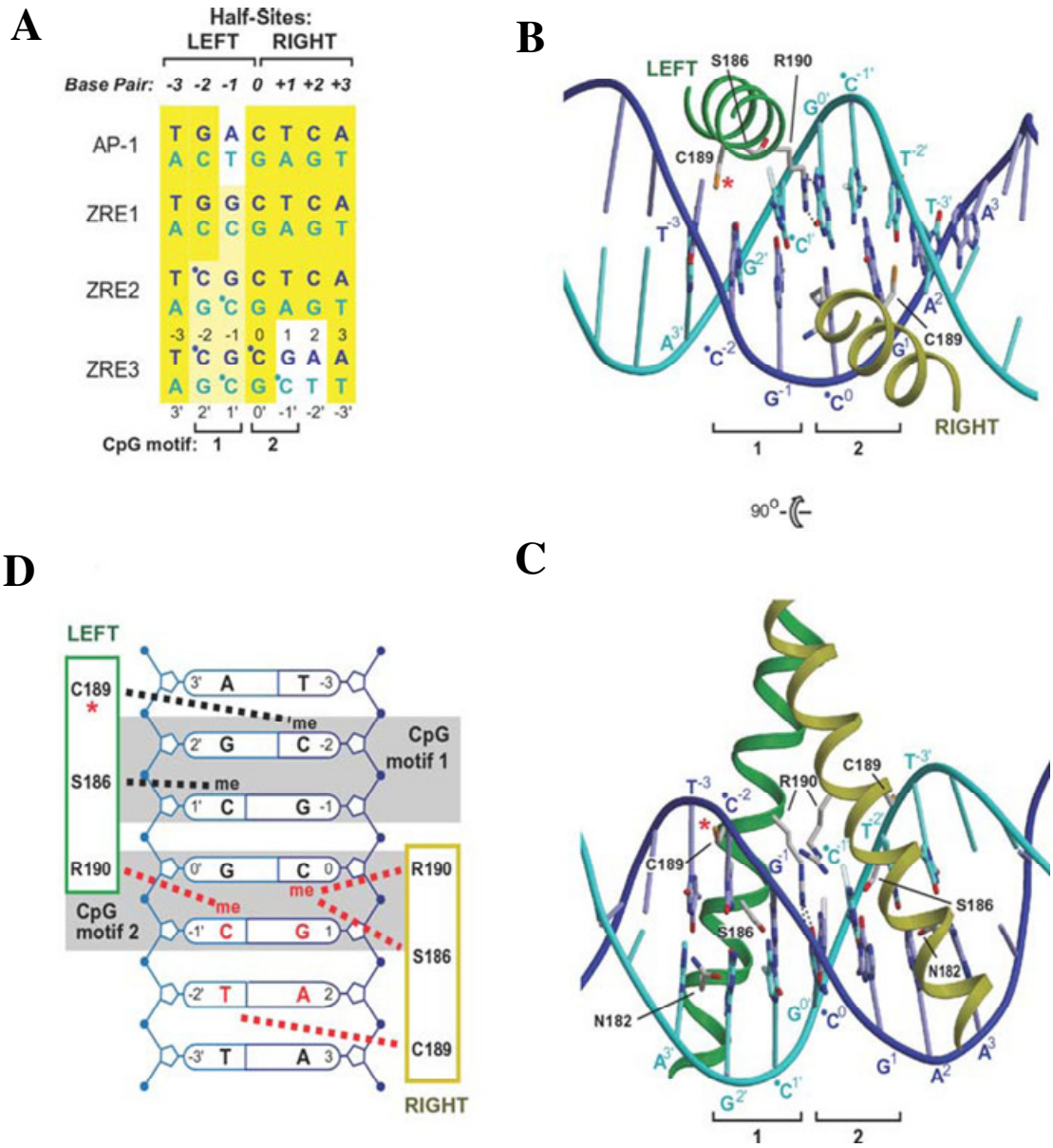

Figure 3.8: Structural model of Zta bound to meZRE3
Modelling of Zta-meZRE3 by Carlos Petosa at EMBL, Grenoble (Karlsson *et al.*, 2008a).
A. Alignment of Zta recognition sequences. The numbering convention is shown for basepair positions (bold italics) and individual nucleotides (plain font). Cytosines modified by methylation are indicated by a dot. **B**. Model of the Zta-meZRE3 complex viewed along the pseudodyad. The methylation sensitive C189 residue (red asterisk) and bidentate hydrogen bond interactions between $R190^{Left}$ and $Guanine^{0'}$ (dotted black lines) are indicated. Cytosine methyl groups are semi-transparent. **C**. Orthogonal view. The hydrophobic contact between $Cytosine^{1'}$ and $S186^{Left}$ (broken blue line) and hydrogen bond network involving $S186^{Left}$, $N182^{Left}$ and $Guanine^{2'}$ (dotted black lines) are shown. **D**. Schematic summary of contacts. van der Waals contacts involving the CpG methyl groups and Zta residues are shown as red and black broken lines.

As the methyl group is electron-donating, methylation of this residue would increase the negative charge in the π-electron system, thus enhancing the interaction. In addition there is an extra van der Waals contact with the arginine side-chain (Karlsson *et al.*, 2008a). The methyl group of cytosine^{0} interacts with Ser-186^{Right} and Arg-190^{Right} (Figure 3.8C). The models suggest contact between Zta and each of the four CpG methyl groups. This agrees with my competition EMSA experimental evidence of a contribution to binding from each of the methyl groups.

The C189S mutation dramatically reduces binding to methylated ZRE3. The modelling postulates that the methylation sensitivity of CpG motif 1 by C189^{Left} is due to a direct contact between the thiol group of C189^{Left} and the methyl group of cytosine^{-2} (Figure 3.9). This interaction would be destabilized by substitution of the hydrophobic cysteine to a more polar serine residue. This methyl group and thus interaction is common to both ZRE2 and ZRE3. This explains the decreased binding affinity as assessed by EMSA for ZtaC189S for methylated ZRE2 and ZRE3 (Figure 3.7). As the thiol-methyl contact is only present in methylated sites this also could explain why ZtaC189S has no effect on binding in unmethylated ZRE2. In motif 2, which is not present in ZRE2, the C189S residue is not close enough to form a direct bond with any cytosine methyl group. However the modelling puts C189^{Right} in van der Waals contact with the methyl group of thymidine$^{-2'}$ (Figure 3.9D). It is probable this bond would be disrupted by mutation to C189S in the same way as the symmetrically equivalent bond between cysteine^{-2} methyl group and C189^{Left}. This would mean that ZtaC189S destabilizes bonds with both half-sites in methylated ZRE3 and could explain the greatly impaired binding of ZtaC189S to meZRE3.

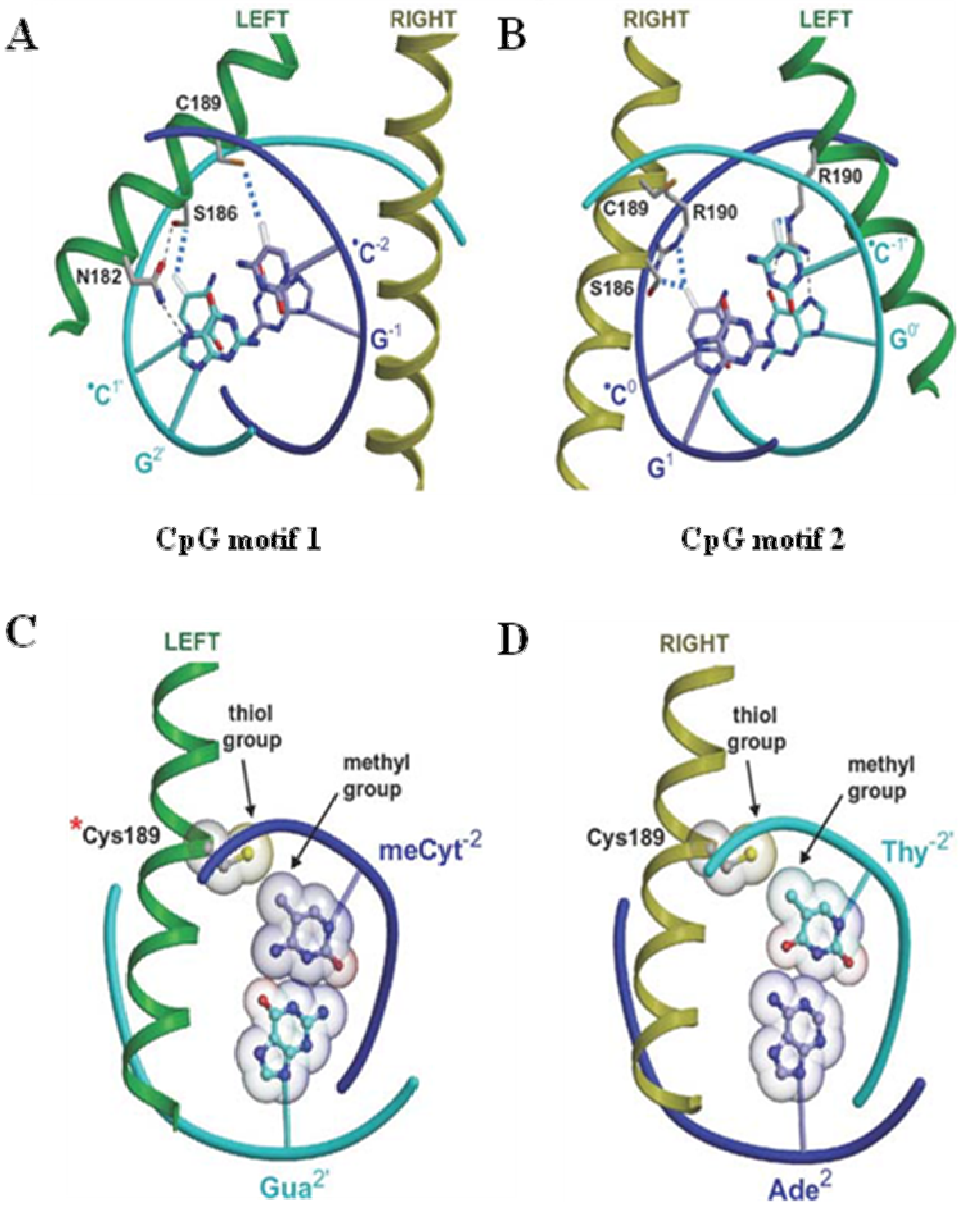

Figure 3.9: Interactions mediated by CpG motifs and C189 and S186 residues
Interactions involvingCpG motif 1 (A) and motif 2 (B) are shown in approximately the same orientation. Hydrophobic contacts are shown in dashed blue lines and hydrogen bonds as dotted black lines. Motif 1 contacts the left bZIP helix (green) only, while motif 2 contacts the Left and Right (yellow) helices of Zta. Thiol-methyl group contacts mediated by C189 in the left (C) and right (D) helices. Cys-189^{Left} contacts the methyl group of cytosine^{-2} while Cys-189^{Right} contacts the methyl group of Thy$^{-2'}$. (Karlsson *et al.*, 2008a)

3.3 Discussion

Zta was the first transcription factor identified to have the ability to preferentially bind to and activate methylated promoters. This appears to be crucial in the function of the virus as it allows a mechanism to escape the otherwise inhibitory effects of viral and potentially host genome methylation. In order to understand the mechanism behind this key ability of Zta it is necessary to elucidate the interactions between the protein and the methylated DNA binding site.

As the key previous experiments by Bhende et al. (Bhende *et al.*, 2004) had utilised a promoter that was only partially methylated, initially I sought to clarify binding of Zta to the fully methylated promoter that would be found *in vivo*. In accordance with the Bhende study (Bhende *et al.*, 2004), Zta binding to unmethylated ZRE3 was not detectable. Full methylation of ZRE3 me(-1', -2, 1', 0) created a site that was 16% better at binding Zta than the partially methylated ZRE3 me(-1', -2). This suggests that methylation at positions 1' and 0 has some additional contribution to creating a stronger Zta binding site.

Further examination of the individual contribution of all 4 methylation sites revealed that all competed for binding to varying degree, suggesting that all 4 methylated sites contribute to the interaction with Zta. The order of site strength is $meC^{1'} > meC^{-2} > meC^{0} \geq meC^{-1'}$. This reveals that the contribution to binding is strongest from CpG motif 1 that is common to both ZRE2 and ZRE3 (Figure 3.8A). The contribution to binding is weaker from CpG motif 2, which is unique to ZRE3. The modelling performed by Carlo Petosa and colleagues (Karlsson *et al.*, 2008a) suggests that residues of Zta make contact with each of the 4 methyl groups which is consistent with my results of the competition binding by each individually methylated cytosine. CpG motif 1 and CpG motif 2 are predicted to have different stereochemical environments although stronger binding by motif 1 was not explained.

C189S is unable to bind to RpZRE3 *in vivo*, while DNA binding to Rp ZRE1 and ZRE2 is maintained (Karlsson *et al.*, 2008a). This selective inhibition of DNA binding implies that Zta interaction through ZRE3 is a critical step in activation of Rp. *In vitro* it was

demonstrated that C189S is defective in binding to methylated ZRE3 (Karlsson *et al.*, 2008a), highlighting this as the potential basis of the inability of C189S to activate Rp and resultant blockage of the lytic cycle.

The Zta mutant C189S is compromised for binding to methylated ZRE3 and to a lesser extent ZRE2, while retaining wild-type level binding to unmethylated sites including ZRE1. This makes C189S valuable as a selective tool for linking the relevance of methylation specific Zta binding to the *in vivo* disruption of latency. ZtaC189S is unable to activate the expression of BRLF1 in Burkitt's lymphoma derived Raji cells (Karlsson *et al.*, 2008a), suggesting that binding to meZRE3 is essential for activation from the Rp promoter in these cells. This supports the theory that recognition of methylated ZREs is a critical step for lytic reactivation of latent EBV in B-lymphocytes. A previous study by Wang et al demonstrated ZtaC189S produced only a slight disruption to reactivation of BRLF1 (Wang *et al.*, 2005) in epithelial BZLF1-KO-293 cells. However *in vivo* lytic reactivation predominantly occurs in B-lymphocytes and the difference in activation by ZtaC189S may be a result of cellular differences in transcription factors or chromatin structure. Raji cells also display a higher level of methylation than BZLF1-KO-293 and some other epithelial cells (Bhende *et al.*, 2005). The modelling of Zta interacting with meZRE3 predicted that C189 would be sensitive to methylation of CpG motif 1 via a thiol-methyl group contact (figure 3.9C). When C189 is substituted with an A or S, this thiol-methyl contact is lost and decreased DNA-binding ability is observed (Figure 3.7). C189 also appears important in the redox sensitivity of Zta DNA-binding. Nitrosylation of C189 has been postulated as a mechanism for down-regulation of EBV reactivation by nitric oxide (Wang *et al.*, 2005). This may be a link between other ways of regulating Zta and Rp activation and methylation.

Chapter 4 Promoter Functions of Zta and ZtaRh

4.1 Introduction

4.1.1 Lymphocryptoviruses

EBV is a member of the lymphocryptovirus (LCV) genus, along with about 50 different LCVs that have been identified in both New and Old World primates (Ehlers *et al.*, 2010). Almost every species of non-human primate is naturally infected by their own LCV which are closely related to EBV. Phylogenetic trees have indicated synchronous evolution of viruses and hosts (Ehlers *et al.*, 2010). LCV genomes are organised in a collinear fashion with the EBV genome (Wang *et al.*, 2001). In general an identical repertoire of genes is present in each LCV, with greater conservation amongst lytic genes than latent genes (Wang *et al.*, 2001). Even genes with weaker homology between EBV and other LCVs such as EBNA 3A, 3B and 3C are functionally conserved, as are repeat structures (Wang *et al.*, 2001). The *in vivo* infection of the related LCVs also closely resembles the natural history of EBV infection (Wang *et al.*, 2001). Asymptomatic, lifelong infection of most occurs in infancy and LCV-induced tumours arise in immune-suppressed primates (reviewed in (Wang *et al.*, 2001)). These similarities in epidemiology and pathogenesis identify simian LCVs as a valuable model system to provide a better understanding about EBV. Despite the presence of LCVs in all Old World primates, initially it was not thought that New World primates were similarly infected as there was an absence of cross-reactive antibodies to EBV infected B cells. This would have meant that LCV infection arose late in primate evolution, approximately 25 million years ago after the divergence of New and Old World primates (Wang, 2005). The discovery of an LCV infecting New World common marmosets by Cho et al (Cho *et al.*, 2001) and evidence of related LCVs in most or all New World species (Ehlers *et al.*, 2003) means that the appearance of EBV-related viruses occurred much earlier in primate evolution, at approximately 40 million years ago.

4.1.2 Rhesus lymphocryptovirus

The complete nucleotide sequence of the rhesus macaque LCV, Cercopithecine herpes virus 15 (Ce-HV15, RhLCV) has been sequenced (Rivailler *et al.*, 2002). Every EBV

gene is represented by a homologue in the same relative position in the RhLCV genome. This identical repertoire of genes has 65% overall similarity with EBV, with 75.6% similarity in open reading frames. This provides support at a genetic level for use of RhLCV as a model system to study the pathogenesis of EBV. Proteins appear to be functionally conserved but display a range of amino acid similarity ranging from 29.4% for EBNA3A to 96.9% for uracyl DNA glucosidase. Latent genes are less well conserved than lytic genes (Wang, 2005). Conservation between the host human and Rhesus macaque genomes is approximately 93% in alignable sequence (Gibbs *et al.*, 2007).

Although they are relatively well conserved, LCVs appear to be mostly host species restricted. RhLCV is unable to immortalize human B-cells and EBV is unable to immortalize cells from rhesus macaques (Moghaddam *et al.*, 1998). This restriction occurs at a later stage than viral entry and may be due to a crucial interaction with a host protein. However immortalization between some closely related species is possible, for example baboon LCV can immortalise rhesus monkey B cells (Moghaddam *et al.*, 1998).

RhLCV has already proved valuable as a model species. For example it is not possible to study the very early stages of primary EBV infection *in vivo* before the onset of any symptoms. However RhLCV naïve rhesus macaques can be orally inoculated with the virus, allowing investigation into the very early stages of infection (Moghaddam *et al.*, 1997) with wild-type or mutant virus. Another valuable use of RhLCV is infection in immunocompromised animals, such as those infected with a simian-human chimeric immunodeficiency virus (SHIV). Infection of rhesus macaques with SHIV results in an immunodeficiency similar to human HIV infection (Reimann *et al.*, 1996). This allows investigation of specific factors that contribute to disease development in LCV infected individuals such as components of the host immune response that control the infection and alterations in LCV-infected cells. Potentially the results from experiments like this could provide strategies to prevent or treat EBV-associated cancer and disease in immunocompromised people.

Further investigation into the similarities and differences between EBV and the related LCVs could provide valuable information to improve the use of viruses such as RhLCV as a model system for EBV. In addition the other LCVs provide a tool to increase our understanding of how EBV works.

My initial aims are to examine the site specific DNA binding function of ZtaRh to investigate how it operates as transcription factor. This will include identification of potential ZREs within the RhLCV genome as well as utilisation of a promoter assay to assess functionality.

4.2 Results

4.2.1 Alignment of Zta and ZtaRh

The RhLCV protein ZtaRh is a homologue to EBV Zta. ZtaRh is a 247 amino acid protein, arranged into the same 4 domains as Zta. Overall ZtaRh displays 71.3% similarity to Zta at the protein level (Figure 4.1). The two proteins share 63% identity in the N-terminal transactivation domain and only 11% of the differences are conservative amino acid substitutions. The C-terminal third of the protein shows a higher degree of similarity (83%) with a total of only 11 amino acid differences in the basic, coiled-coil and CT regions. In contrast to the transactivation domain, 89% of the differences are conservative amino acid changes.

The ability and specificity of the ZtaRh interaction with DNA was questioned because there are two amino acid differences in the basic (DNA contact) region (K192R and Q195N) and the region immediately adjacent to the bZIP region of ZtaEBV has been shown to influence the DNA-binding specificity of Zta.

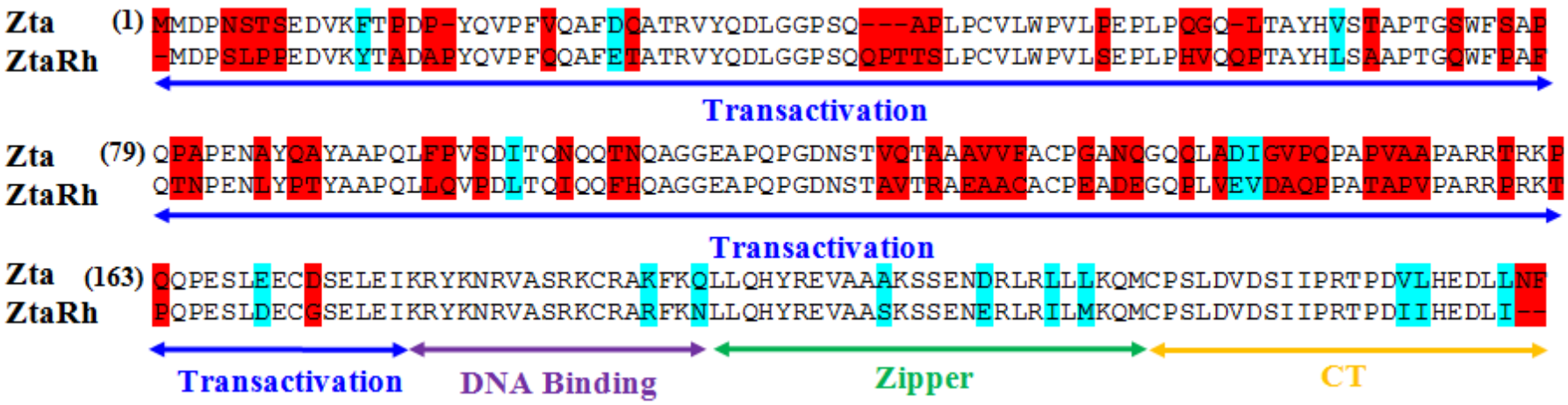

Figure 4.1: Amino acid alignment of Zta and ZtaRh proteins
The residues highlighted in blue are conservative differences and non-conservative differences are highlighted in red. The amino acid numbering of the Zta protein is bracketed to the left of the alignment. The transactivation, DNA binding, Zipper and CT domains are indicated below the residues. The alignment was originally done using Invitrogen Vector NTI.

4.2.2 Electrophoretic Mobility Shift Assay (EMSA)

The ability of ZtaRh to bind known Zta Response Elements (ZREs) was examined through Electrophoretic Mobility Shift Assays (EMSAs).

Radio-labelled Zta and ZtaRh proteins were produced from expression vectors using *in vitro* transcription and rabbit reticulocyte *in vitro* translation. The RhLCV Zta had been cloned by a previous member of the Sinclair lab, Mirjam Mayer. [^{35}S] Methionine was incorporated into the proteins during translation to allow detection on a phosphor imager.

Double-stranded ^{33}P end-labelled probes were created for six ZRE sequences that Zta is known to bind (Figure 4.2).

Figure 4.2: EMSA probe sequences
The sequences of the 8 ZRE probes used in the EMSA experiments are shown, aligned by the highlighted core binding sequence. The red cytosine bases are methylated. Probes were labelled with ^{33}P then annealed to the reverse complement oligo.

These probe sequences are all derived from ZREs within promoters or the lytic origin of replication (oriLyt) from the EBV genome (Table 4.3). The probes ZRE1, ZRE2 and ZRE3 are from the promoter of the EBV gene BRLF1. ZRE2 contains one CpG methylation site and ZRE3 contains two methylation sites. These probes were tested separately in the methylated and unmethylated forms. The AP1, ZREIIIB, ZRE1 and ZRE2 sites are fully conserved in the RhLCV genome. The ZRE used for the oriLyt probe differs by 1 base in RhLCV and ZRE3 is divergent at 4 bases as shown in Table 4.3.

ZRE probe	EBV location	EBV sequence	RhLCV
AP1	BMRF1 promoter	TGACTCA	conserved
oriLyt	ori Lyt 1	TTACACA	TTGCACA
ZREIIIB	BZLF1 promoter	TTAGCAA	conserved
ZRE1	BRLF1 promoter	TGAGCCA	conserved
ZRE2	BRLF1 promoter	TCGCTCA	conserved
ZRE3	BRLF1 promoter	TTCGCGA	TCCGGCG

Table 4.3: Location and conservation of EMSA probe ZREs
Five of the six ZRE sequences used in initial EMSA experiments are located within three different EBV promoters. oriLyt is derived from the ZRE oriLyt1 within the oriLyt-left region. The sequences of AP1, ZREIIIB, ZRE1 and ZRE2 are fully conserved in RhLCV. The divergent RhLCV sequences of oriLyt and ZRE3 are shown.

For these experiments oligos were methylated at CpG sites during synthesis (Sigma) as indicated in Figure 4.2. Equivalent amounts of each protein were used in EMSA reactions for each probe. A negative control (IVT), containing all the translation components except the RNA, was used to determine if proteins in the rabbit reticulocyte bind to the specific DNA probe used. Following quantitation of DNA-probe complexes with phospho image analysis, the binding efficiency relative to Zta was calculated (Figures 4.4, 4.5, 4.6). It was important to establish that there was excess probe in each reaction, seen as bands at the bottom of the gel. This determines that the binding reaction is not limited due to lack of probe. All experiments were duplicated.

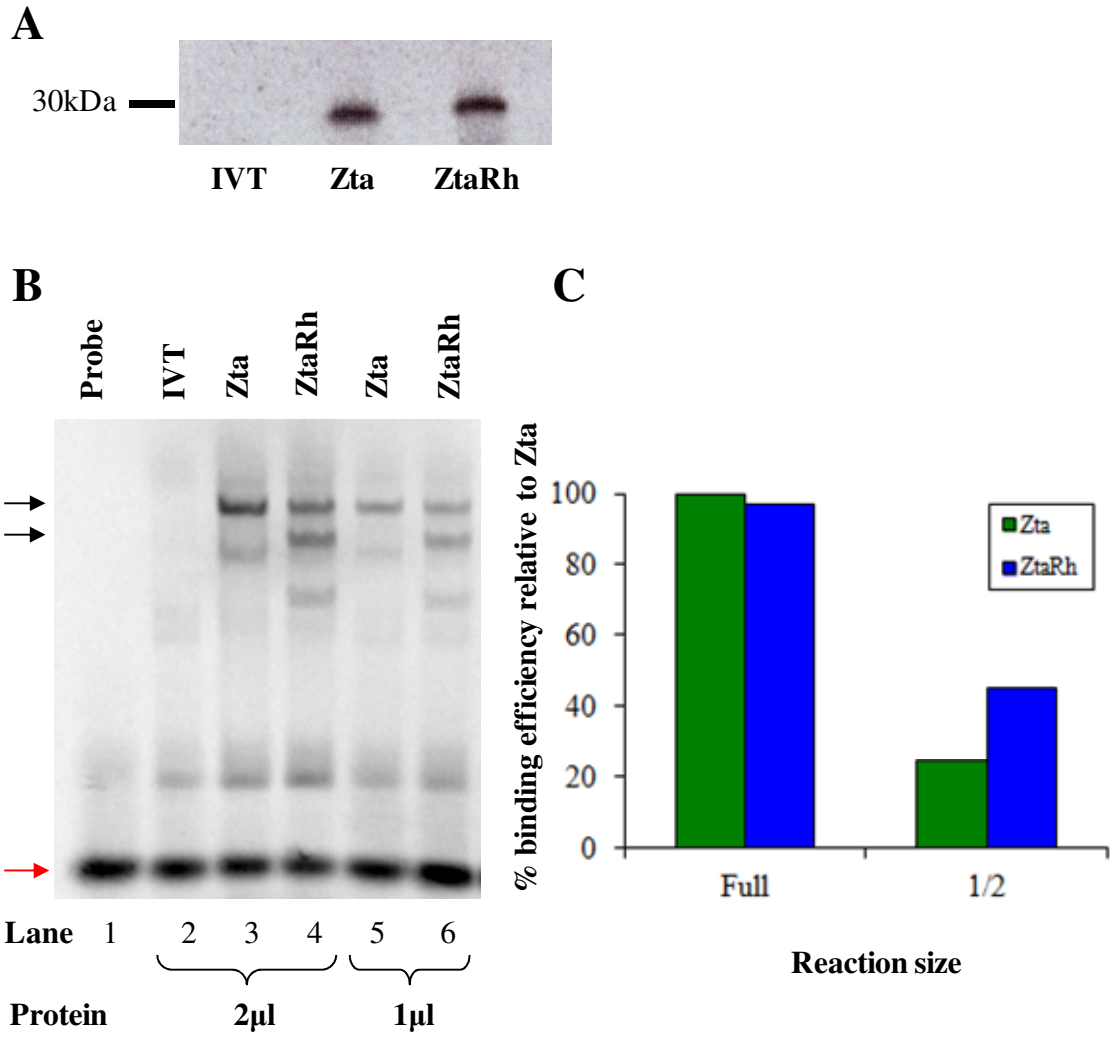

Figure 4.4: Binding by Zta and ZtaRh to AP1 ZRE

Zta and ZtaRh protein was radiolabelled with [^{35}S] met during *in vitro* translation with Promega Rabbit Reticulocyte Lysate, separated by SDS-PAGE and visualised using a phosphoimager. Equivalent amounts of protein **(A)** were used in all EMSA analysis **(B)** with [^{33}P]-labelled AP1 DNA probe (**GATCCATGACTCAGAGGAAAACATACG)** . Black arrows indicate DNA/protein complexes. A strong second lower band (indicated with lower black arrow) was consistently seen in ZtaRh lanes. The red arrow shows unbound free probe. Experiments were performed in duplicate and in full (2µl protein) and half (1µl protein) size reactions and average values are shown. Probe alone is in lane 1 and translation reaction omitting RNA (IVT) as a control is in lane 2. Images were scanned on a phosphoimager (Molecular Dynamics Storm 860). Band size was quantitated with Imagequant software (Molecular Dynamics) to determine binding efficiency relative to full size Zta **(C)**. For ZtaRh samples the two bands indicated with arrows were quantitated and binding efficiency calculated from the combined value.

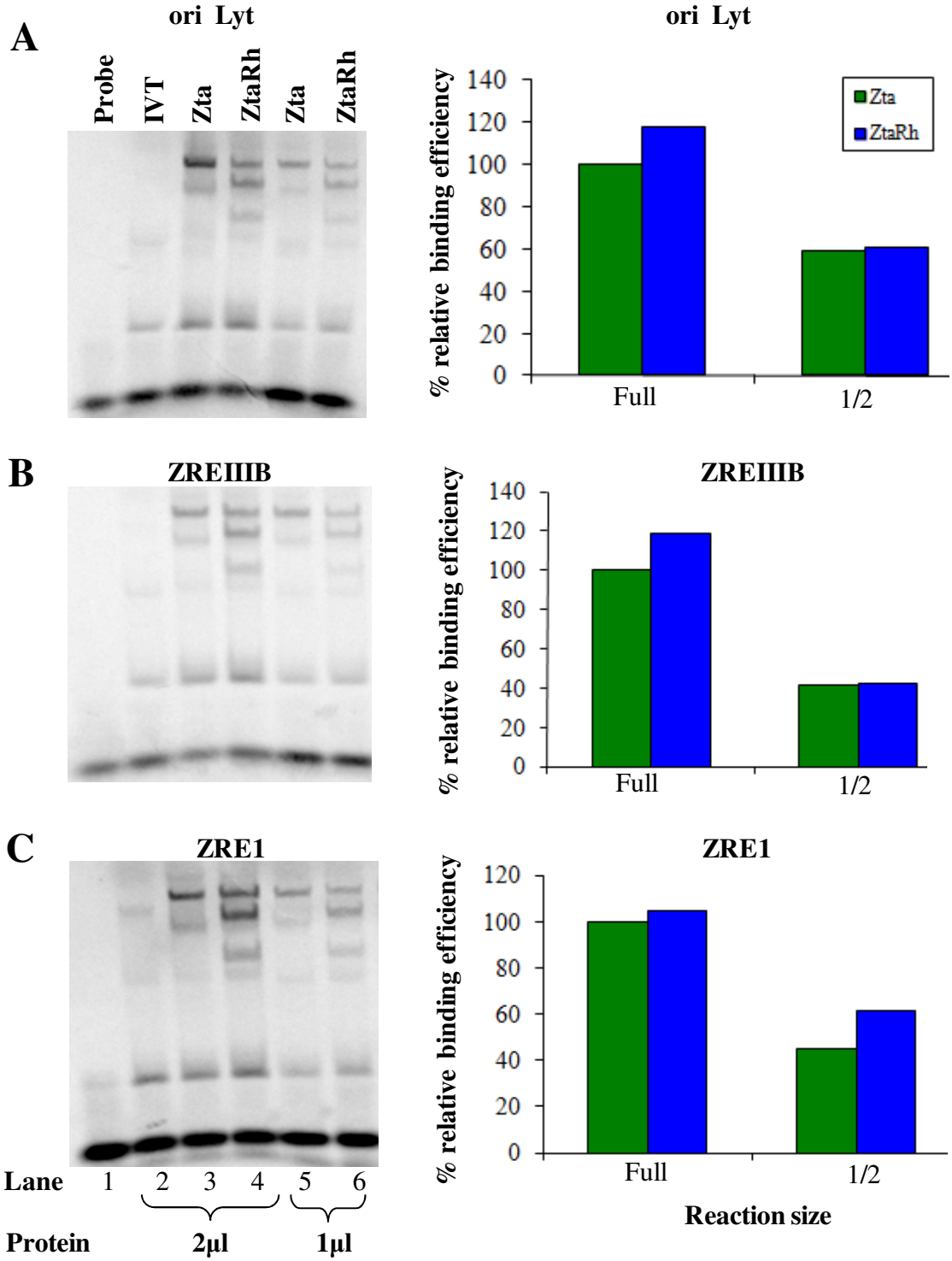

Figure 4.5: ori Lyt, ZREIIIB and ZRE1 EMSAs
EMSA gels and relative binding efficiency graphs for **(A)** ori Lyt (probe- CCTTAAAGTATTACACAGAG), **(B)** ZREIIIB (probe- GTACATTAGCAATGCCTG) and **(C)** ZRE1 (probe- GATCTCTTTTATGAGCCATTGGCA). Reactions were performed as in Figure 4.4.

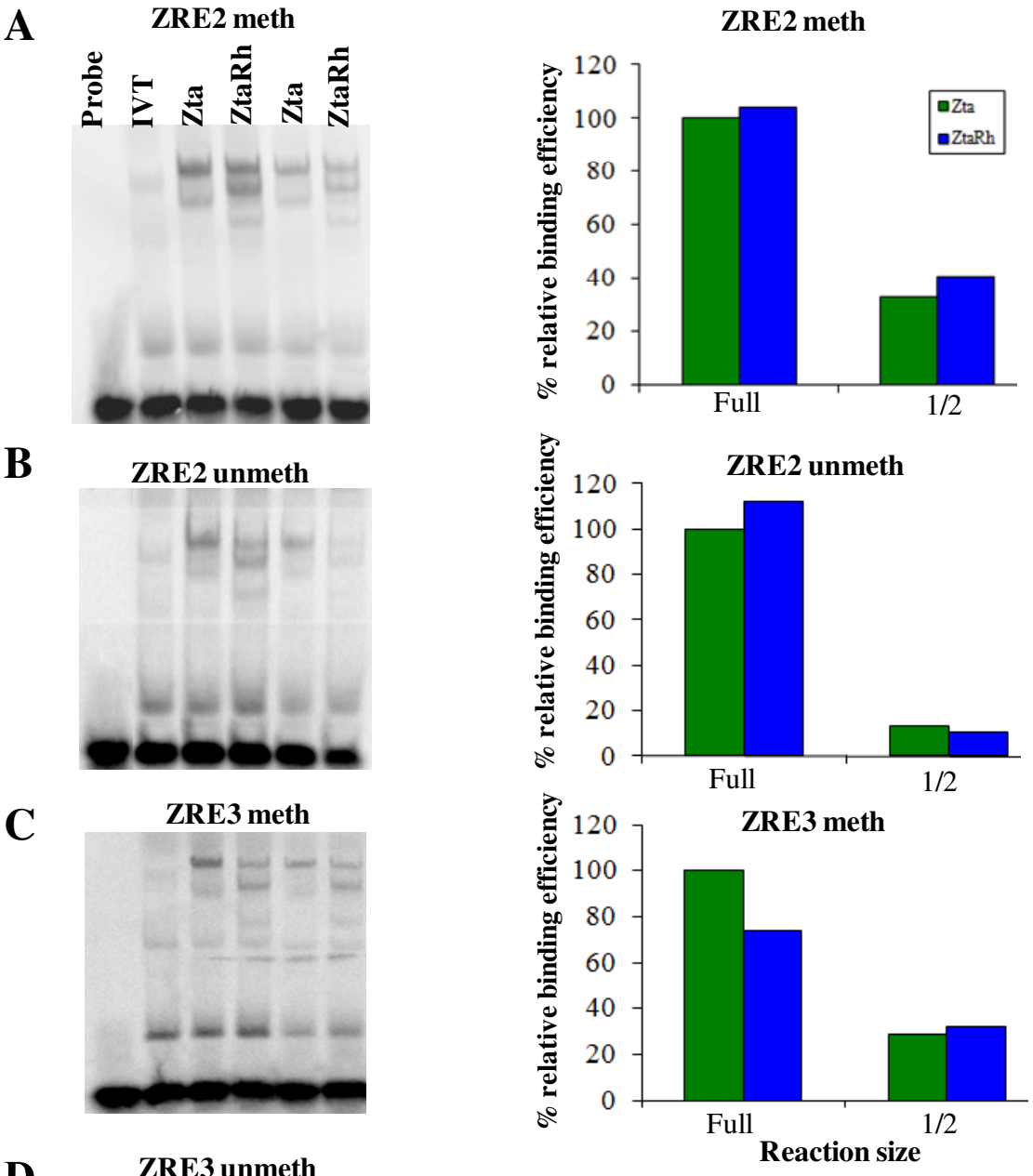

Figure 4.6: ZRE2 and ZRE3 EMSAs
EMSA gels and relative binding efficiency graphs for **(A)** ZRE2 methylated (probe-**GATCATAAAATCGCTCATAAGCTT**), **(B)** ZRE2 unmethylated and **(C)** ZRE3 methylated (probe-GATCTATAGCATCGCGAATTTTGA) and **(D)** ZRE3 unmethylated**.** As there was no binding to ZRE3 unmeth these reactions and gels were performed alongside other probes as a control. Full and half size reactions were performed as in Figure 4.4. In the probe sequence the red cytosine is methylated.

Neither protein was able to bind to the unmethylated ZRE3 probe so no numerical data was obtained from this experiment. The binding ability of Zta and ZtaRh to the probes tested was similar (Figure 4.7) with the greatest difference in binding of ZtaRh to ZRE3 methylated which was reduced by 26%.

This demonstrates that the repertoire of DNA binding sites that ZtaRh is capable of binding to overlaps with that of Zta.

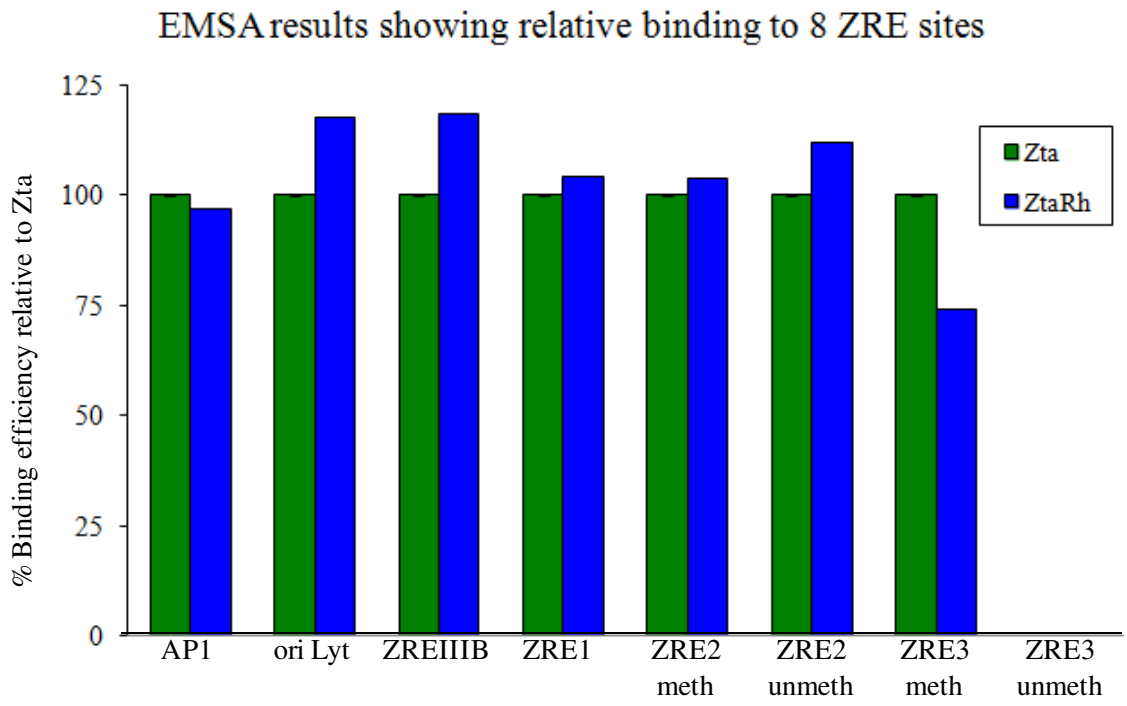

Figure 4.7: Similar binding ability of Zta and ZtaRh to 8 ZRE probes
Summary graph showing the average relative binding of Zta and ZtaRh to 8 EMSA ZRE probes. This graph summarises the data shown in Figures 4.4, 4.5 and 4.6. There was no binding for either protein to ZRE3 unmethylated. Experiments were duplicated and the average value shown.

4.2.3 ZREs in RhLCV oriLyt

As the binding ability of the proteins appears to be conserved between the two species, I next compared the conservation of ZRE sites within the EBV and RhLCV genomes. The left and right origins of lytic replication (oriLyt) are conserved with 88-90% identity for both regions. Figure 4.8 shows an alignment of the oriLyt Left for EBV and RhLCV with the seven ZREs in this region highlighted. 4 of the ZREs are completely conserved with a sequence difference in the remaining three; oriLyt 1, 6 and 7. RhLCV oriLyt 1 and 6 both differ from EBV by a single base, while oriLyt 7 has two differences. Results are very similar for oriLyt Right which is located in the Rh LCV genome at 138,134 - 139,200 bp.

I designed EMSA probes for oriLyt 1, oriLyt 6 and oriLyt 7 using the RhLCV sequence as shown in Figure 4.9A. I compared binding with the EBV and LCV Zta proteins using duplicate EMSAs as previously. The data suggests binding by ZtaRh to oriLyt 6 and oriLyt 7 was reduced by 50% and 40% respectively (Figure 4.9), however further experimental replications would need to be performed to quantify these obsevations.

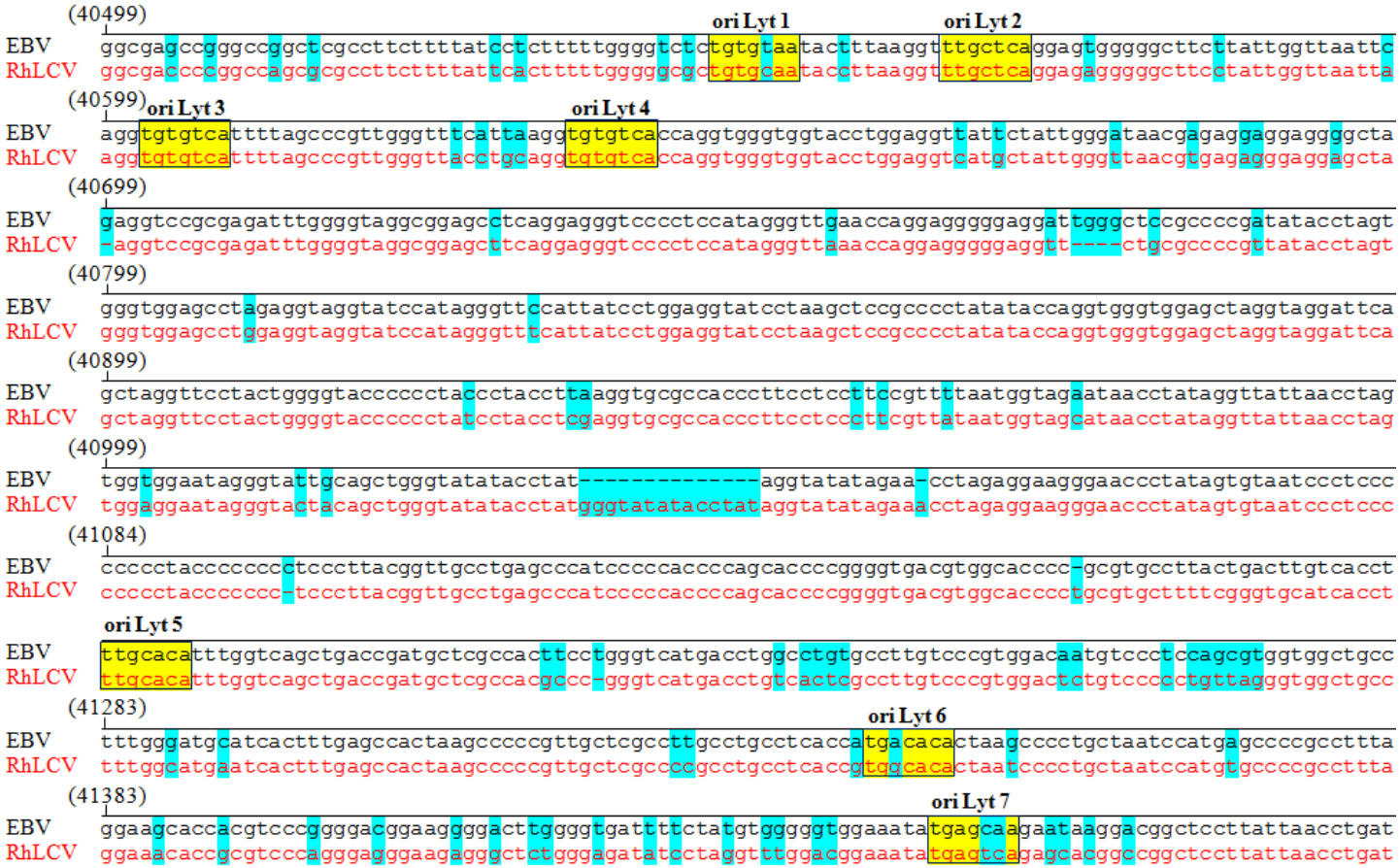

Figure 4.8: Alignment of the oriLyt-Left region of the EBV and RhLCV genomes
EBV nucleotide sequence is in black and RhLCV sequence is in red. Sequence differences are highlighted in blue. The seven Zta Response Elements, oriLyt 1-7, are boxed in yellow and numbered. The EBV genomic numbering is shown in brackets. In the RhLCV genome this sequence is located at 34339-35331 bp. This oriLyt region shows an 88.3% identity between the two genomes.

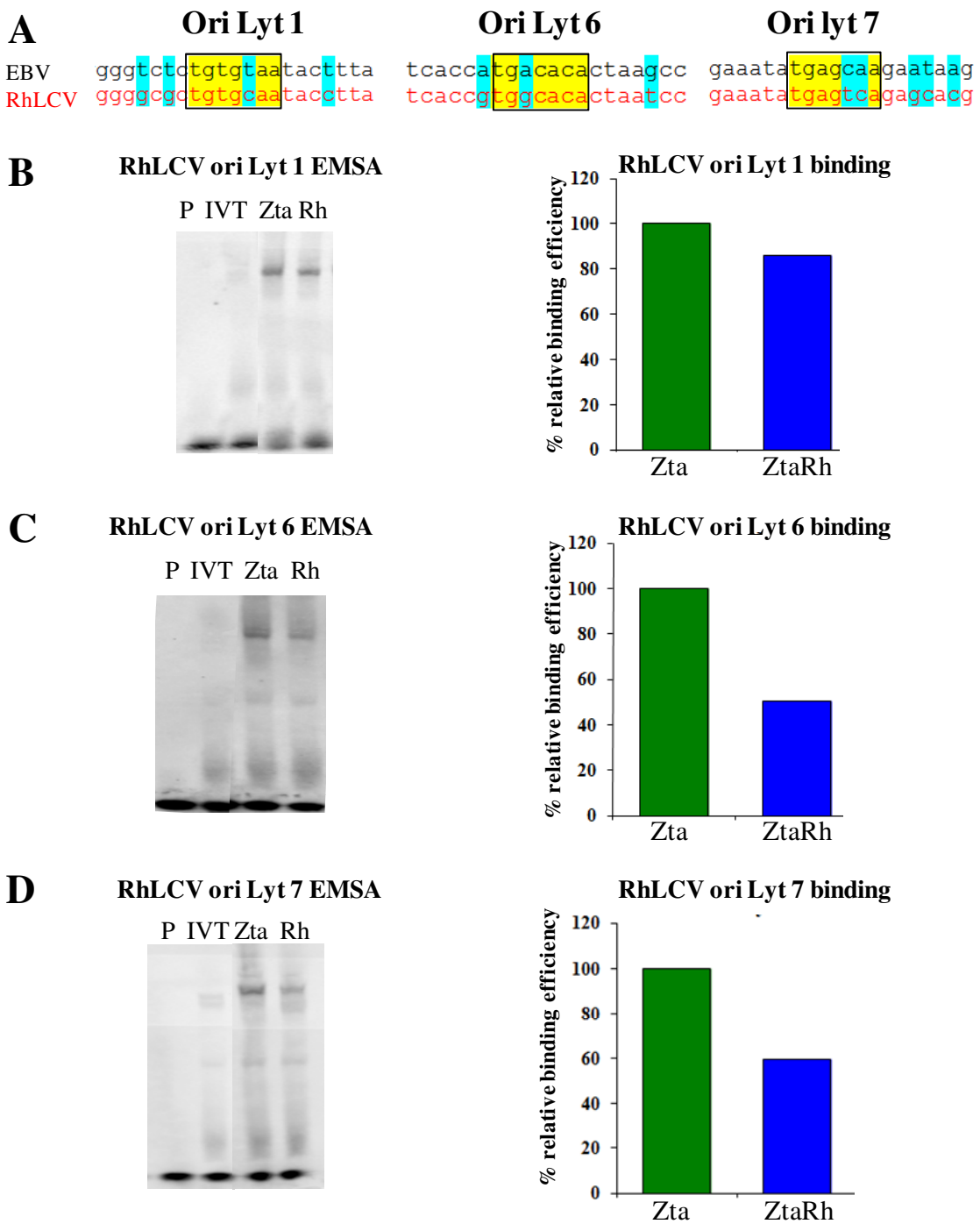

Figure 4.9: Binding by Zta and ZtaRh to three ZREs from RhLCV ori Lyt
Alignment of the ori Lyt region from EBV and RhLCV showed a difference in three ZREs; ori Lyt 1, 6 and 7 (**A**). EMSA probes were created using the RhLCV sequence. EMSAs were performed as in Figure 4.4 using Zta and ZtaRh proteins for oriLyt 1 (**B**), ori Lyt 6 (**C**) and ori Lyt 7 (**D**). Example gels and the relative binding graphs are shown. All experiments were duplicated and the average value shown.

4.2.4 ZREs in RhLCV BRLF1 promoter

The promoter of the EBV BRLF1 (Rp) gene contains three ZREs and encodes the protein Rta. These were included in the initial EMSA experiments and ZtaRh was able to bind to all three EBV sites. EBV Rp ZRE2 contains a single CpG methylation site and ZRE3 contains two. As binding to these three ZRE sequences is conserved, I aligned the sequences for EBV Rp and RhLCV Rp (Figure 4.10) to see if the sequences are retained in the RhLCV genome. This revealed that ZRE1 and ZRE2 are completely conserved, however ZRE3 is not. Through sequence alignment the sequence in the equivalent position is CGCCGGA. This sequence only has 3 bases in the same position (highlighted) as the EBV sequence, TCGCGAA. The RhLCV sequence also has 2 CpG motifs but they are in a different configuration. The RhLCV Rp sequence is located in the RHLCV genome at 88050 – 88446bp and the sequence identity is 85%. In order to establish if the RhLCV site could potentially operate as a ZRE, I created an EMSA probe of the sequence (RhLCV ZRE3) in both methylated and unmethylated versions (Figure 4.11). EMSAs were performed as previously. Neither Zta nor ZtaRh were able to bind to methylated or unmethylated RhLCV ZRE3, suggesting it is non-functional. Analysis of the RhLCV promoter with a Microsoft Word macro to search for known ZREs from a database compiled by Kirsty Flower in the Sinclair lab revealed that there are no other known functional ZRE sites within the RhLCV promoter (Flower *et al.*, 2011).

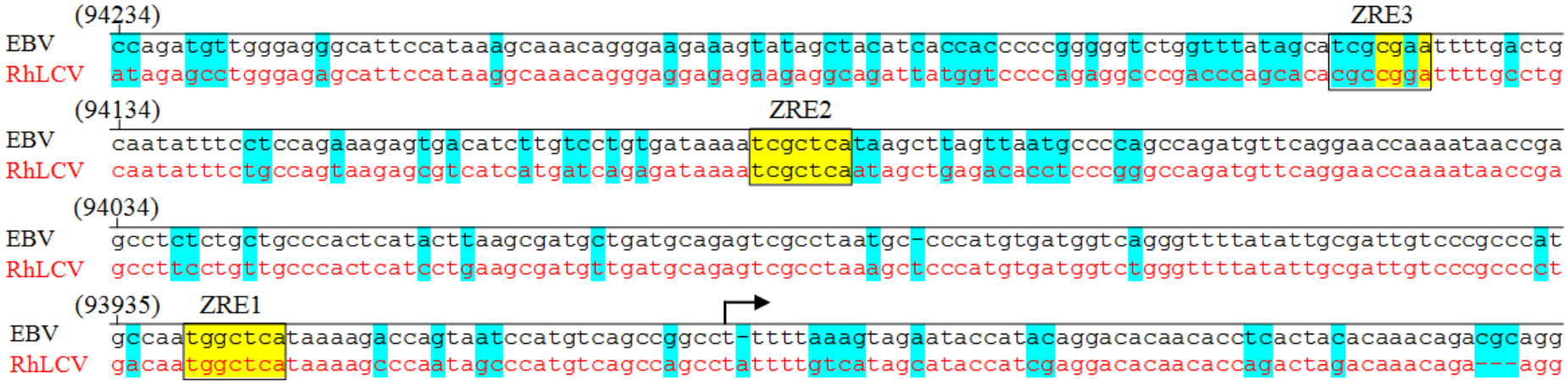

Figure 4.10: Alignment of BRLF1 gene promoter from EBV and RhLCV
EBV nucleotide sequence is in black and RhLCV sequence is in red. Sequence differences are highlighted in blue. The transcription start site is marked with an arrow. The three Zta Response Elements; ZRE1, ZRE2 and ZRE3, are boxed in yellow and numbered. The EBV genomic numbering is shown in brackets. The RhLCV sequence is located in the genome at 88050 – 88446bp. There is 85% sequence identity between the two viruses in this region.

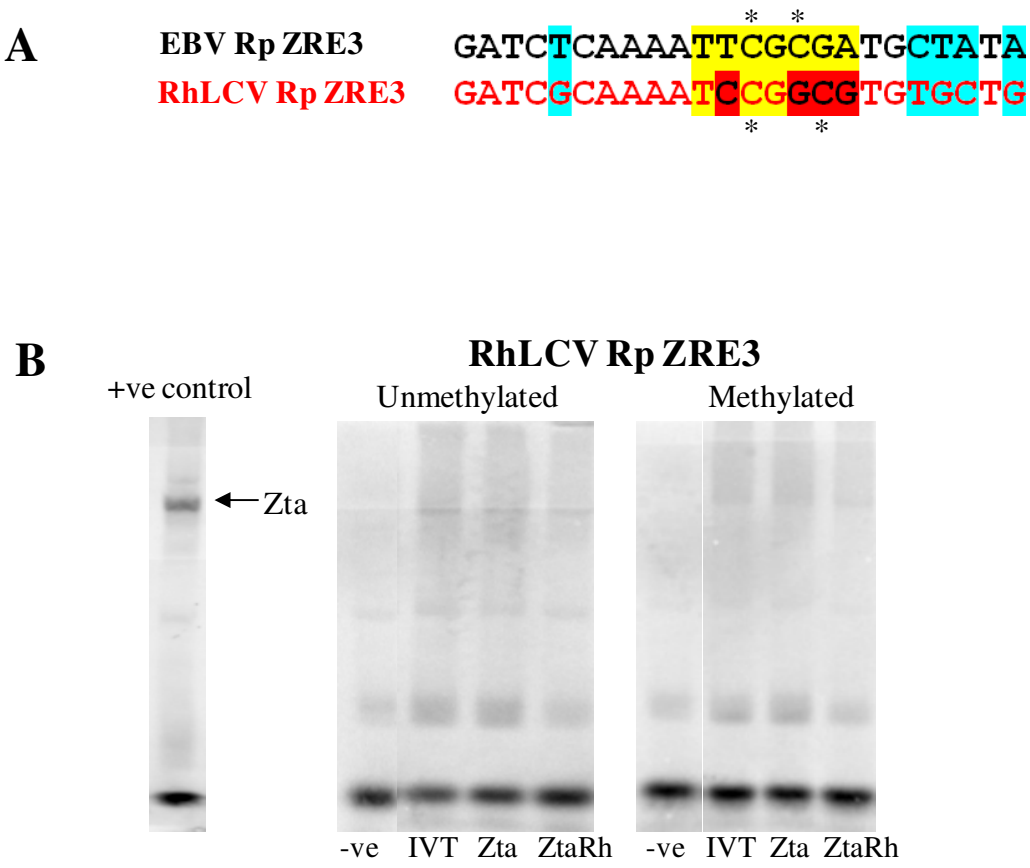

Figure 4.11: Zta and ZtaRh are unable to bind to ZRE3 from RhLCV Rta promoter

An aligned comparison of the region around ZRE3 is shown for both viruses **(A)**. Potential methylation sites are indicated with asterixes. Methylated and unmethylated EMSA probes were created using the RhLCV sequence. EMSAs were performed **(B)** as in Figure 4.4. No binding was seen for either protein. The left hand panel shows the expected position of bound, labelled Zta in a positive control.

4.2.5 Determination of methylation dependent promoter efficiency

In order to compare the effectiveness of RhLCV Rp with the equivalent promoter from EBV and to establish the importance of the ZRE3 site in the context of the whole promoter region, I performed a luciferase assay. This allows quantification of transcriptional activity from a promoter using luciferase as a reporter gene. It involves inserting the promoter of interest into an expression vector, directly upstream of the luciferase gene. This brings the luciferase gene under control of the promoter being studied and allows ready detection of gene expression.

I cloned the Rp from each virus into the vector pGL2 (Promega). The pGL2 vector encodes the firefly (*Photinus pyralis*) luciferase gene. Expression of the gene through promoter activation results in the oxidation of a luciferin, coelenterazine, by luciferase to produce a luminescent protein, coelenteramide. This can then be quantitated using a luminometer. This assay would enable a comparison of the relative strength of the promoters from EBV and RhLCV. Inserting a functional ZRE3 into the Rh promoter would help ascertain if there is a possible function for this site in RhLCV.

4.2.5.1 Cloning EBV and RhLCV Rp

The aim was to clone the promoters of EBV BRLF1 (Rp) and RhLCV BRLF1 (RhRp) immediately upstream from the luciferase gene in the pGL2 vector. This makes it possible to readily measure gene expression by detection of luciferase. I designed PCR primers to amplify approximately 1000bp encoding the promoter region of EBV Rp and RhLCV RhRp. Originally I incorporated restriction enzyme cutting sites for MluI and XhoI at the primer ends to enable cloning into the multiple cloning region of the pGL2 vector. EBV Rp was amplified using PCR using Rp-CAT as a template. Rp-CAT is a plasmid containing the promoter region of BRLF1 coupled to the chloramphenicol acetyltransferase (CAT) gene (Sinclair *et al.*, 1991). The PCR template DNA for RhRp was Cosmid LV28, containing RhLCV DNA from 70,760 to 111,969 bp in the SuperCos vector (a gift from Prof. Fred Wang).

Both Rp fragments were successfully amplified (Figure 4.12A), restriction digested with MluI and XhoI and purified from agarose gel using QIAquick gel extraction

(Qiagen). The pGL2 vector was also digested and purified in the same way. However multiple attempts at ligating the fragments into the digested pGL2 vector failed.

I then repeated the PCR reactions and digested newly amplified, purified products with XhoI alone. The pGL2 vector was sequentially digested with the blunt cutter SmaI (in place of MluI) then XhoI. After overnight ligation reactions, products were transformed into chemically competent E. coli cells and grown on agar plates. Colonies were picked and grown before plasmid DNA was extracted using a Qiagen Miniprep kit. Successful cloning of EBV Rp was detected by the presence of 3 restriction bands (sizes 277bp, 462bp and 217bp) when cut with HindIII. Cutting cloned RhRp with SmaI produced a band of 395bp. Vectors were sequenced to confirm cloning of the appropriate region was successful. The pGL2 vectors now contain Rp from EBV or RhLCV (Figure 4.12B).

A

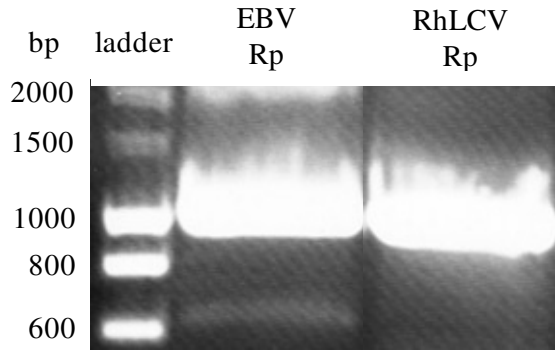

B

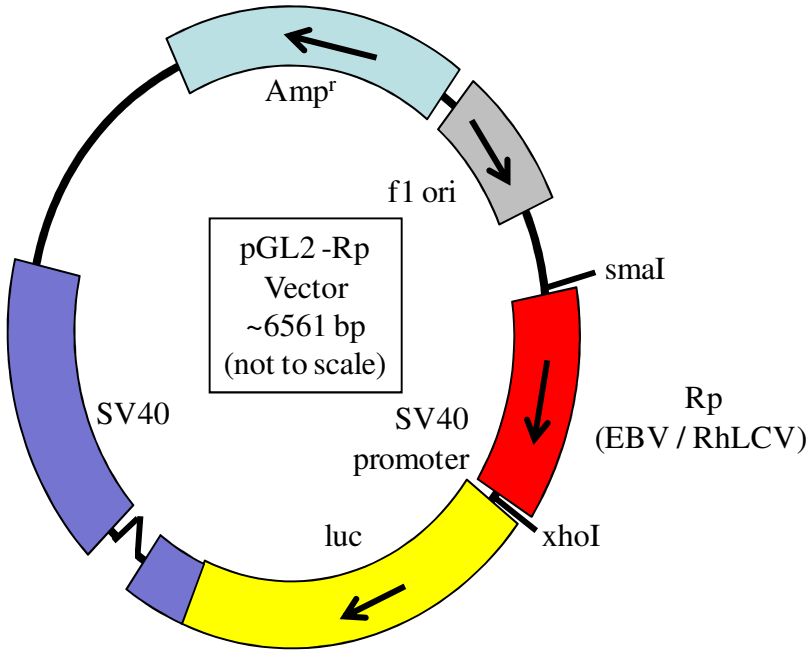

Figure 4.12: Cloning EBV Rp and RhLCV Rp and ZRE3 mutants
The promoter regions of EBV Rp and RhLCV Rp were amplified using PCR **(A)**. Products were restriction digested using SmaI and XhoI and ligated into Promega pGL2 vector **(B)** which contains the gene for firefly luciferase (luc).

Mutagenesis to knock out EBV ZRE3

I designed mis-matched primers (Figure 4.13A) to convert ZRE3 in EBV Rp into a non-functional site using site-directed mutagenesis, creating the vector EBVΔZRE3. This was undertaken successfully as shown by sequencing of the mutant in Figure 4.13C. The mutant sequence (CCGTCAA) is the same sequence used by Bhende et al (Bhende *et al.*, 2004) in their investigations into Rp.

Mutagenesis to insert functional ZRE3 into Rh

Through sequence alignment the equivalent position of ZRE3 in RhLCV Rp (Figure 4.10) was identified. Site-directed mutagenesis was used to introduce a ZRE3 site into this position (Figure 4.13B) to create the vector Rh+ZRE3. Rh+ZRE3 was sequenced to verify the mutations were accurate (Figure 4.13D).

Cloning his-tagged ZtaRh into pBabe

ZtaRh is not detected by the BZ1 antibody used to identify Zta in western blots, so I subcloned ZtaRh and Zta into pBabe vectors, incorporating a 6x-histidine (his) tag. I designed a forward PCR primer for each gene including 6 repeats of the sequence CAT, preceded by ATG. This encodes for a 5' tag of 6 histidine residues which can be detected by a his-Tag antibody. The his-tagged Zta gene was able to reactivate EBV from latency to an equivalent level as non-his-tagged Zta.

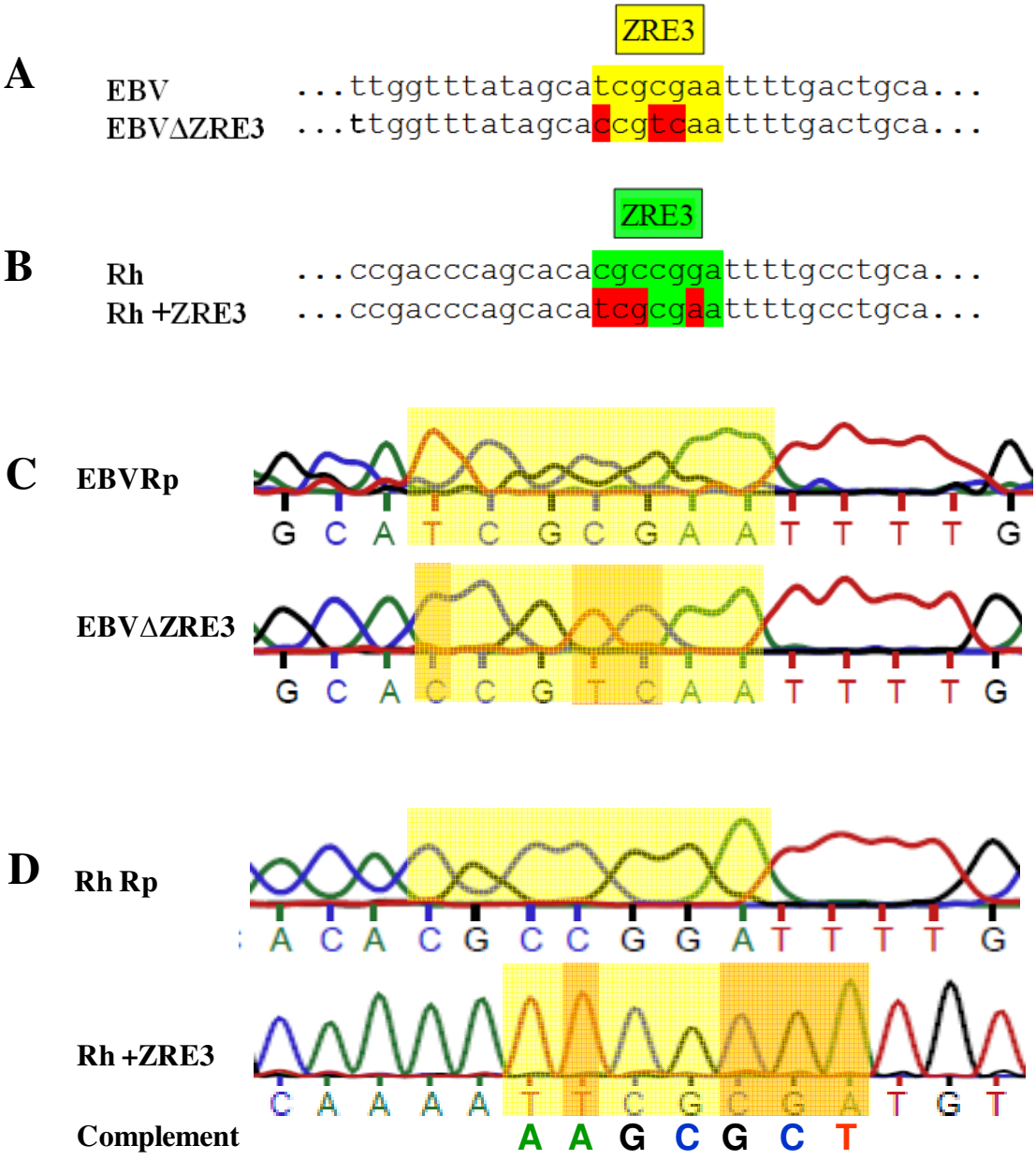

Figure 4.13: Site directed mutagenesis of Rp luciferase vector
Site directed mutagenesis (sdm) was performed on EBV Rp to render ZRE3 non-functional **(A)**. The bases shown in red were altered in the sdm reaction to create EBVΔZRE3. Sdm was performed on the RhLCV Rp vector to insert an EBV ZRE3 into in the aligned sequence position **(B)**, creating Rh+ZRE3. Vectors were sequenced to confirm changes **(C and D)**. ZRE sites are highlighted in yellow and altered bases in EBVΔZRE3 **(C)** and Rh+ZRE3 **(D)** are highlighted in orange. Rh+ZRE3 was sequenced in reverse and the complement sequence is shown below.

4.2.5.2 Methylation of vectors

In order to assess the effect of methylation on promoter efficiency, I had to create methylated versions of each vector. This was achieved using the CpG Methyltransferase M.SssI (NEB). This enzyme methylates the cytosine residue in all double-stranded CpG motifs. 10µg of each vector (EBVRp, RhRp, EBVΔZRE3 and Rh+ZRE3) was incubated with 50U SssI enzyme, NEB Buffer 2 (to 1x), 1 µl of 32mM S-adenosylmethionine (SAM) and H_20. After 1 hour at 37°C, the reaction was stopped by incubating at 65°C for 20 minutes. Each vector was also mock-methylated in reactions excluding enzyme. Reactions were digested with the methylation-dependent restriction enzyme BstUI, which is unable to digest CpG methylated DNA. Protection from digestion in this reaction confirmed methylation (Figure 4.14).

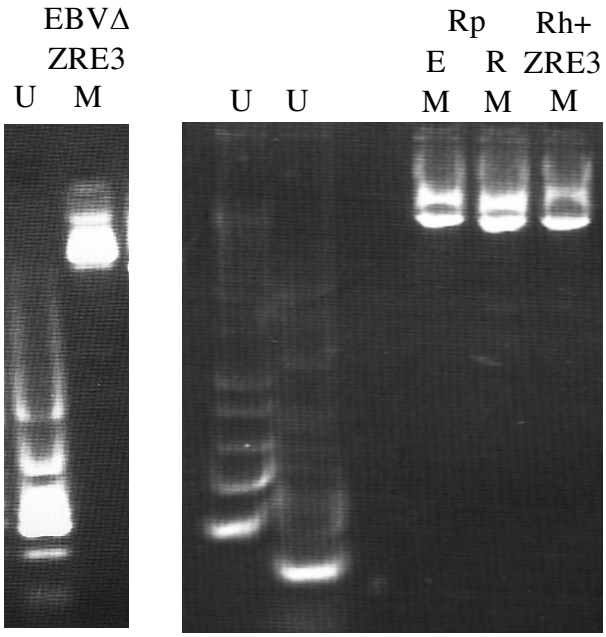

Figure 4.14: Methylation of Rta Promoter Vectors
pGL2 luciferase vectors containing EBV Rp, RhLCV Rp, EBVΔZRE3 and Rh+ZRE3 were methylated and mock-methylated (no enzyme) with SssI methylase. Reactions were then cut with the methylation dependent BstUI restriction enzyme and run on agarose gels to confirm methylation. The left panel shows digested unmethylated (U) DNA and methylated (M) EBVΔZRE3 which was protected from digestion. The right panel has 2 unmethylated controls and methylated EBV (E) Rp, RhLCV (R) Rp and Rh+ZRE3.

4.2.5.3 Luciferase assay

HEK293 cells were co-transfected with pBabe Zta, pBabe ZtaRh or empty pBabe and methylated or non-methylated pGL2 containing EBV Rta promoter (EBVRp), RhLCV Rta Promoter (RhRp), EBVRp with non-functional ZRE3 (EBVΔZRE3) or RhRp with EBV ZRE3 (Rh+ZRE3). Cells were harvested and lysed after 24 hours growth and bioluminescence was measured on a luminometer. The entire experiment was duplicated.

Western blots for expression of cdk2 were performed as a loading control (Figure 4.15A). Samples were also analysed for Zta and ZtaRh levels with western blots using an α-his antibody (Figure 4.15B). Equivalent levels of protein were observed.

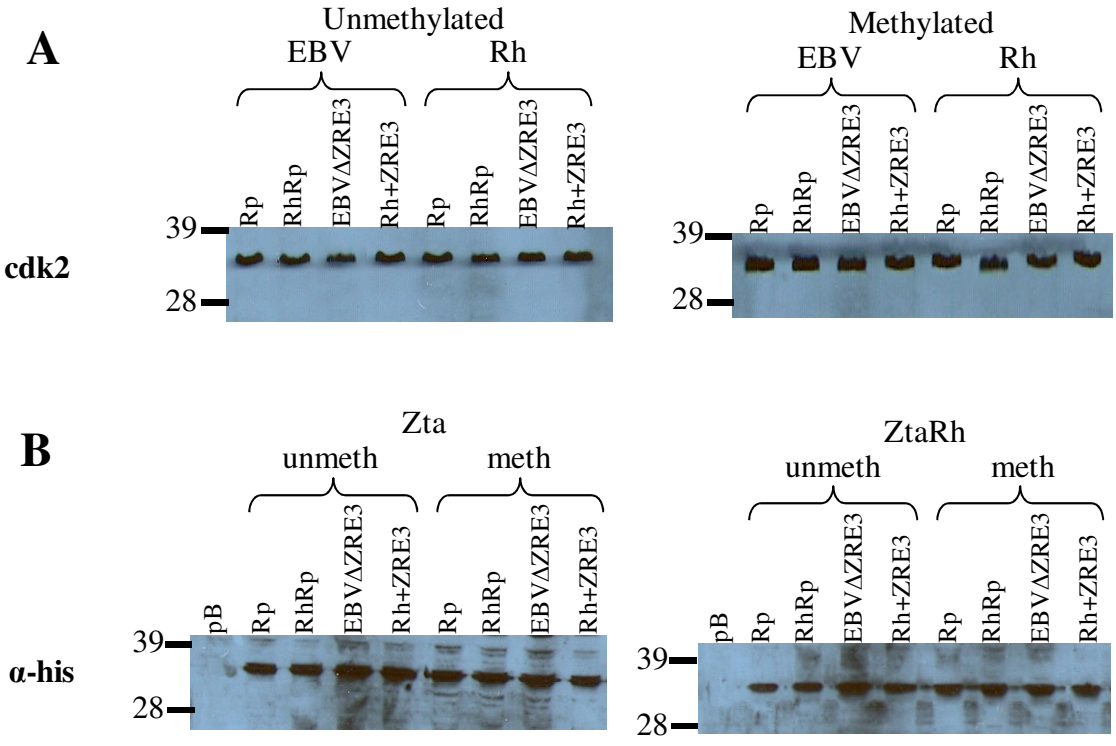

Figure 4.15: Western blots for luciferase assay
A western blot of cdk2 is shown as a loading control (**A**). α-his antibody detected his-Zta and his-ZtaRh for methylated and unmethylated samples used in the luciferase assay (**B**).

Figure 4.16 shows the relative luminescence levels detected for unmethylated promoters. As can be seen in the graph neither Zta or ZtaRh were able to activate any of the four unmethylated promoters. As luciferase levels for these samples are not above the levels of empty pBabe vector, it can set the background for activation from methylated promoters. This also clearly demonstrates that both EBVRp and RhRp are not capable of enabling transcription in the absence of methylation. It can be seen in Figure 4.16 that the background level of activation varied widely from 2 to 20. This variability could arise from differences in transfection efficiency, cell viability or pipetting and should be considered when interpreting results from this method.

The methylated versions of these promoters were activated by the addition of Zta or ZtaRh as shown in Figure 4.17. EBVRp was activated by both Zta and ZtaRh. The resulting luciferase level after activation by Zta is 3 fold higher than from activation by ZtaRh. The wild-type RhRp promoter is also activated by both proteins, although it is a weaker promoter in this system with 4 fold lower luciferase levels from Zta and 5 fold less from ZtaRh. Despite the loss of a functional methylation dependent ZRE3 within the RhRp, the promoter is still methylation dependent when activated by Zta or ZtaRh.

The loss of a functional ZRE3 site in EBVΔZRE3 reduced the activation by both Zta and ZtaRh. There was a 32% reduction in activation by Zta from EBVΔZRE3 compared to the EBVRp which contains an intact ZRE3 site. This is a smaller effect than was observed by Bhende et al (Bhende *et al.*, 2004). The reduction in activation for ZtaRh from EBVΔZRE3 is slightly more pronounced at 53%. This data indicates that both proteins contribute to the activation of the promoter through binding at ZRE3.

Addition of a functional ZRE3 site into the RhRp promoter was not sufficient for either protein to increase the activation from the wild-type RhRp promoter. The lack of a ZRE3 element in RhRp does not appear to account for the lower level of activation in comparison to EBVRp. ZtaRh was considerably weaker at activating all 4 promoters in comparison to Zta, using this system. Reducing the experimental variability and further experiments would provide greater evidence of the influence of the individual promoter elements on expression levels.

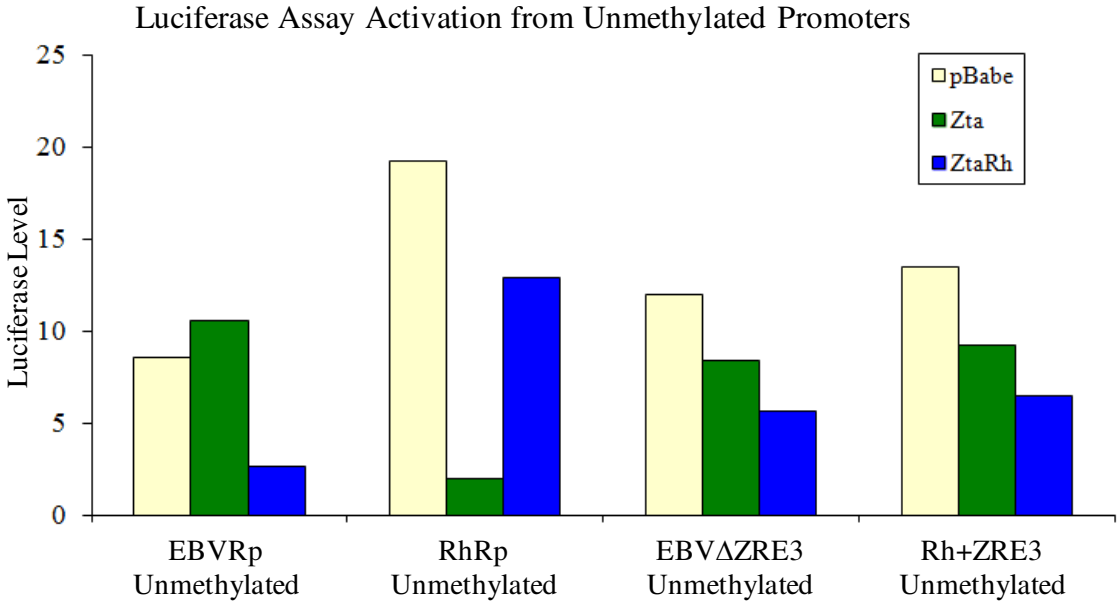

Figure 4.16: Rta Promoter luciferase assay with unmethylated promoters
HEK293 cells were co-transfected with pBabe vector encoding Zta, ZtaRh or empty and unmethylated pGL2 vectors containing EBV Rta Promotor (EBVRp), RhLCV Rta Promotor (RhRp), EBVRp with nonfunctional ZRE3 (EBVΔZRE3) or RhRp with EBV ZRE3 (Rh+ZRE3). Cells were harvested and lysed after 24 hours and the luciferase level was detected by a luminometer. Experiments were performed in duplicate and average values are shown.

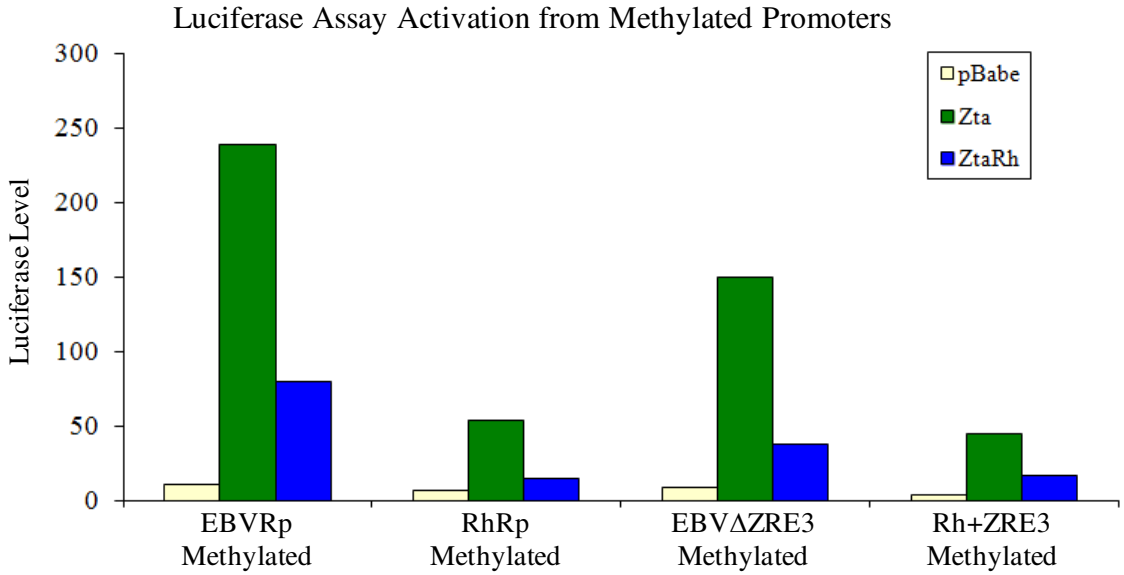

Figure 4.17: Rta Promoter luciferase assay with methylated promoters
HEK293 cells were co-transfected with pBabe vector encoding Zta, ZtaRh or empty and methylated pGL2 vectors containing EBV Rta Promotor (EBVRp), RhLCV Rta Promotor (RhRp), EBVRp with nonfunctional ZRE3 (EBVΔZRE3) or RhRp with EBV ZRE3 (Rh+ZRE3). Cells were harvested and lysed after 24 hours and the luciferase level was detected by a luminometer. Experiments were performed in duplicate and average values are shown.

4.3 Discussion

Zta is relatively well conserved between RhLCV and EBV. There is a smaller degree of conservation in the N-terminal transactivation domain of the protein. As this region is assumed to interact with host proteins to transactivate transcription, species specific differences in host proteins may have driven selection for these differences.

There are 2 amino acid changes located in the basic DNA contact domain of ZtaRh. As this region influences the specificity of Zta DNA-binding, binding of ZtaRh was investigated.

EMSA DNA-binding experiments revealed there were no differences in binding by Zta and ZtaRh to any of the six DNA probes analysed or to 2 methylated variants. This included 2 sites, ori Lyt and Rp ZRE3, which are not conserved in the RhLCV genome. Despite the changes in ZtaRh sequence and some relevant differences in the target binding sites, the range of sites that ZtaRh can bind overlaps with binding by Zta. Analysis of ZREs in the EBV and RhLCV genomes revealed some differences between the two viruses. There were alterations in three (oriLyt 1, 6 and 7) of the seven ZREs in the left oriLyt. When oriLyt 1, 6 and 7 from RhLCV oriLyt were utilised as EMSA probes, both Zta and ZtaRh were able to bind with with considerable strength, although ZtaRh was weaker.

The Rp promoter elements ZRE1 and ZRE2 were conserved but ZRE3 differed at 4 bases. The ZtaRh Rp ZRE3 site still has 2 methylation sites although the conformation is different. When used as an EMSA probe, neither Zta nor ZtaRh were able to bind to methylated or unmethylated versions of RhLCV Rp ZRE3. Analysis of the RhLCV Rp promoter found no additional known functional ZRE sites. For EBV, activation via ZRE3 is required for activation of Rp, as demonstrated by the Zta mutant C189S (Karlsson *et al.*, 2008a). Without a functional ZRE3, RhLCV must act in a different way to activate Rp.

The Rp promoters from EBV and RhLCV were cloned into a luciferase expression vector and 2 mutant variants of the promoters were created. The first mutant was EBV

Rp containing a non-functional ZRE3 and the second mutant was RhLCV Rp with the insertion of a functional EBV ZRE3 in the equivalent position. Each vector was methylated and analysed in both the unmethylated and methylated forms using an luciferase assay in HEK293 with Zta and ZtaRh. The resultant bio-luminescence was analysed to reveal the magnitude of activation. Neither Zta nor ZtaRh were able to activate any of the four unmethylated promoters. Both methylated wild-type EBVRp and RhRp were activated by both proteins, although EBVRp was a stronger promoter. This suggests that methylation is of critical importance for activation from both promoters in these cells. Removal of ZRE3 from EBVRp resulted in weaker binding for Zta and ZtaRh. This indicates that both proteins contribute to activation of EBVRp through ZRE3. This observation for Zta is in agreement with (Bhende *et al.*, 2004). However the addition of a functional ZRE3 into RhRp did not result in higher levels of activation than from wild-type RhRp for either protein. In all experiments ZtaRh was 3-4 times weaker than Zta in promoter activation. As there was a high level of variability in the background luciferase levels, further experiments could provide stronger evidence for the influence of individual elements on promoter activation.

These results suggest that in these cells for EBV methylation of ZRE3 is dominant for promoter activation. However for RhLCV, methylation is important but this does not occur via ZRE3. As ZRE2 contains the only other methylation site within a ZRE in this promoter, it is possible that methylation of ZRE2 plays a more critical role in RhLCV. These experiments were completed in human cells and experiments performed with ZtaRh in the natural Rhesus monkey host cells, with the different complement of host cell proteins present would produce a result that is more informative for ZtaRh. There is currently no suitable Rh cell line in existence.

Chapter 5 Lytic Reactivation and Cell Cycle

5.1 Introduction

The previous chapter has shown that ZtaRh is functional for DNA binding. This chapter assesses whether ZtaRh is also able to perform other important functions of Zta, namely lytic reactivation and enabling cell cycle arrest. Any divergence of ZtaRh from the normal functions of Zta may help to further characterise key regions of this important protein.

5.1.1 Lytic Reactivation

One of the key functions of Zta is reactivation of EBV from latency. The transcriptional activation function of Zta is critical for this lytic reactivation function. As part of this process Zta is required for both lytic cycle gene expression and DNA replication (Zhang *et al.*, 1996).

The ability to reactivate EBV from latency can be assessed using HEK 293 ZKO cells (Feederle *et al.*, 2000). These cells are stably transfected with the EBV genome containing a defective BZLF1 gene. Transfection with a vector capable of expressing functional Zta results in activation of the lytic cycle and consequent replication of the EBV genome as shown in Figure 5.1. The level of lytic activation can then be assessed using QPCR.

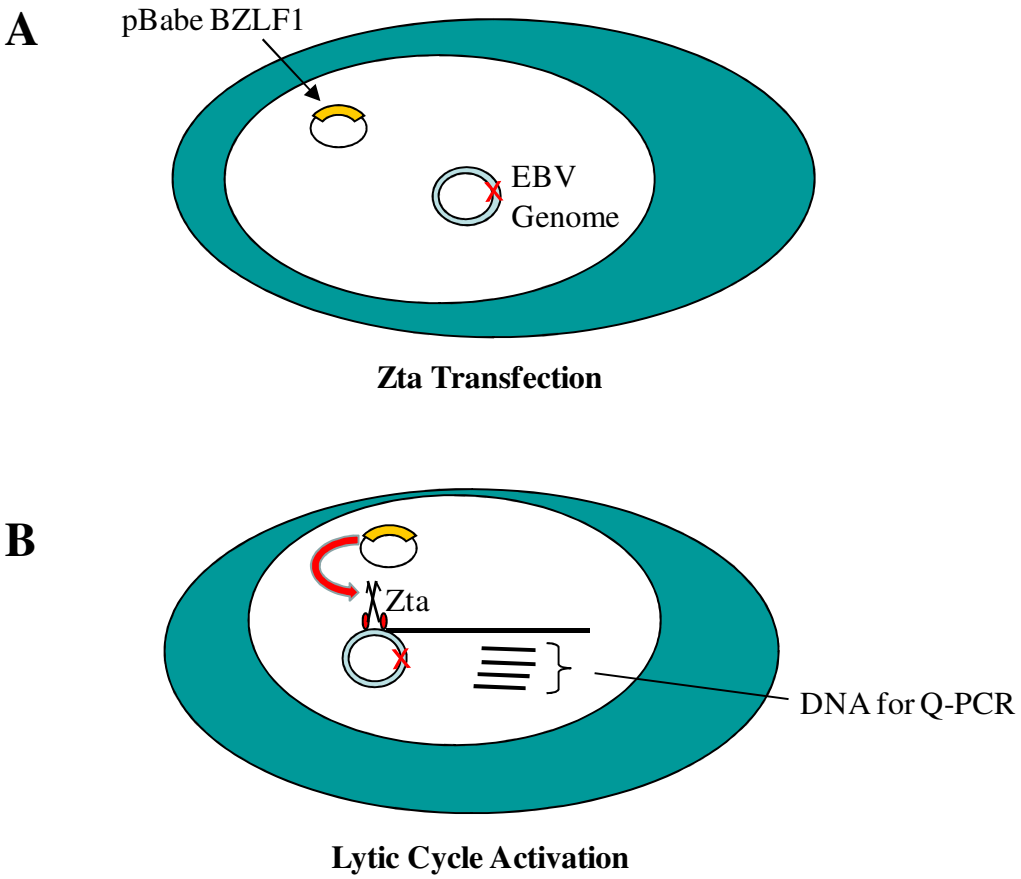

Figure 5.1: Schematic of lytic reactivation experiment
An expression vector containing the BZLF1 gene encoding Zta is transfected into HEK293-ZKO cells (**A**). These are human embryonic kidney cells stably transfected with the EBV genome containing a defective copy of the BZLF1 gene. **B.** Zta protein produced by the incoming vector is able to activate the lytic cycle of EBV. This produces DNA which is then extracted along with host cell DNA and analysed using QPCR.

5.1.2 Zta and the cell cycle

Zta has the ability to modulate the environment of the host cell to provide optimum conditions for EBV replication during the lytic cycle . This includes the ability to cause cell cycle arrest in some cell types (Figure 1.11). The benefit of this activity to the virus during the lytic cycle is likely to be two-fold. Firstly as EBV relies on the expression of some cellular genes for viral DNA replication, arrest ensures that these proteins are available. Secondly mitosis is prevented until the viral lytic cycle has been completed. This allows the virus to escape competition with the host genome for cellular components required for DNA replication.

5.1.3 RhLCV and the cell cycle

It is probable that an equivalent mechanism of cell cycle arrest occurs in rhesus LCV. In order to investigate this, ZtaRh was tested in a cell cycle assay. This could also highlight any contribution to functionality of amino acid differences between the two homologues. Ideally experiments would be conducted in both rhesus cells and human cells, however as rhesus cells were not available, experiments were conducted in human HeLa cells.

This chapter aims to assess whether ZtaRh is capable of performing two important functions of Zta, lytic reactivation and enabling cell cycle arrest.

5.2 Results

5.2.1 Lytic reactivation

The ability of ZtaRh to reactivate EBV from latency, as determined by increased EBV genome levels, was assessed using his-tagged Zta and ZtaRh. HEK293 ZKO cells were transfected with his-tagged Zta, ZtaRh or empty vector (pBabe). Cells were incubated for 96 hours to enable EBV genome replication to occur before harvesting. A sample of cells was used for western blotting to determine the presence of Zta and ZtaRh using an anti-His Tag antibody. This control determined that equivalent levels of each protein

was expressed (Figure 5.2A). In addition a western blot for the gene *blc2* served as a loading control for each sample. However apoptosis status may vary for different experimental samples, resulting in variable expression levels of *bcl2*. This means that *bcl2* was not an appropriate loading control to use for this experiment. The genomic DNA was extracted from the remaining cells. In order to assess if EBV DNA abundance was equivalent, the amount of EBV genome present was assessed using quantitative real time PCR (QPCR) using primers within the EBV DNA polymerase gene (Schelcher *et al.*, 2005) (Figure 5.2B). For each sample the level of human genome present was measured using QPCR with primers for the human gene β-globin as detailed in Table 2.2. The relative expression of β-globin was used to standardise the samples for DNA level. The experiments are duplicated. Transfection with Zta resulted in increased EBV genome levels. However after transfection with ZtaRh the amount of EBV genome detected was only 23% of that Zta transfection (Figure 5.2). The EBV genome levels following transfection with ZtaRh are very low and barely higher than seen as background detection following transfection with the empty pBabe vector. As the loading control used was inappropriate these experiments should be repeated with another control to ensure accurate results. However it appears that expression of the EBV genome is greatly reduced or absent following transfection with ZtaRh in comparison to Zta.

As regions in the C-terminal domains of Zta have previously been shown to be important in lytic reactivation (Taylor *et al.*, 1991; Schelcher *et al.*, 2005) it was of interest to see if differences in this portion of Zta and ZtaRh could account for the loss of reactivation ability of ZtaRh. The three C-terminal domains of Zta contain 11 amino acids differences from ZtaRh (Figure 5.3A). The possible contribution of these divergent residues in the reduced lytic reactivation ability of ZtaRh was assessed through the creation of three domain swap mutants (Figure 5.3B-D).

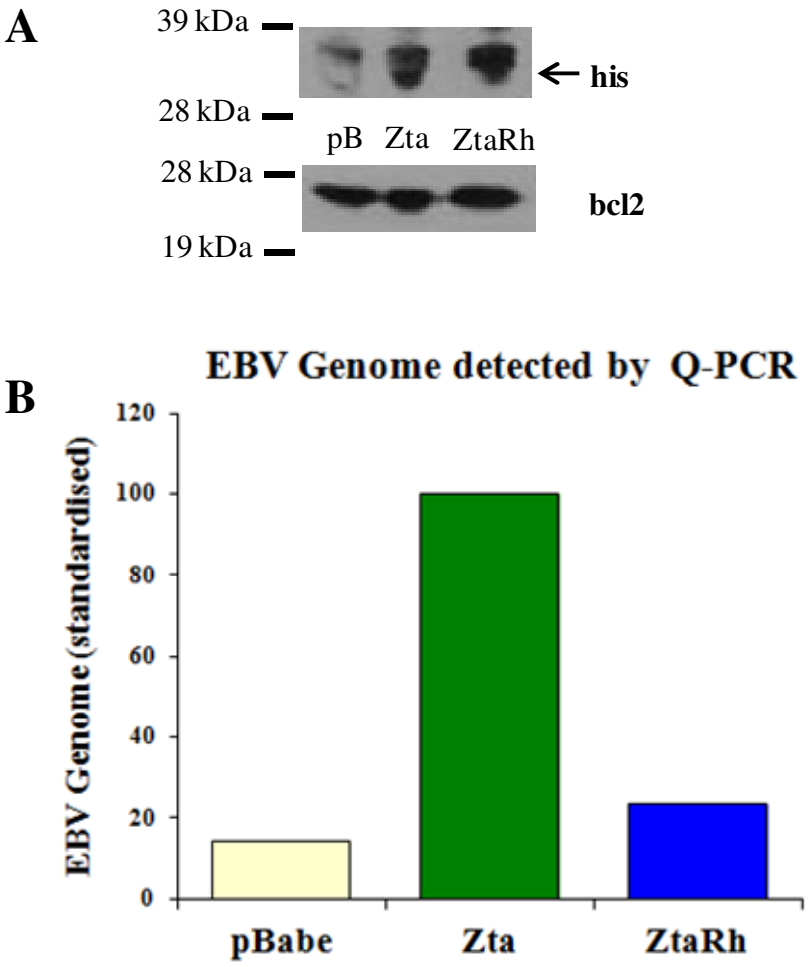

Figure 5.2: Reactivation of lytic cycle by Zta and ZtaRh
HEK293-BZLF1-KO cells were transfected with his-tagged Zta, ZtaRh or empty vector (pBabe). Cells were harvested after 96 hours and genomic DNA was extracted. Western blots confirm that approximately equal amounts of protein were present (**A**). Molecular weight markers are shown on the left. A Western Blot of bcl2 is shown as a loading control. Quantitative Real Time PCR (QPCR) was used to detect the presence of the EBV genome and beta-globin (**B**). Results were standardised by the amount of beta-globin present. Experiments were duplicated and average value shown.

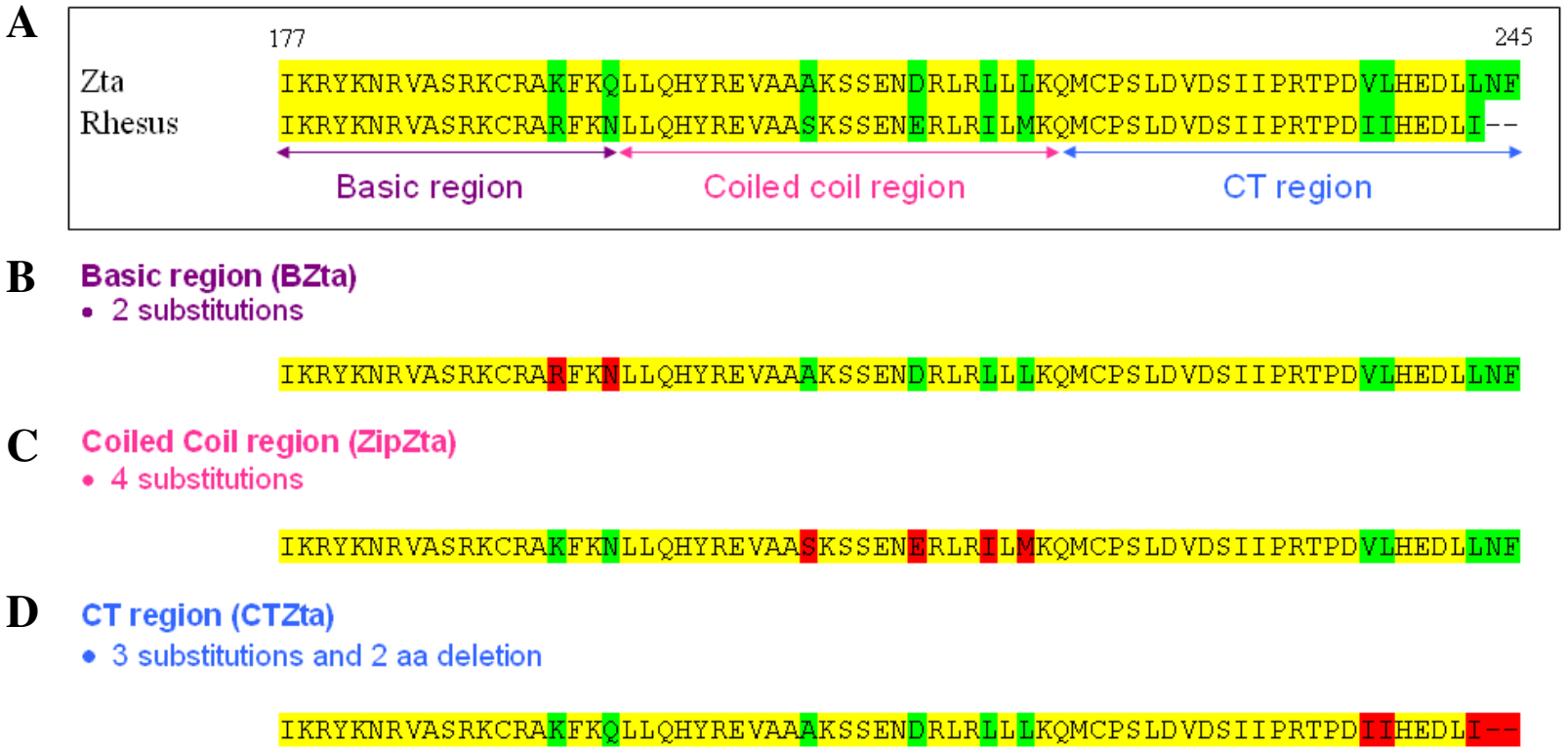

Figure 5.3: Zta and ZtaRh alignment and Domain swap mutants
A. An alignment of the three terminal domains of Zta and ZtaRh from amino acids 177-245. Differences between the 2 proteins are highlighted in green and the functional domains are indicated below. Mutants of Zta were constructed with each domain in turn containing ZtaRh sequence. The sequence of the basic region domain swap mutant (BZta) is shown in **B**, the coiled coil mutant (ZipZta) in **C** and the CT region mutant (CTZta) in **D**. Amino acids altered to match ZtaRh are highlighted in red and remaining differences are in green. The entire transactivation domain of these mutants is encoded by Zta.

5.2.2 Creation of domain swap mutants

The basic region of Zta (aa 177 - 195) differs from ZtaRh at two residues, Lys-192 and Gln-195. Both substitutions are conservative; positively charged Lys-192 is substituted in ZtaRh for positively charged Arg and polar Gln-195 is substituted by polar Asn. A mismatched primer pair for site-directed mutagenesis (sdm) was designed to introduce the mutations K192R and Q195N (Figure 5.4). The template for amplification was his-tagged Zta in the pBabe vector. The vector was sequenced to confirm creation of the domain swap mutant BZta (Figure 5.4 C).

Creation of zipper domain swap mutant, ZipZta.

The coiled coil or zipper domain of Zta (aa 196 - 219) contains 4 residues that vary from ZtaRh. There are 3 conservative substitutions, acidic Asp-212 to acidic Glu, hydrophobic Leu-216 to hydrophobic Ile and hydrophobic Leu-218 to hydrophobic Met. Position 206 is changed from hydrophobic Ala to hydrophilic Ser. However A206S is a polymorphism that occurs naturally as a variant of EBV (Grunewald *et al.*, 1998) and does not alter dimerisation stability or DNA binding (Hicks *et al.*, 2001). Two sequential rounds of sdm were required to create firstly L216I and L218M, then the mutation D212E (Figure 5.5A,B) was added. Attempts to mutate Ala-206 to Ser failed. As this is a polymorphic site, it was decided to leave this residue as Ala in the mutant. ZipZta contains the amino acid changes L216I, L218M and D212E (Figure 5.5 C,D).

Creation of CT domain swap mutant, CTZta.

The extreme C-terminus of ZtaRh lacks the final two amino acids, Asn-244 and Phe-245 found in Zta. The terminal residue of ZtaRh is Leu-243, while Zta contains an Ile at position 243. This means that the final amino acid in Zta is Phe compared with Leu in ZtaRh. The terminal domain contains 2 additional conservative differences between Zta and ZtaRh, V237I and L238I (Figure 5.6A). Two cycles of sdm were undertaken to create the domain swap mutant CTZta (Figure 5.6B-D). All mutants were sequenced to confirm the changes.

A

```
ATAAAGCGATACAAGAATCGGGTGGCTTCCAGAAAATGCCGGGCCAAGTTTAAGCAACTGCTGCAGCACTACCGTGAGGTGGCT
GCTGCCAAATCATCTGAAAATGACAGGCTGCGCCTCCTGTTGAAGCAGATGTGCCCAAGCCTGGATGTTGACTCCATTATCCCC
CGGACACCAGATGTTTTACACGAGGATCTCTTAAATTTCTAA
```

B

B1: K192R and Q195N

```
F:  CGGGTGGCTTCCAGAAAATGCCGGGCCAGGTTTAAGAATCTGCTGCAGCACTACCGTGAGGTGGCTGC
```

C

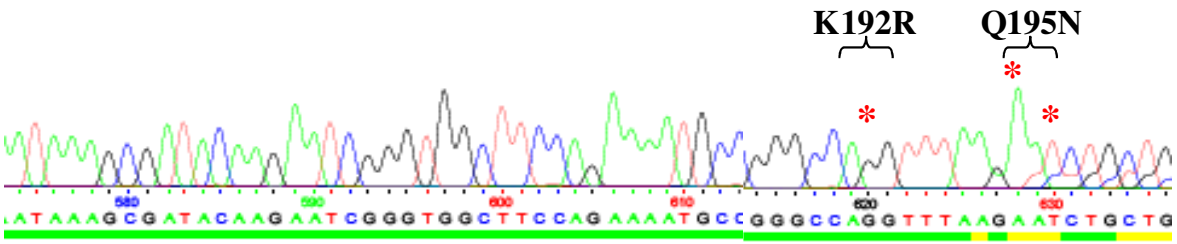

D

```
. . IKRYKNRVASRKCRARFKNLLQHYREVAAAKSSENDRLRLLLKQMCPSLDVDSIIPRTPDVLHEDLLNF
```

Figure 5.4: Basic Region Domain Swap
A. The nucleotide sequence of the three C-terminal domains of Zta. The Basic domain is in blue with the two codons causing an amino acid difference in ZtaRh highlighted. The bases that will be mutated to encode the ZtaRh residue are shown in red. **B.** The sequence of the site directed mutagenesis (sdm) forward primer with the alterations highlighted. The reverse primer is the reverse complement of this sequence. The template for the sdm was Zta in a pBabe vector. A chromatogram of the mutated DNA is shown in **C** with altered bases indicated with a red asterisk. **D.** The amino acid sequence encoded by the domain swap mutant BZta.

A

ATAAAGCGATACAAGAATCGGGTGGCTTCCAGAAAATGCCGGGCCAAGTTTAAGCAACTGCTGCAGCACTACCGTGAGGTGGCT
GCTGCCAAATCATCTGAAAATGACAGGCTGCGCCTCCTGTTGAAGCAGATGTGCCCAAGCCTGGATGTTGACTCCATTATCCCC
CGGACACCAGATGTTTTACACGAGGATCTCTTAAATTTCTAA

B

Zip1: L216I and L218M

F: GCCAAATCATCTGAAAATGACAGGCTGCGCATCCTGATGAAGCAGATGTGCCCAAGCCTGGATGTTGAC

Zip2: D212E

F: CCAAATCATCTGAAAATGAAAGGCTGCGCATCCTGATGAAGC

C

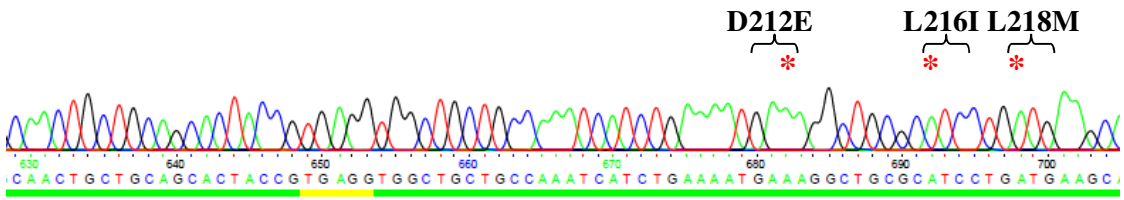

D

..IKRYKNRVASRKCRAKFKNLLQHYREVAAAKSSENERLRILMKQMCPSLDVDSIIPRTPDVLHEDLLNF

Figure 5.5: Coiled Coil Domain Swap

A. The nucleotide sequence of the three C-terminal domains of Zta. The coiled coil or zipper domain is in green with the five codons causing an amino acid difference in ZtaRh highlighted. A206 is not mutated as this site is polymorphic. The bases that will be mutated to encode the ZtaRh residue are shown in red. **B.** The sequences of the two sequential sdm forward primers are shown**,** with the alterations highlighted. In primer Zip2 the blue bases were mutated in the previous stage of sdm. **C.** A chromatogram of the mutated DNA is shown with altered bases indicated with a red asterisk. **D**. The amino acid sequence encoded by the domain swap mutant ZipZta.

A

```
ATAAAGCGATACAAGAATCGGGTGGCTTCCAGAAAATGCCGGGCCAAGTTTAAGCAACTGCTGCAGCACTACCGTGAGGTGGCT
GCTGCCAAATCATCTGAAAATGACAGGCTGCGCCTCCTGTTGAAGCAGATGTGCCCAAGCCTGGATGTTGACTCCATTATCCCC
CGGACACCAGATCTTTTACACGAGGATCTCTTAAATTTCTAA
```

B

CT1: V237I and L238I

```
F:  GTTGACTCCATTATCCCCCGGACACCAGATATTATCCACGAGGATCTCTTAAATTTCTAACTCCCG
```

CT2: L243I, Δ244N and Δ245F

```
F:  CCGGACACCAGATATTATCCACGAGGATCTCATATAACTCCCGTTATTGAAACCACGCCTGCTTC
```

C

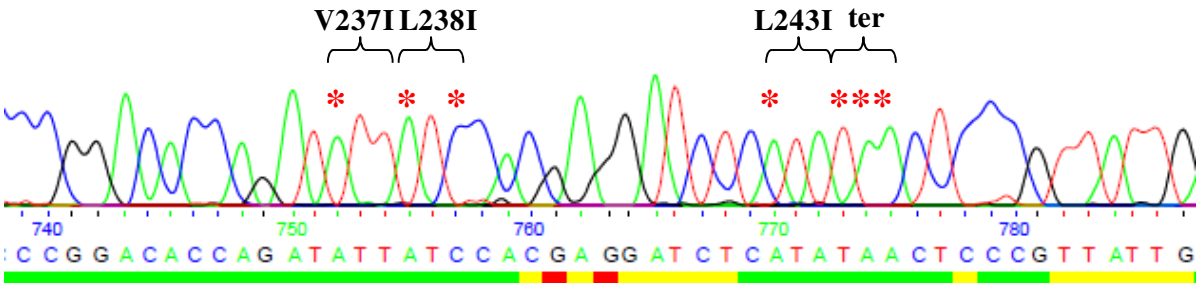

D

```
..IKRYKNRVASRKCRAKFKQLLQHYREVAAAKSSENDRLRLLLKQMCPSLDVDSIIPRTPDIIHEDLI--
```

Figure 5.6: CT Domain Swap

A. The nucleotide sequence of the three C-terminal domains of Zta. The CT domain is in purple with the six codons causing an amino acid difference to ZtaRh highlighted. The bases that will be mutated to encode the ZtaRh residue are shown in red. **B.** The sequences of the two sequential sdm forward primers with the alterations highlighted. In primer CT2 the blue bases were mutated in the previous stage of sdm. A stop codon was introduced to delete residues 244 and 245. Sdm was done using pBabe Zta as template. A chromatogram of the mutated DNA is shown in **C** with altered bases indicated with a red asterisk and the stop codon labelled ter. **D**. The amino acid sequence encoded by the domain swap mutant CTZta.

5.2.3 EBV reactivation by domain swap mutants

In order to attempt to localise the loss of reactivation ability to one or more regions of the ZtaRh protein, lytic reactivation assays were undertaken using the three domain swap mutants. Experiments were performed as previously for ZtaRh. BZta, ZipZta and CTZta were analysed in comparison to Zta and empty pBabe. Western blots using his antibody were performed to confirm that equivalent levels of protein were present in each sample (Figure 5.7A). The gene bcl2 was used as a loading control, although as this gene is associated with apoptosis it was not an appropriate control. All three of the domain swap mutants were able to reactivate the lytic cycle to some degree, although none were equivalent to Zta reactivation (Figure 5.7B). BZta reactivation was reduced by 24% in comparison to Zta. There was a greater inhibition of lytic reactivation shown by the other two mutants. Transfection by the mutant ZipZta resulted in a 60% decrease in detected EBV genome. CTZta transfection demonstrated a 78% reduction in EBV genome in comparison to wild type Zta and is only marginally above the background level shown by transfection with the empty vector pBabe. The loss of lytic reactivation effect was stronger towards the CT end of the protein; indeed reactivation by both CTZta and ZtaRh was very weak or may be background noise. This data suggests that differences in the basic, zipper and CT regions of Zta and ZtaRh do have an effect on the ability of the protein to reactivate EBV from latency, however further experiments and use of a different loading control may further elucidate the levels of activation achieved by each variant.

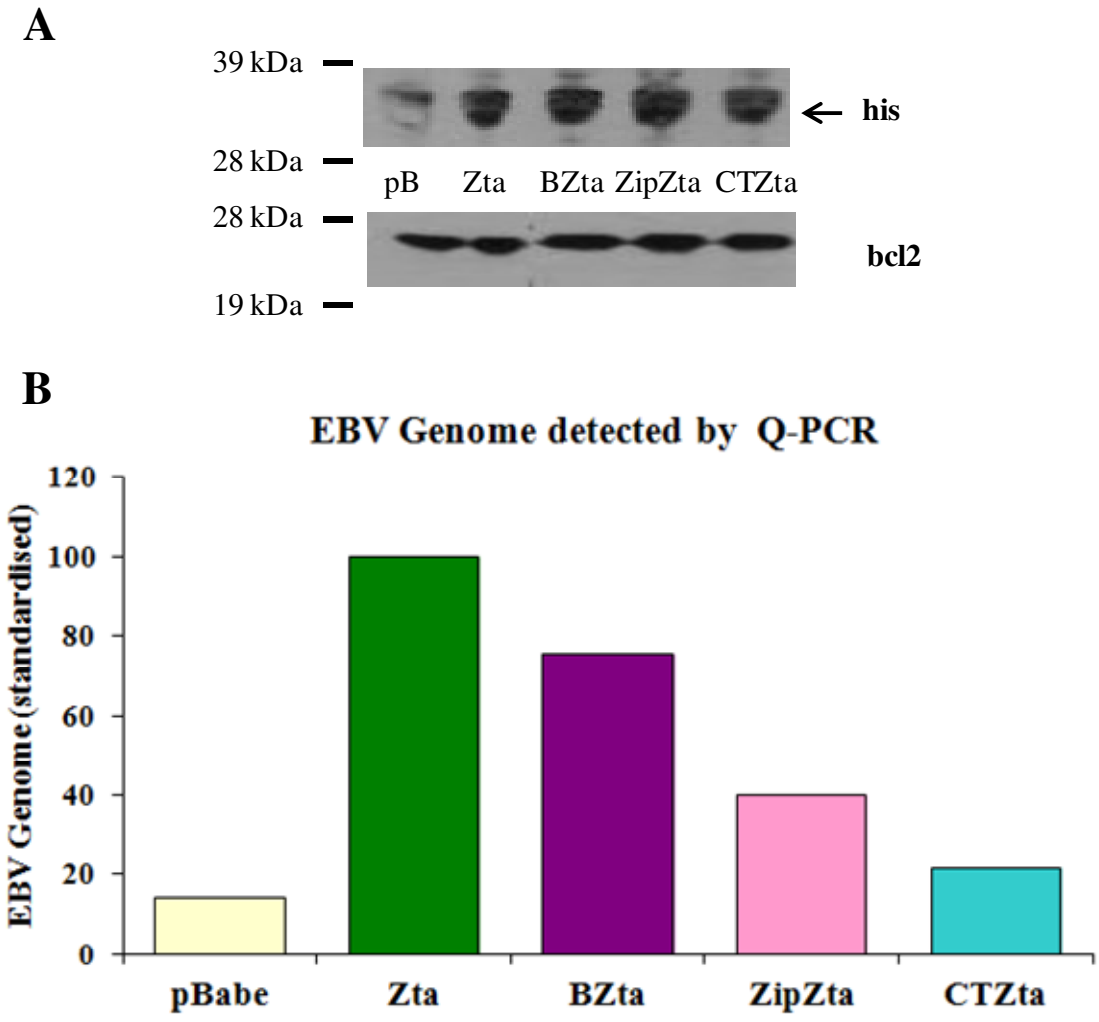

Figure 5.7: Reactivation of lytic cycle by Zta and ZtaRh domain swap mutants
Three domain swap mutants containing ZtaRh domains in a Zta background, BZta, ZipZta and CTZta were utilised to reactivate the lytic cycle in Hek293-ZKO cells. Western blots confirm that approximately equal amounts of protein were present (**A**). Transfection and QPCR were carried out as described in Figure 5.2 and levels of EBV genome detected are shown in **B**. Experiments were duplicated and average value shown.

5.2.4 Analysis of extreme CT mutants

One of the key differences between the CT regions of the two proteins is that ZtaRh lacks the two terminal amino acids (NF). As the most substantial reduction in lytic reactivation was observed in the CT region, a closer analysis of mutants in this area may further clarify the importance of individual residues for this function. Celine Schelcher had previously constructed three mutants of Zta with each of the three extreme CT amino acids converted to alanine (L243A (ANF), N244A (LAF) and F245A (LNA)) and one with all three changed to AAA (LNF243-245AAA (AAA)) (Figure 5.8A).

I sub-cloned these LNF mutants from an SP64 vector into pBabe as a way to further analyse the effect of this CT region on lytic reactivation ability. The same EBV reactivation experiment was repeated using the LNF mutants. BZ1 western blots to reveal expressed protein levels showed that the Zta was expressed at equivalent levels for the Zta sample and all mutants with the exception of ANF, which was approximately half that of the other proteins (Figure 5.8B).

In the mutant AAA, with all three extreme CT amino acids altered, the ability for lytic cycle reactivation was abrogated, as expression of the EBV genome was below that of background (pBabe) (Figure 5.8C). This suggests that these three terminal amino acids may fully account for the reduction in lytic cycle reactivation of ZtaRh. Although the strongest effect appears to be from ANF, Zta was expressed at a lower level in both experiments for this protein, as can be seen on the western blot, so activation may be under-represented. Both AAA and ANF EBV genome levels are lower than that of empty pBabe, suggesting that these mutants have complete loss of lytic reactivation ability. As the expression of the EBV genome for AAA and ANF is below that of the pBabe control containing no EBV genome, this represents a variation in the experimental system that should be addressed in further experiments. The level of EBV genome detected in cells transfected with ANF was reduced by 93.6% compared to Zta, LAF by 37.5 %, LNA by 70.9 % and AAA by 89.3 %.

These lytic reactivation assays suggest that the extreme CT region of Zta is essential for lytic reactivation, however further experiments should be conducted to allow significant data to be generated. This would also determine if the results showing a lower level of EBV genome activation than the empty pBabe vector are accurate.

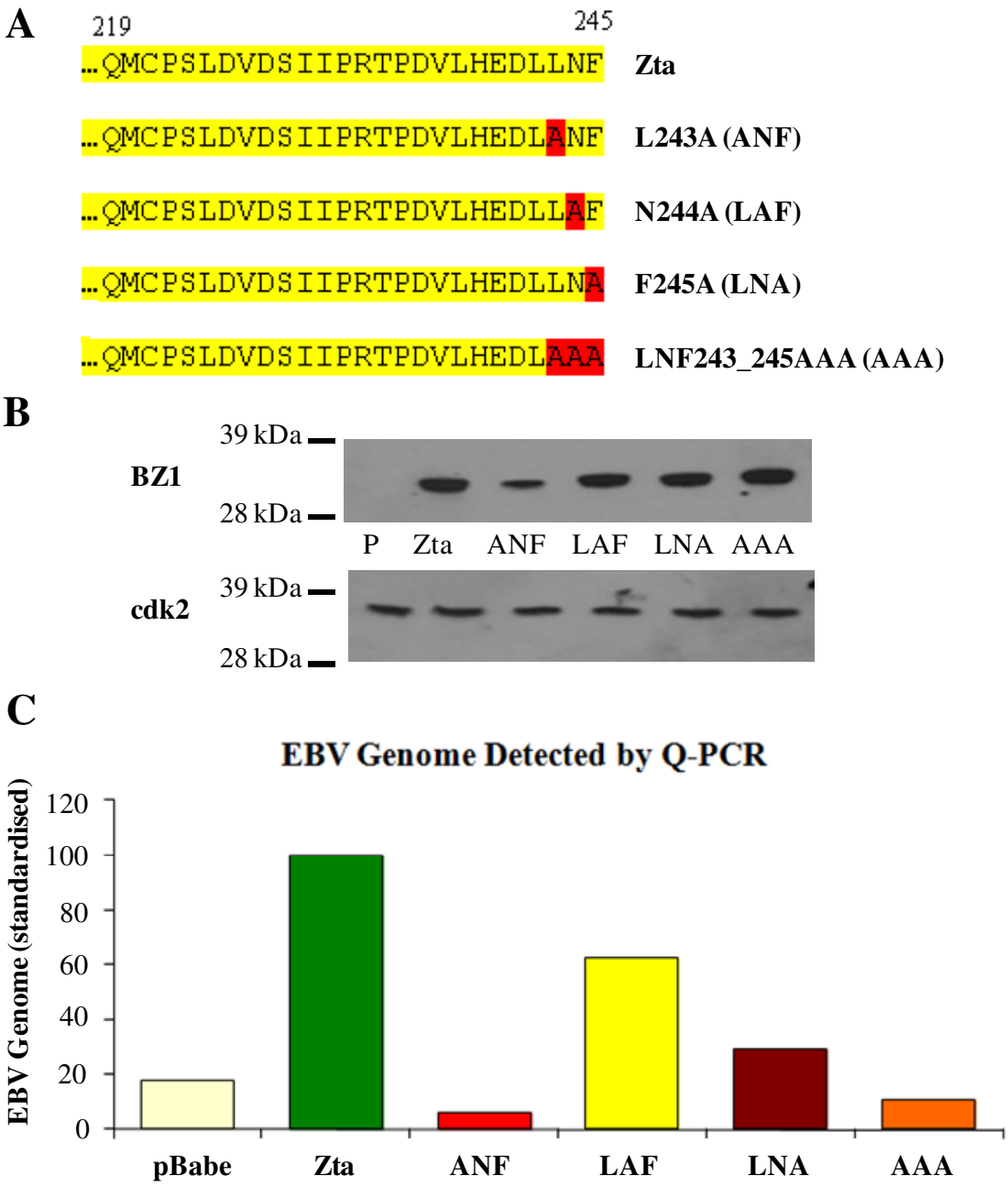

Figure 5.8: Reactivation of lytic cycle by Zta and C-terminal LNF mutants
pBabe expression vectors containing Zta and mutants with substitutions to alanine of 1 or all 3 of the terminal amino acids LNF (**A**), created by Celine Schelcher, were transfected into HEK293-ZKO cells. Western blots used BZ1 antibody to detect Zta and mutants and cdk2 as a loading control (**B**). The level of Zta protein detected by BZ1 antibody for ANF was approximately half the rest of the samples. QPCR was performed on the genomic DNA to determine levels of EBV genome present (**C**). Transfection and QPCR were carried out as described in Figure 5.2. Experiments were duplicated and the average value is shown.

5.2.5 Regulation of the Cell Cycle by Zta and RhZta

In the next series of experiments the effect of ZtaRh on the cell cycle was assessed. Zta has the ability cause cell cycle arrest in some cell types including HeLa cells (Cayrol and Flemington, 1996b). This occurs through several mechanisms as detailed in section 1.4.8. I wanted to investigate if the ability of Zta to cause cell cycle arrest is shared with RhZta.

HeLa cells were co-transfected with GFP vector and Zta, ZtaRh or empty vector (pBabe) expression vectors. Cells were harvested after 48 hours and a sample of cells was used for western blot analysis using an anti-his antibody. This was to determine that an equivalent level of protein expression of Zta or ZtaRh is observed in each sample. Prior to establishment of cell cycle status, a sample of cells were prepared for analysis of transfection efficiency for each experiment. Cells were resuspended in PBS and analysed with a flow cytometer. In order to calculate transfection efficiency, healthy cells were gated and the proportion that were positive for GFP was determined (Figure 5.9). Cells that are expressing GFP are assumed to also be successfully transfected with the experimental expression vector.

A third fraction of cells was fixed in 80% ethanol and stained with propidium iodide. The cell cycle profile was determined for these cells by flow cytometry analysis. As propidium iodide binds stoichiometrically to DNA, cells are selected according to DNA content and thus are categorised to cell cycle phase; G1/G0, S or G2/M (Figure 5.10)

The transfection efficiency in the initial experiment was between 61% and 67% (Figure 5.9). Transfection efficiency remained consistently at that approximate level for all experiments. Cells that were transfected with Zta showed on average a 12.6% increase in the G1 cell population over cells transfected with empty pBabe (Figure 5.11). However cells transfected with ZtaRh had only a 2.6% increase in G1 cells. The results are significantly different using a Mann-Whitney U test ($U=16$, $n1 = n2 = 4$, $P=0.02857$). The experiment was repeated 4 times. The western blots in Figure 5.11 confirm that an equivalent amount of his-tagged protein was expressed for Zta and

ZtaRh. ZtaRh shows an almost complete inability to promote cell cycle arrest in HeLa cells.

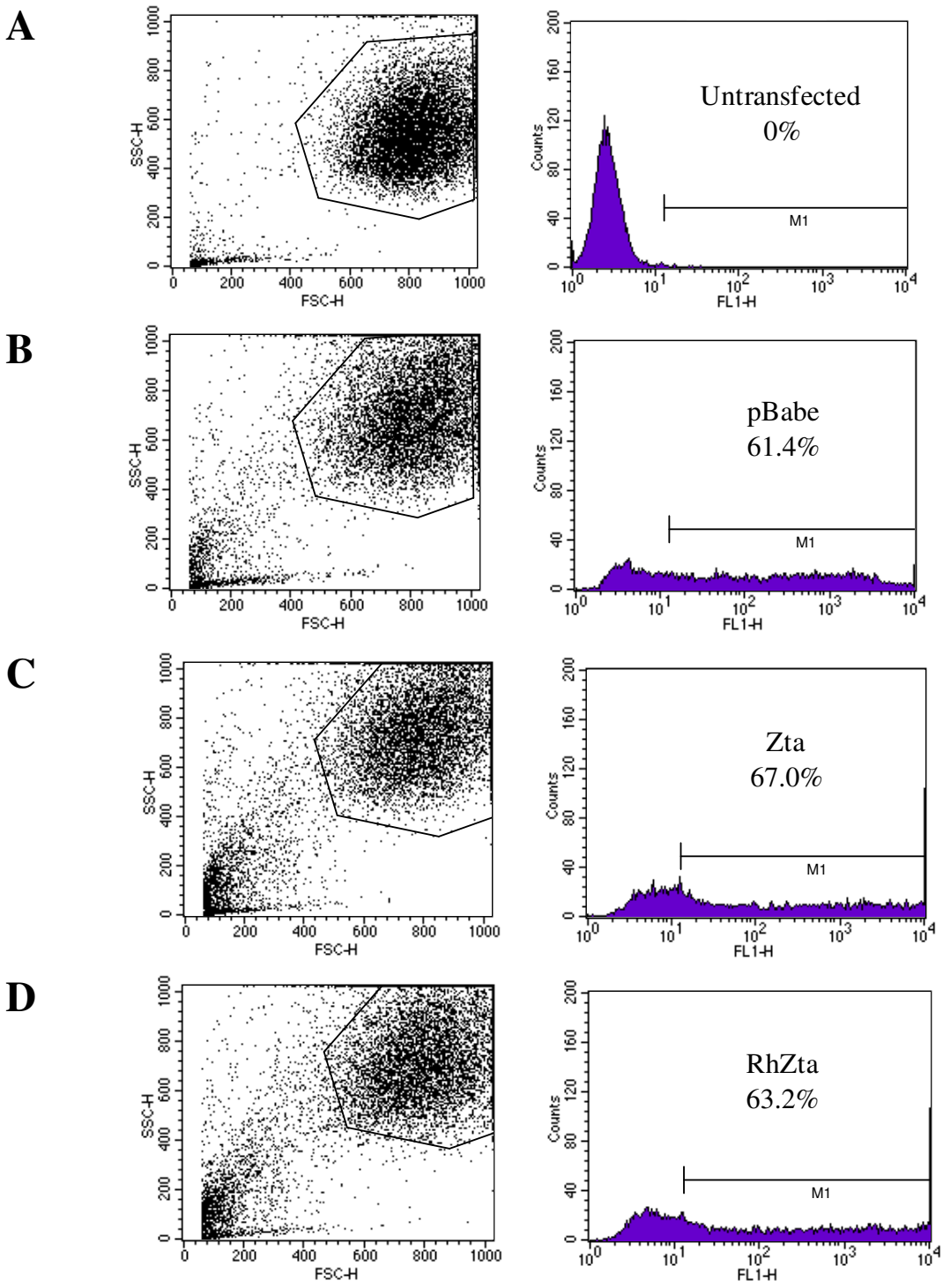

Figure 5.9: Transfection Efficiency as determined by FACS analysis
HeLa cells were untransfected (**A**) or transfected using Calcium Phosphate with pBabe (**B**), Zta (**C**) or ZtaRh (**D**), along with 250ng of GFP vector. A sample of cells harvested after 48 hours were tested for transfection efficiency using flow cytometry. Healthy cells were gated (left panels) and then selected for presence of GFP, giving a transfection efficiency percentage (right panel).

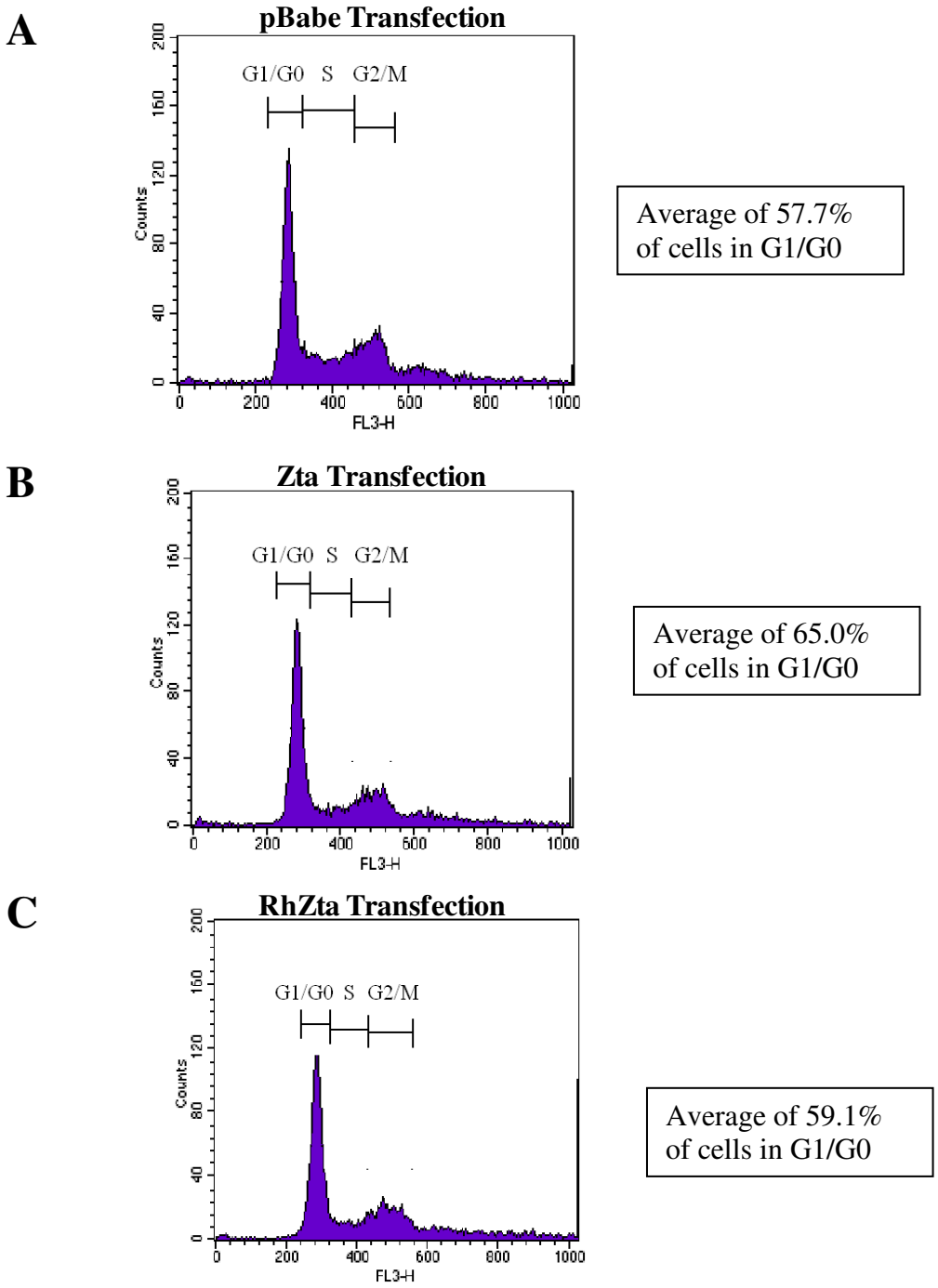

Figure 5.10: Cell cycle analysis of Zta and ZtaRh
HeLa cells transfected with pBabe vector (**A**), Zta (**B**) or ZtaRh (**C**) were treated with RNAse and stained with propidium iodide (PI). Flow cytometry (FACS) was used to detect the fluorescence from PI bound to DNA to show the distribution of cells in G1/G0, S and G2/M of the cell cycle. The average number of cells in G1/G0 is shown to the right of each graph.

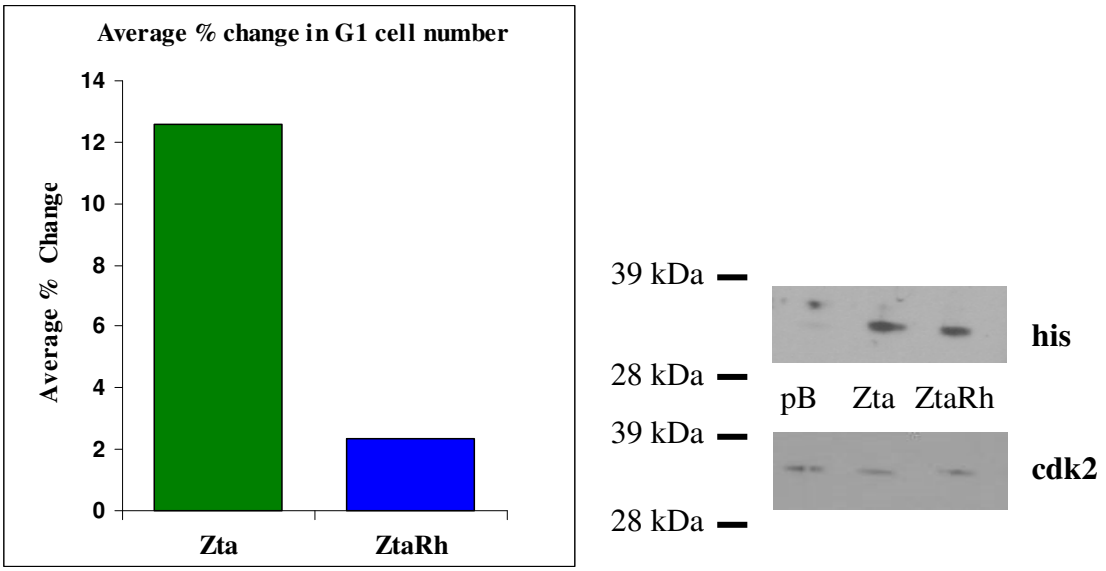

Figure 5.11: ZtaRh is compromised in Human Cell Cycle arrest function
The graph shows the average increase in G1 cells compared to cells transfected with pBabe alone, as detected by FACS analysis. This experiment was repeated 4 times. The results are significantly different with a Mann-Whitney U test (U=16, n1 = n2 = 4, P=0.02857). The western blot using his-antibody shows the presence of the his-tagged proteins. Cdk2 is shown as a loading control.

In order to localise this loss of cell cycle arrest function that ZtaRh displayed, the same experiments were repeated using the domain swap mutants, BZta, ZipZta and CTZta, described in Figure 5.3. There was no change from Zta in the increase in G1 cells in cells transfected with BZta or ZipZta (Figure 5.12). There was a slight reduction in cell cycle arrest function seen in the mutant CTZta (7.1% compared with 11.9% for Zta). However this does not account for the entire reduction seen with cells transfected with ZtaRh.

The cell cycle assay was repeated using the extreme CT LNF mutants, to reveal if the reduction in cell cycle arrest function seen in the mutant CTZta could be localised. However the level of reduction observed with each of the three mutants was slight (Figure 5.13).

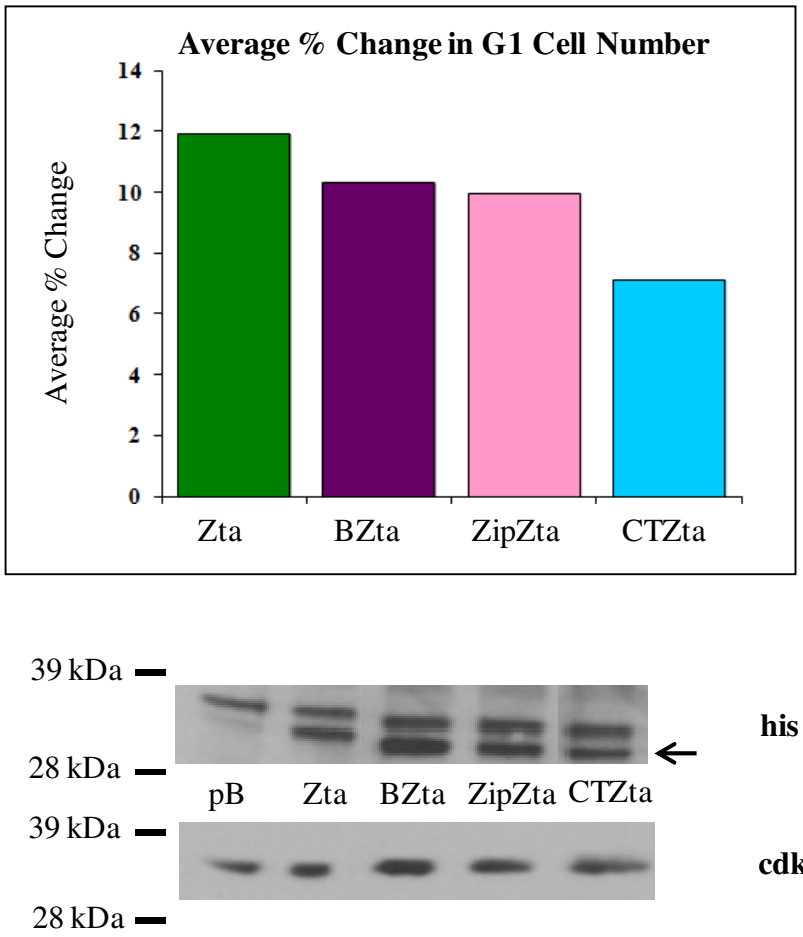

Figure 5.12: Cell cycle analysis of Zta and domain swap mutants
HeLa cells were transfected with pBabe vector, Zta, BZta, ZipZta and CTZta and cell cycle assays were performed as in Figure 5.10. Experiments were duplicated and average value shown. Western blot shown his-Zta and mutants detected by α-his antibody and cdk2 as a loading control are shown.

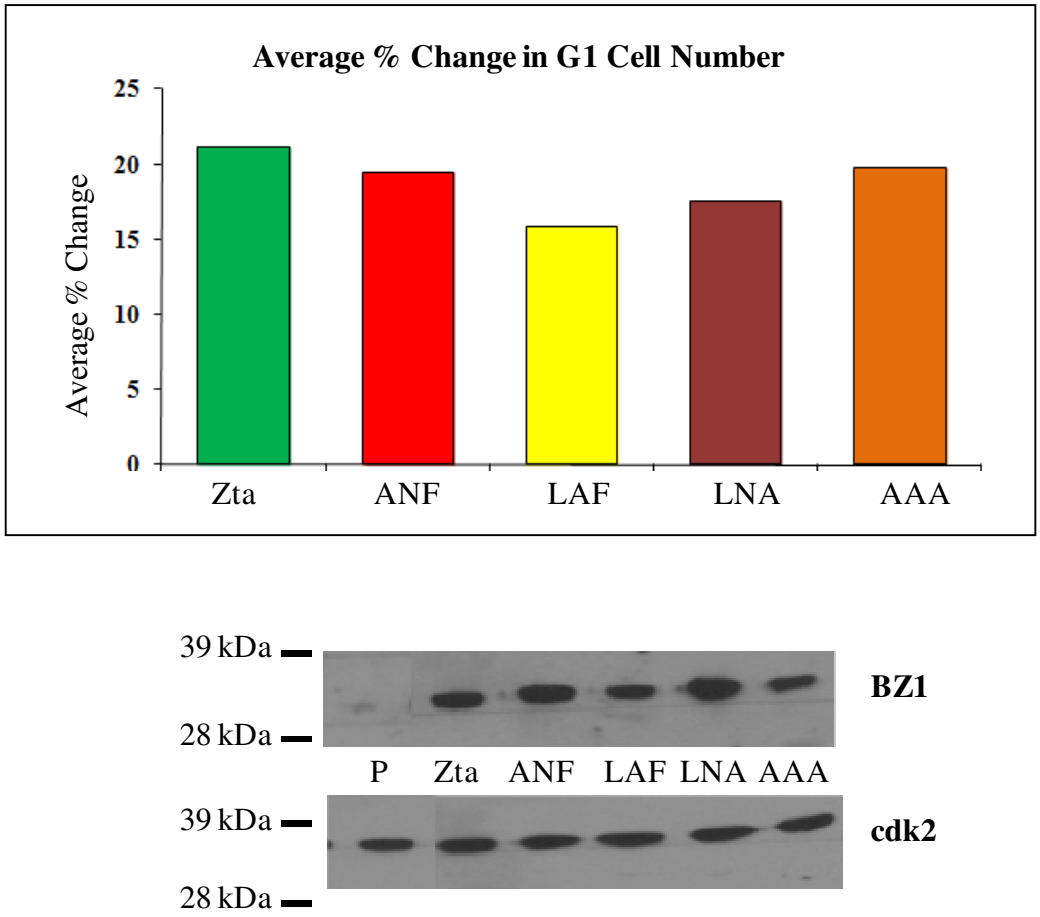

Figure 5.13: Ability of extreme C-terminal Zta mutants to cause cell cycle arrest
Four substitution mutants of the three C-terminal amino acids of Zta, as described in Figure 5.8 were used to transfect HeLa cells. The cell cycle arrest assay was performed as in Figure 5.11. Western blots showing Zta detection by BZ1 and cdk2 as a loading control are shown below the graph.

The loss of lytic reactivation ability of ZtaRh could not be accounted for by the same mechanism as the reduced ability of ZtaRh to cause cell cycle arrest as the extreme CT region is not implicated in the latter function. In order to further characterise the loss of lytic reactivation I developed a series of QPCR probes to span the lytic reactivation cascade. This could reveal when in this cascade of activation the extreme CT of Zta is critical for the process and give an insight into the possible mechanism.

5.2.6 Analysis of lytic cycle cascade

Replication of EBV genes in the lytic cycle occurs in a cascade of sequential gene activation (Figure 5.14). This commences with the immediate early transcription factors Zta and Rta, which transactivate their own promoters as well as early genes. The early genes transcribe proteins involved in viral DNA replication, resulting in the creation of linear viral genomes. Late genes are involved in the packaging of this viral DNA into complete virions. Further information about the mechanism responsible for the loss of reactivation by CT mutants of Zta could be uncovered by revealing the stage at which lytic reactivation is compromised.

The immediate early genes BZLF1 and BRLF1, early genes BBLF2/3, BHLF1 and EBV DNA polymerase (BALF5) and the late gene BLLF1 were selected for further QPCR analysis. QPCR primers were designed for BBLF2/3, BHLF1 and BLLF1 and also for the latent gene LMP1. I attempted to design primers that crossed splice sites to ensure that the quantitative PCR would analyse cDNA only and not background genomic DNA. However this was not possible for all genes. Primers for BBLF2/3, LMP1, Zta and Rta do cross splice sites but other primer pairs do not.

HEK 293 ZKO cells were transfected with Zta, ZtaRh or empty vector (pBabe) and harvested as in the earlier experiments. RNA was extracted and treated with RQ1 DNase to degrade genomic DNA that could contaminate the QPCR. cDNA was produced from the DNase-treated RNA. This was analysed using QPCR to determine the level of gene expression for BRLF1, BBLF2/3, EBV polymerase, BHLF1, BLLF1 and LMP1 (Figure 5.15A). Expression levels were normalised to the host ribosomal protein L32. Rta was expressed by ZtaRh to 45% the level of activation by Zta. ZtaRh shows markedly reduced relative levels of expression for all 3 early genes (12-20% of activation by Zta).

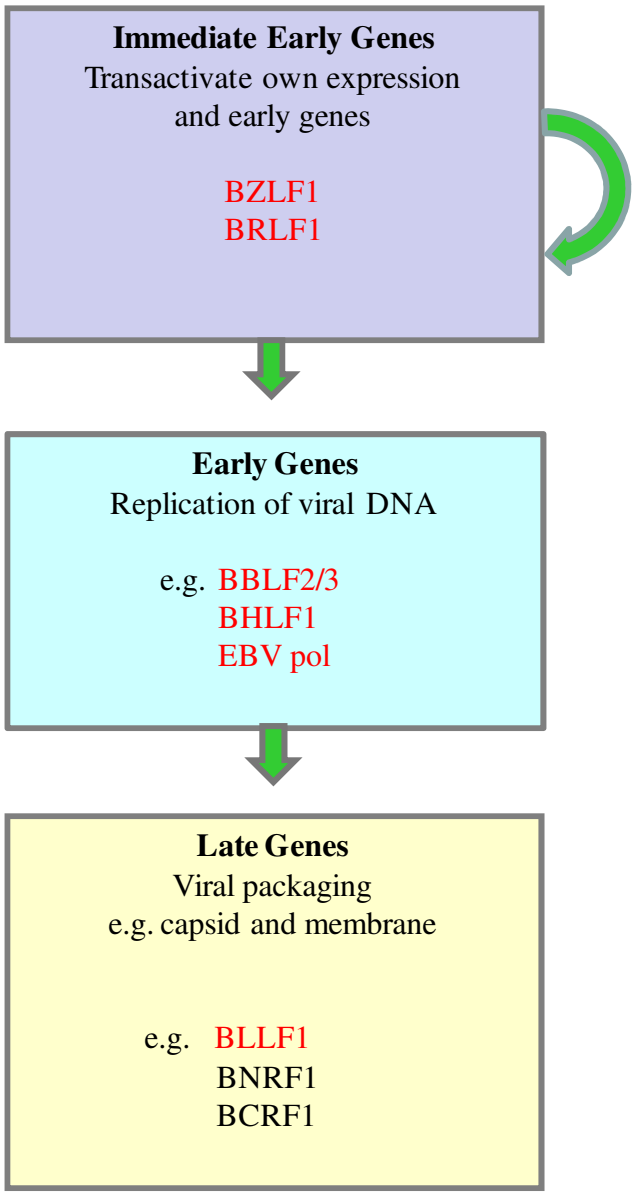

Figure 5.14: Cascade of lytic gene activation
EBV replication in the lytic cycle proceeds through a cascade of sequential gene activation. Initially the immediate early transcription factors BZLF1 and BRLF1 are expressed, transactivating their own promoters and early genes. Early genes are involved in the replication of viral DNA , creating linear viral genomes. Late genes transcribe proteins including viral capsid, membrane and tegument proteins for packaging this DNA into complete virions. Genes highlighted in red were used for RT-PCR to determine at which stage of lytic activation ZtaAAA is defective.

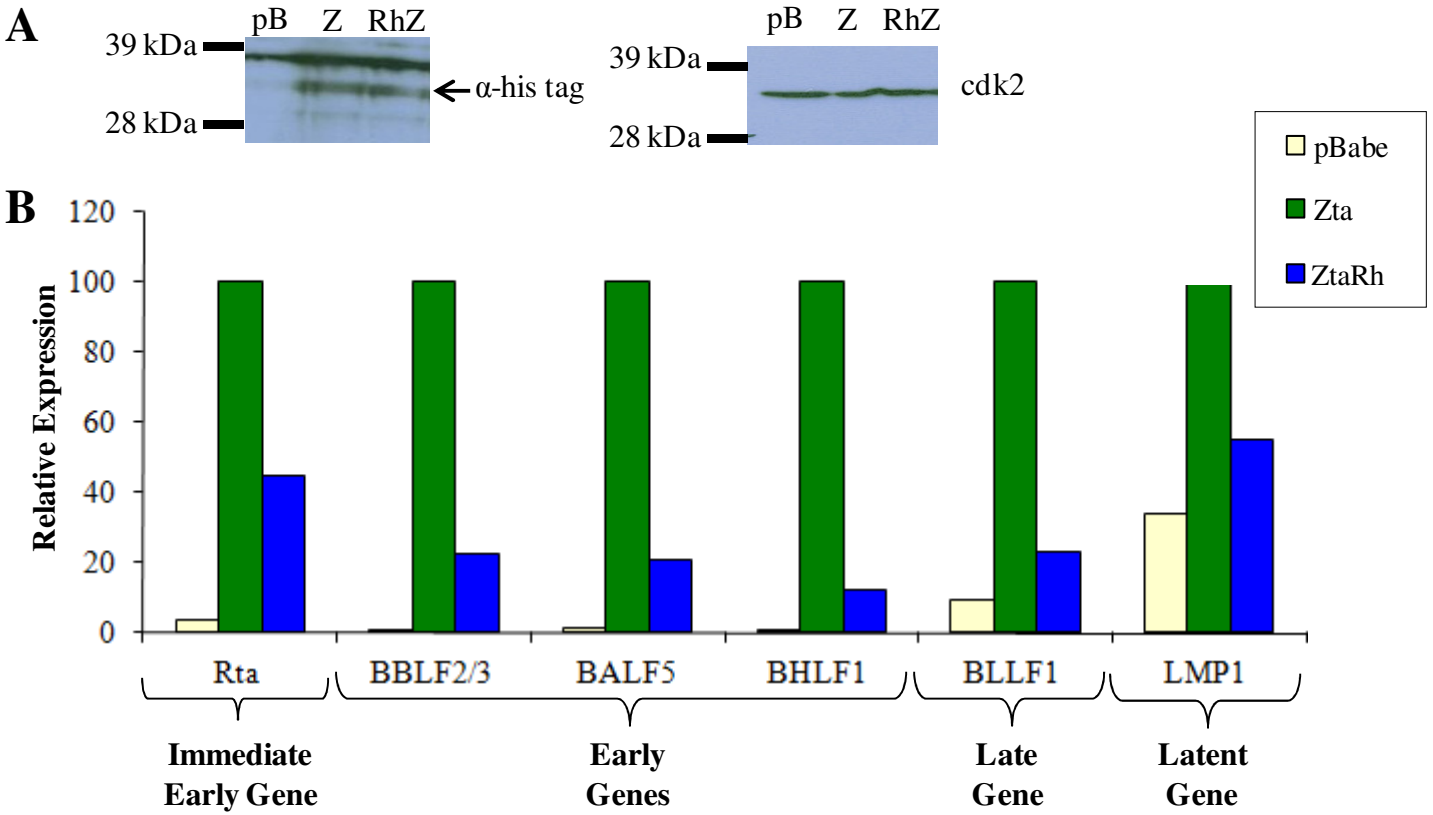

Figure 5.15: RT-PCR of Zta and ZtaRh for selected EBV genes
HEK293-BZLF1ko Cells were transfected with 0.8µg of DNA (Zta, ZtaRh or empty vector (pBabe)) and harvested after 48 hours. Total RNA was extracted, DNase treated and cDNA was synthesized. Western blots using α-his tag and cdk2 antibodies confirmed equivalent expression of pBabe (pB), Zta (Z) and ZtaRh (RhZ) proteins and provided a loading control (**A**). 1 µl of each diluted cDNA sample was used in a real time PCR reaction with 0.5 µM of each primer and 12.5 µl SYBR Green mastermix (Qiagen). Each sample was standardised for cDNA amount using the housekeeping gene L32. The ability of each protein to activate gene expression was assessed using primers for Rta, BBLF2/3, BALF5 (EBV pol), BHLF1, BLLF1 and LMP1 (**B**). Values have been normalised to Zta expression for each gene. The experiment has been duplicated and average value shown.

The experiment was repeated using DNase treated RNA from HEK 293 ZKO cells transfected with Zta, ZtaAAA or empty vector (pBabe). A western blot for BZLF1 confirmed that equivalent levels of protein were expressed and a western blot for cdk2 was performed as a loading control (Figure 5.16A).

ZtaAAA demonstrated a different distribution of expression for these selected genes (Figure 5.16B). AAA demonstrated higher levels of expression for BZLF1 (60% higher), BRLF1 (135%) and the early gene BBLF2/3 (187%) than Zta. However for the other two early genes, EBV pol and BHLF1 and the late gene BLLF1, expression had dropped to approximately similar levels to ZtaRh (16%, 26% and 27% respectively). This indicates that the reduced expression from ZtaRh is via an additional mechanism affecting activation of Rta. For the latent gene LMP1 expression through ZtaRh activation was reduced to 54% of the level of Zta, while expression by AAA is approximately similar to Zta.

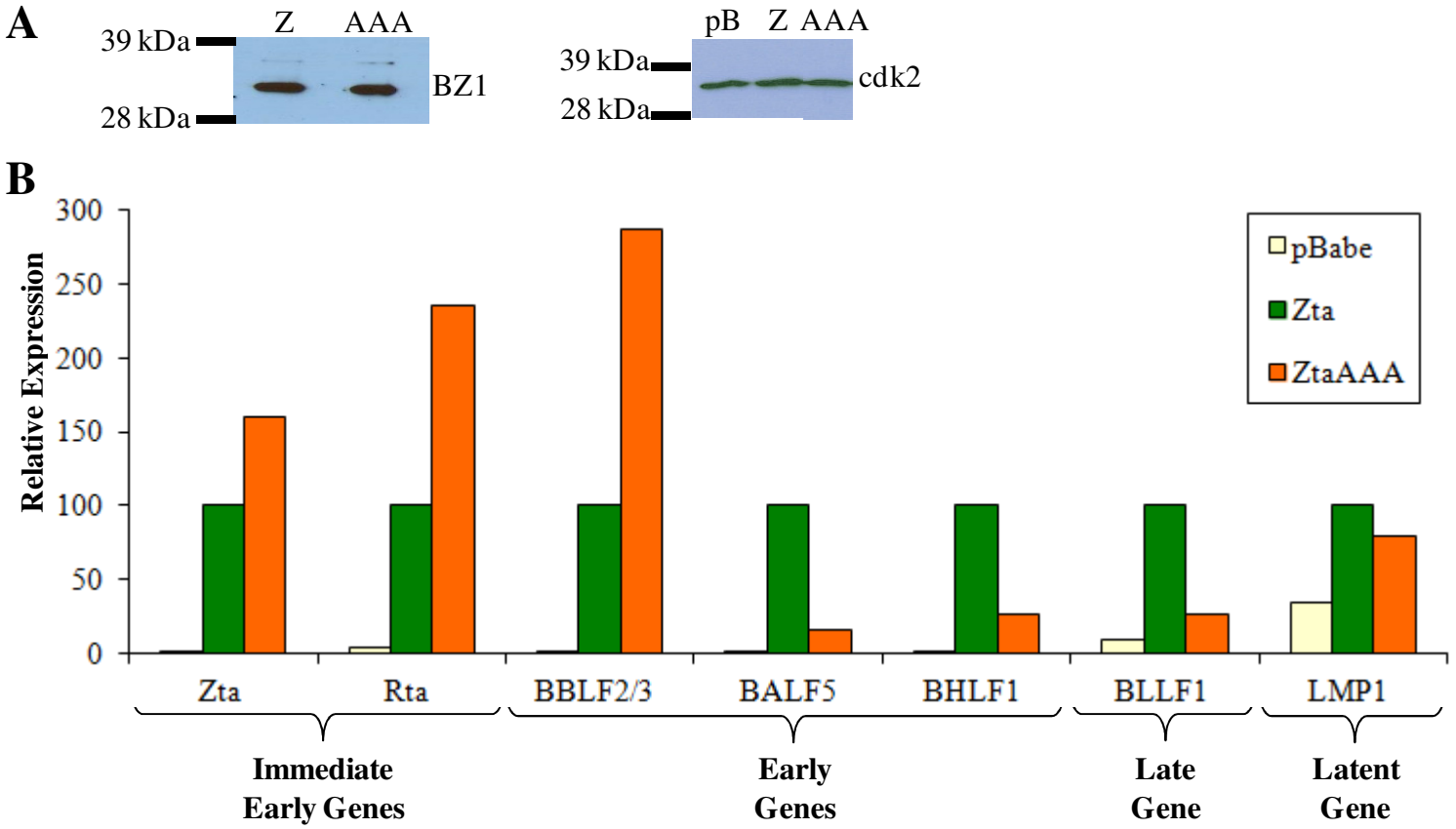

Figure 5.16: RT-PCR of Zta and ZtaAAA for selected EBV genes
HEK293-BZLF1ko Cells were transfected with 0.8µg of DNA (Zta, ZtaAAA or empty vector (pBabe) and harvested after 48 hours. Experiments were performed as in Figure 5.15. A BZ1 western blot showing equivalent expression of Zta (Z) and ZtaAAA (AAA) is shown and a cdk2 western blot is a loading control (**A**). The ability of each protein to activate gene expression was assessed using primers for Zta, Rta, BBLF2/3, BALF5 (EBV pol), BHLF1, BLLF1 and LMP1 (**B**). Values have been normalised to Zta expression for each gene. The experiment has been duplicated and average value ahown.

ZtaRh displayed poor activation and EBV replication. This could be caused by the changes in the transactivation domain or in combination with differences to Zta in the three C terminal domains. As ZtaAAA is only defective in expression of two early (BHLF1 and BALF5) and one late gene (BLLF1), it is possible that the extreme CT of ZtaRh has also contributed to decreased expression of these genes. In order to examine this two new mutants were designed; Rh_LNF and Zta_IΔΔ as shown in Figure 5.17A. Rh_LNF is comprised of ZtaRh sequence with the terminal Ile-247 replaced with Leu, Asn and Phe, the three terminal amino acids of Zta. Conversely Zta_IΔΔ is comprised of Zta sequence with the three terminal residues (LNF) replaced with Ile. Both mutants were created using mis-matched primers with PCR site-directed mutagenesis (Figure 5.17B-C). Mutants were sequenced to confirm changes.

Zta_IΔΔ does not appear to mimic the pattern of gene expression shown by ZtaRh (Figure 5.18). This suggests that the low expression seen in cells transfected with ZtaRh is not caused by the extreme CT of the ZtaRh gene. This is supported by the mutant Rh_LNF which does show expression at an almost equivalent level to ZtaRh. The only exception was higher expression of Rta in cells transfected with Rh_LNF (131% of Zta cell expression, compared with 45% in ZtaRh cells). The reduced expression of EBV polymerase, BHLF1 and BLLF1 seen with ZtaRh was not seen with Zta_IΔΔ. Considerably higher expression was seen for Zta, Rta, BBLF2/3 and EBV polymerase with Zta_IΔΔ than with Zta. As the differences in these proteins are restricted to the extreme CT, this further suggests that this region may be important to the function of Zta. This in turn may have a role in influencing the expression of multiple genes. As experiments were only duplicated, further replicates would have to be performed to provide results with any measure of significance. A summary of the expression for each protein is shown in Table 5.19.

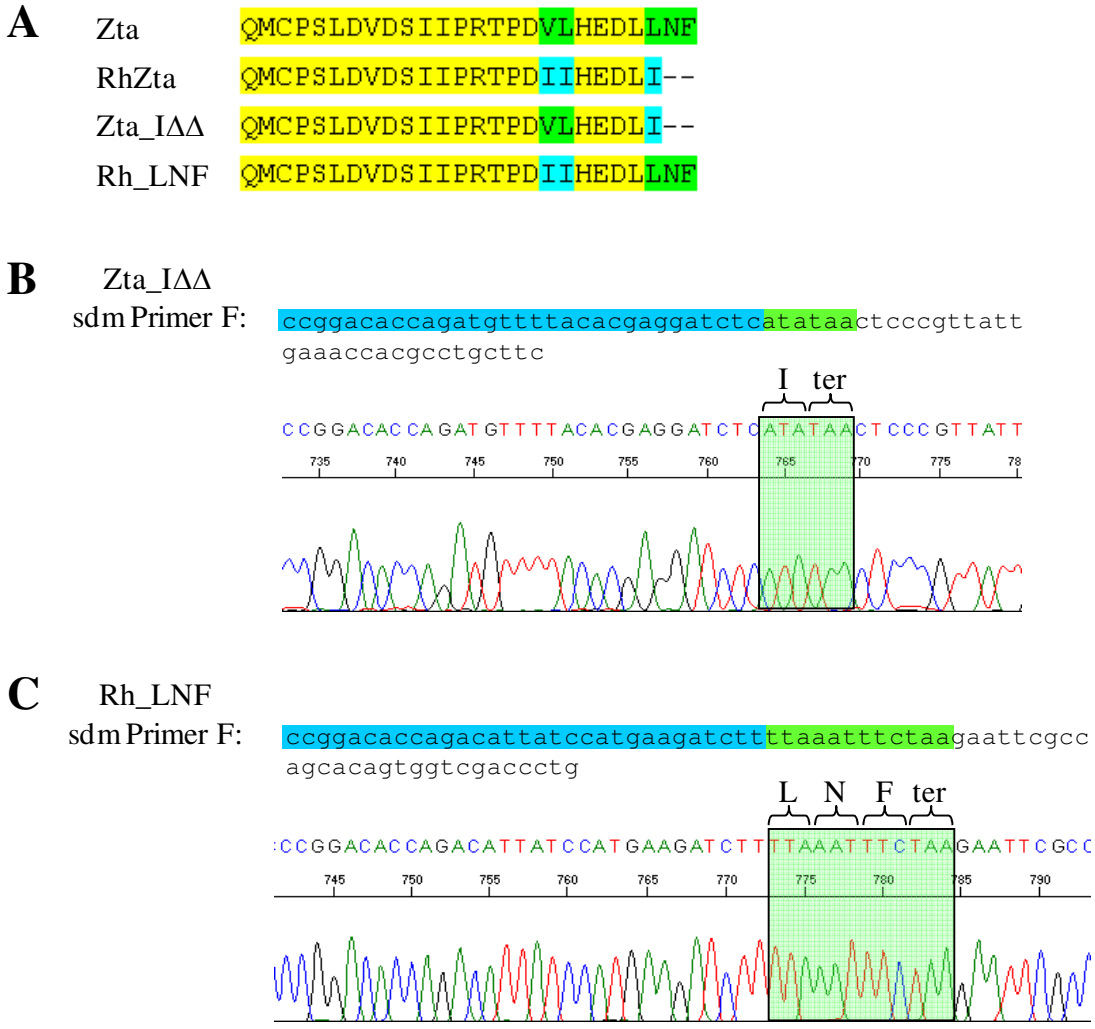

Figure 5.17: Construction of extreme CT mutants
A. Site directed mutagenesis was used to create two mutants that differ from Zta or ZtaRh only in the extreme CT residues. Zta_IΔΔ is Zta sequence with the terminal LNF replaced with I from Rh. The sdm primers and the sequence chromatogram are shown with the changed residues highlighted (**B**). Rh_LNF is ZtaRh sequence with the terminal I replaced with LNF from Zta (**C**).

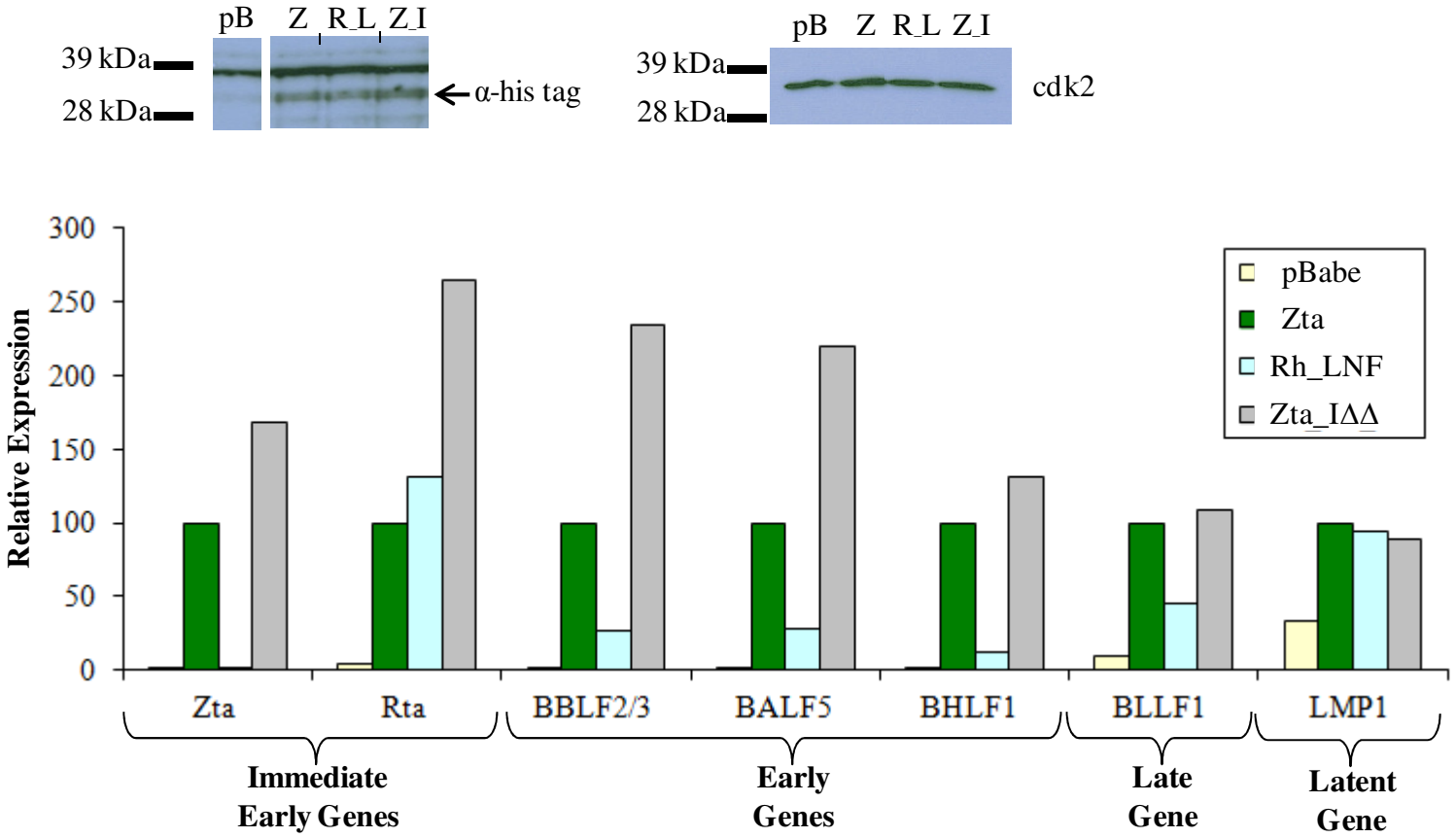

Figure 5.18: RT-PCR of Zta, Rh_LNF and Zta_IΔΔ for selected EBV genes
HEK293-BZLF1ko Cells were transfected with 0.8µg of DNA (Zta, Rh_LNF, Zta_IΔΔ or empty vector (pBabe)) and harvested after 48 hours. Western blots using α-his tag and cdk2 antibodies confirmed equivalent expression of pBabe (pB), Zta (Z), Rh_LNF (R_L) and Zta_IΔΔ (Z_I) proteins and provided a loading control (**A**). cDNA was produced and RT-PCR was performed as in figure 5.15 . The ability of each protein to activate gene expression was assessed using primers for Zta, Rta, BBLF2/3, BALF5 (EBV pol), BHLF1, BLLF1 and LMP1 (**B**). Values have been normalised to Zta expression for each gene. The experiment has been duplicated and average value shown.

		ZtaRh	ZtaAAA	Rh_LNF	Zta_IΔΔ
Immediate Early	Zta		+		+
	Rta	--	++	0	++
Early	BBLF2/3	--	++	--	++
	BALF5	--	--	--	++
	BHLF1	--	--	--	0
Late	BLLF1	--	--	--	0
Latent	LMP1	-	0	0	0

Table 5.19: Expression of EBV genes in cells transfected with ZtaRh and mutants in comparison with Zta cells.
Quantitative PCR was used to determine expression of EBV in cells transfected with Zta, ZtaRh, ZtaAAA, Rh_LNF or Zta_IΔΔ as described in Figure 5.16 and 5.18. Expression is shown realative to Zta transfected cells. **++** indicates greater than 1 fold increase over expression by Zta. **--** indicates greater than 1 fold decrease over expression by Zta. **0** indicates no difference in expression levels.

5.3 Discussion

ZtaRh has been shown to be defective in several key functions of Zta. ZtaRh was almost totally deficient in causing lytic reactivation in HEK 293 ZKO cells and in activating cell cycle arrest in HeLa cells. In addition ZtaRh was deficient in causing expression of selected early and late EBV genes. ZtaRh is not compromised in DNA binding so the loss of these other functions is via a different mechanism. ZtaRh differs markedly from Zta in the N-terminal transactivation and contains some more modest differences in the three C-terminal regions (Figure 5.3). The CT region has been shown previously to be important in lytic reactivation so I examined the contribution of differences between Zta and ZtaRh using three domain swap mutants. This showed that there was a small influence from the basic region and a stronger effect from differences in the zipper and CT regions. Use of four CT terminal mutants showed that mutation of Zta L243 to alanine (ANF mutant) was sufficient to lose lytic reactivation function. In addition a mutant with the three terminal amino acids, LNF, converted to AAA, ZtaAAA (AAA) was entirely compromised for this function. Examination of the domain swap and extreme CT mutants in a cell cycle assay revealed that despite a small decrease in cell cycle arrest from ZtaCT, the loss of this function maps outside of these domains. This means that differences in the transactivation domain most probably account for the loss of the cell cycle arrest function in ZtaRh.

To understand the mechanism of reactivation loss, it was of interest to determine at which stage of lytic reactivation ZtaRh and ZtaAAA are defective. ZtaRh showed reduced expression of Rta to 50% of the level shown by Zta, and was at very low levels for all early and late genes. In comparison ZtaAAA showed strong expression of Rta and the early gene BBLF2/3 with expression loss of the other early and late genes. This suggests an additional mechanism for some of the loss of activity by ZtaRh which affects Rta activation. The mutant Zta_IΔΔ showed that this is an effect from part of the protein prior to the CT region, probably the transactivation domain. Conversion of the ZtaRh terminal to LNF (Rh_LNF), mimicking Zta, restored replication of Rta to the same level as Zta. This shows that the reduced levels of Rta were not responsible for the loss of replication of genes later in the lytic reactivation cascade. In addition the latent gene LMP1 was expressed at wild-type levels with Rh_LNF, showing that the terminal three amino acids have no influence on transcription of this gene.

It is reasonable to assume that as RhLCV is a functional virus, ZtaRh would be a functional replication factor when operating on the right genome in the right cells. As yet little is known about the specific mechanisms of RhLCV and differences in protein co-factors, cellular environment and DNA sequence are likely to be critical for the optimal functioning of ZtaRh in rhesus cells and account for the loss of function observed in human cells.

The data presented in this chapter shows that the last three amino acids of Zta are critical for key functions of the protein. The extreme CT is conserved in all isolates of EBV suggesting the functional importance of this region (Grunewald *et al.*, 1998; Hicks *et al.*, 2001). The exact conformation of this region of Zta is not yet known as the terminal nine amino acids are missing from the current crystal structure (Petosa *et al.*, 2006). The preceding nine amino acids in the resolved Zta structure, D228-D236, have been shown to fold back, making stabilising contacts with the zipper domain for dimerisation (Petosa *et al.*, 2006). These interactions have been shown to be critical for DNA replication, but not for promoter transactivation (McDonald *et al.*, 2009). Cross-linking experiments have indicated that the extreme CT residues continue this contact with the zipper region (Schelcher *et al.*, 2007)(Figure 5.20). This is one possible mechanism by which the ZtaAAA mutant has such an impact on functions of Zta. As DNA binding is not obviously compromised in ZtaRh, the mechanism of reactivation loss may be due to a disruption in interactions with one or more proteins. The first example of a specific function to be ascribed to the extreme CT of Zta is the interaction of 53BP1 and Zta (Bailey *et al.*, 2009). Interaction between 53BP1 and Zta is greatly diminished with a deletion mutant of the three terminal amino acids, LNF. Additionally, Bailey and colleagues demonstrated that the knockdown of 53BP1 expression reduced EBV replication, which indicates that the association between Zta and 53BP1 is involved in the viral replication cycle (Bailey *et al.*, 2009).

ZtaRh contains a cysteine at the equivalent position to C189 of Zta. It would be interesting to investigate if a serine mutation at this position in ZtaRh would also result in methylation sensitive binding and if there would be any change in lytic reactivation. As ZtaRh is defective in lytic reactivation of EBV, this would have to be investigated in a cell-line containing CeHV-15, which we currently do not have.

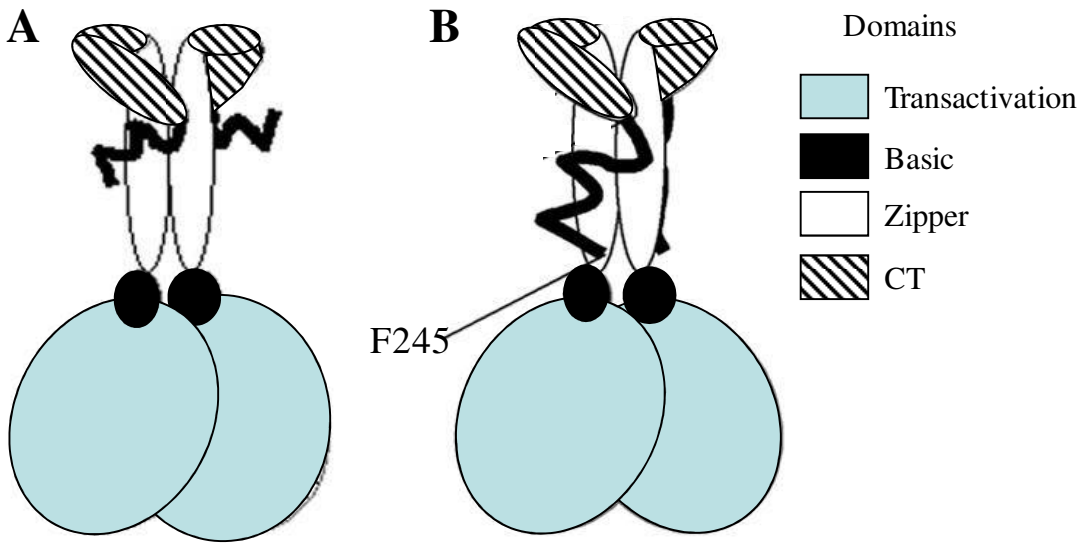

Figure 5.20: Schematic diagram of Zta structure
This schematic diagram of Zta is based on the crystal structure of Zta, as determined by Petosa and colleagues (Petosa *et al.*, 2006) which ends at D236. The distal CT region of Zta interacts with the zipper region (**A**). The wavy black line shows the extreme terminal CT region of unknown structure. Experimental cross-linking evidence shows that the extreme CT of Zta also makes contact with the zipper region (**B**) (Schelcher *et al.*, 2007)
(Diagram adapted from (Schelcher *et al.*, 2007)

Chapter 6 The impact of Zta on host cell proteins

6.1 Introduction

6.1.1 Zta Interactions

Zta interacts with a variety of different cellular and viral proteins. Many interactions occur through the transactivation domain, but several are dependent on the zipper dimerisation domain. As the CT region has contact with this domain, it is possible that alterations to the CT region may have an influence on the ability of Zta to form these contacts. It would be interesting to investigate how mutants of Zta in the CT region would affect the following Zta interactions, both *in vitro* and *in vivo*. If differences between Zta and ZtaRh influenced these interactions, it would be informative on the role of Zta in human cells.

6.1.2 Protein Interactions

A potential mechanism for the loss of function of Zta when mutated at the CT would be if interaction with an important protein was disrupted by alterations to the extreme CT region of Zta. This interaction could be with either a viral or cellular protein. This will be investigated in two stages. Initially known binding partners of Zta could be tested *in vitro* and *in vivo* for disruption to binding with alterations to this region.

CBP

CREB-binding protein (CBP) is a histone acetylase and a co-activator of transcription. CBP has been shown through an immunoprecipitation assay to positively regulate Zta transactivation (Adamson and Kenney, 1999). The acetylation of histones by CBP leads to a weakened association between the histones and DNA, resulting in a more open chromatin structure and better access for the basal DNA transcription machinery. Meanwhile Zta decreases the transactivation function for the transcription factor CREB. This may occur through competitive CBP binding between Zta and CREB (Adamson and Kenney, 1999). As a transcriptional activator, Zta may direct histone acetylase activity to target promoters, possibly through its interaction with CBP. Interaction with Zta occurs in two regions of CBP and requires the transactivation as well as zipper region of Zta (Adamson and Kenney, 1999).

C/EBPα

Zta interacts with another bZIP protein, CCAAT/enhancer binding protein α (C/EBPα), which acts as a positive regulator of Zta. The protein is stabilised by Zta interaction leading to increased levels of C/EBPα (Wu *et al.*, 2003). This results in induction of the cyclin dependent kinase inhibitor p21, ultimately resulting in G1 cell cycle arrest (Wu *et al.*, 2003). This interaction requires the basic domain of Zta and some residues from the zipper.

NFκB p65 subunit

The p65 subunit of NFκB has been shown to negatively regulate Zta transactivation both *in vitro* using GST fusion proteins and *in vivo* with co-immunoprecipitation (Gutsch *et al.*, 1994). As NFκB p65 inhibits Zta from transactivating viral genes, this may be a mechanism for maintaining viral latency (Gutsch *et al.*, 1994). This interaction occurs in the zipper dimerisation domain of Zta.

RARα and RXRα

The retinoic acid receptors (RARα and RXRα) repress activation by Zta of the viral gene BMRF1 (Sista *et al.*, 1993). The interaction between RXRα and Zta occurs through the zipper domain (Sista *et al.*, 1995).

p53

p53 is a key protein in the cellular response to viral infection, both by inducing apoptosis and inducing a type I interferon response. Interaction between Zta and p53 occurs *in vitro* and *in vivo* and each protein is capable of inhibiting the other (Zhang *et al.*, 1994). Zhang et al proposed that the balance of p53 and Zta in latently infected cells may be important in regulation of lytic cycle activation. If Zta is activated and overcomes inhibition by p53, it may in turn inhibit p53-dependent transactivation. The zipper domain of Zta is required for contact with p53 (Zhang *et al.*, 1994).

BGLF4

BGLF4 is a serine/threonine protein kinase and is the only protein kinase encoded by EBV (Smith and Smith, 1989).

A study by Asai and colleagues has shown that BGLF4 mediated phosphorylation of Zta leads to formation of a stable BGLF4-Zta complex (Asai *et al.*, 2009). BGLF4 downregulates transactivation by Zta from its own promoter. The site of phosphorylation that is necessary for interaction is Ser-209 in the zipper region of Zta (Asai *et al.*, 2009).

BMRF1

The viral polymerase processivity factor (BMRF1) interacts directly with Zta and this has been shown to affect lytic reactivation (Zhang *et al.*, 1996).

6.1.3 Expression array

Another approach to question how Zta impacts host cell proteins is to examine the effects of Zta on host gene expression using quantitative PCR. This could reveal novel genes that Zta is able to influence as well as explore the effects of Zta mutants. The results of a QPCR array are presented, which analysed the expression of 600 human genes from the cDNA of HEK293 cells, transfected with either Zta or the mutant ZtaAAA.

This chapter aims to investigate how the binding of Zta to known interacting proteins is affected by different mutations. In addition I aim to identify potentially new changes to the host cell as a result of Zta expression by use of a QPCR array.

6.2 Results

6.2.1 Protein Co-expression

Initially two viral genes and six human genes encoding proteins that interact with Zta outside of the transactivation domain were selected to investigate interactions with Zta and mutants. They were the viral genes BMRF1 and BGLF4 and human genes CBP, C/EBPα, NFκB p65, p53, RARα and RXRα (Table 6.1). The target vector for cloning was pcDNA3. This vector was chosen as it is suitable for use in bacterial or mammalian expression systems. The addition of a flag-tag in the cloning primers was included to allow detection of cloned proteins via a flag antibody.

Protein	Critical Zta Residues	WB size (kDa)	References
p53	200-227	53	(Zhang *et al.*, 1994; Mauser *et al.*, 2002b)
C/EBPα	124-134, 204	45	(Watt and Molloy, 1988; Wu *et al.*, 2003)
RARα	179-245	45	(Sista *et al.*, 1993; Pfitzner *et al.*, 1995; Sista *et al.*, 1995)
RXRα	140-227, 200-227	53	(Sista *et al.*, 1993; Pfitzner *et al.*, 1995; Sista *et al.*, 1995)
NF-κβp65	200-227	65	(Gutsch *et al.*, 1994; Hong *et al.*, 1997)
BMRF1	138-245, 200, 214/218	48	(Schepers *et al.*, 1996)
BGLF4	209	54	(Asai *et al.*, 2006; Asai *et al.*, 2009)

Table 6.1: Proteins known to interact with Zta targeted for cloning
The table shows 5 human and 2 EBV genes known to bind to Zta. The region of Zta that is critical for interaction is shown. C/EBPα was cloned by Celine Schelcher and BGLF4 was given by Dr Tarakanova (Tarakanova *et al.*, 2007). The expected molecular size on a western blot (WB) is shown in kDa.

6.2.1.1 Cloning of viral genes

Primers for cloning BMRF1 were designed to amplify by PCR the 1212bp coding region, as well as incorporating a flag-tag at the 5' end of the gene and restriction enzyme sites at both ends to enable ligation into the pcDNA3 vector. The BMRF1 gene was amplified in a PCR reaction using these primers, with cDNA from LCL cells as a template. Digested, purified PCR product was ligated into digested pcDNA3 to create flag BMRF1 pcDNA3 (Figure 6.2A). The vector was also digested again and run on agarose to check insertion of the cloned gene (Figure 6.2B). All evidence suggested the gene had been correctly cloned however sequencing of the final vector revealed a deletion of 3 basepairs (ΔATT) in the flag-tag (Figure 6.2C). As primers were ordered with the full flag-tag sequence, this could have been either an error in the synthesis of the primer or an enzymatic error during PCR. Complementary primers containing the correct sequence were ordered and used in a site directed mutagenesis reaction to correct the flag-tag error. This correction was confirmed by sequencing (Figure 6.2C).

A vector containing flag-tagged BGLF4 was kindly given by Tarakanova (Tarakanova *et al.*, 2007).

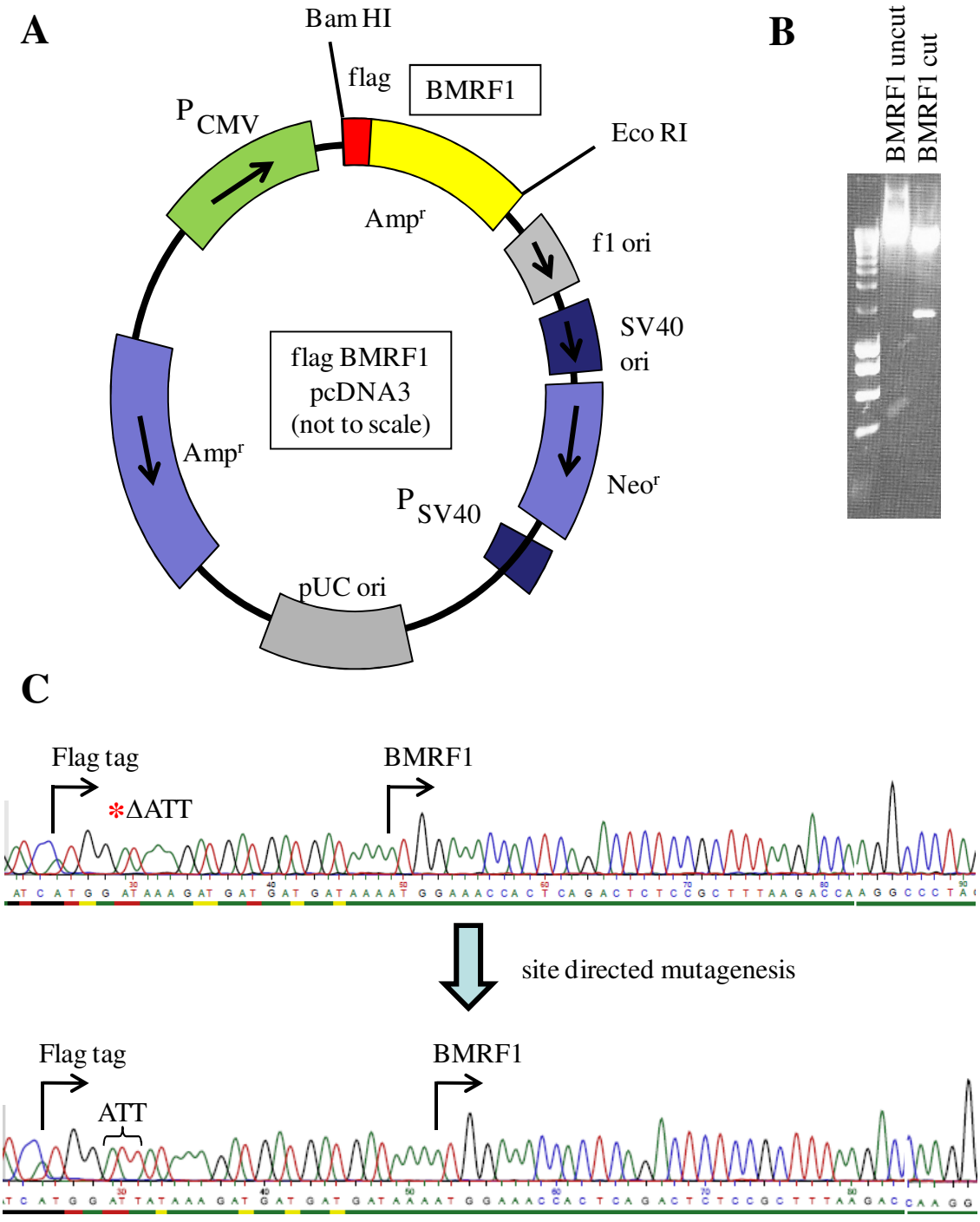

Figure 6.2: Cloning of BMRF1
A shows a vector map of pcDNA3 with cloned EBV gene BMRF1 containing a flag-tag. BMRF1 was PCR cloned using cDNA from LCL cells. Primers contained a flag tag and PCR product was digested with BamHI and Eco RI and ligated into digested pcDNA3 vector. Product was digested and run on an agarose gel to check insertion (**B**). The vector was sequenced to confirm (**C**). There was an error (ΔATT) in the flag-tag which was corrected using site-directed mutagenesis.

6.2.1.2 Cloning of human genes

C/EBPα had already been cloned by a previous member of the Sinclair lab, Celine Schelcher in pcDNA3 with a flag-tag.

PCR primers were designed for each of the remaining five human genes; CBP, NFκB p65, p53, RaRα and RxRα. For the gene CBP it was not possible to amplify the entire gene as it encodes for a very large protein (2405 amino acids long). As Zta interacts with two domains of this protein (Adamson and Kenney, 1999; Zerby *et al.*, 1999), primers were designed to amplify these two domains separately. CBP target domain 1 is comprised of amino acids 301 -585 and domain 2 is amino acids 1680 - 1915.

PCR reactions using cDNA obtained from Ak31 and LCL3 cells were performed to amplify these five human genes. Initially PCR bands were obtained only for p53. The other 5 PCR reactions produced no discernable products. Optimisation of reactions, including reducing the specificity of the reaction by lowering the annealing temperature, utilising a touchdown PCR protocol and re-designing primers resulted in PCR bands for NFκB p65, CBP1 and CBP2. However all products were both weak and contained multiple unspecific bands. No products were obtained under any condition of RXRα or RARα. After purification, multiple attempts at ligating the purified, digested PCR products of NFκB p65, CBP1 and CBP2 into the digested pcDNA3 failed and no cloned genes were created.

The probable reason for the lack of success at amplifying the target genes was cDNA template that was not of adequate quality. Use of commercially available human cDNA template for PCR cloning may have produced improved results. Ligation of the target genes into pcDNA3 was probably not successful because of the low concentration and poor quality of the PCR products.

In order to continue with the planned pulldown experiments Image Clones of NFκB p65, RXRα and RARα were purchased from Invitrogen. These were amplified in PCR reactions using the primers designed for the initial failed amplifications. Strong PCR products were obtained for all three genes, confirming the initial amplification problems stemmed from a poor quality template or low levels of mRNA expression in that cell type. PCR products were digested and ligated into digested pcDNA3 (Figure 6.3A).

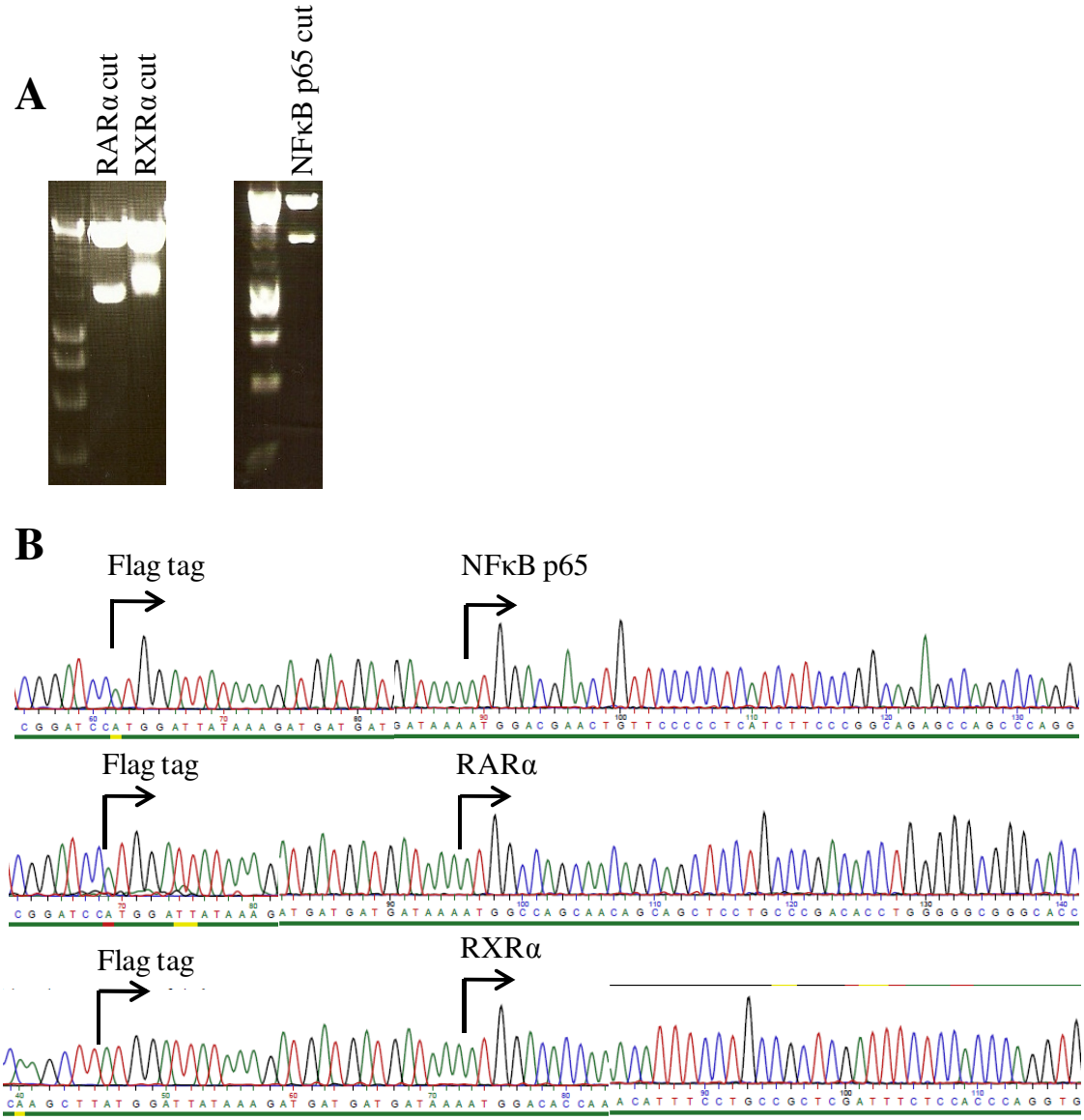

Figure 6.3: Cloning of NFκB p65, RARα and RXRα.
Initial attempts to clone NFκB p65, RARα and RXRα from cDNA failed. Image Clones containing these genes were bought from Invitrogen. These were amplified by PCR using primers containing restriction enzyme sites and the flag-tag. PCR products were digested and ligated into digested pcDNA3. Product was digested and run on an agarose gel to check insertion (**A**). Vectors were sequenced to confirm (**B**).

Ligation was again quite problematic and required several rounds of optimisation, however it was ultimately successful for all three genes. Vectors were sequenced to confirm the correct sequence had been cloned (Figure 6.3B). A pcDNA3 vector containing a flag-tagged version of p53 was bought from Addgene. The required domains of CBP were not found to be commercially available so this gene was excluded at this stage.

Expression vectors containing the flag-tagged viral genes BMRF1 and BGLF4 and human genes C/EBPα, NFκB p65, p53, RXRα and RARα were now available for investigating the interactions with Zta and mutants.

6.2.1.3 *in vivo* expression of proteins

Expression of these proteins in cell culture was tested by transfecting HEK293 cells with each vector DNA. After 72 hours cells were harvested and lysate was run on protein gels. Detection of flag-tagged proteins was done using western blotting with the flag M2 antibody. Strong expression was seen for BGLF4, BMRF1, C/EBPα and NFκB p65 (Figure 6.4A). Longer exposure of the blot also revealed weaker expression of RARα (Figure 6.4B). Expression of p53 and RXRα was not detected. Subsequent experiments resulted in p53 expression, however RXRα expression was not achieved.

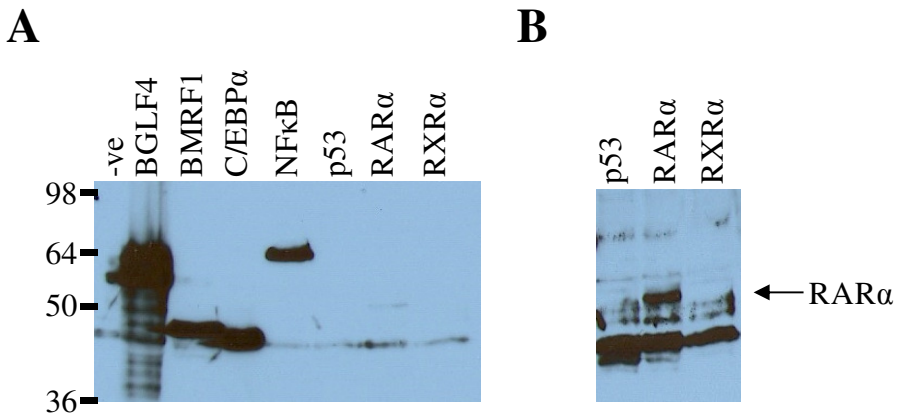

Figure 6.4: Expression of proteins
HEK293 cells were transfected with 3.5µg of vector DNA using effectene (Qiagen). Cells were harvested and lysed after 72 hours and lysate was run on a protein gel. Proteins were detected using western blotting with flag M2 antibody (Sigma) (**A**). Longer exposure of right-hand lanes (**B**) show expression of RARα (indicated by arrow). RXRα and p53 were not detected. Expected band sizes are shown in Table 6.1.

As expression of BGLF4 was strong, this gene was selected to test the pulldown procedure. HEK293 cells were co-transfected with vectors containing his-Zta and BGLF4 (Zta/BGLF), as well as controls comprised of his-Zta or BGLF4 along with the complementary empty vector (pBabe or flag-pcDNA3). Cells were harvested and lysed after 48 hours. Supernatant was incubated with HIS-Select Nickel Affinity Gel (Sigma) overnight. These nickel-linked agarose beads bind to his-tagged proteins, i.e. his-Zta, thus also capturing any associated proteins. The agarose is washed multiple times and then mixed with sample buffer, denatured at 95°C and run on a protein gel. Gels were then western blotted with BZ1 and flag antibodies. Figure 6.5A shows that BZ1 bands were detected for both Zta and Zta/BGLF4. This is as expected as both should be captured by the Ni agarose. However in the α-flag western blot, bands were visible for Zta/BGLF4 and BGLF4 alone. As this does not contain a his-tag, it should not have been captured by the Ni agarose. This shows that there has been non-specific binding to the agarose so the experiment does not provide valid results.

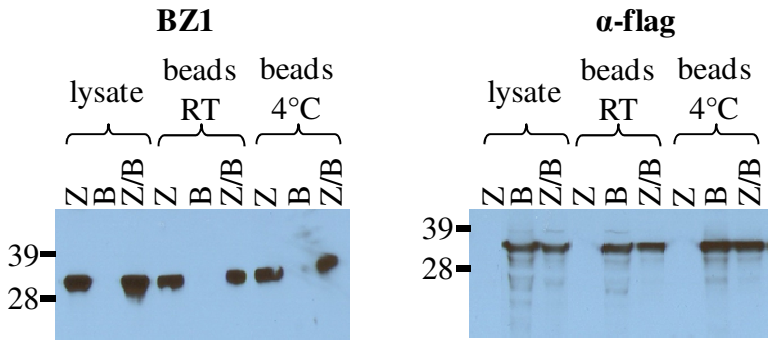

Figure 6.5: BGLF4 pulldown
HEK293 cells were transfected with 5 ng of vector containing Zta or BGLF4 with empty vector or Zta and BGLF4. After 48 hours cells were lysed and freeze thawed three times. 250 µl of supernatant was added to 180 µl of Ni-NTA Agarose (Qiagen) and bound overnight at 4°C or at room temperature (RT). After washing agarose was mixed 1:1 with Laemmli Sample buffer and run on a protein gel. This was western blotted with BZ1 and α-flag antibodies

This same experiment was repeated with CEBP/α, with the same inconclusive results. The lysis and wash buffers used originally are shown in Table 6.6 as Sinclair lab. As suggested by Qiagen, I tried increasing the imidizole concentration to provide more stringent washing conditions and also added 5mM of DTT as a reducing agent. Neither strategy was successful so I identified two alternative pairs of buffers as detailed in Table 6.6 that had been used successfully in similar experiments; Qiagen (Protocol 15: Buffers for purification from mammalian cells using Ni-NTA agarose beads) and Zou (Zou *et al.*, 2007). Neither pair of buffers was successful in reducing the non-specific binding. In addition incubation time was adjusted and experiments were performed at 4°C, however the non-specific binding remained.

A reverse approach was tried using EZview Red Anti-FLAG M2 Affinity Gel (Sigma), in order to select proteins via the flag-tag instead and determine if this also pulled down Zta. However the same problem with sticky proteins was encountered so again valid results were unobtainable.

Sinclair lab	Qiagen	Zou
Lysis Buffers		
10% glycerol 2mM EDTA 0.1% NP40 2mM DTT 150mM NaCl 10mM NaF in PBS	50 mM NaH2PO4 10 mM imidazole 0.05% Tween 20 pH to 8.0 with NaOH	1% NP-40 10mM imidizole in PBS
Wash Buffers		
20mM imidizole 0.5% NP-40 in PBS	50 mM NaH2PO4 300 mM NaCl 20 mM imidazole 0.05% Tween 20 pH to 8.0 with NaOH	1% NP-40 20mM imidizole in PBS

Table 6.6: Buffer conditions used for Ni-affinity gel pulldown experiments
Three different combinations of lysis and wash buffers were tried for the his-pulldown of Zta-interacting proteins. The Qiagen buffers are from www.quiagen.co.uk (Protocol 15: Buffers for purification from mammalian cells using Ni-NTA agarose beads) and the Zou buffers from Zou et al (Zou *et al.*, 2007). Buffers also all contained complete protease inhibitors (EDTA free)(Roche).

6.2.1.4 Co-expression observations

Although the pulldown experiments failed to produce the wanted results, some interesting observations were obtained when proteins were co-expressed with Zta. Co-expression with C/EBPα resulted in a double band for Zta. The band is larger than Zta and is visible in Figure 6.7B. Co-expression of Zta and p53 resulted in degradation of Zta over time. After 72 hours detection of Zta is barely discernable (Figure 6.7D).

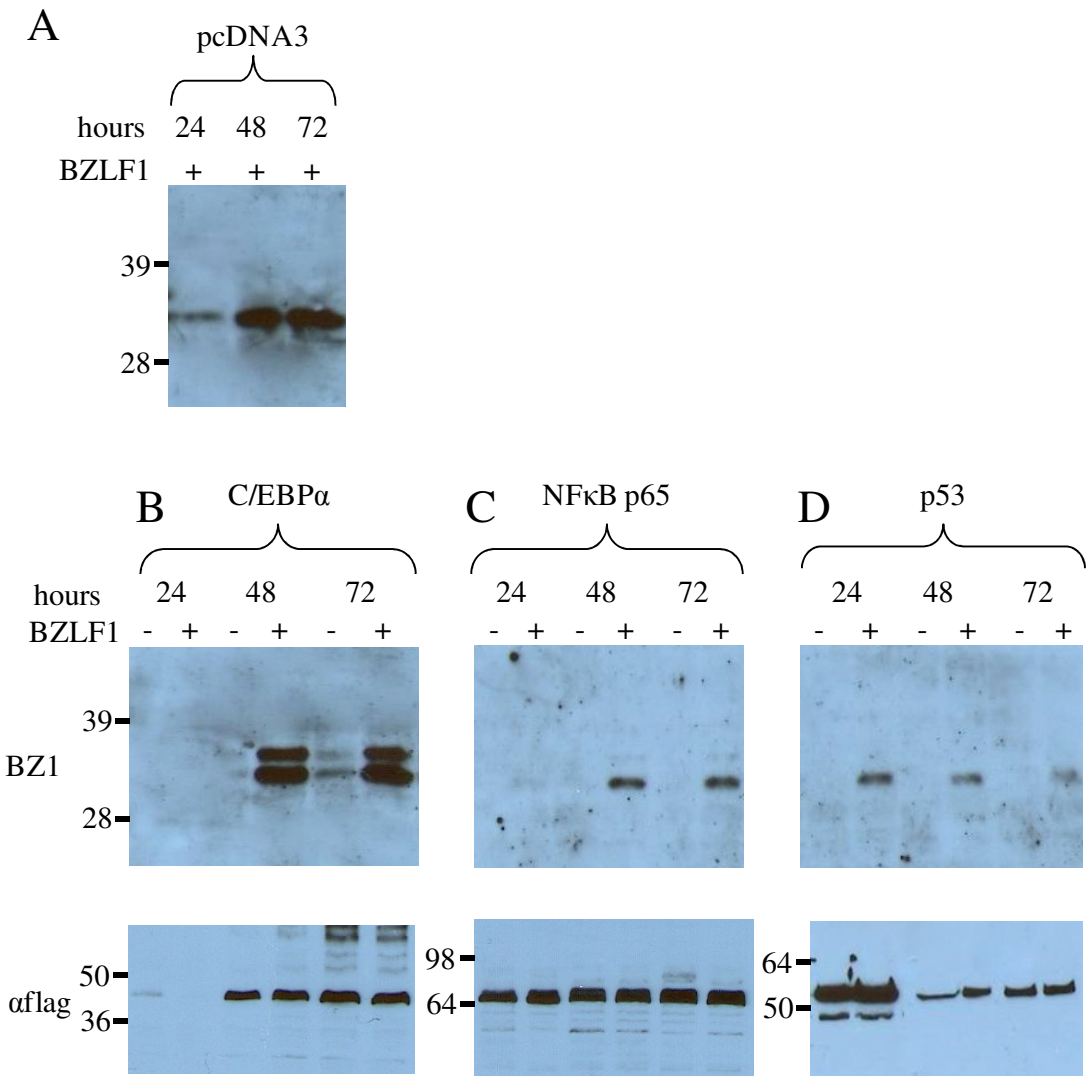

Figure 6.7: Expression of Zta at time points following cotransfection
HEK293 cells were co-transfected using effectene with pcDNA3-flag vector (**A**), C/EBPα (**B**), NFkB p65 (**C**) or p53 (**D**) +/- pBabe Zta. Cells were harvested after 24, 48 and 72 hours. Protein gels were western blotted with BZ1 and αflag antibodies.

In order to see if the mutant ZtaAAA would have a similar effect on C/EBPα and p53 as Zta, I performed co-transfection experiments using ZtaAAA. Western blots with α-flag antibody detected equivalent levels of each protein when co-transfected with Zta or ZtaAAA (Figure 6.8A). As expected only non-specific bands were seen in the α-flag western blot from transfection of Zta or ZtaAAA with empty pcDNA3 vector. Blotting with BZ1 antibody revealed that expression of Zta and ZtaAAA were equivalent in the control samples (Figure 6.8B).

Zta co-transfected with C/EBPα showed the larger additional band, however it was completely absent in the ZtaAAA / C/EBPα sample. The level of Zta protein detected by BZ1 antibody in the Zta / p53 sample was visible but drastically reduced from the levels seen in the control samples. In ZtaAAA / p53, the level of protein detected was again reduced from the controls, however it was considerably stronger than seen for Zta. This raises the possibility that the mutation of the three terminal amino acids of Zta to AAA may provide protection against degradation when co-expressed with p53.

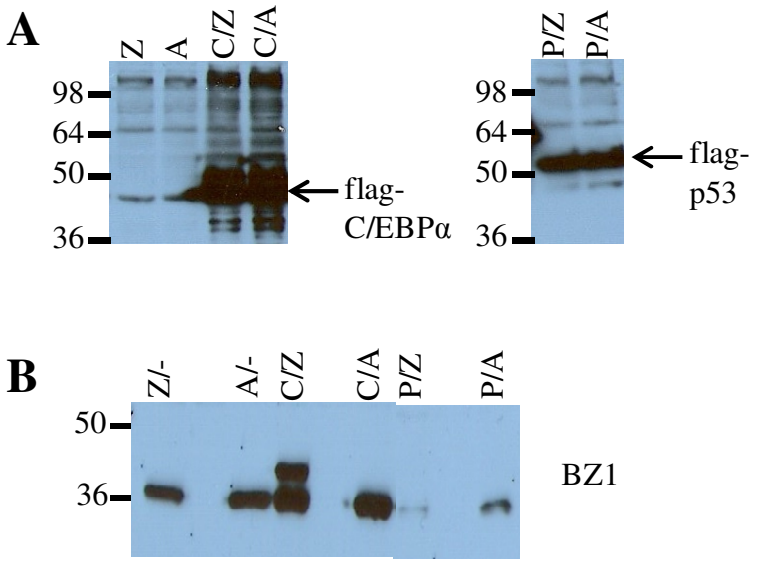

Figure 6.8: Expression of C/EBPα and p53 with ZtaAAA
Zta (Z) or ZtaAAA (A) expression vectors were co-transfected into HEK293 cells with vectors for flag-tagged C/EBPα (C), p53 (P) or empty PCDNA3 vector (-). Cells were harvested after 48 hours and western blots with α-flag (**A**) and BZ1 (**B**) antibodies were performed.

6.2.1.5 Protein half-life

In order to further determine what is happening in the co-expression of these proteins, a protein half-life experiment was performed (figure 6.9). HEK293 cells were co-transfected with empty flag-pcDNA3, C/EBPα, NFκB p65 or p53 +/- pBabe Zta. 48 hours later cycloheximide was added to cells and cells were then harvested at 0, 4, 8 and 24 hours. Cycloheximide is an inhibitor of eukaryotic protein biosynthesis that works via blocking translational elongation.

The results revealed that expression of Zta when transfected along with empty flag-pcDNA vector, as detected by BZ1 antibody on western blots, is stable for 8 hours after cycloheximide addition (Figure 6.9A). Expression then drops dramatically by 24 hours. However when Zta is co-expressed with C/EBPα, an additional band larger than the expected 35kDa band for Zta is clearly visible (Figure 6.9B). C/EBPα also appears to have a stabilising effect on Zta as the protein is still strongly expressed after 24 hours. The level of C/EBPα is also unchanged at 24 hours.

In contrast co-expression of Zta and p53 results in a dramatic reduction of Zta expression within 2 hours of cycloheximide addition (Figure 6.9C). This degradation was co-ordinated with a reduction in p53 expression.

The levels of Zta when co-expressed with NFκB p65 are not considerably changed from expression of Zta alone (Figure 6.9D). NFκB p65 expression is approximately halved by 2 hours and gradually reduces after that.

Although the associations of Zta and its known binding partners were not able to be assessed in pulldown experiments, co-expression with some proteins provided interesting results. The additional band produced during co-expression of Zta and C/EBPα and the degradation of Zta when expressed with p53 show there is a direct or indirect association between these proteins. In contrast expression with C/EBPα did not result in an additional protein band for ZtaAAA, and the p53 associated degradation of ZtaAAA was much reduced from Zta levels. This shows that the three CT amino acids of Zta, that are key to many functions of Zta, also have an influence on these protein interactions.

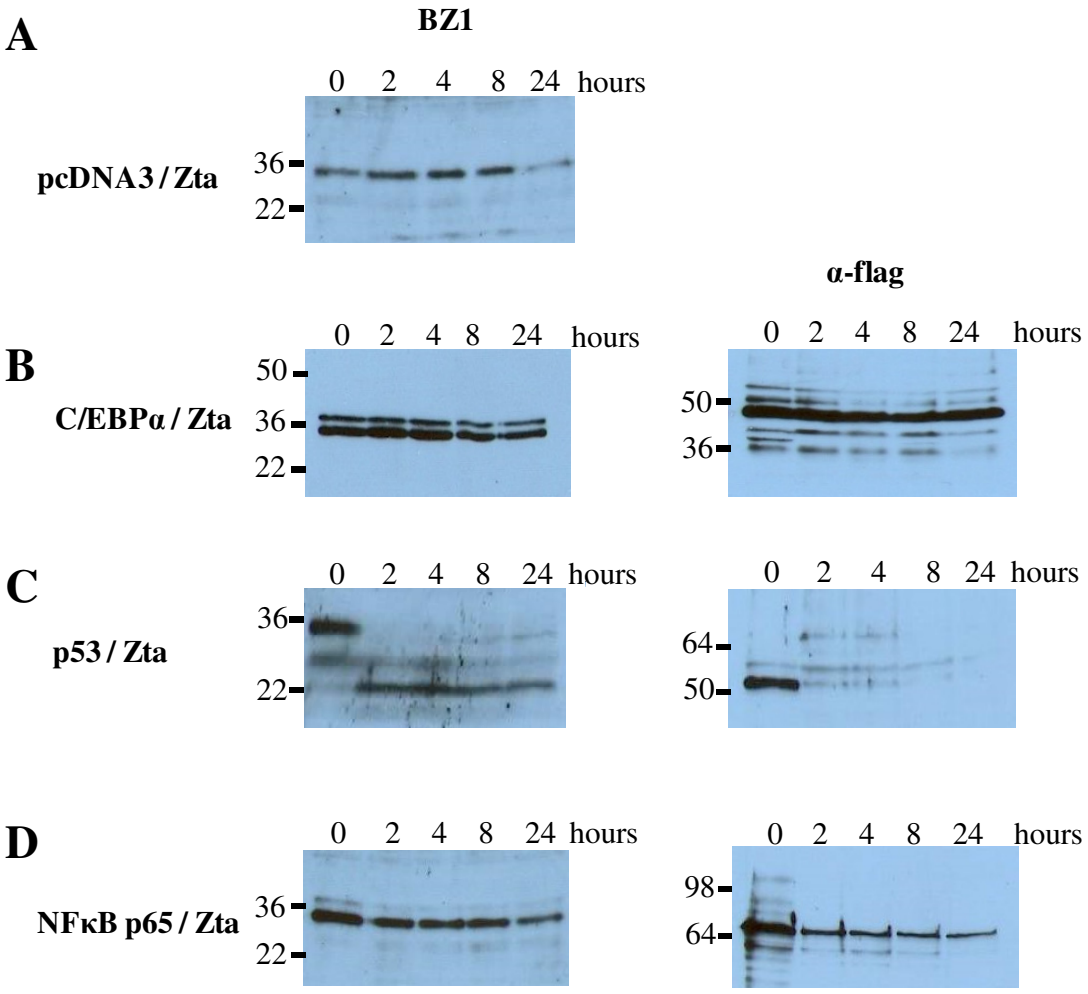

Figure 6.9: Expression of Zta at time points following cotransfection and cycloheximide
HEK293 cells were co-transfected using effectene with pcDNA3-flag vector (**A**), C/EBPα (**B**), p53 (**C**) or NFkB p65 (**D**) or +/- pBabe Zta. After 48 hours 100µg of cycloheximide was added to each well. Cells were harvested at 0, 4, 8 and 24 hours. Cells were counted using a hematocytometer and $1x10^6$ cells were lysed at each time point and loaded on a protein gel. Protein gels were western blotted with BZ1 and α-flag antibodies.

6.2.2 QPCR cancer array

A second approach was adopted to assess the effect of Zta on host cell proteins, using a QPCR expression array with probes for 600 genes with an association with cancer. By comparing changes to the expression of host genes in cells transfected with Zta, ZtaAAA or a control empty vector, host genes that are influenced by Zta or ZtaAAA may be revealed. In addition acyclovir was used to treat some Zta-transfected cells. Acyclovir is a nucleoside analogue with far greater affinity for viral polymerase than cellular polymerase. Acyclovir is phosphorylated by EBV encoded thymidine kinase then by cellular kinases to generate acyclovir triphospate, an active acyclo-GTP. Incorporation of acyclovir triphosphate into a growing DNA chain results in termination of elongation, resulting in the inhibition of viral DNA replication (Lin *et al.*, 1984). These acyclovir-treated cells would therefore be restricted from expressing late lytic cycle genes. Different patterns of host cell gene expression observed in these cells could be attributed to early EBV lytic events.

6.2.2.1 Method

HEK293-ZKO cells were transfected with a vector encoding Zta, ZtaAAA or empty vector (pBabe) as summarised in figure 6.10. Cells were harvested after 48 hours and RNA was extracted. This time point was selected as infectious viral particles are present 48 hours after transfection. In addition a duplicate set of Zta transfected cells was treated with 100 ug/ml acyclovir following transfection. Two separate experimental sets of total RNA were sent to the Biotrove laboratory (now part of Applied Biosystems) as biological replicates. There it was converted to cDNA with a high capacity cDNA RT kit (Applied Biosystems). The cDNA was used at a concentration of 100ng/µl for 32 cycles of Quantitative PCR. This was performed using an OpenArray technology which is a nanolitre fluidics platform. A microscope slide sized plate with 3,072 holes is coated with hydrophilic and hydrophobic coatings. Reagents and samples for the QPCR reactions are retained in the holes via surface tension. The primers used were for 595 human genes with an association with cancer as shown in Table 6.11. This comprises the Biotrove Cancer OpenArray. The Cancer OpenArray panel includes genes associated with DNA repair, angiogenesis and cell

adhesion. It also contains genes that are differentially expressed in early cancer and metastatic disease involved in apoptosis, cell cycle, kinases and transcription factors.

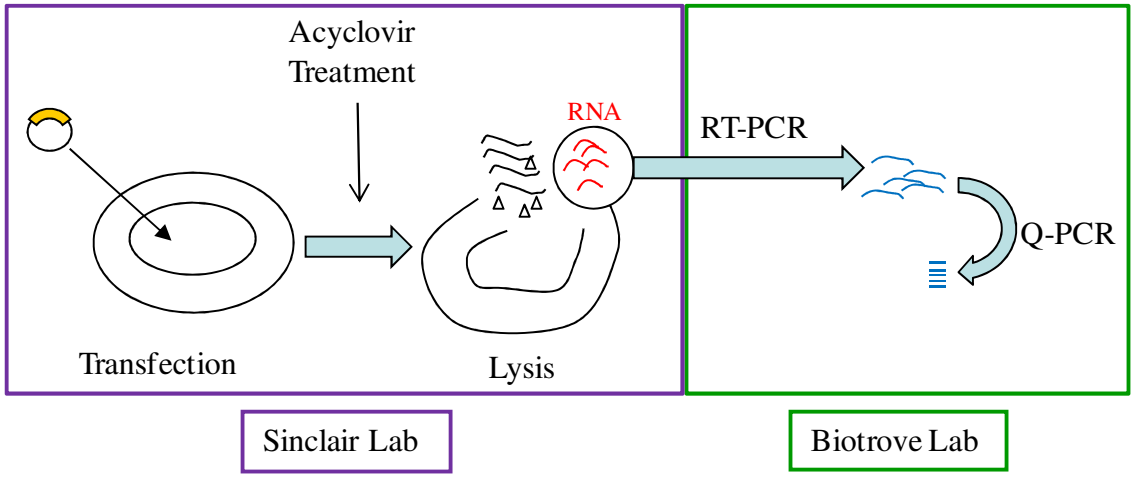

Figure 6.10: QPCR Cancer OpenArray Flow Chart
HEK293-ZKO cells were transfected with a vector encoding Zta, ZtaAAA or empty vector (pBabe). One duplicate set of Zta-transfected cells were treated with 100 ug/ml acyclovir. Cells were harvested after 48 hours and RNA was extracted using RNeasy kit (Qiagen). This was sent to the Biotrove Laboratory where it was converted to cDNA with high capacity cDNA RT kit (Applied Biosystems). The DNA was used at 100 ng/ul for 32 cycles of Quantitative PCR (QPCR) using primers for 595 human genes with an association with cancer included in the Biotrove (now Applied Biosystems) Cancer OpenArray. All experiments were performed with biological replicates.

AARS	CAV1	CRAT	FASTK	HSPA5	MAPK3	NME3	PRKCB1	SFN	TLE1
ABCB1	CBFB	CRHR1	FBN1	HSPA8	MAPKAPK3	NMU	PRKCD	SFPQ	TMEFF1
ABCC4	CBLB	CSF1	FBN2	HSPB1	MAPRE1	NONO	PRKCE	SFRS7	TMEM45A
ABCG2	CCL2	CSF1R	FBP1	HSPH1	MARS	NOTCH1	PRKCG	SHB	TNF
ABI2	CCNB1	CSF3	FBXO5	HYAL1	MAS1	NOTCH2	PRKCZ	SIAH2	TNFRSF10B
ABL1	CCNB2	CSK	FES	HYOU1	MATN3	NOTCH4	PRKD2	SKI	TNFRSF1A
ABL2	CCND1	CSNK1G2	FGD6	ICAM1	MCC	NPM1	PRL	SKIL	TNFRSF1B
ACTB	CCND2	CTNNA1	FGF3	ID1	MCCC1	NQO1	PRNP	SLC16A1	TNK1
ACY1	CCND3	CTNNB1	FGF8	ID2	MCM2	NR1D1	PSMA1	SLC1A4	TNK2
ADM	CCNE1	CTPS	FGFR1	IDUA	MCM4	NR2F1	PSMD2	SLC20A1	TOB1
ADSL	CCNE2	CTSB	FGR	IER3	MCM6	NR2F6	PTCH1	SLC2A3	TP53
AK1	CCT5	CTSC	FKBP8	IFITM1	MDM2	NR4A1	PTEN	SLC7A1	TP53BP2
AKR1C2	CD24	CTSE	FLT1	IGF1	MDM4	NRAS	PTGS1	SMAD1	TP53I3
AKT1	CD34	CTSL2	FN1	IGF2	MELK	NRG1	PTMA	SMO	TPBG
ALAS	CD44	CUL1	FOS	IGF2R	MGST1	ODZ1	PTN	SMPD1	TPT1
ALB	CD59	CYB5A	FOSL1	IGFBP3	MIB1	ODZ3	RAB27B	SNAI2	TRADD
ALDH4A1	CD68	CYC1	FOSL2	IGFBP4	MICB	ORC6L	RAB5A	SND1	TRAM1
ANPEP	CD70	CYP19A1	FOXO1	IGFBP5	MKI67	OSM	RAB6B	SNRPB2	TRIP13
ANXA5	CDC20	CYR61	FRAP1	IHPK2	MLF1IP	OXCT1	RAC1	SOCS1	TRRAP
ANXA7	CDC25A	DCC	FTL	IL1B	MLLT10	PA2G4	RAD21	SOCS3	TSG101
AP2B1	CDC25B	DCK	FUT8	ILK	MLLT3	PABPC1	RAD50	SOD1	TUBA1B
AP2M1	CDC25C	DCN	FZD2	ING1	MLN51	PAQR3	RAD51	SORT1	TUFM
APC	CDC2L5	DDX10	FZD5	INS	MME	PCNA	RAF1	SP1	TXNRD1
AR	CDC42BPA	DEGS1	G6PD	IRF3	MMP1	PCTK1	RAI2	SPINT2	TYK2
ARHGAP5	CDH1	DEK	GAPDH	ITGA3	MMP11	PCTK2	RALBP1	SPRY2	TYRO3
ARHGEF5	CDK10	DEPDC1	GAS6	ITGA6	MMP14	PCTK3	RAP1A	SRC	UBC
ARID4A	CDK2	DHCR7	GBE1	ITGB3	MMP17	PDGFA	RARA	SRPX	UbcH5B
ARMC1	CDK4	DHRS2	GCN1L1	JAK1	MMP2	PDGFB	RARB	STAT1	UBE2L6
ASNS	CDK5	DHX8	GCN5L2	JARID1A	MMP9	PDGFRA	RASGRF1	STAT2	UCHL1
ASPM	CDK9	DLG3	GDF15	JUN	MNDA	PEA15	RASL11B	STAT3	UCHL5
ATAD2	CDKL1	DTL	GMPS	JUND	MRPL13	PECAM1	RB1	STAT5B	USP7
ATF4	CDKN1A	DVL1	GNA13	KIF14	MS4A7	PECI	RBBP4	STC1	VDAC1
ATM	CDKN1B	DVL3	GNAZ	KIF21A	MSH2	PFDN4	RBL2	STK3	VEGFA
ATP5B	CDKN1C	E2F1	GNB2	KIF3B	MSH6	PFDN5	REL	STK32B	VHL
ATP5O	CDKN2A	E2F3	GNB2L1	KIT	MT3	PFKP	RELA	STMN1	VIL2
AURKA	CDKN2B	E2F5	GPR126	KITLG	MTDH	PGAM1	RELB	STX1A	VIM
AXL	CDKN2D	ECT2	GPR180	KLK10	MUC1	PGK1	RET	SYNCRIP	WEE1
B2M	CEACAM5	EF1A	GPR39	KLK13	MX1	PGR	RFC2	TAF1	WISP1
BAG1	CEBPG	EGF	GRB2	KPNA2	MYB	PHB	RFC4	TBL3	WNT1
BAG3	CENPA	EGFR	GSK3A	KRAS	MYBL1	PIK3CA	RGS19	TBP	WNT2
BARD1	CENPC1	EGLN1	GSPT1	KRT18	MYBL2	PIK3CB	RHOA	TBRG4	WNT2B
BAX	CGRRF1	EGR1	GSTM3	KRT19	MYC	PIK3CG	RHOB	TBX3	WNT3
BBC3	CHAF1A	EGR3	GTF2I	KRT2	MYCL1	PIM1	RHOC	TCF7L2	WNT5A
BCL2L1	CHPT1	EIF2C2	GusB	KRT9	MYD88	PIR	RHOD	TFAP2C	WT1
BHLHB2	CIB1	EIF5	H2AFZ	LAMB1	MYL9	PKM2	RIPK1	TFDP1	XRCC1
BIRC5	CIRBP	EPHA2	HADHA	LCK	MYLK	PKMYT1	RPL19	TFDP2	XRCC3
BLMH	CKMT1B	ERBB2	HDAC1	LCN2	MYRIP	PLG	RPLP0	TFRC	XRCC4
BMP6	CKS2	ERBB3	HDGF	LDHA	NDC80	PLK2	RPN2	TGFA	XRCC5
BNIP3	CLK1	ERBB4	HLA-C	LEP	NDRG1	POLR2A	RPS4X	TGFB1	XRCC6
BRAF	CLK2	ERCC3	HLA-G	LITAF	NEO1	PPARD	RPS6KB1	TGFB2	YBX1
BRCA1	CLK3	ERGIC1	HMBS	LONP1	NF1	PPARG	RRM1	TGFB3	YES1
BRCA2	CLNS1A	ESM1	HMGA1	LTF	NF2	PPIA	RRM2	TGFBI	YWHAB
BTG2	CLTC	ETV1	HMGB1	LYN	NFKB1	PPIH	SACS	TGFBR2	YWHAZ
BTK	CNBP	ETV3	HMGB3	LZTR1	NFKB2	PPP2R5A	SEC14L2	TGFBR3	ZAP70
BUB1	COL1A1	ETV6	HMGN2	M6PR	NID1	PRAME	SELENBP1	THBS1	ZMYND8
CA9	COL4A2	EVL	HMMR	MAD2L1	NINJ1	PRC1	SEMA3C	TIE1	
CANX	COL6A3	EXT1	HPRT	MAP2K2	NMB	PRDX2	SEMA4D	TIMP1	
CAP1	COX6C	EZH2	HRB	MAP3K8	NMBR	PRDX4	SEPP1	TIMP3	
CAPN1	COX7A2	F2R	HSP90AB1	MAPK12	NME1	PRKAR1A	SERPINE1	TJP1	
CAPNS1	CP	FAS	HSPA4	MAPK13	NME2	PRKCA	SERPINH1	TK1	

Table 6.11: Table of Genes used in QPCR
Primers for these 595 genes were used in QPCR for the Cancer OpenArray

To verify the expression of Zta and EBV genes, I also analysed the samples with quantitative PCR for Zta and EBV DNA polymerase genes (Figure 6.12). Results were standardised to the expression of the housekeeping ribosomal gene L32. Zta, Zta + acyclovir and ZtaAAA all showed similar levels of expression of Zta. Expression of EBV DNA polymerase was greatly reduced for Zta +acyclovir and ZtaAAA. Application of acyclovir in cell culture is expected to result in a decreased mRNA levels for EBV polymerase (Halder *et al.*, 2009). As ZtaAAA is defective in lytic reactivation, low levels of EBV polymerase expression were also expected.

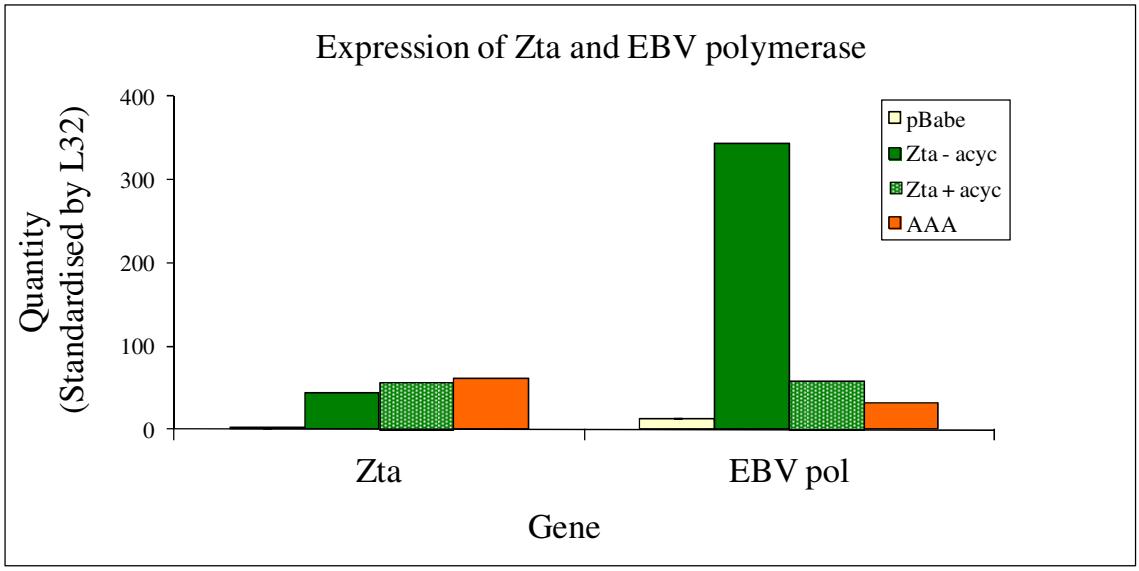

Figure 6.12: Expression of Zta and EBV polymerase in Biotrove samples
The four samples sent for analysis with the Biotrove Cancer OpenArray were analysed using QPCR for expression of Zta and EBV polymerase. The average result is shown. Results were standardised to the expression of the housekeeping ribosomal gene L32.

6.2.2.2 Analysis

The results provided by Biotrove were in the form of two replicate CT values for each gene from the QPCR analysis. I converted these values to ΔCT for each sample by normalisation to 4 housekeeping control genes selected and previously validated by Biotrove, that were analysed on the same array, for each sample. These housekeeping genes were Actin B, GAPDH, keratin 18 and keratin 19.

I calculated the average of each data point from the two measured QPCR values. This average value was used to determine the ΔΔCT for each comparison pair e.g. ΔΔCT Zta/pBabe. This figure then allows the calculation of the Fold Difference (FD) for the comparison pair.

An error in the analysis by Biotrove provided 46 samples with CT values of 26.00. These results were in fact invalid and subsequently these genes had to be removed from the analysis. In total there were 532 genes from the array with data for all samples.

6.2.2.3 Results

I plotted scattergraphs of the comparison pairs to give an overview of the data. These are shown in Figure 6.13. In panel A, values for Zta compared to pBabe are shown. The majority of the data points are distributed closely to the diagonal line of FD=0, indicating low fold differences. Several outlying values with a high fold difference are highlighted. The highest fold difference for this comparison is for the gene PSMD2 (FD = 147.7), followed by CD70 (FD = 26.86) and Notch2 with a FD of 14.7. A similar pattern is observed in panel B for the comparison of ZtaAAA/pBabe. The highest value for this pairing is again PSMD2 (FD = 106.3). The data in panel C for Zta/ZtaAAA is clustered more tightly around the central line, indicating in general less difference between the two samples. The highest fold difference was seen for CD70 (FD = 24.05).

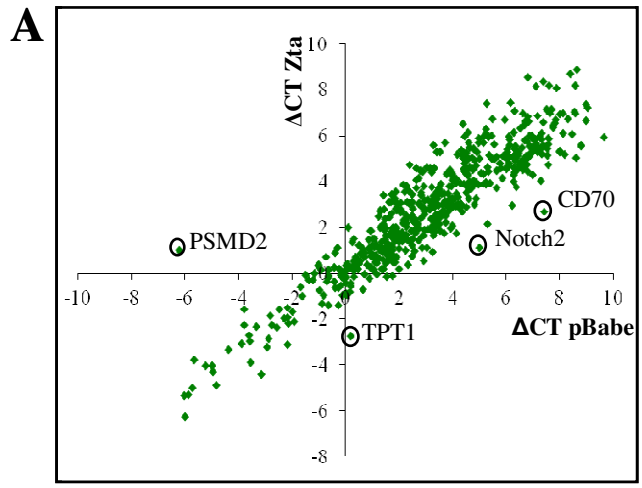

Figure 6.13: Scattergraphs of average ΔCT for Zta and ZtaAAA.
QPCR was performed using the Biotrove Cancer OpenArray. Scattergraphs showing a comparison of gene expression levels, using ΔCT, are shown for Zta and pBabe (**A**), ZtaAAA and pBabe (**B**) and Zta and ZtaAAA (**C**). Some outlying results are highlighted in each graph and the Fold Difference (FD) in expression for these genes are shown to the right of the graphs.

Table 6.14 gives a summary of the 37 genes with a FD in expression greater than 4 between cells transfected with Zta vs. pBabe. This threshold was selected as with only duplicate samples in the analysis, I wanted to focus on large differences as these are more likely to be real than small differences. 31 of the genes showed higher expression in Zta (yellow in Table 6.14) while the remaining 6 were expressed at reduced levels in Zta transfected cells.

The FD for genes with a greater than 4 fold difference between ZtaAAA and pBabe are shown in Table 6.15. There are 51 differentially expressed genes, and all but 1 were expressed at a higher level in cells transfected with ZtaAAA.

There were very few differences in expression between Zta and ZtaAAA. Only 5 genes, CD70, MTDH, NFKB2, SOCS1 and ID1, had a difference in expression greater than 4 fold (Table 6.15B). Figure 6.16 shows the 21 genes in common between Zta and ZtaAAA that have expression with a greater than 4 FD from pBabe.

The results from cells transfected with empty pBabe in comparison with cells transfected with Zta then treated with acyclovir (acZta) are shown in the scattergraph in Figure 6.17. The highest ranking gene in this experiment is CKS2 with a FD of 9.73. Expression was highest for this gene in acZta. There were only 7 genes with a fold difference in expression greater than 4 for these two samples and a summary of these is shown in Table 6.18.

Gene	FD
PSMD2	147.74
CD70	26.86
NOTCH2	14.74
CP	13.43
WNT2	12.05
LCK	9.71
SKIL	9.55
MATN3	9.49
FOS	9.41
PFDN4	9.00
SOCS1	8.10
TPT1	7.71
DCN	7.22
DCC	6.54
CDKN2B	6.47
TNK1	6.46
PDGFA	6.18
RAI2	5.29
CDK2	5.27

Gene	FD
NDC80	5.25
IGF1	5.13
TNF	5.12
CA9	5.04
HMBS	5.01
E2F3	5.01
PLK2	4.90
CDKN2A	4.89
PKM2	4.58
PKMYT1	4.40
CDK10	4.39
ITGB3	4.36
WISP1	4.31
MYD88	4.30
CYP19A1	4.27
TNFRSF1B	4.14
MME	4.12
ABCG2	4.04

Table 6.14: Genes with a greater than 2 fold difference in expression in cells transfected with Zta vs pBabe.
QPCR analysis was performed by Biotrove on RNA from cells transfected with Zta and pBabe (empty vector) as described in figure 6.10. My analysis of the QPCR results showed that 37 genes had a greater than 4 fold difference (FD) in expression. Genes highlighted in yellow had higher expression in Zta cells and blue highlighted genes had higher expression in pBabe cells.

A

Gene	FD
PSMD2	106.27
SOCS1	41.64
NOTCH2	39.98
PFDN4	15.17
TPT1	12.16
SKIL	12.12
CDK2	10.51
CP	9.68
PDGFA	9.41
FOS	9.00
MTDH	8.84
NDC80	8.22
CDKN2B	7.75
E2F3	7.74
ARHGAP5	7.08
MYD88	6.98
BAG3	6.83

Gene	FD
ERBB4	6.81
SERPINE1	6.68
TIMP3	6.68
RAD50	6.56
CEACAM5	6.15
BRCA2	6.01
COX6C	5.63
ITGA3	5.60
CHPT1	5.60
ASPM	5.50
TNK1	5.38
ATF4	5.33
TNF	5.23
HMGN2	5.05
ITGB3	5.03
DCN	4.98
PTGS1	4.92

Gene	FD
MATN3	4.81
MT3	4.81
TNFRSF1B	4.74
RAP1A	4.68
STK3	4.59
DEPDC1	4.58
KIF21A	4.56
CA9	4.54
TGFBR2	4.32
MLF1IP	4.31
FGD6	4.30
KIF14	4.29
FAS	4.27
PIK3CA	4.04
NMU	4.03
REL	4.02
RARB	4.00

B

Gene	FD
CD70	24.05
MTDH	4.05
NFKB2	4.87
SOCS1	5.14
ID1	8.25

Table 6.15: Genes with a greater than 2 fold difference in expression
QPCR analysis was performed on RNA from cells transfected with Zta, pBabe (empty vector) and ZtaAAA as described in figure 6.10. 51 genes had a greater than 4 fold difference (FD) in expression for ZtaAAA and pBabe (**A**). Genes highlighted in yellow had higher expression in ZtaAAA cells and blue genes had higher expression in pBabe cells. **B** shows the 5 genes with more than 4 fold expression difference between Zta and ZtaAAA. Expression was higher in Zta cells for blue and higher for ZtaAAA in yellow.

Gene	FD (Zta/pBabe)	FD (AAA/pBabe)	FD (Zta/acZta)
PSMD2	147.74	106.27	156.39
NOTCH2	14.74	39.98	27.40
CP	13.43	9.68	
SKIL	9.55	12.12	14.88
MATN3	9.49	4.81	
FOS	9.41	9.00	
PFDN4	9.00	15.17	
SOCS1	8.10	41.64	19.01
TPT1	7.71	12.16	10.45
DCN	7.22	4.98	
CDKN2B	6.47	7.75	9.05
TNK1	6.46	5.38	11.09
PDGFA	6.18	9.41	9.22
CDK2	5.27	10.51	7.06
NDC80	5.25	8.22	7.90
TNF	5.12	5.23	6.62
CA9	5.04	4.54	
E2F3	5.01	7.74	4.26
ITGB3	4.36	5.03	34.13
MYD88	4.30	6.98	15.15
TNFRSF1B	4.14	4.74	15.22

Figure 6.16: Genes with altered expression in Zta/pBabe and ZtaAAA/pBabe
21 genes had fold differences greater than 4 in both Zta/pBabe and ZtaAAA/pBabe. One gene showed higher expression in cells transfected with pBabe and is shown in blue. The fold difference for Zta/acZta is shown when greater than 4.

A

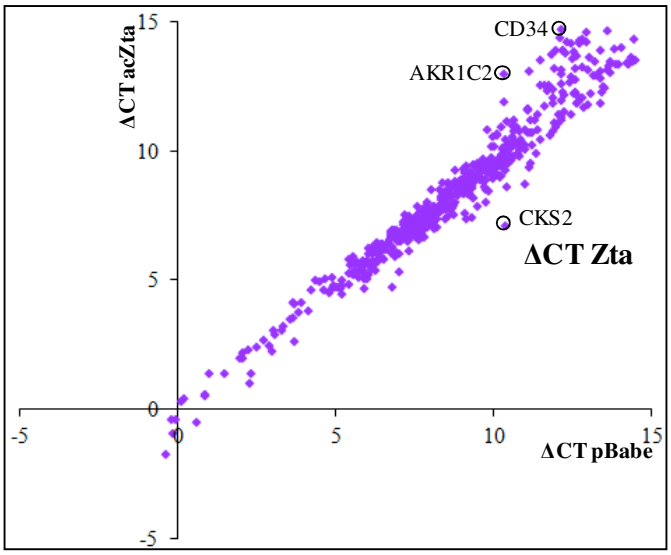

pBabe / acZta

CKS2: FD=9.73
AKR1C2: FD=6.21
D34: FD=5.92

B

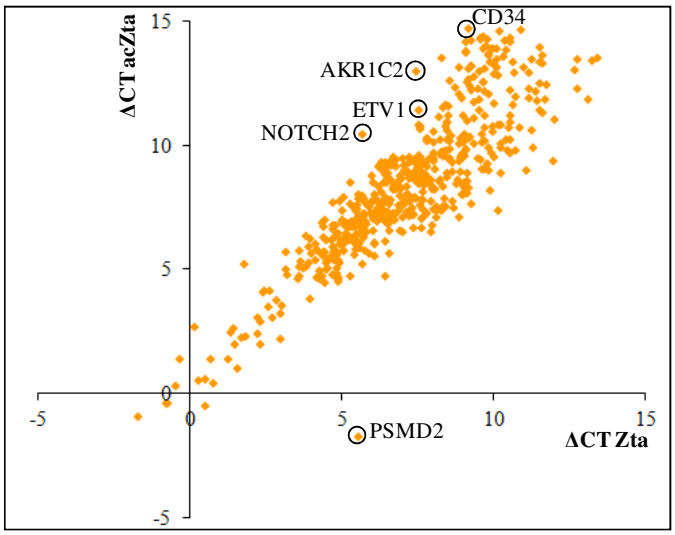

Zta / acZta

PSMD2: FD=156.4
CD34: FD=45.92
AKR1C2: FD=45.44
ETV1: FD=36.81
NOTCH2: FD=27.40

Figure 6.17: Scattergraphs of average ΔCT for Zta and acZta
QPCR was performed using the Biotrove Cancer OpenArray. Scattergraphs showing a comparison of gene expression levels, using ΔCT, are shown for acyclovir treated Zta (acZta) and pBabe (**A**) and Zta and acZta (**B**). Some outlying results are highlighted in each graph and the Fold Difference (FD) in expression for these genes are shown to the right of the graphs.

Gene	FD
CKS2	9.73
AKR1C2	6.21
CD34	5.92
NMBR	4.88
TRIP13	4.82
COX7A2	4.08
ETV1	4.04

Table 6.18: Differentially expressed genes for acZta and pBabe
QPCR analysis was performed on RNA from cells transfected with Zta then treated with acyclovir and pBabe (empty vector). 7 genes had a greater than 4 fold difference (FD) in expression for Zta treated with acyclovir (acZta) and pBabe. Genes highlighted in yellow had higher expression in acZta cells and blue genes had higher expression in pBabe cells.

Figure 6.17B shows the scattergraph of Zta vs. acZta. The shape of this graph differs from the other scattergraphs in that the majority of points are located closer to the ΔCT acZta axis, indicating that expression for most genes was higher in the untreated cells. There were 6 genes, PSMD2, CD34, AKR1C2, ETV1, ITGB3, and TGFB1 with a fold difference greater than 30. Of the 132 genes differentially expressed at greater than 4 fold between Zta and acZta, only 4 were expressed at a higher level in acZta. These are detailed in Table 16.19.

It would be expected that expression profiles of ZtaAAA and acZta would be similar as ZtaAAA is defective in lytic reactivation and acZta is prevented from expressing late lytic genes. However there were a considerable number of differences between the two data sets. The scattergraph for this comparison is shown in Figure 6.20. Similarly to Zta/acZta, lower levels of expression were detected for most genes in the acyclovir treated cells. In total 136 genes were expressed at greater than 4 FD between ZtaAAA and acZta. These genes are shown in Table 6.21. Of these 136 genes only 5 (PSMD2, SERPINE1, IGFBP4, TIMP3 and CDKN2A) were expressed at higher levels in acZta cells.

Gene	FD	Gene	FD	Gene	FD	Gene	FD
PSMD2	156.39	MRPL13	10.99	HSPA5	7.01	PCTK2	5.10
CD34	45.92	CRHR1	10.87	YES1	6.90	EGLN1	5.10
AKR1C2	45.44	PDGFRA	10.71	CDKN2A	6.76	MLF1IP	5.09
ETV1	36.81	UCHL5	10.69	FAS	6.69	BRCA2	5.05
ITGB3	34.13	ERBB3	10.57	STK3	6.63	CD59	4.99
TGFBI	30.23	RAI2	10.52	TNF	6.62	RALBP1	4.95
NOTCH2	27.40	TPT1	10.45	ITGA3	6.36	REL	4.93
NMBR	26.47	SOCS3	10.27	KIF14	6.31	PRNP	4.79
WNT2	26.34	MYB	9.61	MYLK	6.27	GTF2I	4.76
TGFB2	26.12	MAPK13	9.48	CDK10	6.18	KRAS	4.66
BTK	25.56	PDGFB	9.27	ABCB1	6.13	MUC1	4.65
GPR126	25.26	APC	9.24	SEMA3C	5.91	NRG1	4.65
NQO1	22.08	PDGFA	9.22	MTDH	5.86	SFN	4.62
IGFBP3	20.73	FGD6	9.20	MLLT3	5.86	DDX10	4.62
EGF	19.61	NF1	9.11	NPM1	5.82	FGR	4.61
ANPEP	19.04	CDKN2B	9.05	HMGN2	5.81	SKI	4.49
SOCS1	19.01	SPINT2	8.98	SFPQ	5.80	PRKCA	4.46
PLK2	16.06	ODZ1	8.49	ABCC4	5.79	TFDP1	4.40
TNFRSF1B	15.22	CLTC	8.46	MDM2	5.68	CEBPG	4.39
MYRIP	15.15	STK32B	8.20	FGFR1	5.64	BRAF	4.38
MYD88	15.15	NDC80	7.90	HMGB1	5.59	GSPT1	4.37
GSTM3	15.06	RB1	7.77	MMP14	5.54	EGR1	4.35
LEP	15.01	DEPDC1	7.73	ARID4A	5.50	KIF21A	4.27
SKIL	14.88	ABCG2	7.72	RAP1A	5.50	E2F3	4.26
CCL2	14.46	DHRS2	7.59	ARHGAP5	5.49	PKMYT1	4.24
AXL	14.40	SEPP1	7.56	CDKL1	5.48	HSPH1	4.19
RET	13.89	TGFA	7.36	PECAM1	5.32	PRKCE	4.18
RAB27B	13.85	TP53BP2	7.30	PRKCB1	5.31	CENPC1	4.17
TIE1	13.52	TGFB3	7.29	TJP1	5.30	KITLG	4.12
CSF3	13.09	FES	7.27	XRCC4	5.27	TAF1	4.12
THBS1	12.34	ASPM	7.19	MYBL1	5.20	CANX	4.07
WNT2B	12.12	CDK2	7.06	KRT18	5.18	NOTCH4	4.07
TNK1	11.09	PFDN4	7.05	USP7	5.13	CDC42BPA	4.01

Table 6.19: Differentially expressed genes for Zta and acZta
132 genes are expressed at greater than 4 fold difference between Zta and acZta. Higher expression in Zta cells is highlighted yellow and higher for acZta is in blue.

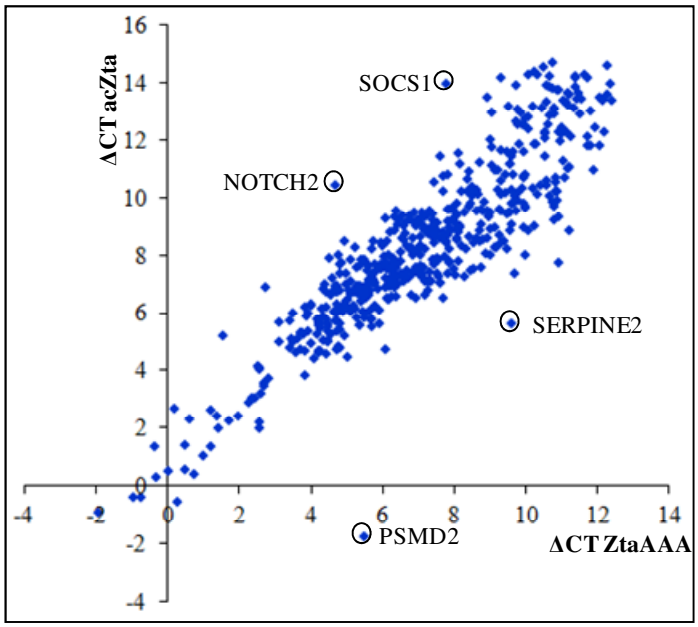

ZtaAAA / acZta

PSMD2: FD=149.94
SOCS1: FD=73.33
NOTCH2: FD=55.76
SERPINE1: FD=15.64

Figure 6.20: Scattergraph of average ΔCT for ZtaAAA and acZta
QPCR was performed using the Biotrove Cancer OpenArray. Scattergraphs showing a comparison of gene expression levels, using ΔCT, are shown for ZtaAAA and acyclovir treated Zta (acZta). Some outlying results are highlighted and the Fold Difference (FD) in expression for these genes is shown to the right of the graphs.

Gene	FD	Gene	FD	Gene	FD	Gene	FD
PSMD2	149.94	MYLK	8.11	HMGB3	5.78	EGLN1	4.80
SOCS1	73.33	MYB	7.97	NFKB2	5.75	TFRC	4.80
NOTCH2	55.76	LEP	7.97	SNRPB2	5.74	MKI67	4.78
ITGB3	29.58	TP53BP2	7.92	COX6C	5.73	PRKCA	4.76
ETV1	23.91	MRPL13	7.72	NPM1	5.69	SYNCRIP	4.68
NQO1	18.48	TGFB2	7.55	MYRIP	5.69	FES	4.66
MYD88	18.42	ASPM	7.44	CDKL1	5.68	AXL	4.66
NMBR	18.02	BTK	7.43	AP2M1	5.64	SMAD1	4.65
MTDH	17.79	DEPDC1	7.37	RB1	5.63	REL	4.65
IGFBP3	17.14	ERBB4	7.31	THBS1	5.62	TMEFF1	4.61
TIE1	15.98	TGFBI	7.21	RAB27B	5.60	MSH6	4.57
CD34	15.71	PLK2	7.09	RALBP1	5.57	MMP9	4.56
SERPINE1	15.64	GPR126	7.06	FAS	5.53	PIK3CA	4.51
AKR1C2	15.31	TNK1	6.93	TGFBR2	5.36	HSPH1	4.46
SKIL	14.16	SKI	6.91	USP7	5.28	CENPC1	4.40
TNFRSF1B	13.09	ITGA3	6.86	GTF2I	5.23	MUC1	4.33
TPT1	12.36	ERBB3	6.85	RAD50	5.22	CLTC	4.33
CCL2	11.90	NF1	6.82	MAPK13	5.22	DDX10	4.28
RAP1A	11.56	MLLT3	6.74	KRAS	5.16	CCNB1	4.27
CDK2	10.57	PRKCB1	6.68	TIMP3	5.14	PCTK2	4.26
PDGFA	10.54	EGF	6.53	EGR1	5.13	PRKAR1A	4.22
ANPEP	10.25	WNT2	6.47	CSF3	5.13	PDGFB	4.22
GSTM3	9.94	UCHL5	6.44	KIF21A	5.11	SEPP1	4.22
RET	9.52	KIF14	6.43	SEMA3C	5.09	MELK	4.21
ARHGAP5	9.45	CHPT1	6.19	TNF	5.07	DHRS2	4.20
NDC80	9.26	HMGN2	6.14	CEBPG	5.06	CDC42BPA	4.18
PFDN4	8.92	TGFA	6.10	MLF1IP	5.05	CCT5	4.13
IGFBP4	8.88	STK3	6.03	GSPT1	5.03	ABCB1	4.12
CRHR1	8.76	HMGB1	6.02	MDM2	5.03	SOCS3	4.10
PDGFRA	8.75	SFPQ	6.01	SPINT2	5.00	FBN2	4.07
ABCC4	8.72	YES1	5.90	CDKN2A	4.98	SRPX	4.07
FGD6	8.45	HSPA4	5.90	E2F3	4.94	E2F5	4.06
BAG3	8.35	BRCA2	5.89	RAI2	4.91	MAPRE1	4.06
CDKN2B	8.14	XRCC4	5.82	ODZ1	4.90	EVL	4.03

Table 6.21: Differentially expressed genes for ZtaAAA and acZta
QPCR analysis was performed on RNA from cells transfected ZtaAAA or with Zta then treated with acyclovir (acZta). 136 genes had a greater than 4 fold difference (FD) in expression for ZtaAAA and acZta. Genes highlighted in yellow had higher expression in ZtaAAA cells and blue genes had higher expression in acZta cells.

Prediction of ZREs in differentially expressed genes

In order to develop a concept of a mechanism that could be responsible for Zta affecting expression of these cellular genes, the presence of ZREs in the promoter regions of differentially expressed genes was examined.

There are 17 genes with a difference in expression greater than 8 fold between Zta and pBabe, ZtaAAA and pBabe or both. These are detailed in Table 6.22. A Biomart (http://www.biomart.org/) query was designed to extract the 1000bp 5' to the coding region for each gene from Ensembl (www.ensembl.org). Each sequence was searched using a MS Word macro (modified from a macro created by James Heather) to identify any potential ZREs located in the DNA sequence. The macro involved matching to 7 bp core ZRE sequences that Zta has been experimentally verified as being able to bind to. Identified sites were classified as ZRE class I, II or III (Karlsson *et al.*, 2008b). Only two genes, Notch2 (FD = 14.74) and TPT1 (FD = 12.16), contained no potential sites. The other 15 genes contained between 1 and 7 ZRE sites.

			ZREs in 1000bp 5' of gene			
Gene	**Pair**	**FD**	**Type I**	**Type II**	**Type III**	**Total**
PSMD2	p/Zta, p/AAA	147.74	1		2	3
SOCS1	AAA/p, Zta/p	41.64	1		3	4
NOTCH2	AAA/p, Zta/p	39.98				0
CD70	Zta/p, Zta/AAA	26.86	1		3	4
PFDN4	AAA/p, Zta/p	15.17	2			2
CP	Zta/p, AAA/p	13.43	4			4
TPT1	AAA/p	12.16				0
SKIL	AAA/p, Zta/p	12.12	1		6	7
WNT2	Zta/p	12.05		1	2	3
CDK2	AAA/p	10.51	2			2
LCK	Zta/p	9.71			1	1
MATN3	Zta/p	9.49			1	1
PDGFA	AAA/p	9.41			3	3
FOS	Zta/p, AAA/p	9.41	2		1	3
MTDH	AAA/p	8.84	1		3	4
ID1	AAA/Zta	8.25	1			1
NDC80	AAA/p	8.22	2	1		3

Table 6.22: Table of number of ZREs in promoter region of genes with differential expression between cells transfected with Zta or ZtaAAA
Genes with a difference in expression between Zta and pBabe, ZtaAAA and pBabe or both of greater than 8-fold were selected. The 1000bp 5' to the coding region of each gene was obtained from Ensembl (www.ensembl.org) using BioMart. Each sequence was searched using a MS Word macro for ZREs that Zta is known to be able to bind to. The number of type I, II and III ZREs is shown for each gene.

41 genes showed a difference in expression between Zta and acZta of 10 fold or more (Figure 6.23). These 41 genes were analysed for ZREs in the same way described above. Only NOTCH2 (FD = 27.40) and TPT1 (FD = 10.45) contained no ZREs.

A genome wide search for ZREs by Kirsty Flower et al (Flower *et al.*, 2011) found that 97.3% of human genes contained at least one potential ZRE in the 1000bp upstream of the gene start. The sites are not thought to be retained in the genome for Zta binding but rather as a result of similarity to other binding sites (AP1) or by chance. However the presence of a ZRE means the site is available for Zta binding to potentially affect gene expression. At least 6 human host genes are known to be directly regulated by Zta through ZREs in the promoters. They are DHRS9 (Jones *et al.*, 2007), EGR1 (Chang *et al.*, 2006), CIITA (Li *et al.*, 2009), IL-8 (Hsu *et al.*, 2008), IL-10 (Mahot *et al.*, 2003) and IL-13 (Tsai *et al.*, 2009). The other genes were not part of the array but EGR1 showed a FD of 5.13 ZtaAAA/acZta, 4.35 for Zta/acZta and 3.93 for AAA/pBabe. Other potential mechanisms for Zta affecting cellular gene expression are as a downstream effect from Zta-regulated activation of a pathway e.g. MAPK pathway (Chang *et al.*, 2006) or activation or repression via a binding partner. One example of this is Zta interacts directly with C/EBPα and C/EBPβ *in vivo*, and is thus able to inhibit activation of TNFR1 by C/EBPα and C/EBPβ (Bristol *et al.*, 2010).

			ZREs in 1000bp 5' of gene			
Gene	**Pair**	**FD**	**Type I**	**Type II**	**Type III**	**Total**
PSMD2	ac/Zta	156.39	1		2	3
CD34	Zta/ac	45.92	2			2
AKR1C2	Zta/ac	45.44	3			3
ETV1	Zta/ac	36.81	1			1
ITGB3	Zta/ac	34.13	2		1	3
TGFBI	Zta/ac	30.23	2			2
NOTCH2	Zta/ac	27.40				0
NMBR	Zta/ac	26.47	1		1	2
WNT2	Zta/ac	26.34		1	2	3
TGFB2	Zta/ac	26.12			5	5
BTK	Zta/ac	25.56	2			2
GPR126	Zta/ac	25.26	1		1	2
NQO1	Zta/ac	22.08	4			4
IGFBP3	Zta/ac	20.73			1	1
EGF	Zta/ac	19.61	2			2
ANPEP	Zta/ac	19.04	1		1	2
SOCS1	Zta/ac	19.01	1		3	4
PLK2	Zta/ac	16.06	3		3	6
TNFRSF1B	Zta/ac	15.22	1	1		2
MYRIP	Zta/ac	15.15	2		2	4
MYD88	Zta/ac	15.15	1			1
GSTM3	Zta/ac	15.06	3			3
LEP	Zta/ac	15.01			2	2
SKIL	Zta/ac	14.88	1		6	7
CCL2	Zta/ac	14.46	6			6
AXL	Zta/ac	14.40	5		1	6
RET	Zta/ac	13.89	1		1	2
RAB27B	Zta/ac	13.85	3			3
TIE1	Zta/ac	13.52	1		1	2
CSF3	Zta/ac	13.09	3		1	4
THBS1	Zta/ac	12.34	1	1	3	5
WNT2B	Zta/ac	12.12	2			2
TNK1	Zta/ac	11.09			1	1
MRPL13	Zta/ac	10.99			1	1
CRHR1	Zta/ac	10.87	1		2	3
PDGFRA	Zta/ac	10.71			1	1
UCHL5	Zta/ac	10.69	2		1	3
ERBB3	Zta/ac	10.57			2	2
RAI2	Zta/ac	10.52	1		3	4
TPT1	Zta/ac	10.45				0
SOCS3	Zta/ac	10.27	1	1	1	3

Figure 6.23: Table of number of ZREs in promoter region of genes with differential expression in cells transfected with Zta and treated with acyclovir
Genes with a difference in expression between Zta and acZta, acZta and pBabe or both of greater than 10-fold were selected and analysed for ZREs in the 1000bp 5' to the gene start as in Figure 6.22.

6.2.2.4 Pathway Interaction Database

An analysis of the data with Pathway Interaction Database (PID) (http://pid.nci.nih.gov/) was performed in order to get an impression of how some of the differentially expressed genes may relate to one another in the cell. The PID is a fully curated database of known biomolecular interactions and signalling pathways of key cellular processes. It can be searched with a group of, for example, experimentally identified genes in order to elucidate potential connections between them. The 44 genes which showed a fold difference in expression greater than 5 between Zta/ ZtaAAA and/or pBabe were entered into the database and pathways containing a significant number of these genes were identified (Table 6.24). The associated p-value was calculated by PID. As the pool of genes on the Biotrove Cancer Array was selected for their relationship to this disease, it was to be expected that many would be involved in the same pathways. However this still provides an interesting starting point for clarifying what possible influence Zta may have in host cells. Interestingly one of the hits was the Transcriptional Targets of AP1 (Fra). As an AP-1 transcription factor, Fra and Zta can recognise and bind the same motifs e.g. tgagtca (Welter *et al.*, 1995). This provides a mechanism for Zta to affect transcription of the same cellular target genes as Fra and other Ap1 transcription factors.

Another interesting match from the PID was the p73 transcription factor network. EBV associated gastric carcinoma shows a loss of p73 expression. In addition specific dense methylation of the 5' UTR and exon 1 is near universal in EBV positive gastric carcinoma samples and absent in almost all EBV negative samples (Ushiku *et al.*, 2007). There is also specific increased methylation of other promoters in EBV positive samples including 10 that were included in the QPCR array (Kang *et al.*, 2002; Kang *et al.*, 2008; Ryan *et al.*, 2010). Six of these genes had results from the array with a greater than 3 fold difference. These are shown in Table 6.25, along with the numbers of ZREs found 5' to the gene. All six contained ZREs in this promoter region. All genes except APC contained at least one type 3 methylation dependent ZRE.

These results give an impression of the potentially wide reaching impact Zta may have both directly and indirectly on host cell gene expression.

Pathway	Genes	P-value
Regulation of nuclear SMAD2/3 signaling	CDK2, CDKN2B, FOS, SERPINE1, SKIL	0.00010
IL2-mediated signaling events	CDK2, FOS, LCK, SOCS1	0.00028
HIF-1-alpha transcription factor network	CA9, CP, FOS, SERPINE1	0.00059
uPA and uPAR-mediated signaling	ITGA3, ITGB3, SERPINE1	0.00184
FOXM1 transcription factor network	BRCA2, CDK2, FOS	0.00184
Ceramide signaling pathway	IGF1, PDGFA, TNF	0.00284
IL12-mediated signaling events	FOS, LCK, SOCS1	0.00669
E2F transcription factor network	CDK2, E2F3, SERPINE1	0.00934
Integrin family cell surface interactions	ITGA3, ITGB3	0.00999
p73 transcription factor network	BRCA2, CDK2, SERPINE1	0.01030
Ephrin B reverse signaling	ITGB3, LCK	0.01310
BARD1 signaling events	CDK2, RAD50	0.01310
Osteopontin-mediated events	FOS, ITGB3	0.01390
IL23-mediated signaling events	ITGA3, TNF	0.01920
Transcriptional targets of AP1 (Fra1 and Fra2)	ATF4, DCN	0.01920
ATR signaling pathway	BRCA2, CDK2	0.02210
amb2 Integrin signaling	LCK, TNF	0.02310
PLK1 signaling events	NDC80, TPT1	0.02840
Regulation of RhoA activity	ARHGAP5, ARHGEF5	0.02840
Transcriptional targets of deltaNp63 isoforms	BRCA2, ITGA3	0.03060
Fanconi anemia pathway	BRCA2, RAD50	0.03170
Downstream signaling in naïve CD8+ T cells	FOS, TNF	0.03170
Signaling events mediated by PTP1B	ITGB3, LCK	0.03510
PDGF receptor signaling network	PDGFA	0.03520
PDGFR-beta signaling pathway	FOS, ITGB3, LCK	0.03520
SHP2 signaling	IGF1, LCK	0.04360
IL4-mediated signaling events	ITGB3, SOCS1	0.05120
Regulation of retinoblastoma protein	CDK2, E2F3	0.05380

Table 6.24: Pathway Interaction Database
Pathways identified using Pathway Interaction Database (http://pid.nci.nih.gov) from genes with > 5 Fold Expression difference in cells transfected with either Zta or ZtaAAA.

	Fold Difference (p-value)				ZREs in 1000bp 5'			
Gene	Zta/pBabe	ZtaAAA/pBabe	Zta/ZtaAAA	Zta/acZta	Type 1	Type 2	Type 3	Reference
APC				9.24	2	-	-	(Kang *et al.*, 2002)
BRCA2	3.86	6.01		5.05	2	1	3	(Ryan *et al.*, 2010)
CCND1								(Ryan *et al.*, 2010)
CDKN2A	0.20 (4.89)			0.15 (6.76)	1	2	3	(Ryan *et al.*, 2010)
ICAM1								(Ryan *et al.*, 2010)
ID2								(Ryan *et al.*, 2010)
IGF2								(Kang *et al.*, 2008)
IGFBP3		3.04		20.73	-	-	1	(Ryan *et al.*, 2010)
PTEN				3.00	-	-	2	(Kang *et al.*, 2002)
THBS1				12.34	1	1	3	(Kang *et al.*, 2002)

Table 6.25: Genes from QPCR array that show increased methylation in EBV positive carcinoma
10 genes that are specifically highly methylated in EBV positive gastric carcinoma were part of the QPCR cancer array (references in right column). Results from the array greater than 3 fold are shown. The ZREs found in 1000 bp 5' to the coding region are shown for these genes.

6.3 Discussion

Attempts to assess the interactions between CT mutants and known Zta interacting proteins using pulldown experiments were unsuccessful. However co-expression of Zta and two other proteins, p53 and C/EBPα, revealed some interesting observations.

Co-expression of p53 and Zta resulted in a rapid degradation of both proteins. In a cycloheximide time course experiment, Zta expression was abolished after 2 hours. p53 expression was almost completely reduced by the same time point. Zta-dependent degradation of p53 has been reported in p53-null human osteosarcoma SaOS-2 and 2KO (mouse embryonic p53-/mdm2- fibroblast) cells (Sato *et al.*, 2009). This ubiquitin-mediated proteasomal degradation of p53 by BZLF1 occurs independently of the key p53 regulator, MDM2. Co-expression of p53 and Zta in IMR-90, HeLa and D98/HE-R1cells by Zhang and colleagues resulted in inhibition of the transactivating function of Zta (Zhang *et al.*, 1994). However the levels of Zta protein expressed remained stable when expressed with p53.

When co-expressed with p53, The CT mutant ZtaAAA was expressed at higher levels than Zta. However this was still considerably decreased from Zta / PCDNA3 expression levels (Figure 6.8). This suggests there is some effect on this interaction either directly from the extreme CT of BZLF1 or as a result of a loss of function due to altered interaction with the extreme CT elsewhere in Zta. This agrees with Zhang and colleagues who found the zipper region of Zta essential for p53 interaction (Zhang *et al.*, 1994).

The coordinated degradation of Zta with p53 observed may be influenced by the cell type and also by the high levels of p53 expression. As p53 regulates the expression of genes involved in apoptosis, it is possible that a downstream target of p53 may influence the levels of Zta.

Co-expression of Zta and C/EBPα led to the expression of both Zta and a smaller amount of a larger species of Zta. This was stable in a cycloheximide time course experiment for 24 hours. Co-expression of the mutant ZtaAAA and C/EBPα did not reveal the same larger form of Zta.

Post-translational modification of Zta may play a pivotal role in both the regulation of gene expression in the lytic cycle and DNA replication (Wang *et al.*, 2005).

Modification of Zta with the ubiquitin-related protein SUMO-1 can occur at lysine 12 (Adamson and Kenney, 2001). Sumoylation of Zta leads to higher levels of BMRF1 following lytic cycle induction, suggesting it may have an important role in EBV lytic replication (Adamson, 2005). Mutation of lysine 12 to alanine, disrupting the sumoylation site, results in a defect in EBV lytic cycle DNA replication (Deng *et al.*, 2001).

Further work on this would establish the type of modification present on Zta, possibly through antibodies directed against different modifications. Analysis with mutants could show which regions of Zta are important for this and confirm the importance of the extreme CT as demonstrated by the single band seen with ZtaAAA co-expression.

It would be interesting to complete both *in vitro* and *in vivo* experiments with the expression vectors for p53, BGLF4, BMRF1, C/EBPα, NFκB p65 and RaRα to establish if any of the mutants of Zta have a disrupted association with these proteins. In addition further work needs to be completed to establish if the double band seen in co-expression with C/EBPα is due to modification of Zta. The band is approximately 12 kDa larger then Zta

The QPCR array provided some evidence that this strategy could be useful in identifying cellular genes influenced by Zta. Two examples are given below.

Expression of the gene EGR-1 was found to be 3.93 fold higher in ZtaAAA cells than pBabe cells. Chang and colleagues have previously shown Zta activation of the cellular transcription factor EGR-1 (Chang *et al.*, 2006). Their promoter assay analysis revealed 2 regions responsive to activation by Zta. They identified two adjacent sequences similar to ZREs in the first site. Analysis of this region with our ZRE macro revealed

one type III ZRE (GGAGCGA). The second region identified as responsive to activation by Zta contains no known ZREs. As an additional mechanism for activating EGR-1, Zta activates the ERK signalling pathway, resulting in binding of the Elk-1 transcription complex to the SRE-Ets site in the EGR-1 promoter (Chang *et al.*, 2006).

The gene TGFβ1 showed a 30 fold difference in expression between Zta and acZta. Cayrol and colleagues have previously shown an increased expression of TGFβ1 in response to Zta (Cayrol and Flemington, 1995) and expression of TGFβ1 can lead to the upregulation of p27, a cyclin dependent kinase inhibitor, causing cell cycle arrest (Toyoshima and Hunter, 1994). In addition, upregulation of TGFβ1 and other immunosuppressive cytokines may function to suppress the immune response of host cells (Israel and Kenney, 2005).

Further investigation into other high scoring genes could potentially clarify the role of Zta in influencing cellular genes.

Some more information is given below on some of the most differentially expressed genes that could be worthy of further experimental investigation:

PSMD2

pBabe / ZtaAAA; FD=106.27

acZta / ZtaAAA; FD=149.94

PSMD2 is a subunit of the 19S proteosome regulator. It also interacts with TNF 1 receptor (Boldin *et al.*, 1995) so may feature in TNF signalling pathway.

CD34

Zta/acZta; FD= 45.92

CD34 is a cell surface glycoprotein and a cell-cell adhesion factor. It is selectively expressed on hematopoietic progenitor cells.

AKR1C2

Zta/acZta; FD= 45.44

AKR1C2 is an aldo/keto reductase with a high affinity for bile acid.

ETV1

Zta/acZta; FD= 36.81

ETV1 is a transcription factor. Altered expression of ETV1 was observed in Primary Effusion Lymphoma which is associated with KSHV and mostly co-infected with EBV (Roy *et al.*, 2011)

It would be useful to elucidate the molecular mechanisms of cellular protein regulation by Zta to increase understanding of the interactions between EBV and host cells and also facilitate the development of anti-viral therapy strategies.

Analysis was limited to duplicate data sets due to cost restraints. Ideally more replcates would be performed to enable a measurement of significance to be applied to the results. However this analysis can be viewed as an initial attempt to identify differentially regulated host genes in response to a replication competent versus a replication incompetent mutant of Zta.

Ideally the array would have been flexible to allow inclusion of other genes of interest as well as EBV genes to provide to more complete context for the results. Further analysis would ideally utilise different cell types to elucidate cell specific or global effects. Results could be verified using additional Q-PCR or TaqMan experiments. Further information about the mechanisms of the influence of Zta on specific host genes could be gained through the use of promoter assays to confirm Zta activity as a transcription factor. Analysis of protein levels could also provide functional confirmation.

For a wider investigation, mass spectrometry following a pulldown of interacting proteins could be utilised. Any proteomic differences identified between cells transfected with Zta, mutant or empty vector could be investigated further.

Chapter 7 Discussion

The importance of methylation dependent recognition by Zta as a critical factor in the EBV infective cycle is becoming increasingly apparent (Bergbauer *et al.*, 2010; Kalla *et al.*, 2010; Flower *et al.*, 2011).

I demonstrated that ZRE3 when methylated at both CpG motifs, was a stronger binding site for Zta than the half methylated site studied by Bhende et al (Bhende *et al.*, 2005). This showed that methylation at sites 1' and 0 also contribute to methylation dependent site recognition by Zta (Figure 3.2). Individual analysis revealed a contribution from each of the methylated cytosines although this was unequal. The strongest individual site was $meC^{1'}$, followed by meC^{-2}, with an approximately equal contribution from meC^{0} and $meC^{-1'}$. This *in vitro* evidence was supported by the structural modelling of Zta bound to methylated ZRE3 performed by Petosa and colleagues (Karlsson *et al.*, 2008a) which showed that all four methylated cytosines make contact with Zta.

Zta was the first transcription factor identified to demonstrate enhanced binding to normally repressive methylated DNA in a sequence dependent manner. Precise elucidation of the DNA:protein interaction that makes this recognition possible through the determination of the contribution of individual methylated cytosines and modelling may help identify other proteins that utilise a similar mechanism.

Zta helps enable EBV to achieve a balance between establishing latency in newly infected cells and the lytic replicative cycle (Kalla *et al.*, 2010). Methylation and the methylation dependent functionality of Zta play a key role in this process. The viral DNA in a newly infected cell is not yet methylated. Zta is unable to activate the lytic cycle, as ZREs in the promoters of key lytic cycle genes, including BMRF1, BSLF2/BMLF1, BSRF1 and BBLF4, are unmethylated so unavailable for activation by Zta (Kalla *et al.*, 2010). This allows establishment of latency and long term persistence of the virus. Methylation of the viral genome occurs progressively after infection, resulting in a heavily methylated genome by 4 weeks post infection, allowing Zta to activate the lytic cycle when conditions permit (Kalla *et al.*, 2010). Bergbauer and colleagues have identified over 20 EBV promoters that are potentially recognised by Zta

in a methylation dependent manner, including BALF2, BMRF1, BBLF4, BALF5 and BSLF2/BMLF1 (Bergbauer *et al.*, 2010).

Zta C189 has been shown to be critical for methylation detection and this residue was conserved in over half of 50 aligned human BZIP proteins (Petosa *et al.*, 2006). It is therefore possible that more cellular BZip proteins possessing a cysteine at this position may demonstrate enhanced binding to methylated DNA recognition sequences. The human transcription factor C/EBPα has recently been shown to possess methylation dependent binding ability (Rishi *et al.*, 2010).

KSHV is closely related to EBV and demonstrates a similar biphasic genome methylation, however it does not possess a Zta homologue. Methylation dependent activation by a cellular transcription factor could provide a potential mechanism for overcoming inhibition by methylation in the reactivation of KSHV and other related viruses lacking a Zta homologue (Flower *et al.*, 2011).

DNA binding experiments revealed that the rhesus LCV homologue ZtaRh acts in a very similar methylation dependent manner to Zta. Thus EBV is probably not unique amongst lymphocryptoviruses to utilise this novel method of overcoming transcriptional repression of methylated DNA. It would be interesting to examine binding by Zta homologues in other LCVs to establish the evolution of this mechanism and if it is conserved across the genus.

ZtaRh can be seen as a natural mutant of Zta in that it utilises the same molecular strategy to perform equivalent biologic tasks (Wang, 2005). Although I demonstrated that the binding recognition of ZREs was similar, there are notable genomic differences in ZREs between EBV and RhLCV. In particular there is no Rp ZRE3 equivalent site in RhLCV. Luciferase reporter assays showed that methylation is still critical for RhRp activation but the addition of a ZRE3 site did not increase RhRp promoter strength. As there are no additional known ZREs in RhRp there may be a more important role in RhLCV for Rp ZRE2. It would be interesting to learn if this is due to physical differences in the proteins or differences in the viral or cellular environment. Development of a suitable Rhesus cell line would be required to fully understand how ZtaRh functions as a transcription factor in the natural host cell.

There is an identical repertoire of both latent and lytic genes between EBV and RhLCV (Rivailler *et al.*, 2002). This close genetic relationship between the two viruses shows RhLCV may be a valuable model for studying how different viral genes contribute to infection and pathogenesis of EBV. Rivailler and colleagues have been successful in producing an LCV positive lymphoma in immunosuppressed rhesus macaques infected with RhLCV (Rivailler *et al.*, 2004). Discovery of differences and similarities between the two viruses such as a variation in viral ZREs and recognition of these sites could be informative in interpreting how the two viruses could prove useful in the development of new treatments or vaccines against EBV.

As ZtaRh is not defective in DNA binding, the inability to cause cell cycle arrest and lytic reactivation must occur via an independent mechanism. Cell cycle analysis using domain swap mutants revealed that differences in the transactivation domain could account for ZtaRh being unable to cause cell cycle arrest. As experiments were not performed in the host cell for ZtaRh, it is not surprising that control over a complex mechanism such as the cell cycle was not maintained. However the loss of lytic reactivation function could be mapped to the three extreme CT amino acids and the mutant ZtaAAA is entirely defective in lytic reactivation. An almost complete loss of expression of selected early and late genes was observed in cells transfected with ZtaRh, with Rta expression at approximately 50% of that in cells transfected with Zta. Cells transfected with ZtaAAA did not have reduced expression of Rta or BBLF2/3, although expression of other early and late genes was compromised. The mutant Rh_LNF restored Rta expression but not BBLF2/3 or later genes showing an independent mechanism. This shows that an extreme CT comprised of either AAA or LNF can express Rta but the ZtaRh sequence of I-- was defective.

The nine extreme CT amino acids have not been crystallised and are not part of any modelling. The preceding amino acids fold back and make contacts with the zipper domain that are stabilising for dimerisation (Petosa *et al.*, 2006). Cross-linking has suggested this contact continues to the extreme CT of Zta (Schelcher *et al.*, 2007) and the loss of this could be causative for the observed functional defects in extreme CT mutants. Alternatively this may be a result of alterations in interactions with host or viral proteins.

Co-expression of Zta and known binding partners in HEK293 cells revealed two interesting observations; Zta and p53 demonstrated instability and a larger additional Zta protein was observed when co-expressed with C/EBPα (Figure 6.7). Both of these effects were abrogated when p53 or C/EBPα were co-expressed with ZtaAAA instead, suggesting these extreme CT residues may be important in interacting with other proteins. Completion of the pulldown experiments could clarify the role of this region in Zta's interaction with key partner proteins.

Further experiments to support the current evidence indicating contact between the extreme CT of Zta and the zipper domain would clarify the remaining unsolved structure of Zta. To validate the structure of this region protein NMR spectroscopy or further crystallisation and modelling of Zta would reveal more clearly the formation the CT of Zta. This would allow the actual effect of mutants in this region on the structure to be revealed.

Results obtained using the QPCR Cancer array suggest this could be a plausible strategy to learn more about the cellular impact of the expression of Zta and Zta mutants. For example ZtaAAA showed a 3.93 fold increase in EGR-1 expression ($p=0.05$). Upregulation of EGR-1 by Zta has been shown by Chang and colleagues to be essential for reactivation of EBV from latency through binding to the EGR-1 promoter (Chang *et al.*, 2006). Activation by Zta is thought to occur through a Serum Response Element and two ZREs (Heather *et al.*, 2009). One of the ZREs contains a CpG site and EGR-1 is methylated in B-cells (Heather *et al.*, 2009). Heather and colleagues demonstrated with EMSA that binding to the methylated ZRE was enhanced 10 fold over the same unmethylated ZRE. Zta C189A was greatly compromised in interaction with the methylated site. Methylation of an EGR-1 promoter construct resulted in 4 fold increase in activation in HeLa cells, although another epithelial cell line showed no increase (Heather *et al.*, 2009).

ZtaAAA is not defective for DNA binding, so increased EGR-1 expression would be expected despite the inability of ZtaAAA to reactivate EBV. Zta also showed increased EGR-1 expression ($FD=2.5$) although this was not significant. The use of more replicates to increase significance and a tailored selection of genes, including viral

genes, could be very informative about the effects of Zta. It would be interesting to analyse C189S using this system as this could be revealing on the effects of methylation sensitive binding by Zta. ChIP-Sequencing (chromatin immunoprecipitation sequencing) could be a useful tool to reveal the role of Zta as a transcription factor, both in the viral and human genome. This could be linked to methylation status to find the impact of methylation sensitive DNA binding by Zta *in vivo*.

In summary, methylation dependent recognition of ZREs in viral and host genes is increasingly being recognised as an important factor in both the infection and activation of EBV. This appears to be a feature shared with RhLCV. The structure of the extreme CT of Zta is not yet clear but these residues are to be important for some functions of Zta, either operating as a stabilising influence in the zipper region or affecting protein interactions. Zta appears to have a wide range of effects on host cell gene expression, probably through actions both as a transcription factor and direct and indirect interactions with host cell proteins.

Chapter 8 References

Adamson, A.L. (2005). Effects of SUMO-1 upon Epstein-Barr virus BZLF1 function and BMRF1 expression. Biochem Biophys Res Commun *336*, 22-28.

Adamson, A.L., Darr, D., Holley-Guthrie, E., Johnson, R.A., Mauser, A., Swenson, J., and Kenney, S. (2000). Epstein-Barr virus immediate-early proteins BZLF1 and BRLF1 activate the ATF2 transcription factor by increasing the levels of phosphorylated p38 and c-Jun N-terminal kinases. J Virol *74*, 1224-1233.

Adamson, A.L., and Kenney, S. (1999). The Epstein-Barr virus BZLF1 protein interacts physically and functionally with the histone acetylase CREB-binding protein. J Virol *73*, 6551-6558.

Adamson, A.L., and Kenney, S. (2001). Epstein-barr virus immediate-early protein BZLF1 is SUMO-1 modified and disrupts promyelocytic leukemia bodies. J Virol *75*, 2388-2399.

Adamson, A.L., and Kenney, S.C. (1998). Rescue of the Epstein-Barr virus BZLF1 mutant, Z(S186A), early gene activation defect by the BRLF1 gene product. Virology *251*, 187-197.

Alfieri, C., Birkenbach, M., and Kieff, E. (1991). Early events in Epstein-Barr virus infection of human B lymphocytes. Virology *181*, 595-608.

Amon, W., and Farrell, P.J. (2005). Reactivation of Epstein-Barr virus from latency. Rev Med Virol *15*, 149-156.

Anagnostopoulos, I., Herbst, H., Niedobitek, G., and Stein, H. (1989). Demonstration of monoclonal EBV genomes in Hodgkin's disease and Ki-1-positive anaplastic large cell lymphoma by combined Southern blot and in situ hybridization. Blood *74*, 810-816.

Asai, R., Kato, A., Kato, K., Kanamori-Koyama, M., Sugimoto, K., Sairenji, T., Nishiyama, Y., and Kawaguchi, Y. (2006). Epstein-Barr virus protein kinase BGLF4 is a virion tegument protein that dissociates from virions in a phosphorylation-dependent process and phosphorylates the viral immediate-early protein BZLF1. J Virol *80*, 5125-5134.

Asai, R., Kato, A., and Kawaguchi, Y. (2009). Epstein-Barr Virus Protein Kinase BGLF4 Interacts with Viral Transactivator BZLF1 and Regulates Its Transactivation Activity. J Gen Virol.

Bailey, S.G., Verrall, E., Schelcher, C., Rhie, A., Doherty, A.J., and Sinclair, A.J. (2009). Functional interaction between Epstein-Barr virus replication protein Zta and host DNA damage response protein 53BP1. J Virol *83*, 11116-11122.

Bartel, D.P. (2004). MicroRNAs: genomics, biogenesis, mechanism, and function. Cell *116*, 281-297.

Baumann, M., Feederle, R., Kremmer, E., and Hammerschmidt, W. (1999). Cellular transcription factors recruit viral replication proteins to activate the Epstein-Barr virus origin of lytic DNA replication, oriLyt. Embo J *18*, 6095-6105.

Bergbauer, M., Kalla, M., Schmeinck, A., Gobel, C., Rothbauer, U., Eck, S., Benet-Pages, A., Strom, T.M., and Hammerschmidt, W. (2010). CpG-methylation regulates a class of Epstein-Barr virus promoters. PLoS Pathog *6*.

Bernardi, R., and Pandolfi, P.P. (2003). Role of PML and the PML-nuclear body in the control of programmed cell death. Oncogene *22*, 9048-9057.

Bhende, P.M., Seaman, W.T., Delecluse, H.J., and Kenney, S.C. (2004). The EBV lytic switch protein, Z, preferentially binds to and activates the methylated viral genome. Nat Genet *36*, 1099-1104.

Bhende, P.M., Seaman, W.T., Delecluse, H.J., and Kenney, S.C. (2005). BZLF1 activation of the methylated form of the BRLF1 immediate-early promoter is regulated by BZLF1 residue 186. J Virol *79*, 7338-7348.

Binne, U.K., Amon, W., and Farrell, P.J. (2002). Promoter sequences required for reactivation of Epstein-Barr virus from latency. J Virol *76*, 10282-10289.

Boldin, M.P., Mett, I.L., and Wallach, D. (1995). A protein related to a proteasomal subunit binds to the intracellular domain of the p55 TNF receptor upstream to its 'death domain'. FEBS Lett *367*, 39-44.

Borza, C.M., and Hutt-Fletcher, L.M. (2002). Alternate replication in B cells and epithelial cells switches tropism of Epstein-Barr virus. Nat Med *8*, 594-599.

Bristol, J.A., Robinson, A.R., Barlow, E.A., and Kenney, S.C. (2010). The Epstein-Barr virus BZLF1 protein inhibits tumor necrosis factor receptor 1 expression through effects on cellular C/EBP proteins. J Virol *84*, 12362-12374.

Burkitt, D. (1958). A sarcoma involving the jaws in African children. Br J Surg *46*, 218-223.

Carey, M., Kolman, J., Katz, D.A., Gradoville, L., Barberis, L., and Miller, G. (1992). Transcriptional synergy by the Epstein-Barr virus transactivator ZEBRA. J Virol *66*, 4803-4813.

Cayrol, C., and Flemington, E. (1996a). G0/G1 growth arrest mediated by a region encompassing the basic leucine zipper (bZIP) domain of the Epstein-Barr virus transactivator Zta. J Biol Chem *271*, 31799-31802.

Cayrol, C., and Flemington, E.K. (1995). Identification of cellular target genes of the Epstein-Barr virus transactivator Zta: activation of transforming growth factor beta igh3 (TGF-beta igh3) and TGF-beta 1. J Virol *69*, 4206-4212.

Cayrol, C., and Flemington, E.K. (1996b). The Epstein-Barr virus bZIP transcription factor Zta causes G0/G1 cell cycle arrest through induction of cyclin-dependent kinase inhibitors. Embo J *15*, 2748-2759.

Chan, C.K., Mueller, N., Evans, A., Harris, N.L., Comstock, G.W., Jellum, E., Magnus, K., Orentreich, N., Polk, B.F., and Vogelman, J. (1991). Epstein-Barr virus antibody patterns preceding the diagnosis of nasopharyngeal carcinoma. Cancer Causes Control *2*, 125-131.

Chang, E.T., and Adami, H.O. (2006). The enigmatic epidemiology of nasopharyngeal carcinoma. Cancer Epidemiol Biomarkers Prev *15*, 1765-1777.

Chang, Y., Chang, S.S., Lee, H.H., Doong, S.L., Takada, K., and Tsai, C.H. (2004). Inhibition of the Epstein-Barr virus lytic cycle by Zta-targeted RNA interference. J Gen Virol *85*, 1371-1379.

Chang, Y., Lee, H.H., Chen, Y.T., Lu, J., Wu, S.Y., Chen, C.W., Takada, K., and Tsai, C.H. (2006). Induction of the early growth response 1 gene by Epstein-Barr virus lytic transactivator Zta. J Virol *80*, 7748-7755.

Chee, A.V., Lopez, P., Pandolfi, P.P., and Roizman, B. (2003). Promyelocytic leukemia protein mediates interferon-based anti-herpes simplex virus 1 effects. J Virol *77*, 7101-7105.

Cho, M.S., and Tran, V.M. (1993). A concatenated form of Epstein-Barr viral DNA in lymphoblastoid cell lines induced by transfection with BZLF1. Virology *194*, 838-842.

Cho, Y., Ramer, J., Rivailler, P., Quink, C., Garber, R.L., Beier, D.R., and Wang, F. (2001). An Epstein-Barr-related herpesvirus from marmoset lymphomas. Proc Natl Acad Sci U S A *98*, 1224-1229.

Clarke, P.A., Sharp, N.A., and Clemens, M.J. (1990). Translational control by the Epstein-Barr virus small RNA EBER-1. Reversal of the double-stranded RNA-induced inhibition of protein synthesis in reticulocyte lysates. Eur J Biochem *193*, 635-641.

Crawford, D.H. (2001). Biology and disease associations of Epstein-Barr virus. Philos Trans R Soc Lond B Biol Sci *356*, 461-473.

Daibata, M., Humphreys, R.E., Takada, K., and Sairenji, T. (1990). Activation of latent EBV via anti-IgG-triggered, second messenger pathways in the Burkitt's lymphoma cell line Akata. J Immunol *144*, 4788-4793.

Daibata, M., Speck, S.H., Mulder, C., and Sairenji, T. (1994). Regulation of the BZLF1 promoter of Epstein-Barr virus by second messengers in anti-immunoglobulin-treated B cells. Virology *198*, 446-454.

Davison, A.J. (2002). Evolution of the herpesviruses. Vet Microbiol *86*, 69-88.

Deaton, A.M., and Bird, A. (2011). CpG islands and the regulation of transcription. Genes Dev *25*, 1010-1022.

Deng, Z., Chen, C.J., Zerby, D., Delecluse, H.J., and Lieberman, P.M. (2001). Identification of acidic and aromatic residues in the Zta activation domain essential for Epstein-Barr virus reactivation. J Virol *75*, 10334-10347.

Dreyfus, D. H., Nagasawa, M., Kelleher, C. A., Gelfand, E. W. (2001). Stable expression of Epstein-Barr virus BZLF-1-encoded ZEBRA protein activates p53-dependent transcription in human Jurkat T-lymphoblastoid cells. Blood *96*, 625-34.

Ehlers, B., Ochs, A., Leendertz, F., Goltz, M., Boesch, C., and Matz-Rensing, K. (2003). Novel simian homologues of Epstein-Barr virus. J Virol *77*, 10695-10699.

Ehlers, B., Spiess, K., Leendertz, F., Peeters, M., Boesch, C., Gatherer, D., and McGeoch, D.J. (2010). Lymphocryptovirus phylogeny and the origins of Epstein-Barr virus. J Gen Virol *91*, 630-642.

Ehlers, B., Ulrich, S., and Goltz, M. (1999). Detection of two novel porcine herpesviruses with high similarity to gammaherpesviruses. J Gen Virol *80 (Pt 4)*, 971-978.

Epstein, M.A., Henle, G., Achong, B.G., and Barr, Y.M. (1965). Morphological and Biological Studies on a Virus in Cultured Lymphoblasts from Burkitt's Lymphoma. J Exp Med *121*, 761-770.

Faller, D.V., Mentzer, S.J., and Perrine, S.P. (2001). Induction of the Epstein-Barr virus thymidine kinase gene with concomitant nucleoside antivirals as a therapeutic strategy for Epstein-Barr virus-associated malignancies. Curr Opin Oncol *13*, 360-367.

Farrell, P.J., Rowe, D.T., Rooney, C.M., and Kouzarides, T. (1989). Epstein-Barr virus BZLF1 trans-activator specifically binds to a consensus AP-1 site and is related to c-fos. Embo J *8*, 127-132.

Faulkner, G.C., Burrows, S.R., Khanna, R., Moss, D.J., Bird, A.G., and Crawford, D.H. (1999). X-Linked agammaglobulinemia patients are not infected with Epstein-Barr virus: implications for the biology of the virus. J Virol *73*, 1555-1564.

Feederle, R., Kost, M., Baumann, M., Janz, A., Drouet, E., Hammerschmidt, W., and Delecluse, H.J. (2000). The Epstein-Barr virus lytic program is controlled by the co-operative functions of two transactivators. Embo J *19*, 3080-3089.

Feng, W.H., Westphal, E., Mauser, A., Raab-Traub, N., Gulley, M.L., Busson, P., and Kenney, S.C. (2002). Use of adenovirus vectors expressing Epstein-Barr virus (EBV) immediate-early protein BZLF1 or BRLF1 to treat EBV-positive tumors. J Virol *76*, 10951-10959.

Fickenscher, H., and Fleckenstein, B. (2001). Herpesvirus saimiri. Philos Trans R Soc Lond B Biol Sci *356*, 545-567.

Fixman, E.D., Hayward, G.S., and Hayward, S.D. (1992). trans-acting requirements for replication of Epstein-Barr virus ori-Lyt. J Virol *66*, 5030-5039.

Flemington, E., and Speck, S.H. (1990a). Autoregulation of Epstein-Barr virus putative lytic switch gene BZLF1. J Virol *64*, 1227-1232.

Flemington, E., and Speck, S.H. (1990b). Epstein-Barr virus BZLF1 trans activator induces the promoter of a cellular cognate gene, c-fos. J Virol *64*, 4549-4552.

Flemington, E., and Speck, S.H. (1990c). Identification of phorbol ester response elements in the promoter of Epstein-Barr virus putative lytic switch gene BZLF1. J Virol *64*, 1217-1226.

Flemington, E.K. (2001). Herpesvirus lytic replication and the cell cycle: arresting new developments. J Virol *75*, 4475-4481.

Flower, K., Thomas, D., Heather, J., Ramasubramanyan, S., Jones, S., and Sinclair, A.J. (2011). Epigenetic Control of Viral Life-Cycle by a DNA-Methylation Dependent Transcription Factor. PLoS One *6*, e25922.

Foss, H.D., Herbst, H., Hummel, M., Araujo, I., Latza, U., Rancso, C., Dallenbach, F., and Stein, H. (1994). Patterns of cytokine gene expression in infectious mononucleosis. Blood *83*, 707-712.

Francis, A.L., Gradoville, L., and Miller, G. (1997). Alteration of a single serine in the basic domain of the Epstein-Barr virus ZEBRA protein separates its functions of transcriptional activation and disruption of latency. J Virol *71*, 3054-3061.

Fruehling, S., and Longnecker, R. (1997). The immunoreceptor tyrosine-based activation motif of Epstein-Barr virus LMP2A is essential for blocking BCR-mediated signal transduction. Virology *235*, 241-251.

Gallagher, A., Armstrong, A.A., MacKenzie, J., Shield, L., Khan, G., Lake, A., Proctor, S., Taylor, P., Clements, G.B., and Jarrett, R.F. (1999). Detection of Epstein-Barr virus (EBV) genomes in the serum of patients with EBV-associated Hodgkin's disease. Int J Cancer *84*, 442-448.

Gao, Z., Krithivas, A., Finan, J.E., Semmes, O.J., Zhou, S., Wang, Y., and Hayward, S.D. (1998). The Epstein-Barr virus lytic transactivator Zta interacts with the helicase-primase replication proteins. J Virol *72*, 8559-8567.

Garcia, V.E., Quiroga, M.F., Ochoa, M.T., Ochoa, L., Pasquinelli, V., Fainboim, L., Olivares, L.M., Valdez, R., Sordelli, D.O., Aversa, G., Modlin, R.L., and Sieling, P.A. (2001). Signaling lymphocytic activation molecule expression and regulation in human intracellular infection correlate with Th1 cytokine patterns. J Immunol *167*, 5719-5724.

Gibbs, R.A., Rogers, J., Katze, M.G., Bumgarner, R., Weinstock, G.M., Mardis, E.R., Remington, K.A., Strausberg, R.L., Venter, J.C., Wilson, R.K., and Consortium, R.M.G.S.a.A. (2007). Evolutionary and biomedical insights from the rhesus macaque genome. Science *316*, 222-234.

Gires, O., Kohlhuber, F., Kilger, E., Baumann, M., Kieser, A., Kaiser, C., Zeidler, R., Scheffer, B., Ueffing, M., and Hammerschmidt, W. (1999). Latent membrane protein 1 of Epstein-Barr virus interacts with JAK3 and activates STAT proteins. Embo J *18*, 3064-3073.

Gires, O., Zimber-Strobl, U., Gonnella, R., Ueffing, M., Marschall, G., Zeidler, R., Pich, D., and Hammerschmidt, W. (1997). Latent membrane protein 1 of Epstein-Barr virus mimics a constitutively active receptor molecule. Embo J *16*, 6131-6140.

Glover, J.N., and Harrison, S.C. (1995). Crystal structure of the heterodimeric bZIP transcription factor c-Fos-c-Jun bound to DNA. Nature *373*, 257-261.

Greenspan, J.S., Greenspan, D., Lennette, E.T., Abrams, D.I., Conant, M.A., Petersen, V., and Freese, U.K. (1985). Replication of Epstein-Barr virus within the epithelial cells of oral "hairy" leukoplakia, an AIDS-associated lesion. N Engl J Med *313*, 1564-1571.

Gruffat, H., Manet, E., and Sergeant, A. (2002). MEF2-mediated recruitment of class II HDAC at the EBV immediate early gene BZLF1 links latency and chromatin remodeling. EMBO Rep *3*, 141-146.

Grunewald, V., Bonnet, M., Boutin, S., Yip, T., Louzir, H., Levrero, M., Seigneurin, J.M., Raphael, M., Touitou, R., Martel-Renoir, D., Cochet, C., Durandy, A., Andre, P., Lau, W., Zeng, Y., and Joab, I. (1998). Amino-acid change in the Epstein-Barr-virus ZEBRA protein in undifferentiated nasopharyngeal carcinomas from Europe and North Africa. Int J Cancer *75*, 497-503.

Gutensohn, N., and Cole, P. (1980). Epidemiology of Hodgkin's disease. Semin Oncol *7*, 92-102.

Gutsch, D.E., Holley-Guthrie, E.A., Zhang, Q., Stein, B., Blanar, M.A., Baldwin, A.S., and Kenney, S.C. (1994). The bZIP transactivator of Epstein-Barr virus, BZLF1, functionally and physically interacts with the p65 subunit of NF-kappa B. Mol Cell Biol *14*, 1939-1948.

Halder, S., Murakami, M., Verma, S.C., Kumar, P., Yi, F., and Robertson, E.S. (2009). Early events associated with infection of Epstein-Barr virus infection of primary B-cells. PLoS One *4*, e7214.

Hammerschmidt, W., and Sugden, B. (1988). Identification and characterization of oriLyt, a lytic origin of DNA replication of Epstein-Barr virus. Cell *55*, 427-433.

Heather, J., Flower, K., Isaac, S., and Sinclair, A.J. (2009). The Epstein-Barr Virus Lytic Cycle Activator Zta Interacts With Methylated ZRE In Promoter Of Host Target Gene Egr1. J Gen Virol.

Henle, G., Henle, W., and Diehl, V. (1968). Relation of Burkitt's tumor-associated herpes-ytpe virus to infectious mononucleosis. Proc Natl Acad Sci U S A *59*, 94-101.

Herrmann, K., Frangou, P., Middeldorp, J., and Niedobitek, G. (2002). Epstein-Barr virus replication in tongue epithelial cells. J Gen Virol *83*, 2995-2998.

Hicks, M.R., Al-Mehairi, S.S., and Sinclair, A.J. (2003). The zipper region of Epstein-Barr virus bZIP transcription factor Zta is necessary but not sufficient to direct DNA binding. J Virol *77*, 8173-8177.

Hicks, M.R., Balesaria, S., Medina-Palazon, C., Pandya, M.J., Woolfson, D.N., and Sinclair, A.J. (2001). Biophysical analysis of natural variants of the multimerization region of Epstein-Barr virus lytic-switch protein BZLF1. J Virol *75*, 5381-5384.

Ho, M., Miller, G., Atchison, R.W., Breinig, M.K., Dummer, J.S., Andiman, W., Starzl, T.E., Eastman, R., Griffith, B.P., Hardesty, R.L., and et al. (1985). Epstein-Barr virus

infections and DNA hybridization studies in posttransplantation lymphoma and lymphoproliferative lesions: the role of primary infection. J Infect Dis *152*, 876-886.

Hochberg, D., Souza, T., Catalina, M., Sullivan, J.L., Luzuriaga, K., and Thorley-Lawson, D.A. (2004). Acute infection with Epstein-Barr virus targets and overwhelms the peripheral memory B-cell compartment with resting, latently infected cells. J Virol *78*, 5194-5204.

Hong, Y., Holley-Guthrie, E., and Kenney, S. (1997). The bZip dimerization domain of the Epstein-Barr virus BZLF1 (Z) protein mediates lymphoid-specific negative regulation. Virology *229*, 36-48.

Hsu, M., Wu, S.Y., Chang, S.S., Su, I.J., Tsai, C.H., Lai, S.J., Shiau, A.L., Takada, K., and Chang, Y. (2008). Epstein-Barr virus lytic transactivator Zta enhances chemotactic activity through induction of interleukin-8 in nasopharyngeal carcinoma cells. J Virol *82*, 3679-3688.

Huen, D.S., Henderson, S.A., Croom-Carter, D., and Rowe, M. (1995). The Epstein-Barr virus latent membrane protein-1 (LMP1) mediates activation of NF-kappa B and cell surface phenotype via two effector regions in its carboxy-terminal cytoplasmic domain. Oncogene *10*, 549-560.

Israel, B.F., and Kenney, S. (2005). EBV Lytic Infection. In: Epstein-Barr Virus, ed. E. Robertson: Caister Academic Press, 571-611.

Jemal, A., Bray, F., Center, M.M., Ferlay, J., Ward, E., and Forman, D. (2011). Global cancer statistics. CA Cancer J Clin *61*, 69-90.

Jones, H.W., Jr., McKusick, V.A., Harper, P.S., and Wuu, K.D. (1971). George Otto Gey. (1899-1970). The HeLa cell and a reappraisal of its origin. Obstet Gynecol *38*, 945-949.

Jones, R.J., Dickerson, S., Bhende, P.M., Delecluse, H.J., and Kenney, S.C. (2007). Epstein-Barr virus lytic infection induces retinoic acid-responsive genes through induction of a retinol-metabolizing enzyme, DHRS9. J Biol Chem *282*, 8317-8324.

Kalla, M., Schmeinck, A., Bergbauer, M., Pich, D., and Hammerschmidt, W. (2010). AP-1 homolog BZLF1 of Epstein-Barr virus has two essential functions dependent on the epigenetic state of the viral genome. Proc Natl Acad Sci U S A *107*, 850-855.

Kang, G.H., Lee, S., Cho, N.Y., Gandamihardja, T., Long, T.I., Weisenberger, D.J., Campan, M., and Laird, P.W. (2008). DNA methylation profiles of gastric carcinoma characterized by quantitative DNA methylation analysis. Lab Invest *88*, 161-170.

Kang, G.H., Lee, S., Kim, W.H., Lee, H.W., Kim, J.C., Rhyu, M.G., and Ro, J.Y. (2002). Epstein-barr virus-positive gastric carcinoma demonstrates frequent aberrant methylation of multiple genes and constitutes CpG island methylator phenotype-positive gastric carcinoma. Am J Pathol *160*, 787-794.

Karlsson, Q.H., Schelcher, C., Verrall, E., Petosa, C., and Sinclair, A.J. (2008a). Methylated DNA recognition during the reversal of epigenetic silencing is regulated by

cysteine and serine residues in the Epstein-Barr virus lytic switch protein. PLoS Pathog *4*, e1000005.

Karlsson, Q.H., Schelcher, C., Verrall, E., Petosa, C., and Sinclair, A.J. (2008b). The reversal of epigenetic silencing of the EBV genome is regulated by viral bZIP protein. Biochem Soc Trans *36*, 637-639.

Keating, S., Prince, S., Jones, M., and Rowe, M. (2002). The lytic cycle of Epstein-Barr virus is associated with decreased expression of cell surface major histocompatibility complex class I and class II molecules. J Virol *76*, 8179-8188.

Kenney, S., Kamine, J., Holley-Guthrie, E., Lin, J.C., Mar, E.C., and Pagano, J. (1989). The Epstein-Barr virus (EBV) BZLF1 immediate-early gene product differentially affects latent versus productive EBV promoters. J Virol *63*, 1729-1736.

Kieff, E., and Rickinson, A.B. (2007). Epstein-Barr virus and its replication. In: Fields Virology, vol. 2: Lippincott Williams & Wilkins, 2603-2654.

Kilger, E., Kieser, A., Baumann, M., and Hammerschmidt, W. (1998). Epstein-Barr virus-mediated B-cell proliferation is dependent upon latent membrane protein 1, which simulates an activated CD40 receptor. Embo J *17*, 1700-1709.

Klose, R.J., and Bird, A.P. (2006). Genomic DNA methylation: the mark and its mediators. Trends Biochem Sci *31*, 89-97.

Kolman, J.L., Taylor, N., Gradoville, L., Countryman, J., and Miller, G. (1996). Comparing transcriptional activation and autostimulation by ZEBRA and ZEBRA/c-Fos chimeras. J Virol *70*, 1493-1504.

Komano, J., Maruo, S., Kurozumi, K., Oda, T., and Takada, K. (1999). Oncogenic role of Epstein-Barr virus-encoded RNAs in Burkitt's lymphoma cell line Akata. J Virol *73*, 9827-9831.

Kouzarides, T., Packham, G., Cook, A., and Farrell, P.J. (1991). The BZLF1 protein of EBV has a coiled coil dimerisation domain without a heptad leucine repeat but with homology to the C/EBP leucine zipper. Oncogene *6*, 195-204.

Krappmann, D., Patke, A., Heissmeyer, V., and Scheidereit, C. (2001). B-cell receptor- and phorbol ester-induced NF-kappaB and c-Jun N-terminal kinase activation in B cells requires novel protein kinase C's. Mol Cell Biol *21*, 6640-6650.

Kudoh, A., Daikoku, T., Sugaya, Y., Isomura, H., Fujita, M., Kiyono, T., Nishiyama, Y., and Tsurumi, T. (2004). Inhibition of S-phase cyclin-dependent kinase activity blocks expression of Epstein-Barr virus immediate-early and early genes, preventing viral lytic replication. J Virol *78*, 104-115.

Kudoh, A., Fujita, M., Kiyono, T., Kuzushima, K., Sugaya, Y., Izuta, S., Nishiyama, Y., and Tsurumi, T. (2003). Reactivation of lytic replication from B cells latently infected with Epstein-Barr virus occurs with high S-phase cyclin-dependent kinase activity while inhibiting cellular DNA replication. J Virol *77*, 851-861.

Landschulz, W.H., Johnson, P.F., and McKnight, S.L. (1988). The leucine zipper: a hypothetical structure common to a new class of DNA binding proteins. Science *240*, 1759-1764.

Lee, M.A., Diamond, M.E., and Yates, J.L. (1999). Genetic evidence that EBNA-1 is needed for efficient, stable latent infection by Epstein-Barr virus. J Virol *73*, 2974-2982.

Lerner, M.R., Andrews, N.C., Miller, G., and Steitz, J.A. (1981). Two small RNAs encoded by Epstein-Barr virus and complexed with protein are precipitated by antibodies from patients with systemic lupus erythematosus. Proc Natl Acad Sci U S A *78*, 805-809.

Levitskaya, J., Sharipo, A., Leonchiks, A., Ciechanover, A., and Masucci, M.G. (1997). Inhibition of ubiquitin/proteasome-dependent protein degradation by the Gly-Ala repeat domain of the Epstein-Barr virus nuclear antigen 1. Proc Natl Acad Sci U S A *94*, 12616-12621.

Li, D., Qian, L., Chen, C., Shi, M., Yu, M., Hu, M., Song, L., Shen, B., and Guo, N. (2009). Down-regulation of MHC class II expression through inhibition of CIITA transcription by lytic transactivator Zta during Epstein-Barr virus reactivation. J Immunol *182*, 1799-1809.

Li, H.P., Leu, Y.W., and Chang, Y.S. (2005). Epigenetic changes in virus-associated human cancers. Cell Res *15*, 262-271.

Lieberman, P.M., Hardwick, J.M., Sample, J., Hayward, G.S., and Hayward, S.D. (1990). The zta transactivator involved in induction of lytic cycle gene expression in Epstein-Barr virus-infected lymphocytes binds to both AP-1 and ZRE sites in target promoter and enhancer regions. J Virol *64*, 1143-1155.

Lin, J.C., Smith, M.C., and Pagano, J.S. (1984). Prolonged inhibitory effect of 9-(1,3-dihydroxy-2-propoxymethyl)guanine against replication of Epstein-Barr virus. J Virol *50*, 50-55.

Liu, S., Borras, A.M., Liu, P., Suske, G., and Speck, S.H. (1997a). Binding of the ubiquitous cellular transcription factors Sp1 and Sp3 to the ZI domains in the Epstein-Barr virus lytic switch BZLF1 gene promoter. Virology *228*, 11-18.

Liu, S., Liu, P., Borras, A., Chatila, T., and Speck, S.H. (1997b). Cyclosporin A-sensitive induction of the Epstein-Barr virus lytic switch is mediated via a novel pathway involving a MEF2 family member. Embo J *16*, 143-153.

Lo, K.W., and Huang, D.P. (2002). Genetic and epigenetic changes in nasopharyngeal carcinoma. Semin Cancer Biol *12*, 451-462.

Lu, J., Chen, S.Y., Chua, H.H., Liu, Y.S., Huang, Y.T., Chang, Y., Chen, J.Y., Sheen, T.S., and Tsai, C.H. (2000). Upregulation of tyrosine kinase TKT by the Epstein-Barr virus transactivator Zta. J Virol *74*, 7391-7399.

Lu, J., Chua, H.H., Chen, S.Y., Chen, J.Y., and Tsai, C.H. (2003). Regulation of matrix metalloproteinase-1 by Epstein-Barr virus proteins. Cancer Res *63*, 256-262.

Macsween, K.F., and Crawford, D.H. (2003). Epstein-Barr virus-recent advances. Lancet Infect Dis *3*, 131-140.

Mahot, S., Sergeant, A., Drouet, E., and Gruffat, H. (2003). A novel function for the Epstein-Barr virus transcription factor EB1/Zta: induction of transcription of the hIL-10 gene. J Gen Virol *84*, 965-974.

Manet, E., Gruffat, H., Trescol-Biemont, M.C., Moreno, N., Chambard, P., Giot, J.F., and Sergeant, A. (1989). Epstein-Barr virus bicistronic mRNAs generated by facultative splicing code for two transcriptional trans-activators. Embo J *8*, 1819-1826.

Marafioti, T., Hummel, M., Foss, H.D., Laumen, H., Korbjuhn, P., Anagnostopoulos, I., Lammert, H., Demel, G., Theil, J., Wirth, T., and Stein, H. (2000). Hodgkin and reed-sternberg cells represent an expansion of a single clone originating from a germinal center B-cell with functional immunoglobulin gene rearrangements but defective immunoglobulin transcription. Blood *95*, 1443-1450.

Mauser, A., Holley-Guthrie, E., Zanation, A., Yarborough, W., Kaufmann, W., Klingelhutz, A., Seaman, W.T., and Kenney, S. (2002a). The Epstein-Barr virus immediate-early protein BZLF1 induces expression of E2F-1 and other proteins involved in cell cycle progression in primary keratinocytes and gastric carcinoma cells. J Virol *76*, 12543-12552.

Mauser, A., Saito, S., Appella, E., Anderson, C.W., Seaman, W.T., and Kenney, S. (2002b). The Epstein-Barr virus immediate-early protein BZLF1 regulates p53 function through multiple mechanisms. J Virol *76*, 12503-12512.

Maxwell, A., McCudden, C., Wians, F., and Willis, M. (2009). Recent Advances in the Detection of Prostate Cancer Using Epigenetic Markers in Commonly Collected Laboratory Samples. Lab Medicine *40*, 171-178.

McDonald, C.M., Petosa, C., and Farrell, P.J. (2009). Interaction of Epstein-Barr virus BZLF1 C-terminal tail structure and core zipper is required for DNA replication but not for promoter transactivation. J Virol *83*, 3397-3401.

Mentzer, S.J., Perrine, S.P., and Faller, D.V. (2001). Epstein--Barr virus post-transplant lymphoproliferative disease and virus-specific therapy: pharmacological re-activation of viral target genes with arginine butyrate. Transpl Infect Dis *3*, 177-185.

Middleton, T., and Sugden, B. (1994). Retention of plasmid DNA in mammalian cells is enhanced by binding of the Epstein-Barr virus replication protein EBNA1. J Virol *68*, 4067-4071.

Moghaddam, A., Koch, J., Annis, B., and Wang, F. (1998). Infection of human B lymphocytes with lymphocryptoviruses related to Epstein-Barr virus. J Virol *72*, 3205-3212.

Moghaddam, A., Rosenzweig, M., Lee-Parritz, D., Annis, B., Johnson, R.P., and Wang, F. (1997). An animal model for acute and persistent Epstein-Barr virus infection. Science *276*, 2030-2033.

Molesworth, S.J., Lake, C.M., Borza, C.M., Turk, S.M., and Hutt-Fletcher, L.M. (2000). Epstein-Barr virus gH is essential for penetration of B cells but also plays a role in attachment of virus to epithelial cells. J Virol *74*, 6324-6332.

Moore, P.S., and Chang, Y. (1995). Detection of herpesvirus-like DNA sequences in Kaposi's sarcoma in patients with and without HIV infection. N Engl J Med *332*, 1181-1185.

Moore, S.M., Cannon, J.S., Tanhehco, Y.C., Hamzeh, F.M., and Ambinder, R.F. (2001). Induction of Epstein-Barr virus kinases to sensitize tumor cells to nucleoside analogues. Antimicrob Agents Chemother *45*, 2082-2091.

Morgenstern, J.P., and Land, H. (1990). Advanced mammalian gene transfer: high titre retroviral vectors with multiple drug selection markers and a complementary helper-free packaging cell line. Nucleic Acids Res *18*, 3587-3596.

Morrison, T.E., and Kenney, S.C. (2004). BZLF1, an Epstein-Barr virus immediate-early protein, induces p65 nuclear translocation while inhibiting p65 transcriptional function. Virology *328*, 219-232.

Morrison, T.E., Mauser, A., Wong, A., Ting, J.P., and Kenney, S.C. (2001). Inhibition of IFN-gamma signaling by an Epstein-Barr virus immediate-early protein. Immunity *15*, 787-799.

Mueller, N., Evans, A., Harris, N.L., Comstock, G.W., Jellum, E., Magnus, K., Orentreich, N., Polk, B.F., and Vogelman, J. (1989). Hodgkin's disease and Epstein-Barr virus. Altered antibody pattern before diagnosis. N Engl J Med *320*, 689-695.

Murray, P.G., and Young, L.S. (2001). Epstein-Barr virus infection: basis of malignancy and potential for therapy. Expert Rev Mol Med *2001*, 1-20.

Nemerow, G.R., Mold, C., Schwend, V.K., Tollefson, V., and Cooper, N.R. (1987). Identification of gp350 as the viral glycoprotein mediating attachment of Epstein-Barr virus (EBV) to the EBV/C3d receptor of B cells: sequence homology of gp350 and C3 complement fragment C3d. J Virol *61*, 1416-1420.

Nemerow, G.R., Wolfert, R., McNaughton, M.E., and Cooper, N.R. (1985). Identification and characterization of the Epstein-Barr virus receptor on human B lymphocytes and its relationship to the C3d complement receptor (CR2). J Virol *55*, 347-351.

Niederman, J.C., Miller, G., Pearson, H.A., Pagano, J.S., and Dowaliby, J.M. (1976). Infectious mononucleosis. Epstein-Barr-virus shedding in saliva and the oropharynx. N Engl J Med *294*, 1355-1359.

Niedobitek, G., Agathanggelou, A., Rowe, M., Jones, E.L., Jones, D.B., Turyaguma, P., Oryema, J., Wright, D.H., and Young, L.S. (1995). Heterogeneous expression of Epstein-Barr virus latent proteins in endemic Burkitt's lymphoma. Blood *86*, 659-665.

O'Shea, E.K., Rutkowski, R., and Kim, P.S. (1989). Evidence that the leucine zipper is a coiled coil. Science *243*, 538-542.

Packham, G., Economou, A., Rooney, C.M., Rowe, D.T., and Farrell, P.J. (1990). Structure and function of the Epstein-Barr virus BZLF1 protein. J Virol *64*, 2110-2116.

Petosa, C., Morand, P., Baudin, F., Moulin, M., Artero, J.B., and Muller, C.W. (2006). Structural basis of lytic cycle activation by the Epstein-Barr virus ZEBRA protein. Mol Cell *21*, 565-572.

Pfitzner, E., Becker, P., Rolke, A., and Schule, R. (1995). Functional antagonism between the retinoic acid receptor and the viral transactivator BZLF1 is mediated by protein-protein interactions. Proc Natl Acad Sci U S A *92*, 12265-12269.

Pfuller, R., and Hammerschmidt, W. (1996). Plasmid-like replicative intermediates of the Epstein-Barr virus lytic origin of DNA replication. J Virol *70*, 3423-3431.

Prokhortchouk, A., Hendrich, B., Jorgensen, H., Ruzov, A., Wilm, M., Georgiev, G., Bird, A., and Prokhortchouk, E. (2001). The p120 catenin partner Kaiso is a DNA methylation-dependent transcriptional repressor. Genes Dev *15*, 1613-1618.

Radkov, S.A., Touitou, R., Brehm, A., Rowe, M., West, M., Kouzarides, T., and Allday, M.J. (1999). Epstein-Barr virus nuclear antigen 3C interacts with histone deacetylase to repress transcription. J Virol *73*, 5688-5697.

Ragoczy, T., and Miller, G. (2001). Autostimulation of the Epstein-Barr virus BRLF1 promoter is mediated through consensus Sp1 and Sp3 binding sites. J Virol *75*, 5240-5251.

Reimann, K.A., Li, J.T., Veazey, R., Halloran, M., Park, I.W., Karlsson, G.B., Sodroski, J., and Letvin, N.L. (1996). A chimeric simian/human immunodeficiency virus expressing a primary patient human immunodeficiency virus type 1 isolate env causes an AIDS-like disease after in vivo passage in rhesus monkeys. J Virol *70*, 6922-6928.

Rishi, V., Bhattacharya, P., Chatterjee, R., Rozenberg, J., Zhao, J., Glass, K., Fitzgerald, P., and Vinson, C. (2010). CpG methylation of half-CRE sequences creates C/EBPalpha binding sites that activate some tissue-specific genes. Proc Natl Acad Sci U S A *107*, 20311-20316.

Rivailler, P., Carville, A., Kaur, A., Rao, P., Quink, C., Kutok, J.L., Westmoreland, S., Klumpp, S., Simon, M., Aster, J.C., and Wang, F. (2004). Experimental rhesus lymphocryptovirus infection in immunosuppressed macaques: an animal model for Epstein-Barr virus pathogenesis in the immunosuppressed host. Blood *104*, 1482-1489.

Rivailler, P., Jiang, H., Cho, Y.G., Quink, C., and Wang, F. (2002). Complete nucleotide sequence of the rhesus lymphocryptovirus: genetic validation for an Epstein-Barr virus animal model. J Virol *76*, 421-426.

Robertson, K.D., and Ambinder, R.F. (1997). Methylation of the Epstein-Barr virus genome in normal lymphocytes. Blood *90*, 4480-4484.

Rochford, R., Miller, C.L., Cannon, M.J., Izumi, K.M., Kieff, E., and Longnecker, R. (1997). In vivo growth of Epstein-Barr virus transformed B cells with mutations in latent membrane protein 2 (LMP2). Arch Virol *142*, 707-720.

Rodriguez, A., Armstrong, M., Dwyer, D., and Flemington, E. (1999). Genetic dissection of cell growth arrest functions mediated by the Epstein-Barr virus lytic gene product, Zta. J Virol *73*, 9029-9038.

Roizman, B., and Baines, J. (1991). The diversity and unity of Herpesviridae. Comp Immunol Microbiol Infect Dis *14*, 63-79.

Rooney, C.M., Rowe, D.T., Ragot, T., and Farrell, P.J. (1989). The spliced BZLF1 gene of Epstein-Barr virus (EBV) transactivates an early EBV promoter and induces the virus productive cycle. J Virol *63*, 3109-3116.

Rowe, D.T. (1999). Epstein-Barr virus immortalization and latency. Front Biosci *4*, D346-371.

Rowe, M., Peng-Pilon, M., Huen, D.S., Hardy, R., Croom-Carter, D., Lundgren, E., and Rickinson, A.B. (1994). Upregulation of bcl-2 by the Epstein-Barr virus latent membrane protein LMP1: a B-cell-specific response that is delayed relative to NF-kappa B activation and to induction of cell surface markers. J Virol *68*, 5602-5612.

Roy, D., Sin, S.H., Damania, B., and Dittmer, D.P. (2011). Tumor suppressor genes FHIT and WWOX are deleted in primary effusion lymphoma (PEL) cell lines. Blood.

Ryan, J.L., Jones, R.J., Kenney, S.C., Rivenbark, A.G., Tang, W., Knight, E.R., Coleman, W.B., and Gulley, M.L. (2010). Epstein-Barr virus-specific methylation of human genes in gastric cancer cells. Infect Agent Cancer *5*, 27.

Sample, J., Henson, E.B., and Sample, C. (1992). The Epstein-Barr virus nuclear protein 1 promoter active in type I latency is autoregulated. J Virol *66*, 4654-4661.

Sample, J., Young, L., Martin, B., Chatman, T., Kieff, E., and Rickinson, A. (1990). Epstein-Barr virus types 1 and 2 differ in their EBNA-3A, EBNA-3B, and EBNA-3C genes. J Virol *64*, 4084-4092.

Sato, Y., Shirata, N., Kudoh, A., Iwahori, S., Nakayama, S., Murata, T., Isomura, H., Nishiyama, Y., and Tsurumi, T. (2009). Expression of Epstein-Barr virus BZLF1 immediate-early protein induces p53 degradation independent of MDM2, leading to repression of p53-mediated transcription. Virology *388*, 204-211.

Sato, Y., Shirata, N., Murata, T., Nakasu, S., Kudoh, A., Iwahori, S., Nakayama, S., Chiba, S., Isomura, H., Kanda, T., Tsurumi, T. (2010). Transient increases in p53-responsible gene expression at early stages of Epstein-Barr virus productive replication. Cell Cycle *9*, 807-14.

Sayos, J., Wu, C., Morra, M., Wang, N., Zhang, X., Allen, D., van Schaik, S., Notarangelo, L., Geha, R., Roncarolo, M.G., Oettgen, H., De Vries, J.E., Aversa, G., and Terhorst, C. (1998). The X-linked lymphoproliferative-disease gene product SAP regulates signals induced through the co-receptor SLAM. Nature *395*, 462-469.

Scharenberg, A.M., Humphries, L.A., and Rawlings, D.J. (2007). Calcium signalling and cell-fate choice in B cells. Nat Rev Immunol *7*, 778-789.

Schelcher, C., Al Mehairi, S., Verrall, E., Hope, Q., Flower, K., Bromley, B., Woolfson, D.N., West, M.J., and Sinclair, A.J. (2007). Atypical bZIP Domain of Viral Transcription Factor Contributes to Stability of Dimer Formation and Transcriptional Function. J Virol *81*, 7149-7155.

Schelcher, C., Valencia, S., Delecluse, H.J., Hicks, M., and Sinclair, A.J. (2005). Mutation of a single amino acid residue in the basic region of the Epstein-Barr virus (EBV) lytic cycle switch protein Zta (BZLF1) prevents reactivation of EBV from latency. J Virol *79*, 13822-13828.

Schepers, A., Pich, D., and Hammerschmidt, W. (1996). Activation of oriLyt, the lytic origin of DNA replication of Epstein-Barr virus, by BZLF1. Virology *220*, 367-376.

Shannon-Lowe, C., and Rowe, M. (2011). Epstein-Barr virus infection of polarized epithelial cells via the basolateral surface by memory B cell-mediated transfer infection. PLoS Pathog *7*, e1001338.

Shannon-Lowe, C.D., Neuhierl, B., Baldwin, G., Rickinson, A.B., and Delecluse, H.J. (2006). Resting B cells as a transfer vehicle for Epstein-Barr virus infection of epithelial cells. Proc Natl Acad Sci U S A *103*, 7065-7070.

Shimizu, N., Tanabe-Tochikura, A., Kuroiwa, Y., and Takada, K. (1994). Isolation of Epstein-Barr virus (EBV)-negative cell clones from the EBV-positive Burkitt's lymphoma (BL) line Akata: malignant phenotypes of BL cells are dependent on EBV. J Virol *68*, 6069-6073.

Sinclair, A.J. (2003). bZIP proteins of human gammaherpesviruses. J Gen Virol *84*, 1941-1949.

Sinclair, A.J. (2006). Unexpected structure of Epstein-Barr virus lytic cycle activator Zta. Trends Microbiol *14*, 289-291.

Sinclair, A.J., Brimmell, M., Shanahan, F., and Farrell, P.J. (1991). Pathways of activation of the Epstein-Barr virus productive cycle. J Virol *65*, 2237-2244.

Sinclair, A.J., Palmero, I., Peters, G., and Farrell, P.J. (1994). EBNA-2 and EBNA-LP cooperate to cause G0 to G1 transition during immortalization of resting human B lymphocytes by Epstein-Barr virus. Embo J *13*, 3321-3328.

Sista, N.D., Barry, C., Sampson, K., and Pagano, J. (1995). Physical and functional interaction of the Epstein-Barr virus BZLF1 transactivator with the retinoic acid receptors RAR alpha and RXR alpha. Nucleic Acids Res *23*, 1729-1736.

Sista, N.D., Pagano, J.S., Liao, W., and Kenney, S. (1993). Retinoic acid is a negative regulator of the Epstein-Barr virus protein (BZLF1) that mediates disruption of latent infection. Proc Natl Acad Sci U S A *90*, 3894-3898.

Smith, P.R., de Jesus, O., Turner, D., Hollyoake, M., Karstegl, C.E., Griffin, B.E., Karran, L., Wang, Y., Hayward, S.D., and Farrell, P.J. (2000). Structure and coding content of CST (BART) family RNAs of Epstein-Barr virus. J Virol *74*, 3082-3092.

Smith, R.F., and Smith, T.F. (1989). Identification of new protein kinase-related genes in three herpesviruses, herpes simplex virus, varicella-zoster virus, and Epstein-Barr virus. J Virol *63*, 450-455.

Spear, P.G., and Longnecker, R. (2003). Herpesvirus entry: an update. J Virol *77*, 10179-10185.

Speck, S.H., Chatila, T., and Flemington, E. (1997). Reactivation of Epstein-Barr virus: regulation and function of the BZLF1 gene. Trends Microbiol *5*, 399-405.

Swaminathan, S. (2008). Noncoding RNAs produced by oncogenic human herpesviruses. J Cell Physiol *216*, 321-326.

Swenson, J.J., Mauser, A.E., Kaufmann, W.K., and Kenney, S.C. (1999). The Epstein-Barr virus protein BRLF1 activates S phase entry through E2F1 induction. J Virol *73*, 6540-6550.

Szekely, L., Selivanova, G., Magnusson, K.P., Klein, G., and Wiman, K.G. (1993). EBNA-5, an Epstein-Barr virus-encoded nuclear antigen, binds to the retinoblastoma and p53 proteins. Proc Natl Acad Sci U S A *90*, 5455-5459.

Takada, K., and Ono, Y. (1989). Synchronous and sequential activation of latently infected Epstein-Barr virus genomes. J Virol *63*, 445-449.

Takase, K., Kelleher, C.A., Terada, N., Jones, J.F., Lucas, J.J., and Gelfand, E.W. (1996). Dissociation of EBV genome replication and host cell proliferation in anti-IgG-stimulated Akata cells. Clin Immunol Immunopathol *81*, 168-174.

Tao, Q., and Robertson, K.D. (2003). Stealth technology: how Epstein-Barr virus utilizes DNA methylation to cloak itself from immune detection. Clin Immunol *109*, 53-63.

Tarakanova, V.L., Leung-Pineda, V., Hwang, S., Yang, C.W., Matatall, K., Basson, M., Sun, R., Piwnica-Worms, H., Sleckman, B.P., and Virgin, H.W.t. (2007). Gamma-herpesvirus kinase actively initiates a DNA damage response by inducing phosphorylation of H2AX to foster viral replication. Cell Host Microbe *1*, 275-286.

Taylor, N., Flemington, E., Kolman, J.L., Baumann, R.P., Speck, S.H., and Miller, G. (1991). ZEBRA and a Fos-GCN4 chimeric protein differ in their DNA-binding specificities for sites in the Epstein-Barr virus BZLF1 promoter. J Virol *65*, 4033-4041.

Thompson, M.P., Aggarwal, B.B., Shishodia, S., Estrov, Z., and Kurzrock, R. (2003). Autocrine lymphotoxin production in Epstein-Barr virus-immortalized B cells: induction via NF-kappaB activation mediated by EBV-derived latent membrane protein 1. Leukemia *17*, 2196-2201.

Thompson, M.P., and Kurzrock, R. (2004). Epstein-Barr virus and cancer. Clin Cancer Res *10*, 803-821.

Thorley-Lawson, D.A., and Gross, A. (2004). Persistence of the Epstein-Barr virus and the origins of associated lymphomas. N Engl J Med *350*, 1328-1337.

Tierney, R.J., Kirby, H.E., Nagra, J.K., Desmond, J., Bell, A.I., and Rickinson, A.B. (2000). Methylation of transcription factor binding sites in the Epstein-Barr virus latent cycle promoter Wp coincides with promoter down-regulation during virus-induced B-cell transformation. J Virol *74*, 10468-10479.

Tomkinson, B., Robertson, E., and Kieff, E. (1993). Epstein-Barr virus nuclear proteins EBNA-3A and EBNA-3C are essential for B-lymphocyte growth transformation. J Virol *67*, 2014-2025.

Toyoshima, H., and Hunter, T. (1994). p27, a novel inhibitor of G1 cyclin-Cdk protein kinase activity, is related to p21. Cell *78*, 67-74.

Tsai, S.C., Lin, S.J., Chen, P.W., Luo, W.Y., Yeh, T.H., Wang, H.W., Chen, C.J., and Tsai, C.H. (2009). EBV Zta protein induces the expression of interleukin-13, promoting the proliferation of EBV-infected B cells and lymphoblastoid cell lines. Blood *114*, 109-118.

Tsurumi, T., Fujita, M., and Kudoh, A. (2005). Latent and lytic Epstein-Barr virus replication strategies. Rev Med Virol *15*, 3-15.

Tugizov, S.M., Berline, J.W., and Palefsky, J.M. (2003). Epstein-Barr virus infection of polarized tongue and nasopharyngeal epithelial cells. Nat Med *9*, 307-314.

Urier, G., Buisson, M., Chambard, P., and Sergeant, A. (1989). The Epstein-Barr virus early protein EB1 activates transcription from different responsive elements including AP-1 binding sites. Embo J *8*, 1447-1453.

Ushiku, T., Chong, J.M., Uozaki, H., Hino, R., Chang, M.S., Sudo, M., Rani, B.R., Sakuma, K., Nagai, H., and Fukayama, M. (2007). p73 gene promoter methylation in Epstein-Barr virus-associated gastric carcinoma. Int J Cancer *120*, 60-66.

Verma, R.P., and Hansch, C. (2006). Chemical Toxicity on HeLa Cells. Curr Med Chem *13*, 423-448.

Vermeulen, K., Van Bockstaele, D.R., and Berneman, Z.N. (2003). The cell cycle: a review of regulation, deregulation and therapeutic targets in cancer. Cell Prolif *36*, 131-149.

Vetsika, E.K., and Callan, M. (2004). Infectious mononucleosis and Epstein-Barr virus. Expert Rev Mol Med *6*, 1-16.

Wagner, H.J., Bein, G., Bitsch, A., and Kirchner, H. (1992). Detection and quantification of latently infected B lymphocytes in Epstein-Barr virus-seropositive, healthy individuals by polymerase chain reaction. J Clin Microbiol *30*, 2826-2829.

Waltzer, L., Bourillot, P.Y., Sergeant, A., and Manet, E. (1995). RBP-J kappa repression activity is mediated by a co-repressor and antagonized by the Epstein-Barr virus transcription factor EBNA2. Nucleic Acids Res *23*, 4939-4945.

Waltzer, L., Logeat, F., Brou, C., Israel, A., Sergeant, A., and Manet, E. (1994). The human J kappa recombination signal sequence binding protein (RBP-J kappa) targets

the Epstein-Barr virus EBNA2 protein to its DNA responsive elements. Embo J *13*, 5633-5638.

Waltzer, L., Perricaudet, M., Sergeant, A., and Manet, E. (1996). Epstein-Barr virus EBNA3A and EBNA3C proteins both repress RBP-J kappa-EBNA2-activated transcription by inhibiting the binding of RBP-J kappa to DNA. J Virol *70*, 5909-5915.

Wang, F. (2005). Epstein-Barr Virus related Lymphocryptoviruses of Old and New World nonhuman primates. In: Epstein-Barr Virus, ed. E. Robertson: Caister Academic Press, 691-709.

Wang, F., Rivailler, P., Rao, P., and Cho, Y. (2001). Simian homologues of Epstein-Barr virus. Philos Trans R Soc Lond B Biol Sci *356*, 489-497.

Wang, P., Day, L., Dheekollu, J., and Lieberman, P.M. (2005). A redox-sensitive cysteine in Zta is required for Epstein-Barr virus lytic cycle DNA replication. J Virol *79*, 13298-13309.

Wang, Y.C., Huang, J.M., and Montalvo, E.A. (1997). Characterization of proteins binding to the ZII element in the Epstein-Barr virus BZLF1 promoter: transactivation by ATF1. Virology *227*, 323-330.

Watt, F., and Molloy, P.L. (1988). Cytosine methylation prevents binding to DNA of a HeLa cell transcription factor required for optimal expression of the adenovirus major late promoter. Genes Dev *2*, 1136-1143.

Welter, J.F., Crish, J.F., Agarwal, C., and Eckert, R.L. (1995). Fos-related antigen (Fra-1), junB, and junD activate human involucrin promoter transcription by binding to proximal and distal AP1 sites to mediate phorbol ester effects on promoter activity. J Biol Chem *270*, 12614-12622.

Westphal, E.M., Mauser, A., Swenson, J., Davis, M.G., Talarico, C.L., and Kenney, S.C. (1999). Induction of lytic Epstein-Barr virus (EBV) infection in EBV-associated malignancies using adenovirus vectors in vitro and in vivo. Cancer Res *59*, 1485-1491.

Williams, H., and Crawford, D.H. (2006). Epstein-Barr virus: the impact of scientific advances on clinical practice. Blood *107*, 862-869.

Williams, H., Macsween, K., McAulay, K., Higgins, C., Harrison, N., Swerdlow, A., Britton, K., and Crawford, D. (2004). Analysis of immune activation and clinical events in acute infectious mononucleosis. J Infect Dis *190*, 63-71.

Wilson, J.B., Bell, J.L., and Levine, A.J. (1996). Expression of Epstein-Barr virus nuclear antigen-1 induces B cell neoplasia in transgenic mice. Embo J *15*, 3117-3126.

Wu, F.Y., Chen, H., Wang, S.E., ApRhys, C.M., Liao, G., Fujimuro, M., Farrell, C.J., Huang, J., Hayward, S.D., and Hayward, G.S. (2003). CCAAT/enhancer binding protein alpha interacts with ZTA and mediates ZTA-induced p21(CIP-1) accumulation and G(1) cell cycle arrest during the Epstein-Barr virus lytic cycle. J Virol *77*, 1481-1500.

Wu, F.Y., Wang, S.E., Chen, H., Wang, L., Hayward, S.D., and Hayward, G.S. (2004). CCAAT/enhancer binding protein alpha binds to the Epstein-Barr virus (EBV) ZTA protein through oligomeric interactions and contributes to cooperative transcriptional activation of the ZTA promoter through direct binding to the ZII and ZIIIB motifs during induction of the EBV lytic cycle. J Virol *78*, 4847-4865.

Wysokenski, D.A., and Yates, J.L. (1989). Multiple EBNA1-binding sites are required to form an EBNA1-dependent enhancer and to activate a minimal replicative origin within oriP of Epstein-Barr virus. J Virol *63*, 2657-2666.

Xia, T., O'Hara, A., Araujo, I., Barreto, J., Carvalho, E., Sapucaia, J.B., Ramos, J.C., Luz, E., Pedroso, C., Manrique, M., Toomey, N.L., Brites, C., Dittmer, D.P., and Harrington, W.J., Jr. (2008). EBV microRNAs in primary lymphomas and targeting of CXCL-11 by ebv-mir-BHRF1-3. Cancer Res *68*, 1436-1442.

Yates, J., Warren, N., Reisman, D., and Sugden, B. (1984). A cis-acting element from the Epstein-Barr viral genome that permits stable replication of recombinant plasmids in latently infected cells. Proc Natl Acad Sci U S A *81*, 3806-3810.

Yoshizaki, T., Sato, H., Murono, S., Pagano, J.S., and Furukawa, M. (1999). Matrix metalloproteinase 9 is induced by the Epstein-Barr virus BZLF1 transactivator. Clin Exp Metastasis *17*, 431-436.

Young, L.S., and Rickinson, A.B. (2004). Epstein-Barr virus: 40 years on. Nat Rev Cancer *4*, 757-768.

Young, L.S., Yao, Q.Y., Rooney, C.M., Sculley, T.B., Moss, D.J., Rupani, H., Laux, G., Bornkamm, G.W., and Rickinson, A.B. (1987). New type B isolates of Epstein-Barr virus from Burkitt's lymphoma and from normal individuals in endemic areas. J Gen Virol *68 (Pt 11)*, 2853-2862.

Zalani, S., Coppage, A., Holley-Guthrie, E., and Kenney, S. (1997). The cellular YY1 transcription factor binds a cis-acting, negatively regulating element in the Epstein-Barr virus BRLF1 promoter. J Virol *71*, 3268-3274.

Zalani, S., Holley-Guthrie, E., and Kenney, S. (1995). The Zif268 cellular transcription factor activates expression of the Epstein-Barr virus immediate-early BRLF1 promoter. J Virol *69*, 3816-3823.

Zalani, S., Holley-Guthrie, E.A., Gutsch, D.E., and Kenney, S.C. (1992). The Epstein-Barr virus immediate-early promoter BRLF1 can be activated by the cellular Sp1 transcription factor. J Virol *66*, 7282-7292.

Zerby, D., Chen, C.J., Poon, E., Lee, D., Shiekhattar, R., and Lieberman, P.M. (1999). The amino-terminal C/H1 domain of CREB binding protein mediates zta transcriptional activation of latent Epstein-Barr virus. Mol Cell Biol *19*, 1617-1626.

Zhang, J., Chen, H., Weinmaster, G., and Hayward, S.D. (2001). Epstein-Barr virus BamHi-a rightward transcript-encoded RPMS protein interacts with the CBF1-associated corepressor CIR to negatively regulate the activity of EBNA2 and NotchIC. J Virol *75*, 2946-2956.

Zhang, Q., Gutsch, D., and Kenney, S. (1994). Functional and physical interaction between p53 and BZLF1: implications for Epstein-Barr virus latency. Mol Cell Biol *14*, 1929-1938.

Zhang, Q., Hong, Y., Dorsky, D., Holley-Guthrie, E., Zalani, S., Elshiekh, N.A., Kiehl, A., Le, T., and Kenney, S. (1996). Functional and physical interactions between the Epstein-Barr virus (EBV) proteins BZLF1 and BMRF1: Effects on EBV transcription and lytic replication. J Virol *70*, 5131-5142.

Zhou, S., Fujimuro, M., Hsieh, J.J., Chen, L., and Hayward, S.D. (2000). A role for SKIP in EBNA2 activation of CBF1-repressed promoters. J Virol *74*, 1939-1947.

Zou, W., Wang, J., and Zhang, D.E. (2007). Negative regulation of ISG15 E3 ligase EFP through its autoISGylation. Biochem Biophys Res Commun *354*, 321-327.